University of Reading

Design, biological and toxicological evaluation of a polymer-insect repellent conjugate for extended release and decreased permeation of PMD

Sayyed Ibrahim Shah

(Pharm-D, M.Phil.)

Thesis submitted to the University of Reading in partial fulfilment of the requirements for the degree of Doctor of Philosophy

School of Pharmacy, University of Reading, United Kingdom

September 2020

Acknowledgements

To my **beloved parents**, **brothers** and **family members**, I will forever be indebted to you because you never gave up supporting me to make this dream become a reality. Especially my mum who always stood by my side and prayed for me.

Extremely grateful to **Abdul Wali Khan University, Mardan (AWKUM)** in Khyber Pakhtunkhwa Province of Pakistan for helping and providing the funding for my PhD Studies.

Finally, I thank **Allah (SWT)** for letting me through all these difficulties. I have experienced Your guidance day by day. I will keep on trusting You for my future.

Ibrahim Shah

September 2020

Dedicated to my beloved parents

Ammi & Baba

Declaration of Original Authorship

This thesis describes research conducted in the School of Pharmacy, University of Reading under the supervision of Professor Adrian Williams and Professor Vitaliy Khutoryanskiy and I Sayyed Ibrahim Shah certify that the research described is original and that I have written all the text therein and Where information has been derived from other sources, I confirm that this has been clearly indicated by suitable citation

Ibrahim Shah

September 2020

Abstract

This PhD project aims to develop a novel polymer-drug conjugate (PDC) *via* free radical polymerisation for extended release and decreased permeation of p-menthane 3,8-diol (PMD) when applied topically onto the skin. The rational behind this was the volatile nature of PMD (evaporates quickly) and reports of the side effects associated with the topical absorption of the PMD. For this purpose, firstly hyaluronic acid (HA) was chosen as a polymer to conjugate PMD but despite exploring various synthetic strategies, and changing reaction parameters including the molecular weight, drug, reaction time *etc*, a conjugate could not be produced. After these initial attempts, an alternative route was selected for the PDC synthesis based on synthesis of polymerisable PMD conjugate and its subsequent co- and homopolymerisation. PMD was conjugated with acryloyl chloride *via* an ester bond to form acryloyl-PMD (APMD), which was subsequently copolymerised with acrylic acid (AA) to form a series of copolymers poly(AA-*co*-APMD). The copolymers were characterised by ^{1}H NMR and FT-IR for their structural elucidation, which was then followed by molecular weight characterisation, thermal analysis by TGA and DSC, reactivity ratio studies, turbidimetric analysis and drug loading. The properties of these copolymers were affected by the molar ratios of AA and APMD, where the AA incorporation into the final copolymer was 3× higher than the APMD. In order to assess the amount of drug (PMD) released from the copolymer, an *in vitro* experiment was performed by using porcine liver esterases (PLEs) to cleave the ester bond from the substrate (copolymer). It was found that ~45% of the drug was released over five days. To investigate the reason for the comparatively modest drug release, two experiments were performed to investigate the effect of copolymer molecular weight and enzyme activity on PMD release. It was found that molecular weight did impact on drug release whilst addition of fresh enzymes showed that ester bond cleavage was not limited by enzyme activity in our study. Penetration and permeation of the copolymer and free drug (PMD) through excised full thickness porcine ear skin was investigated. The Franz diffusion cell studies showed no permeation of the copolymer as compared to the PMD. Moreover, tape stripping revealed that almost ~90% of the copolymer was found on the outer surface of the skin as compared to PMD which was found in all the layers of the skin. A new model using planaria fluorescence assay was developed as a novel method to pre-screen potential irritants such as our copolymer or PMD. The model was developed using a range of known skin irritants to include non-, mild-, moderate- and strong-irritants. The results showed that this model was able to successfully differentiate strong irritants from the non-irritants, whilst the other irritant classes also showed good correlation between the fluorescence intensity (FI) of the

planaria after irritant and then fluorescent dye exposure and the known literature primary irritation index (PII). This test demonstrated that that the copolymer is unlikely to be a significant irritant when applied topically. Overall, this project has demonstrated the feasibility of the copolymer approach as strategy to develop extended-release insect repellents whilst reducing transdermal permeation of the small molecular weight active ingredient and hence minimising any adverse systemic effects.

Table of contents

1. Introduction: Polymer drug conjugates: A potential drug carrier system for topical application

List of Abbreviations

AA	Acrylic acid
ACN	Acetonitrile
AIBN	2,2-Azobis(2-methyl-propionitrile)
ANOVA	Analysis of variance
API	Active Pharmaceutical Ingredients
APMD	Acryloyl-p-menthane 3,8 diol
Am-B	Amphotericin B
AGA	Androgenetic alopecia
CL	Cutaneous Leishmaniasis
CMC	Critical Micelle Concentration
CR	Complement receptor
DDS	Drug Delivery Systems
DMF	Dimethylformamide
DMSO	Dimethyl Sulfoxide
DNA	Deoxyribonucleic acid
DOX	Doxorubicin
DSC	Differential Scanning Calorimetry
DIPEA	N,N Diisopropyletylamine
EC	Ethyl cellulose
EDTA	Ethylene-Diamine tetra-acetic acid
EE	Entrapment Efficiency
EPR	Enhance Permeation and Retention
EGF	Epidermal growth factor
EtOH	Ethanol
FDA	Food and Drug Administration
5-FU	5-Fluorouracil

FTIR-	Fourier Transformed Infrared spectroscopy
GP63	Metalloproteinase glycoprotein 63
GPC	Gel permeation chromatography
GTS	Glyceryl Tri-stearate
HFSC	Hair follicle stem cells
HA	Hyaluronic acid
HPLC	High Performance Liquid Chromatography
IFN-γ	Interferon Gamma
IL-10	Interleukin-10
IMC	Indomethacin
IU	International Unit
LCMS	Liquid chromatography-mass spectroscopy
LPG	Lipo-phospho-glycan
MDR	Multidrug resistance
μg	Microgram
μL	Microlitre
μm	Micrometer
μM	Micromolar
MIC	Minimal inhibitory concentration
Milt	Miltefosine
MXD	Minoxidil
mL	Millilitre
MTT	3-(4,5-dimethylthiazol-2-yl)-2,5-diphenyltetrazolium bromide
NSAID	Non-Steroidal Anti-inflammatory Drug
PAA	Poly (acrylic acid)
PBS	Phosphate Buffered Saline
PCD	Programmed cell death
PDCs	Polymer-drug conjugates
PDI	Polydispersity Index
PEG	Poly-ethylene glycol
PEI	Poly-ethyleneimine
PEO	Poly-ethylene Oxide

PNIPAM	Poly-(*N*-isopropylacrylamide)
PLGA	Poly (Lactic-c-glycolic) acid
PVA	Polyvinyl-Alcohol
PVP	Polyvinyl-pyrrolidone
PyBOP	Benzotriazol-1-yloxy)tripyrrolidinophosphonium hexafluorophosphate
QS	Quorum sensing
RNA	Ribonucleic acid
ROS	Reactive Oxygen Species
SDS	Sodium Dodecyl Sulfate
SEM	Scanning Electron Microscopy
SLN	Solid Lipid Nanoparticles
SSG	Sodium Stibogluconate
TEER	Transepithelial Electrical Resistance
TEM	Transmission Electron Microscopy
TGA	Thermogravimetric Analysis
TGF-β	Transforming Growth Factor-Beta
XRD	X-Ray Diffraction
XTT	2,3-Bis-(2-Methoxy-4-Nitro-5-Sulfophenyl)-2*H*-Tetrazolium-5-Carboxanilide

List of Conferences and Presentations

Pharmacy PhD Showcase 2017, University of Reading, 10th March, 2017 – Poster

Pharmacy PhD Showcase 2018, University of Reading, 10th April 2018 – Talk

Pharmacy PhD Showcase 2019, University of Reading, 14th April 2019 - Talk

Postgraduate Symposium on Biomaterials, University of Lancaster, 7th February 2019

Publication from this Thesis

Syed Ibrahim Shah, Adrian C.Williams, Lau W.M, Vitaliy V.Khutoryanskiy. **2020**. Planarian toxicity fluorescent assay: A quick and cheap pre-screening method for potential skin irritants. Tox.In vitro. **Accepted**

List of Tables

LIST OF FIGURES

Chapter 1. Introduction

Polymer-Drug Conjugates: A Potential Drug Carrier System for Topical Application

1.1 Introduction

The skin is the largest and one of the most physiologically intricate organs in the human body, accounting for 15-16% of the total body mass and has a surface area of 1.7-2.5 m^2. It is responsible for creating a barrier between the host and the external environment as well as the maintenance of homeostasis by permitting communication between the endo- and exogenous environments (Alberti et al*.,* 2001; N'Da, 2014; Williams, 2003).

The concept of polymer-drug conjugates (PDCs) began in 1950s, but it was in 1975 when Helmut Ringsdorf validated this approach as a mean of realizing drug targeting (Ringsdorf, 2007). Since then, research in PDCs orientated around their application in cancer to achieve delivery of chemotherapeutic drugs to tumor tissues (Kopeček, 2013), with passive accumulation occurring by the enhanced permeability and retention effect (EPR) (Natfji et al., 2017). Later, the application of this approach of conjugating drugs to polymers as carriers was extended to develop therapeutic systems for diseases other than cancers including infections, inflammation, cardiovascular disease, nervous system disorders, digestive system ailments, endocrine disease, eye infections, bone and wound-related problems (Pang et al*.,* 2014).

At present polymers are widely used in topical formulations, and serve as a vehicle for the skin formulations (Park et al., 2005). Selection of polymers depend upon the formulation type, ranging from polyethylene and polyacrylates in transdermal patches to thickening or gelling agents like cellulose in semisolid systems (Prausnitz and Langer, 2008). The most common polymers applied to skin are cellulose derivatives, chitosan, polyacrylates, hyaluronic acid, polyvinyl alcohol, polyvinyl-pyrrolidone and silicones. These polymers have varied functions in diverse applications from wound dressings, to anti-nucleants in super-saturated systems and lubricants (Valenta and Auner, 2004).

This chapter focuses on the application of PDCs for the skin rather than other routes, with a focus on the rationales and the key considerations that have underpinned their design (Table 1, Table 2), with information summarised according to the therapeutic area. We finish the chapter with brief introduction about insect repellents with especial focus on p-menthane 3,8 diol (PMD).

1.2. Skin as a Potential Site for Drug Delivery

The skin provides an approachable and convenient site for the administration of drugs and can be used for both topical and systemic drug delivery (Prow et al., 2011). Drugs are provided to various body parts by applying traditional hypodermic needles and metal lancets *e.g.,* intramuscular and subcutaneous injections, which produce discomfort and can transmit various biohazardous pathogens like Hepatitis-C, HIV and now COVID-19 causing SARS-nCOV-2. The skin, on the other hand, offers potential for non- or minimally invasive drug delivery due to its large surface area and the trans-dermal route avoids the first-pass impact of the liver. Likewise, constant blood pharmacons (biologically active substances other than drugs) and drug concentrations can be achieved by the transdermal route, thus reducing variations of the drug concentration in the blood, reducing related harm and inefficacy. Additionally, ingesting difficulties and drug absorption complications in the gastrointestinal region can be bypassed. Due to many immune cells like macrophages, the skin presents potential for delivering different vaccines (van der Maaden et al., 2015). However, the skin, and in particular the stratum corneum, presents a formidable barrier to passive absorption of most drugs.

The skin comprises of three layers, the epidermis, dermis and hypodermis (Figure 1.1). The outermost layer of the skin is the epidermis which is approximately 180μm thick but is up to 0.8mm on the hand palms and feet soles (Alkilani et al., 2015). Epidermis, depending upon the location is divided into 4-5 layers, from deep to superficial these layers are the stratum basale, stratum spinosum, stratum granulosum and stratum corneum, whilst the epidermis of the palms and feet consist of a fifth layer called stratum lucidum (Duracher et al., 2009). All these layers except the stratum basale consist of specialised cells called keratinocytes made up of a protein called keratin (van der Maaden et al*., 2015). The stratum basale is the deepest layer of the epidermis which connects the epidermis with basal lamina, this is then followed by stratum spinosum which got its name due to the spiny appearance of the cells. This layer of the epidermis consists of specialised macrophages called Langerhans cells (Honari and Maibach, 2014). Next layer is the stratum granulosum which got its name from the grainy appearance of the cells. Due to the death of the cells of this layer, it gives rise to another layer called stratum lucidum, which is a smooth layer of the cell located in between the stratum corneum and stratum granulosum. This is then followed by the uppermost layer of the epidermis called stratum corneum (SC) which helps to prevent the penetration of the microbes and keep the skin

hydrated. The SC is dead, anucleate and so the underlying epidermal layers are sometimes referred to as the viable epidermis to distinguish this from the overlying barrier layer (Delgado-Charro, 2013; Hadgraft and Valenta, 2000; Piérard et al., 2003).

Epidermal layers are site for various diseases (and hence a potential drug delivery site) like psoriasis (a disease of stratum basale), atopic dermatitis (associated with depletion of SC lipids) (Sahle et al., 2015) and different bacterial and fungal infections (Edlich et al., 2005; Mueller et al., 2002). Most of these epidermal diseases, *e.g.* psoriasis, rosacea, allergic reactions due to food, eczema result in the disruption of the SC (Alkilani et al., 2015) and thus should be a point of consideration whilst designing the drug delivery system for these diseases.

Underneath the epidermis is the dermis which is typically ~2000μm thick (Figure 1.1). The dermis contains blood vessels, hair follicles, nerves, nociceptors (pain-sensors), connective tissues (collagen and elastin), lymph vessels, sebaceous and sweat glands (Abdo et al., 2020; Barcaui et al., 2015; Kolarsick et al., 2006; van der Maaden et al., 2015). Approximately 2.5 million sweat glands regulate body's temperature by producing sweat. The sebaceous glands are mostly located on the forehead, scalp and face, and are moderately prominent on the upper trunk and secrete sebum which regulate pH and keep the skin moist (Benson, 2012; Rossi et al., 2009). Hair follicles are found almost all over the skin with varying densities except on the hands, feet and lips. Dermis is a disease site for the diseases like cellulitis, acne vulgaris (Boulanger, 2007), fibromatosis (Lebwohl et al., 1990), benign fibrous histiocytoma and dermal changes (premature wrinkling) in aging. Moreover, the hair follicles in the dermis offer a potential route for non-invasive transdermal drug delivery (Patzelt and Lademann, 2013).

Below the dermis is hypodermis which connects the skin to underlying fibrous tissues of the bones and the muscles. The border between the hypodermis and the dermis is difficult to distinguish. By some, it is not considered strictly as a part of the skin. Hypodermis is a site for various skin infections (Paul, 2020).

Intracellular route

Transcellular route

Intrafollicular route

Stratum corneum

Extruding lamellar granule

Stratum granulosum

Desmosomal junction

Stratum spinosum

Stratum basale

Basement membrane

A

Stratum corneum

Epidermis

Dermis

Hypodermis

Langerhans cell

Nerves

Hair follicle

Blood vessels

Sweat gland
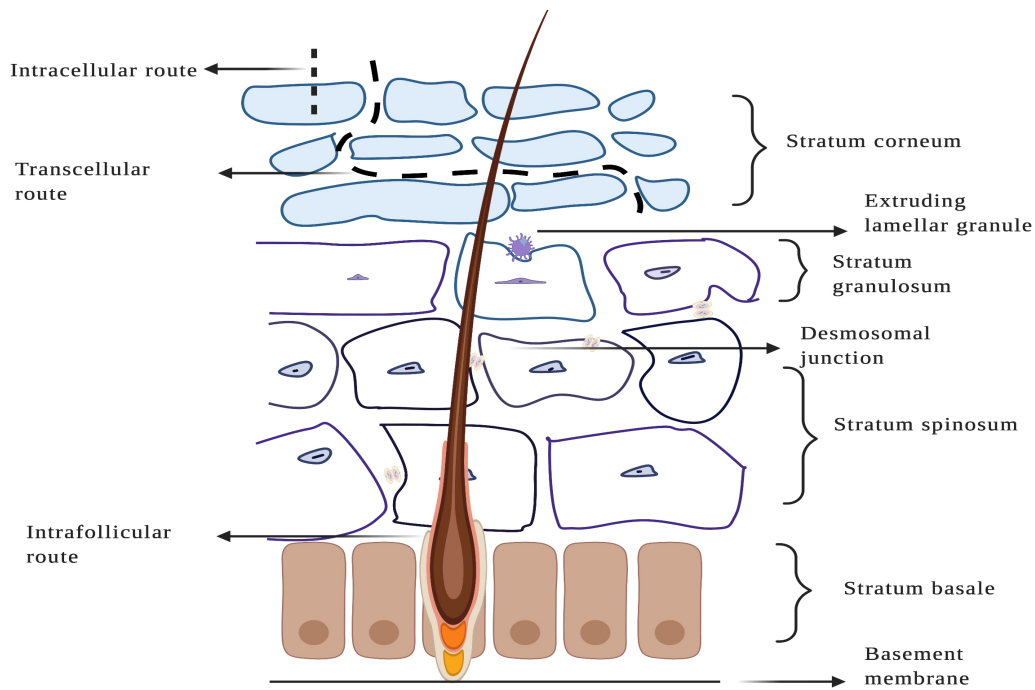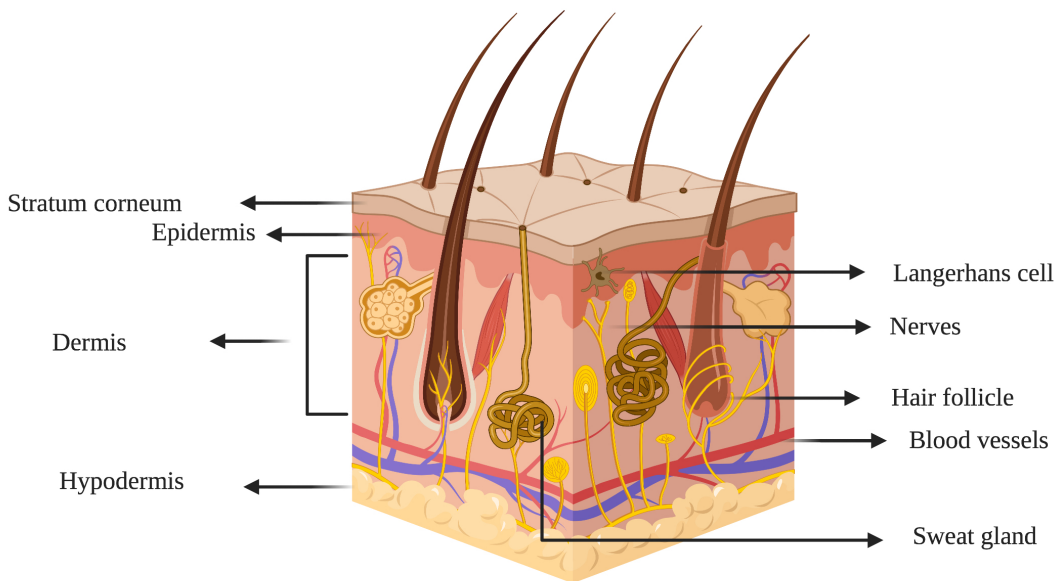
B

Figure 1.1. Illustration representing A) Possible drug delivery routes into and through the skin, image adapted from (Williams, 2003) B) Microanatomical configuration of Human skin

4

One other important characteristics of human skin is the presence of various enzymes such as alcohol dehydrogenase, aldehyde dehydrogenase, Cytochrome P-450 and carboxyl esterases. These enzymes act as a first line of defence against foreign substances by transforming and thus helping in excretion or elimination of these harmful substances. Moreover, these enzymes has been utilised in the drug delivery and various studies have exploited these enzymes as a mean for extended as well as the controlled drug release (Lau et al*.,* 2012; Mizukami et al*.,* 2017; Pyo and Maibach, 2019). Due to considerable number of cells, the skin retains a biotransformation activity equal to approximately one-third of the liver, therefore, the skin is an important organ with an elevated enzyme activity and is suitable for designing delivery of dermally controlled medications (Alkilani et al*.,* 2015).

1.3.Polymer-Drug Conjugates

1.3.1. An Overview

Since the ground-breaking efforts of Hermann Staudinger (Staudinger, 1920), polymer science has substantial impacted on humanity in numerous areas, both positively and negatively with over 400 million tons of plastics manufactured yearly world-wide since 2015. Due to rapid advances in synthetic instruments and knowledge of biomolecular composition and performance, polymer bioconjugates are seen not only in biomedical applications, but can also provide inventive concepts in other materials sciences. Different chemistries for site-specific conjugation, distinct methodologies to standardize the size, topology, distribution, and role of the polymers, alongside adjustable exploitation of bioconjugate structural design were introduced. Recent innovations in polymer bioconjugates focus on nucleic acids, proteins, lipids, carbohydrates and even living cells (Chen et al., 2009; Webber et al., 2016).

Since Ringsdorfs early work (Ringsdorf, 1975), extensive research has been reported using polymer drug conjugates as drug delivery systems (DDS) for various purposes, starting from cancer therapy and later on extending to the treatment of inflammatory, infectious and cardiovascular diseases (Larson and Ghandehari, 2012). The polymer is often used as an "inert" carrier for covalently bound drug molecules, though in some cases the polymer itself may also have some functionality in drug targeting. The benefits of drug conjugation to polymeric transporters, for instance polyethylene glycol (PEG), include improved drug solubilization, decreased immunogenicity, controlled drug release, drug targeting, extended circulation, and enhanced safety (Ekladious et al*.,* 2019).

Polymer-drug conjugates (Figure 1.2) can be regarded as polymer-based prodrugs and are often used to improve aqueous solubilization of various drugs, and consequently enhance bio-accessibility. Polymer-drug conjugate drug delivery system commonly contains a biocompatible water-soluble polymer backbone to which a hydrophobic drug moiety is linked directly or *via* a biological responsive linker ("spacer") (Kim et al*.,* 2012). The spacer is typically a 'bio-reactive' chemical bond, implicating that it undergoes dissociation in a biological setting. These bio-conditions can be in the form of chemical, *i.e.,* change in pH or the presence of enzymes such as esterases, lipases or proteases. The selection of the spacer is thus dependent on the desired site of action and the physiological conditions of the part of the body where delivery of PDC is intended (Seifu and Nath, 2019).
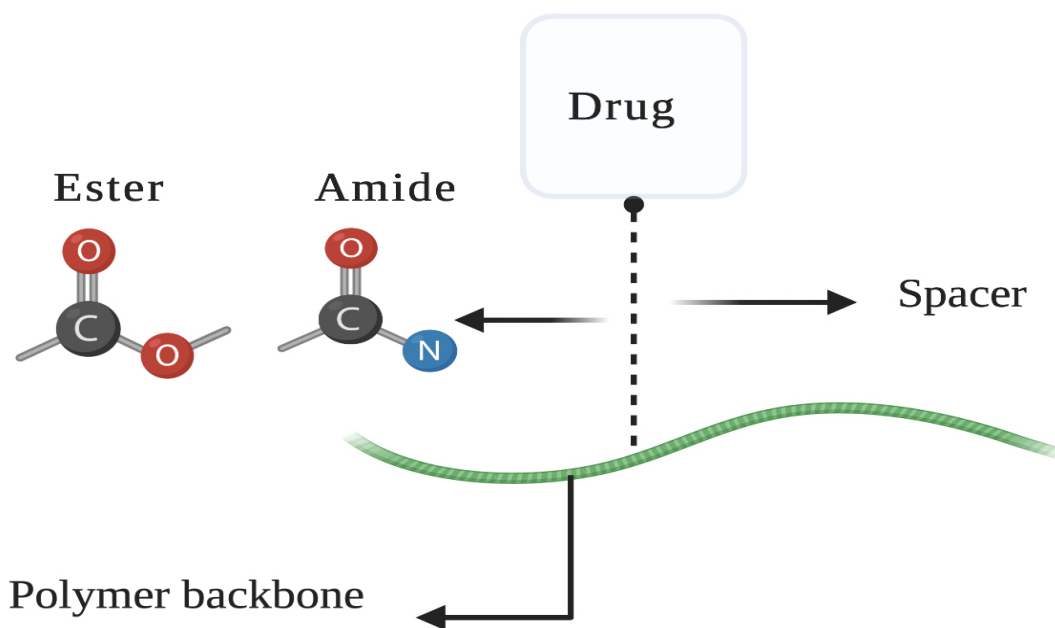
Figure 1.2. Schematic description of PDCs. Figure adapted from (Natfji et al.,2017)

On the basis of architecture, there are four common types of PDCs namely linear polymers, dendrimers, polymeric micelles and polymeric nanoparticles (Figure 1.3). Examples of linear PDCs include polyethylene glycol *e.g., N*-(2-hydroxypropyl) methacrylamide (HPMA) copolymers used in various lysosomally-cleavable PDCs *e.g.,* peptide-polymersomes

modernized with anti-EGFR antibody for systemic cancer therapy. Dendrimers are branched polymers having star like structures which provides multiple sites for drug conjugation onto their surfaces, hence increasing the chances of biological interactions. The most widely used dendrimers are poly-amidoamine (PAMAM), polypropylene imine in brain diseases, poly-aryl ether dendrimer, and biodegradable poly-lysine dendron in ocular drug delivery. Another form of the PDCs are polymeric micelles; these are amphiphilic macromolecules, that in aqueous medium form micelles. Examples includes polysorbates and sodium dodecyl sulphate, used as a permeation enhancer in transdermal drug delivery. Similarly, polymeric nanoparticles are soft colloidal structures in the range 10-1000 nm. They can be synthesised from various degradable and non-degradable polymers; examples include but are not limited to hyaluronic acid (HA) for targeting cell surface receptor CD44 and chitosan used to entrap nucleic acids (Feng and Tong, 2016; Yu et al., 2013)
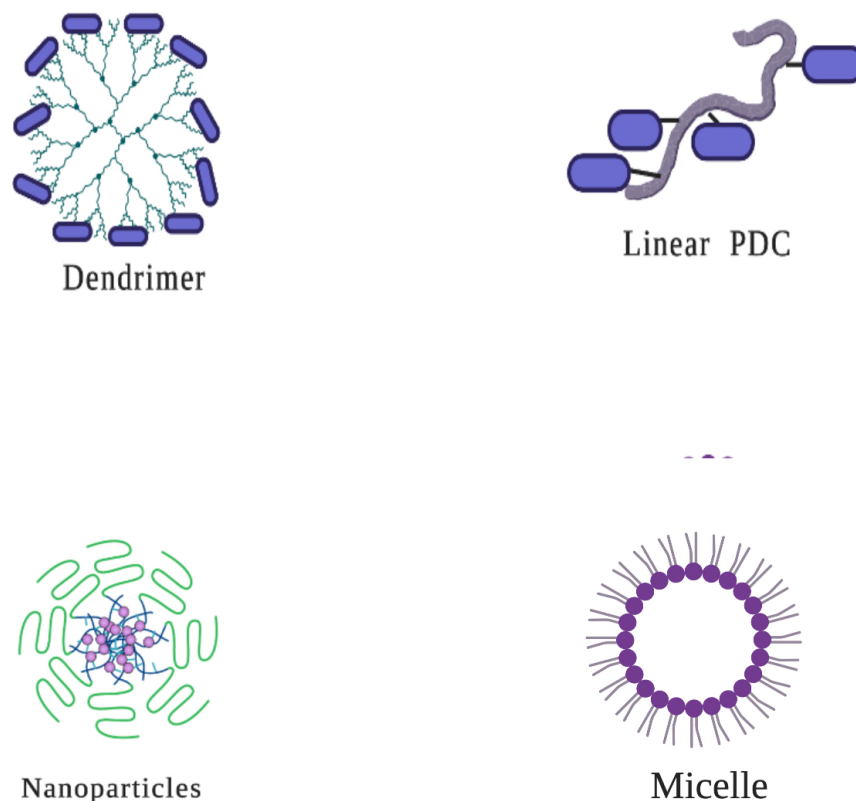
Figure 1.3. Different types of PDCs

1.3.2. Mechanism of Action of Polymer-drug Conjugates

Polymers present exceptional and multipurpose opportunities for drug delivery, and can be "bio-tailored" for therapies such as medical appliances, implants, and application of polymer-drug conjugates, whilst synthetic polymers have been used to aid delivery of therapeutic small molecule drugs the full benefits of polymer-based drug delivery has not yet been realised (Joralemon et al., 2004). Presently, effective uptake of polymeric systems by different isolated cancer cell lines persists as a major challenge, predominantly because many of the biocompatible polymers are highly hydrophilic with a neutral surface charge, and hence with low affinity to plasma membranes. To mitigate this challenge, ligand alteration and stimuli reaction site-specific moieties have been shown to and increase intracellular uptake of the

copolymer-drug conjugates, shown by utilizing HPMA-copolymer anticancer drug conjugates (Pang et al., 2016).

Recent investigations have led to dynamic release systems, which contain sustained release and site-specific targeted drug delivery. Pharmaceutical nanobiotechnology seeks to combine both the diagnosis and therapy of diseases using varied drug delivery vehicles *e.g.*, liposomes, polymeric nanoparticles, niosomes, and curative polymers as "smart," biocompatible systems (Mogoşanu et al., 2016).

For therapeutic impact, a drug must interact with or bind to its target. The bulk (60%) of drug targets are proteins stationed at the plasma membranes of various cells. In addition to plasma membrane intracellular proteins, ribosomes or DNA are other targets for delivering drugs. An ideal PDC should release the drug only at the target location. In the case where an active drug target is extracellular, then delivery is relatively easy. Where the drug target is in cytosol (intracellular) and the polymer delivery system can easily enter, then drug will be released intracellularly. However, if the conjugate does not have the ideal properties to enter a cell where the target site may reside, then drug release may be extracellular, but the drug will then need to enter the cell and diffuse to its target site. Fortunately, due to different biochemistry of the environment outside (extracellular) and inside of the cells (cytosol), designing and creation of linkage between the drug molecule and polymer that break down under particular conditions, control of the drug release site is possible (Borke et al., 2018)
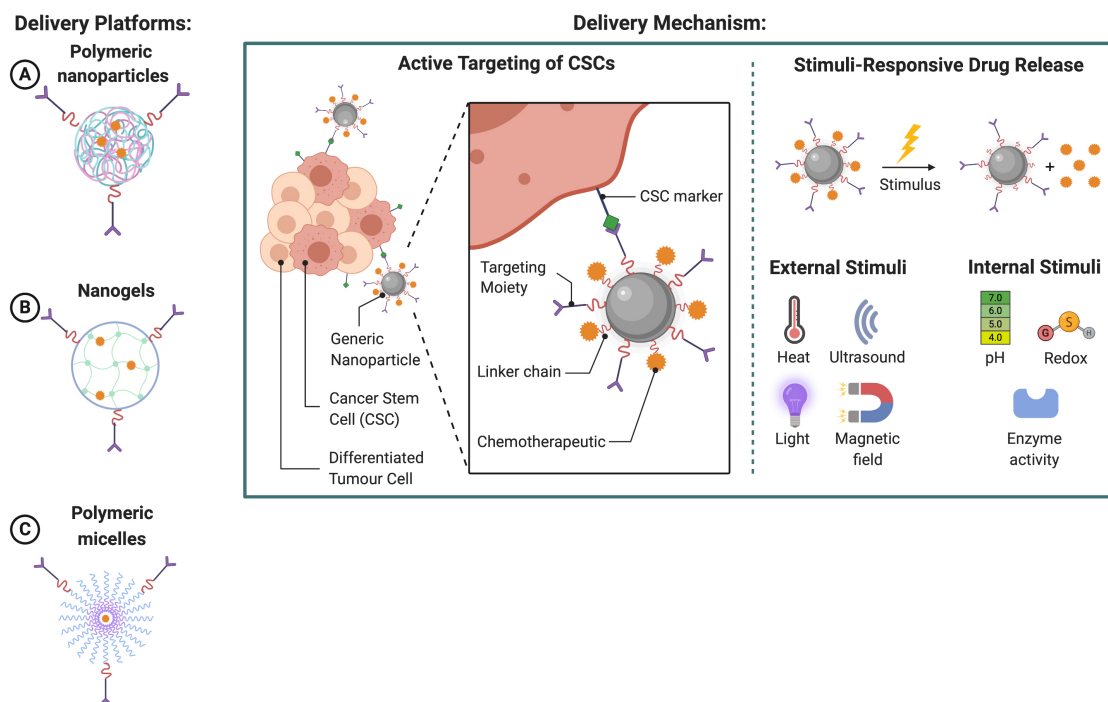
Figure 1.4. Illustration showing PDCs drug delivery mechanism to a cancer stem cell

Dependent on the pathophysiology of the target site, the design of PDCs and the mechanism of drug release can be tailored as summarised in Table 1.1.

Table 1.1. Rationale for Polymer-Drug Conjugate Design

Rationale	Mechanism of Action	Examples
Controlled and Sustained Drug Delivery	pH-dependent release	HPMA-copolymer Anticancer drug conjugates (Pang et al., 2016)
Release and Enhanced Drug Targeting	Enzyme-dependent release	Tragacanthin-tyramine conjugate (Lett et al., 2019)
	Receptor-mediated activation.	HA-Growth hormone conjugate (Yang et al., 2012)
	Tissue affinity	PEG-Adenovirus conjugate (Kim et al., 2011)
	Targeting by increase of vasculature	HPMA-Doxorubicin (Etrych et al., 2008)

Increased water solubility	Linking to a water-soluble polymer	8-Aminoquinoline-HPMA conjugate (Nan et al., 2001)
Enhanced stability and prolonged half-life ($t_{1/2}$)	Reduced renal filtration	PEG-vancomycin conjugates (Greenwald et al., 2003)
	Reduced enzymatic degradation	Sodium-carboxymethylcellulose–Bowman–Birk conjugate (Marschütz and Bernkop-Schnürch, 2000)
Combination therapy	Polymer and drug have therapeutic effects. Loading two drugs simultaneously.	Polyacetal-curcumin conjugate (Requejo-Aguilar et al., 2017) PGA-paclitaxel+ carboplatinum conjugate (Vicent and Duncan, 2006)
Localised effect	Prevention of Blood- Brain Barrier penetration	PEG-haloperidol conjugate (Natfji et al., 2020)

1.3.3. Advantages of Polymer-Drug Conjugates

PDCs offer numerous advantages over traditionally used micro and macromolecule formulations including improved solubility and stability in aqueous medium, precise (or rather more precise) delivery and an improved pharmacokinetic profile (Zhu et al., 2014). The principle difference between other polymeric systems and polymer-drug conjugates is that in the later, one or more drug molecules can be linked to a single polymer chain through a linker, a spacer or a drug may be directly attached whereas the other polymeric carrier systems only physically encapsulate the drug (Maeda et al., 2001; Pan et al., 2014; Pang et al., 2016). PDCs thus possess, and can have tailored, suitable physico-chemical properties (Figure 1.4) to:

(1) Increase in water solubility of poorly water-soluble drugs, *i.e.,* by attaching the drug to a linear polymer like PEG, which also helps in the rapid excretion of the drug from the body.

(2) Protect the drug from deactivation or degradation *e.g.,* PEG-protein conjugates.

(3) Improve in the pharmacokinetic profile of the drug, such as prolonging its circulation before elimination

(4) Decrease an immune response to a drug.

(5) Allow site-specific targeting of the drugs such as with the EPR effect for tumours.

(6) Enhance therapeutic outcomes by either attaching two drugs on the same polymer chain or where both polymer and the drug have synergistic activity.

(7) PDCs due to their unique nature are more resistant to the efflux mechanism employed by the multidrug resistance bacteria (Pang et al., 2013).

1.3.4. Synthesis and Characterisation of Polymer-Drug Conjugates

For the synthesis of PDCs, various methods are used, among which there are two most widely used routes; 1) conjugation of the polymer with the drug, 2) polymerisation of the monomer drug conjugate to form homo or copolymer, 3) Polymerizable drug. For conjugation of the polymer with the drug, different methods are used, the most common is the coupling method. This method involves the use of activating agents like N-hydroxysuccinimide esters (NHS), or carbodiimides (Hamley, 2014). Another method used for the conjugation of drugs with the polymers is the click coupling reaction (a reaction involving high grafting efficiencies) where low to medium size (molecular weight) polymers are conjugated with the drugs. Major disadvantage of this method includes relatively lower drug loading (Zolotarskaya et al., 2015). Similarly, an alternate route for the synthesis of PDCs is the polymerisation of the monomer drug conjugate with itself (homopolymer) or with another monomer (copolymer). For this purpose, various methods are used, namely, free radical polymerisation, ring-opening polymerisation, reversible addition-fragmentation chain transfer polymerisation (RAFT) reaction etc. The selection of these method depends upon the requirement, i.e. molecular weight and polydispersity index (PDI) etc. Amount of drug loaded can be controlled by the molar ratio of the feed mixture whilst the drug release can be controlled by the selection of a rational linker in between the drug and the monomer. Disadvantages of this method include uncontrollable and inconsistent side conjugation with the polymer backbone whilst the advantages include better drug loading than the conjugation of the drug to the polymer backbone (Hasirci et al., 2017; Nicolas, 2016). Similarly, third method to synthesise a PDC is the use of a polymerizable drug, for example 10-hydroxycamptothecin. The use of this strategy includes advantages like

better drug loading, whilst disadvantages include; not many drugs fit for such category, moreover, as most of these drugs are polymerised through the polycondensation route, so this chemistry does not yield high molecular weight polymers. In addition, introduction of responsive functional groups is not easy and requires complex chemistry (Feng and Tong, 2016). In order to investigate the structure and properties of the PDCs various techniques are used, few of them are NMR, FT-IR, UV, TEM, GPC and thermal analysis (Chang et al., 2012).

Conjugation to

Conjugation through

Monomer drug
conjugate

polymerization

Drug

Polymerizable drug

polycondensation
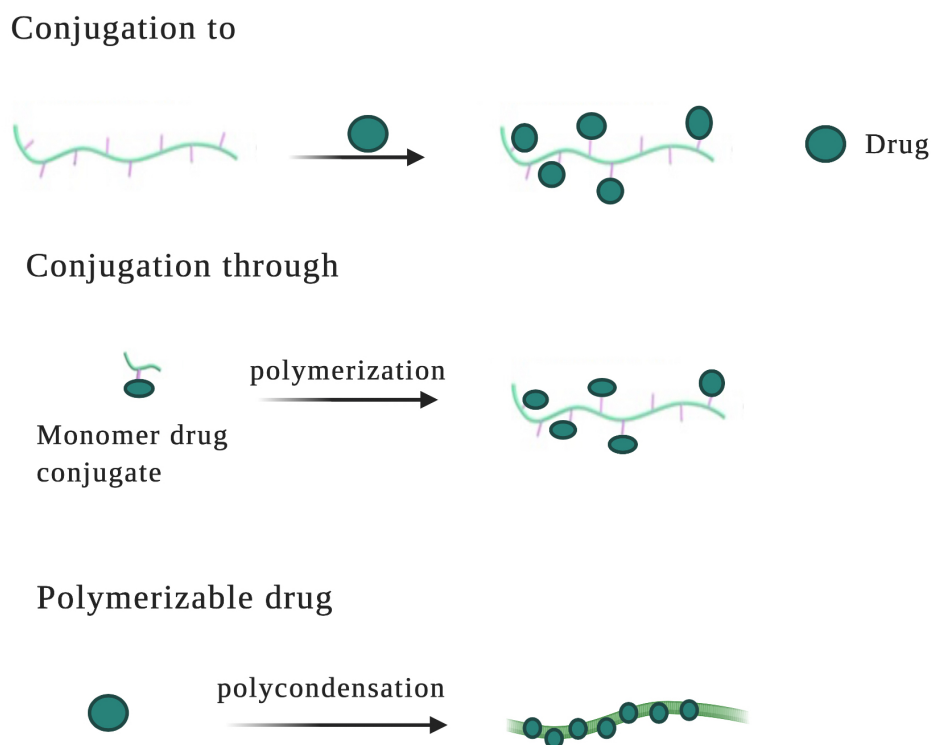
Figure 1.5. Synthetic strategies for the synthesis of PDCs. Illustration adapted from (Feng and Tong, 2016)

1.4. Applications of Polymer-Drug Conjugates for Skin Drug Delivery

Traditionally PDCs have been used in chemotherapy to optimise the drug delivery profile and reduce the adverse drug reactions (ADRs) by exploiting the EPR effect. Till now, there is only one commercial example of PDCs which is Movantik[Rx] (a PEG-Naloxol conjugate) used to treat opioid induced constipation and is given orally. Beside this, PDCs have also been used for other indications including cardiovascular diseases, nervous system diseases and endocrine system diseases *etc* mostly delivered *via* intravenous route. Here, we focus on topical

application of PDCs. This may initially appear somewhat counterintuitive as skin is a well-established effective barrier to drug delivery, and only relatively small molecular weight (typically <500 Da) and lipophilic molecules can be delivered to or through the skin to therapeutic levels. However, this is advantageous where the drug to be conjugated should remain at the skin surface and not permeate, perhaps where surface action or release at the skin surface is desired (as with insect repellents described below), or for use where the skin barrier is compromised in conditions such as psoriasis or for wound healing.

1.4.1. Polymer-Drug Conjugates in Wound Healing

Wound healing is a complicated, biochemical, molecular and cellular activity including inflammation, propagation, and movement of different cell types, resulting in tissue rebuilding and transformation as shown in Figure 1.6. This activity is accelerated or hampered by matrix production, collagen accumulation, neovascularization, re-epithelialization and formation and differentiation of various cells and the interplay with growth factors and cytokines. The prominent growth factors which are important modulators of wound healing include fibroblast growth factor (FGF), platelet-derived growth factor (PDGF), insulin-like growth factor (IGF), transforming growth factor (TGF), epidermal growth factor (EGF) and vascular endothelial growth factor (VEGF). The ultimate result of this cellular-molecular cross talk results in tissue repair that affect chemotaxis and promote mitosis of inactive cells which then lead to angiogenesis (Barrientos et al., 2008; Singer and Clark, 1999).
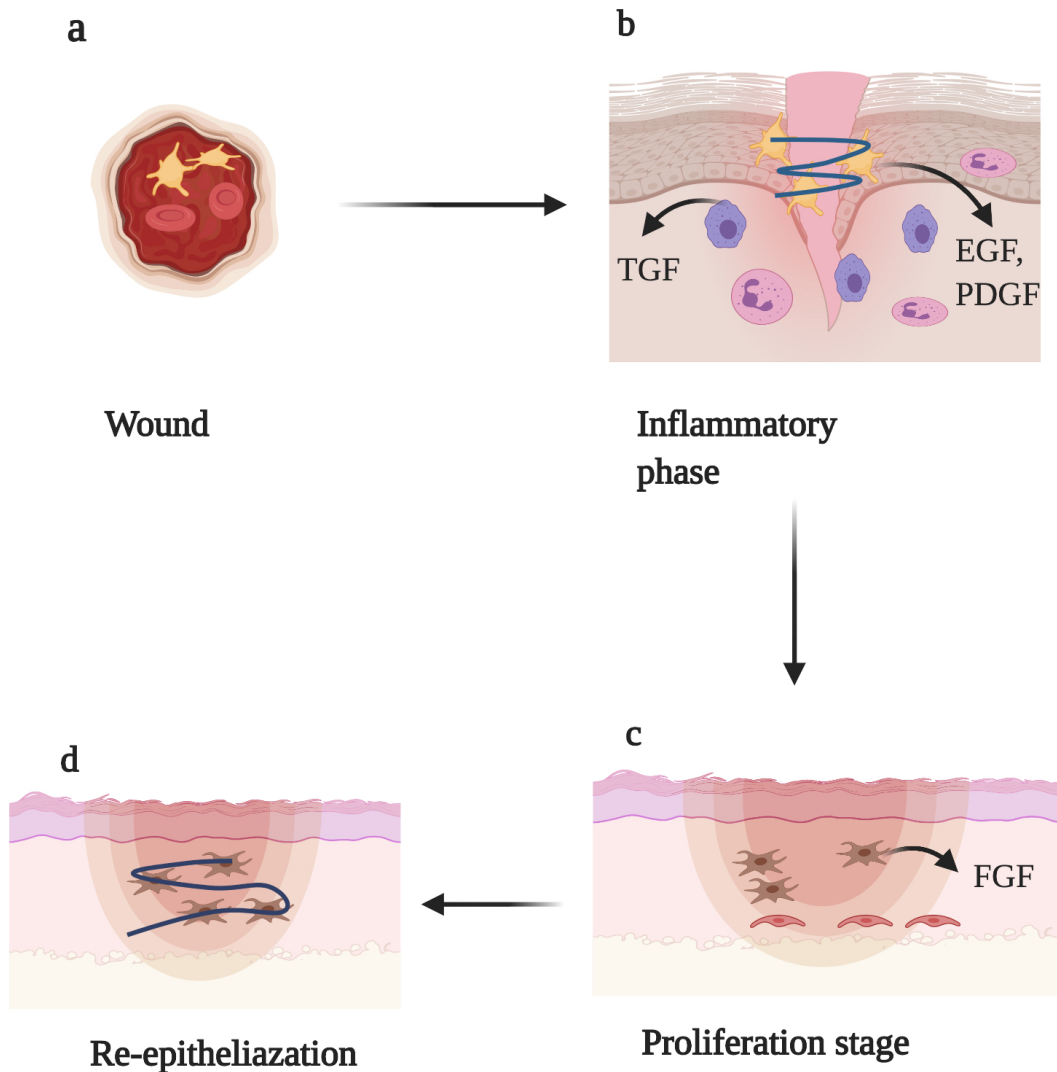
Figure 1.6. Illustration representing the wound healing process a) Beginning of homeostasis by the release of erythrocytes and platelets to form a clot, b) Activation of platelets by thrombin resulting in the release of growth factors, *i.e.* EGF, PDGF to attract neutrophils and macrophages, c) Fostered by the proangiogenic factors like FGF, there is formation of the new blood vessels and capillaries, d) Re-epithelization phase characterised by the gradual appearance of the newly formed collagen.

Wound healing is a highly synchronised process and depends on signalling pathways within the cell. Substantial progress has been made in the identification of these signalling molecules and the underlying mechanism in both the healthy and diseased states. As a result, there has been a significant interest in using these signalling pathways for better therapeutic outcomes,

i.e., healing or facilitating the healing process that may otherwise not occur naturally. An ideal drug delivery system (DDS) for wound healing would have the following characteristics:

(1) It should maintain its therapeutic activity throughout the wound bed,

(2) It must prevent rapid dilution in the wound and associated systemic uptake,

(3) It would facilitate the release of the drug within the wound at relevant therapeutic rate and duration, and

(4) It would increase the water solubility and stability of the drug (Rădulescu et al., 2016).

One approach to achieve the above is the use of PDCs.

Acidic fibroblast growth factor (aFGF), a protein that activates division in the cells of mesodermal and neuroectodermal origin, exhibits biological activity in wound healing by stimulating the proliferation of fibroblasts and promoting angiogenesis, resulting in wound healing. However, use of aFGF is limited due to its instability and short half-life. To address these problems Huang and the coworkers reported conjugation of PEG with recombinant human acid fibroblast growth factor (rhaFGF) by the site specific PEGylation of rhaFGF with mPEG-butyraldehyde (20KDa). The obtained product was purified by using Sephadex-G 25-gel filtration. *In vivo* immunogenecity was significantly decreased whilst the *in vivo* half life was significantly elongated, due to which wound healing was much quicker when BALB/c mice were treated with PEGylated rhaFGF as compared with the treatment alone with rhaFGF (Huang et al., 2011). It was concluded that this was due to the better thermal activity at physiological temperature and an improvement in half-life as seen by other researchers (Papanas and Maltezos, 2007).
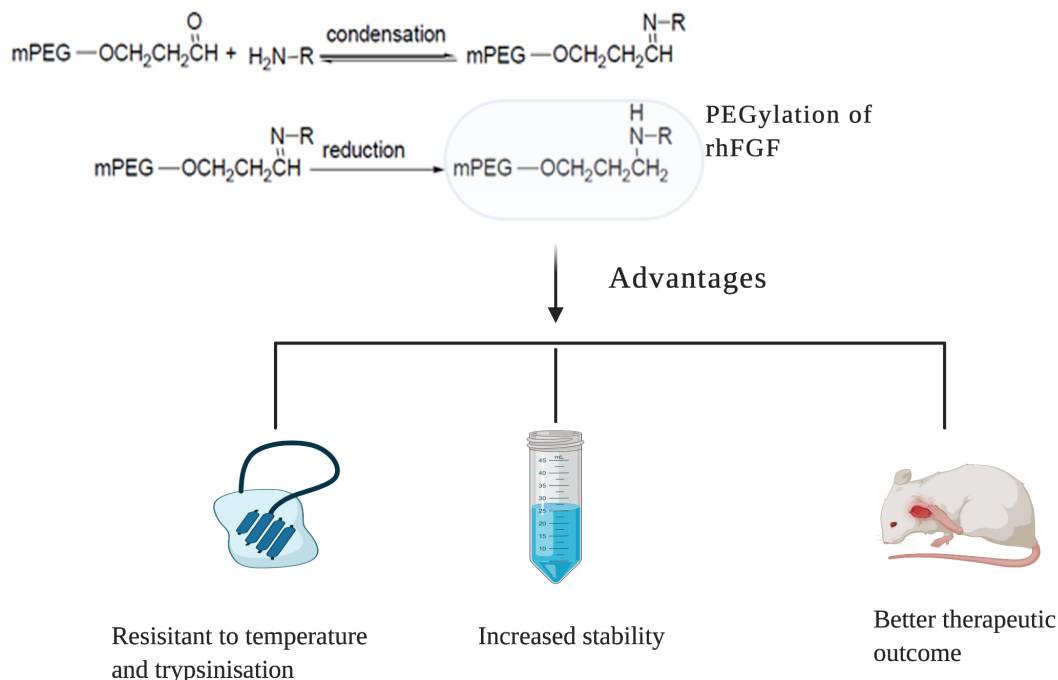
Figure 1.7. Illustration showing the synthesis and the advantages of the PEGylated rhFGF

In another study Choi et al. (2012) reported the successful conjugation of low-molecular weight protamine (LMWP) with recombinant epidermal growth factor (rEGF) to form a rLMWP-EGF conjugate. Conjugation was achieved by linking a highly positive charged protamine molecule to the n-terminal of EGF and was used to treat diabetic and burn wounds. In both cases, *in vitro* results showed well-preserved cell proliferation activity of the conjugate. Moreover, after the application of this conjugate onto the skin of BALB/c mice, the *in vivo* results showed that as compared to controls, *i.e.* EGF alone, the physical mixture of EGF and LMWP and the conjugate itself. The results (Figure 1.9) showed that the conjugate permeability into the mice skin was 11 times higher than the free protamine and was responsible for the quicker wound closure. These experiments suggest that topically applied conjugate of protamine with EGF (rLMWP-EGF) has the potential to be used in diabetic wounds as shown in Figure 1.9 b and c.
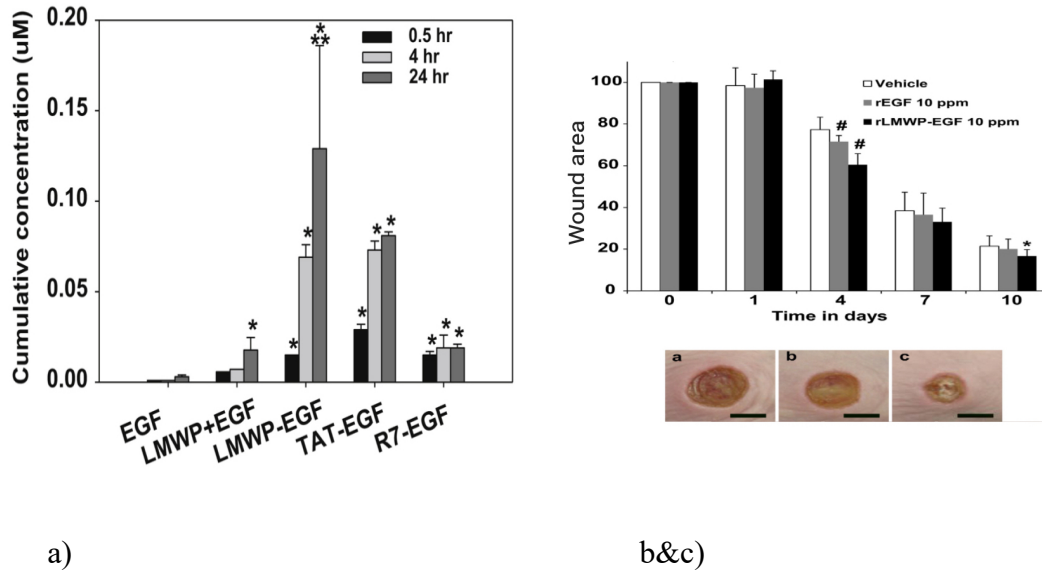
Fig 1.8. ***In vitro*** **permeation through the artificial skin constructs. (a) Time-course of cumulative concentrations of epidermal growth factor (EGF) and EGF covalently conjugated with low-molecular-weight protamine (LMWP), transactivating transcription activator (TAT), and oligo-arginine (R7). Effect of epidermal growth factor (rEGF) or low-molecular-weight protamine (LMWP) conjugated EGF (rLMWP-EGF) on wound area reduction in the full thickness model. (b) Percentages of wound area were measured for 10 days. (c) Lower panels provide typical wound images. The data are plotted as mean ± standard deviation (*n* = 4). *p < 0.05 *vs.* EGF. **p < 0.05 *vs.* TAT-EGF (Choi et al., 2012).**

In an alternative wound repair model, Requejo-Aguila et al. (2017) applied PDCs for spinal cord injury (SCI); curcumin, a natural anti-inflammatory, was conjugated to polyacetal (PA) in order to increase its water solubility and stability and provide controlled release of the drug. *In vitro* studies showed pH-dependent release of the drug, *i.e.,* curcumin with increasing release at acidic pH. *In vivo* studies using Sprague Dawley rats revealed that a single administration of the conjugate produced a significant increase in motor activity due to the various factors among which top of the list is the elongation of the axon due to the inhibition of Rho kinase enzyme. Other factors included a decreased volume of cavitation, decreased astrogliosis (glial scar formation) and increased number of neurons fibres after the injury as compared to controls or PA as shown in Figure 1.10. Notably, the conjugate treatment offered a neuroprotective effect supplemented by reduced levels of apoptosis and inflammation. The

combined therapy of PA-curcumin and ependymal progenitor (epSCi) improved functional recovery from chronic spinal injury, with a notable reduction in scar area.
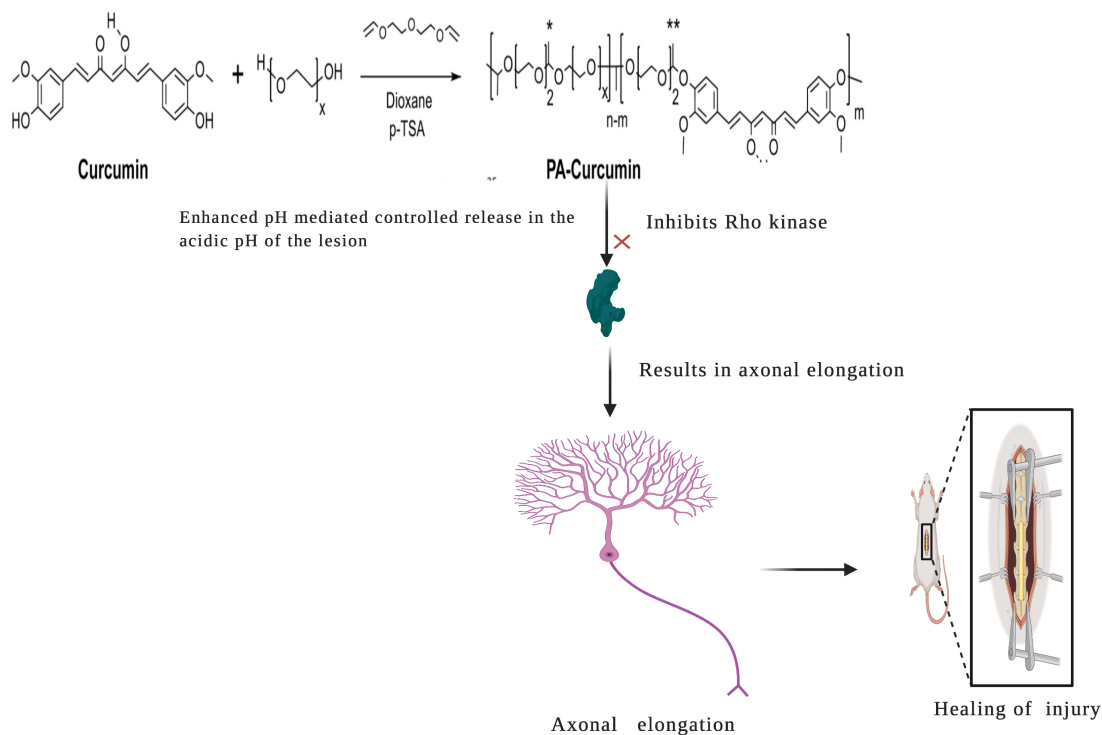
Figure 1.9. Illustration showing the synthesis PA-Curcumin conjugate, and the mechanism by which the PDC heals the spinal wound

Hatanaka et al. (2019) assessed biocompatible polymeric nanosheets for topical and transdermal drug delivery by using two-dimensional nanostructures. Their sheets properties included high transparency, elasticity, and glueyness. Betamethasone valerate (BV) was used as a model drug conjugated to poly (L-lactic acid) or poly (lactic-co-glycolic) acid. Films were constructed by a spin-coating-assisted layer-by-layer technique utilizing a water-soluble sacrificial tissue/membrane. These fabricated formulations had higher incorporation and release of BV as compared to a commercial ointment and controlled-release membranes enabled application to any area of skin for an extended period. The auditors reported that this bio-friendly polymeric nanosheet preparation offers a novel and encouraging topical and transdermal drug delivery system for pharmaceutical or cosmetic uses including the usage as a dressing for the wounds.

1.4.2. Topical Conjugates for Local Anaesthetics

Pain management, whether acute or chronic, is a substantial clinical challenge requiring both pharmacological and behavioural (*e.g.* cognitive behavioural therapy) interventions. Local anaesthetics disrupt neural transmission by preventing the influx of sodium ions via ionophores inside neuronal tissues and are commonly applied to manage post-surgical pain and for acute and chronic pain therapy. A range of methodologies are presently applied to extend the duration of local anaesthetics, but long term sustained neuronal obstruction (*e.g.* for >24 hrs) remains elusive. Whilst local anaesthetics have been extensively used in clinical practice, due to their toxicity and short half-lives their benefits are limited and hence are the target of multiple research groups attempts to develop innovative drug delivery systems such as microparticles, liposomes, niosomes and nanoparticles (Becker and Reed, 2012).

Hyaluronic acid (HA) is a non-immunogenic polysaccharide naturally found in valves of heart, vitreous humour of the eyes, synovial fluid and extracellular matrix. Due to its biodegradability, bio-similarity and viscoelastic traits, HA has been extensively used in numerous therapeutic products (Abduljabbar and Basendwh, 2016). One of the important drugs used as anaesthetic is bupivacaine (BUP), but its usage has got limitations due to its short duration of action. As discussed in Table 1.1, one of the major advantages of the PDCs is the increased half-life of the drug. Thus, by keeping this into consideration Gianolio et al. (2005) conjugated BUP to the HA derivative, Hylan B particles; *in vitro* BUP drug release was extended to ~100 hours from HA-BUP particles, substantially higher than that of free BUP showing approximately 5 hours (Figure 1.10). This translated to extended *in vivo* efficacy where HA-BUP demonstrated a twenty-fold lengthier block time in weakening motor nerve functions, as compared to free BUP.
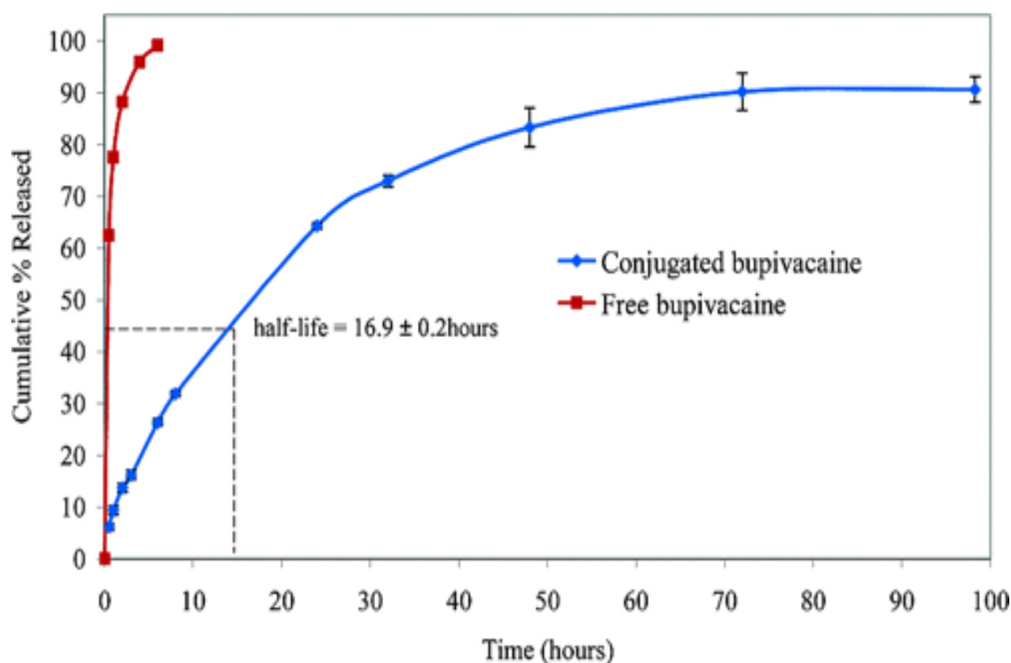
Figure 1.10. Figure showing the cumulative release of BUV from the PDC over the period of time (Gianolio et al., 2005)

Polylactic acid (PLA) polymerized from lactic acid is a multipurpose material, primarily utilized for biodegradable goods such as plastic bags and containers. PLA was conjugated to bupivacaine (BUP) and was used as a delivery system to lengthen percutaneous response of superficial neurons. Another anesthetic lidocaine (LID) was coated onto poly-L-lactide-polylactic acid (PLLA) microneedle arrays. Dip-coating permitted LID to only cover the needle tips and substantially decreased painkiller loss, so this drug delivery system prolonged the duration of anesthesia (Baek et al., 2017).

Among the recombinant proteins, polypeptides are engineered genetically from various cell types. Covalent bonding of the peptide and drug *via* a cleavable linker produces peptide-drug conjugates which have been evaluated as drug delivery system. Among these systems, transcriptional trans-activator peptide (TAT), is a well-established peptide. Wang et al. (2013) produced a liposomal formulation using lidocaine loaded TAT-peptide-conjugates for transdermal delivery of the lidocaine. The formulation was tested for its stability and encapsulation efficacy, showing better stability and encapsulation efficacy ($80.05 \pm 2.64\%$) as compared to the conventional liposomal formulation (CLs). *In vivo* experiments using BALB/c

mouse skin penetration of the fluorescent dye calcein (also called as fluorexon) encapsulated in liposomes and TAT-conjugated liposomes delivery vehicles showed that the conjugated formulation had improved skin permeation, *i.e.* 4.17 and 1.75 times higher than the LID solution and LID-CLs (shown in Figure 1.11) as well as the stability in the mouse model. This better permeability profile can be attributed to the TAT, as it is a well-known cell-penetrating peptide that can increase the skin delivery of drugs.
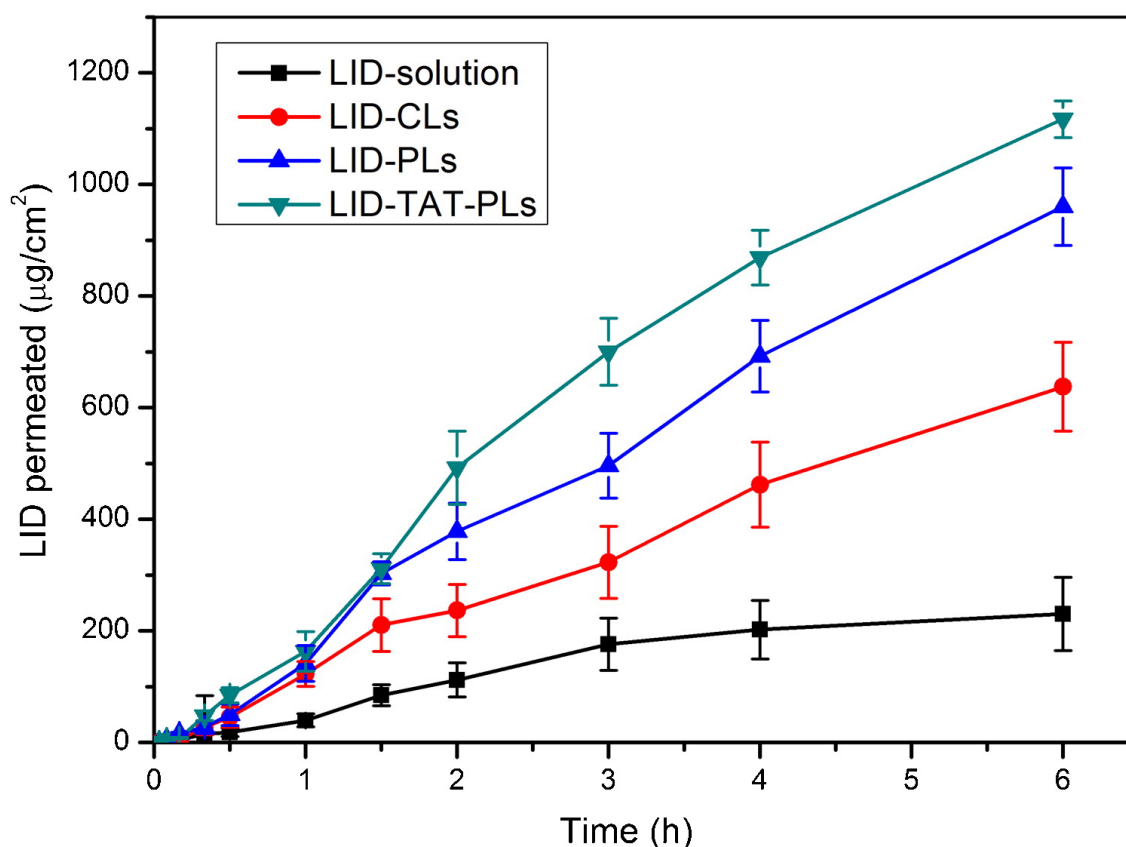
Figure 1.11. Figure showing the permeation profile of the Lidocaine from the PDC (Wang et al., 2013)

Leu-enkephalin (LENK) is an endogenous opioid peptide neurotransmitter with an amino acid sequence of Tyr-Gly-Gly-Phe-Leu. It is naturally occurring in the brains of several organisms, including humans and has been identified as a promising painkiller. It is considered as a strong anaesthetic attributed to its strong affinity towards the δ -opoid receptors, however, its utilization is restricted due to its instability in the plasma and transport across the BBB. In order to address these problems, Feng et al. (2019) conjugated LENK with squalene assembling the conjugate to form nanoparticles. *In vivo* studies using rats with carrageenan-stimulated paw

oedema resulting in hyperalgesia (extreme sensitivity to pain) to mimic human pain evaluated the therapeutic activity of the formulation. The anti-hyperalgesic impact of LENK-SQ nanoparticles was twice as long as that of morphine. Fluorescent images showed the biodistribution of the formulation in the rat model paw oedema where, in contrast to LENK alone, the majority of the conjugate was observed at the site of application, *i.e.,* is an inflamed paw, with relatively little accumulation within the rat's brain so overcoming the problems linked with the use of the peptide (LENK) only.
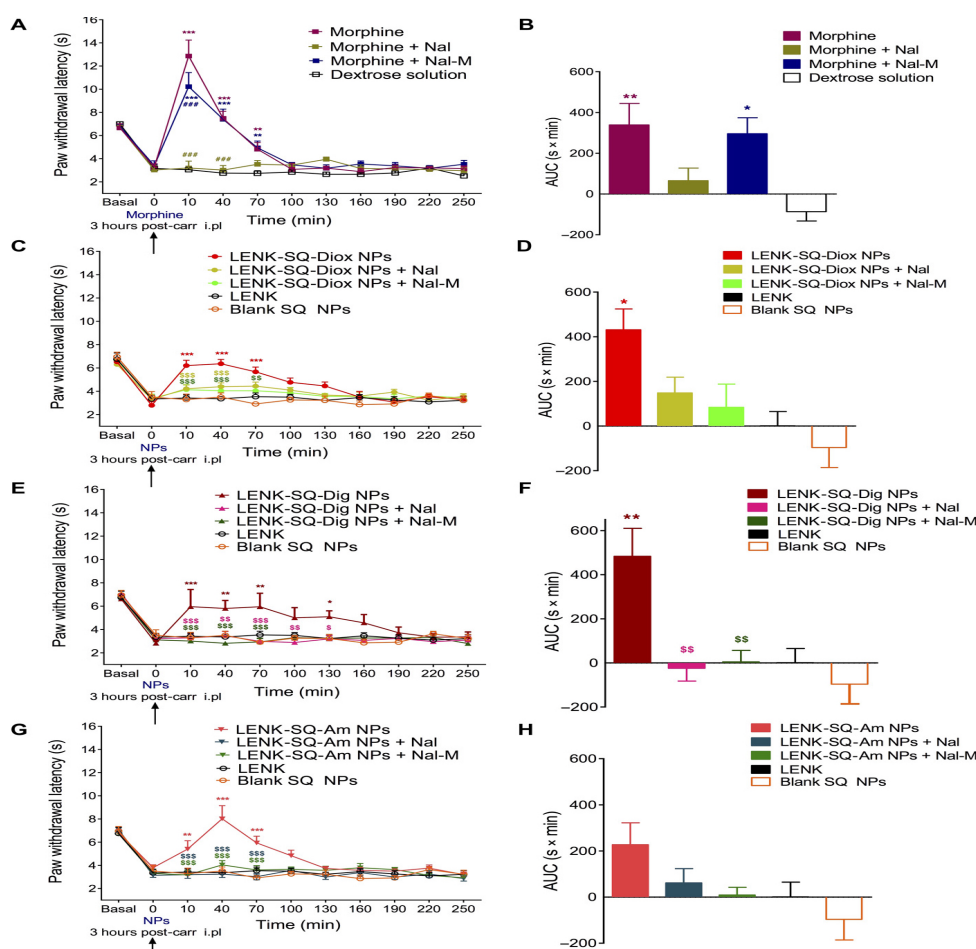
Figure 1.12. Antihyperalgesic effects of acute treatment with morphine (A and B), LENK-SQ-Diox NPs (C and D), LENK-SQ-Dig NPs (E and F), and LENK-SQ-Am NPs (G and H) in λ-carrageenan–induced inflammatory pain injected rats. Administration of morphine, LENK-SQ NPs, Nal, Nal-M, LENK, blank SQ NPs, or dextrose solution (vehicle) was performed (arrows, 0 on abscissa) 3 hours after λ-carrageenan injection into the right hind paw. Morphine (A), LENK-SQ-Diox NPs (C), LENK-SQ-Dig NPs (E), and LENK-SQ-Am NPs (G) induced an increase in PWL (in seconds, means ± SEM of

independent determinations in five to nine animals per group) in the Hargreaves test. *P* < 0.05, **P* < 0.01, ***P* < 0.001, compared to dextrose solution or LENK solution; ###*P* < 0.001, compared to morphine; $*P* < 0.05, $$*P* < 0.01, $$$*P* < 0.001, compared to LENK-SQ NPs. Two-way analysis of variance (ANOVA) with repeated measures, Bonferroni post-test. Nal or Nal-M was administered 15 min before morphine or LENK-SQ NP injection. Basal on abscissa: Control (naïve) rats (before λ-carrageenan injection). (B, D, F, and H) Bars are the means ± SEM of AUCs (seconds × minutes) of the cumulative durations derived from the time course changes (A, C, E, and G) in PWL after the various treatments. *P* < 0.05, **P* < 0.01, ***P* < 0.001, one-way ANOVA, Tukey post-test, compared to dextrose (vehicle) or LENK solution; $*P* < 0.05, $$*P* < 0.01, $$$*P* < 0.001, compared to LENK-SQ NPs (Feng et al., 2019).
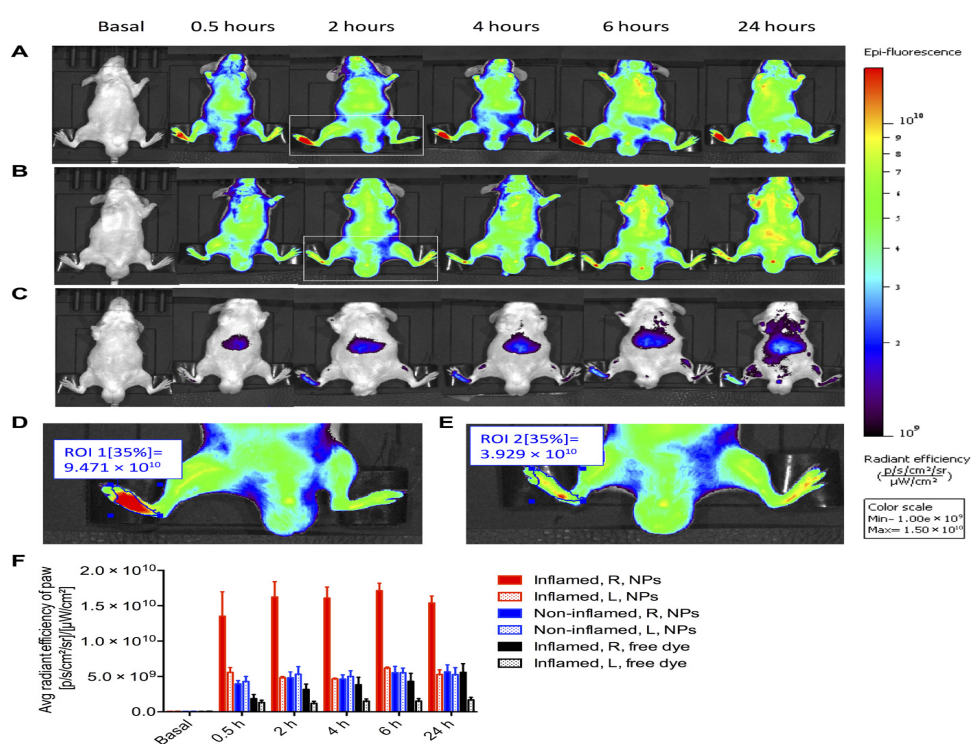
Figure 1.13. (A) Biodistribution of fluorescent LENK-SQ-Am NPs in mice with inflamed right hind paw. (B) Biodistribution of fluorescent LENK-SQ-Am NPs in mice with non-inflamed hind paw (saline injected only into the right hind paw). (C) Biodistribution of free dye in mice with inflamed right paw. (D) Zoom of group A at 2 hours. (E) Zoom of group B at 2 hours. (F) Quantitative analysis of the paws with the same region of interest (ROI). R, right hind paw; L, left hind paw (Feng et al., 2019).

1.4.3. Polymer-Drug Conjugates for the Treatment of Psoriasis

Psoriasis (Greek *psōriasis*, from *psōra* 'itch' and *psōrian* 'have an itch') is an inflammatory chronic illness facilitated by the immune system with a primarily cutaneous contribution. Psoriasis is a lifelong autoimmune disease exemplified by patches of abnormal skin. Affected sites are normally red, purple on certain individuals with darker skin, itchy, dry, and encrusted. Psoriasis coverage varies from discrete patches to full body coverage. Clinical phenotypes of psoriasis are described by the appearances of the disease, patient age at disease commencement, degree of coverage and morphology (Raychaudhuri et al., 2014). Plaque psoriasis is the most common form of psoriasis which has encrusted (scaly) skin, erythematous plaques, and inflammatory cell infiltration (Nestle et al., 2009). It also affects nails, skin and joints, is a persistent, agonizing, disfiguring and immobilizing noncommunicable disease (NCD) for which there is no appropriate remedy. It adversely effects the quality of living, most common among 49-69 years old with a registered prevalence rate of 0.09% to 11.4% in the world, making it a significant health concern (Rendon and Schäkel, 2019; WHO, 2016).

Common first line therapy for psoriasis uses corticosteroids but as the condition resolves and the stratum corneum barrier reforms, then decreasing amounts of the drug are delivered at the target site. Retention of corticosteroids within the epidermis can manage skin inflammation, erythema and scaling linked with psoriasis, whilst preventing potential side effects associated with oral delivery. Dolz-Pérez et al. (2020) used both *in vitro* and *ex vivo* assays to show that a poly-L-glutamic acid (PGA)-fluocinolone acetonide (FLUO) conjugate (PGA-FLUO) suppressed pro-inflammatory cytokine (TNF-α, IL-1β, IL-6, IL-10) released by the leukocytes, suggesting this system for the treatment of psoriasis. Furthermore, PGA-FLUO was shown as a reservoir within the epidermis by employing *ex vivo* human skin permeation studies with confocal microscopy; negligible conjugate was seen in the dermis, suggesting a reduced likelihood of FLUO entering the systemic blood circulation. PGA-FLUO applied within a hyaluronic acid (HA)-poly-L-glutamate cross polymer (HA-CP) vehicle successfully decreased psoriasis-linked phenotypes in an *in vivo* mouse model of human psoriasis with minimum pro-inflammatory cytokines in body tissue and blood serum. Together, the results show that the conjugate combined with a HA-CP penetration enhancer could be an effective topical therapy for psoriasis.
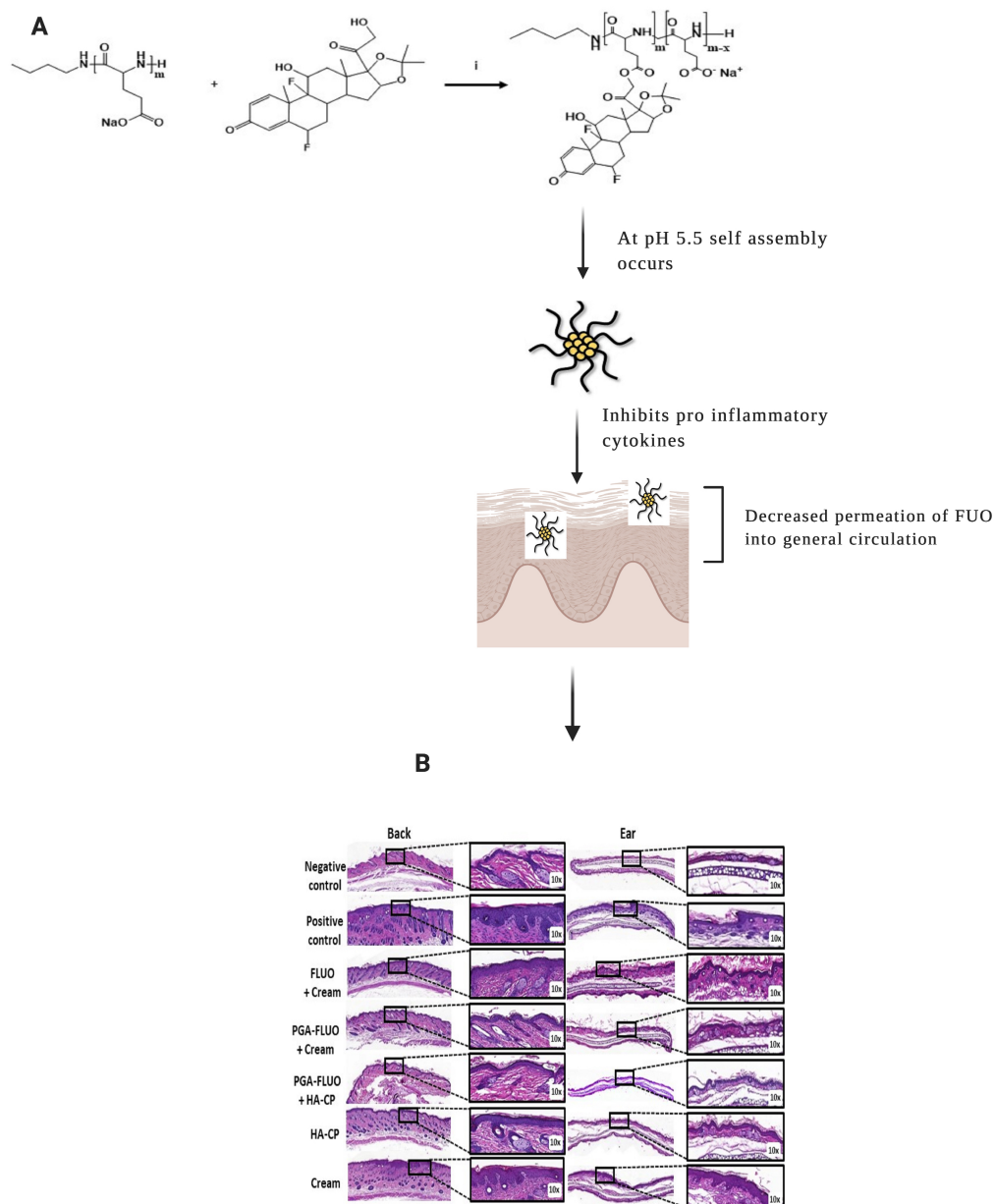
Figure 1.14. A) Illustration showing the synthesis and the permeation of the PDC, B) Histological analysis of mouse tissues after five days of anti-psoriatic treatment in an IMQ-induced skin inflammation model. The images demonstrate a marked reduction of the epidermal thickening in the group treated with PGA-FLUO compared to free FLUO. One representative picture is shown for each treatment regimen (Dolz-Pérez et al., 2020)

Topical anti-inflammatory medications with inadequate percutaneous penetration is a major reason restricting their use in psoriatic skin. Although curcumin has demonstrated effectiveness in the treatment of psoriasis, its permeation through the stratum corneum remains a main

obstacle to transdermal delivery. Mao et al. (2017) used skin-permeating nanoparticles to enable delivery of curcumin to the lower skin layers. Polymeric nanoparticles were synthesized from an innovative amphiphilic polymer called RRR-α-tocopheryl succinate-grafted-ε-poly lysine conjugates with a diameter of 25.45 nm and a positive Zeta potential of 19.65 mV. The particles were evaluated in mouse skin *in vivo,* (it should be noted that mouse skin is a relatively poor and fragile model of human skin). Curcumin was effectively encapsulated in the polymeric nanoparticles with an encapsulating efficiency of 78.45%. To prolongation retention of the curcumin-nanoparticles (CUR-NPs) in skin, silk fibroin was applied as a hydrogel-based matrix which, *in vitro,* demonstrated slower release of curcumin than the plain CUR-gel, with no alteration in the skin penetration ability of CUR-NPs. *In vivo* experiments on psoriatic mice showed that the CUR-NPs-gel displayed a better therapeutic outcome than CUR-NPs alone as the former enhanced skin permeation resulting in successful anti-keratinization activity. Interestingly, CUR-NPs-gel also prevented the appearance of pro-inflammatory and inflammatory cytokines particularly TNF-α, NF-κB, IL-10 and IL-6 to a greater extent than the CUR-NP's alone.
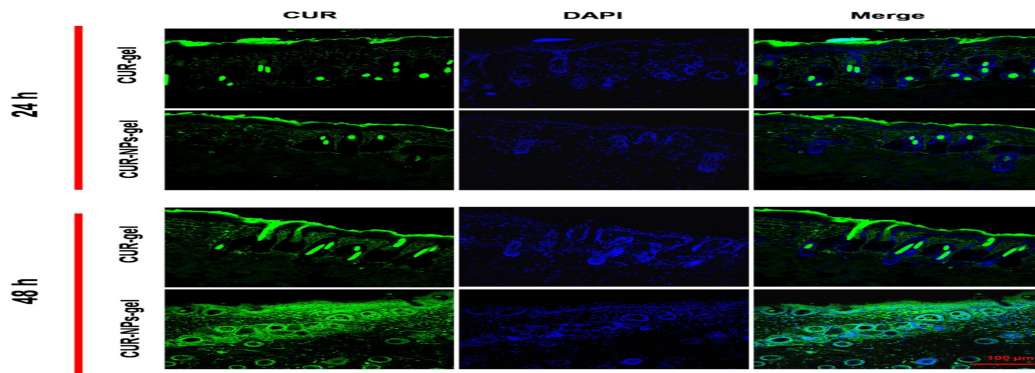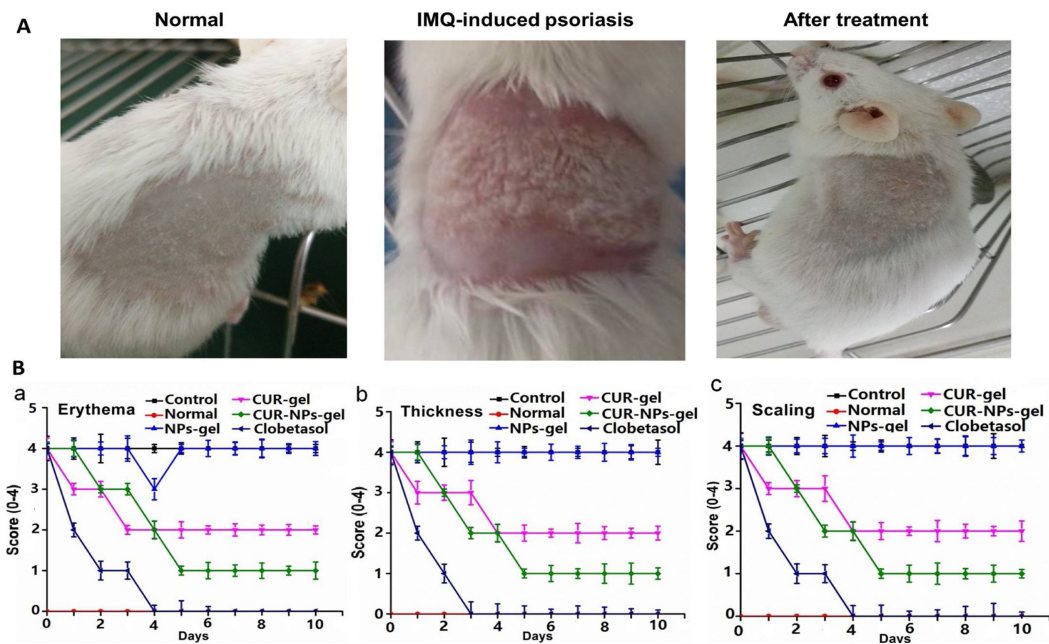
Figure 1.15. Permeation of nanoparticles in mice skin at 24 h and 48 h. Original magnification: 20×. (A) Mice skins on the back were exposed to the IMQ suspension for 8 days (IMQ exposure alters keratinocyte proliferation and differentiation), **(B)** PASI scoring of psoriatic skin after treatment with various formulations: **(a)** Erythema, **(b)** thickness and **(c)** scaling of the back skins. The score is presented (Mean ± SD, n = 12) (Mao et al., 2017).

Antibodies such as TNF-α–Ab are potent therapeutics for the treatment of psoriasis. Three immuno-biological drugs are used to target tumour necrosis factor (TNF-α), with etanercept, adalimumab and infliximab authorized to treat mild-to-serious cutaneous psoriasis. These biologics are delivered by intravenous infusion or subcutaneous injection but are expensive with potential for side effects. The key challenge for topical delivery of TNF-α–Ab is their poor penetration into and permeation through the stratum corneum (Carrasquillo et al., 2020). Korkmaz et al. (2016) used the approach of combining TNF-α–Ab conjugated to hyaluronic acid (HA) with tip loaded dissolvable microneedle arrays (TL-dMNAs) for local application, *i.e.* into the skin. The results showed that: (1) TL-dMNAs can be effectively moulded to incorporate anti-TNF-α-Ab-HA at the tip of the microneedles whilst maintaining the required biological activity for antibody ligand binding; (2) Anti-TNF-α-Ab-HA can be efficiently distributed into human skin using TL-dMNAs; and (3) polymer conjugation successfully prevented antibody diffusion from the delivery locus. Taken together, these outcomes

encourage the development of microneedle array–based delivery system of varying polymer-antibody conjugates for the treatment of psoriasis.
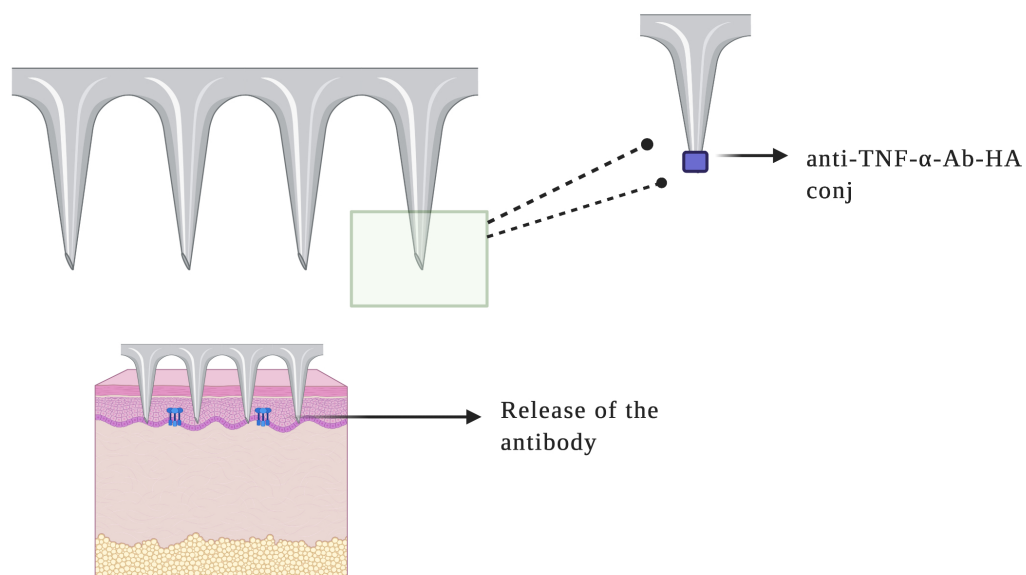
Figure 1.16. Illustration showing the use of microneedles coated with the conjugated polymer in the skin

Tretinoin, also called as all-trans retinoic acid (ATRA), a metabolite of vitamin A is used to treat acute promyelocytic leukaemia and skin disorders such as psoriasis. ATRA is used in the form of creams or emulsions, delivering the drug as a single bolus which is immediately taken up by the skin and contributes to the side effects such as skin irritation and hair loss. To address these problems Castleberry et al. (2017) synthesised a polymer-drug conjugate by conjugating ATRA with a hydrophilic polymer, namely polyvinyl alcohol (PVA), through an ester bond. This resulted in the formation of amphiphilic nanoparticles which were water soluble. *In vitro* drug release studies using pig skin showed that the ATRA from the conjugate was within the skin for up to 10 days, thus providing a sustained drug release (as compared to single bolus). Moreover, *in vivo* results showed that the conjugate formulation reduced inflammation at the site of inflammation as compared to the free drug and ensured retention of the drug at the site of application at detectable concentrations for up to 6 days.
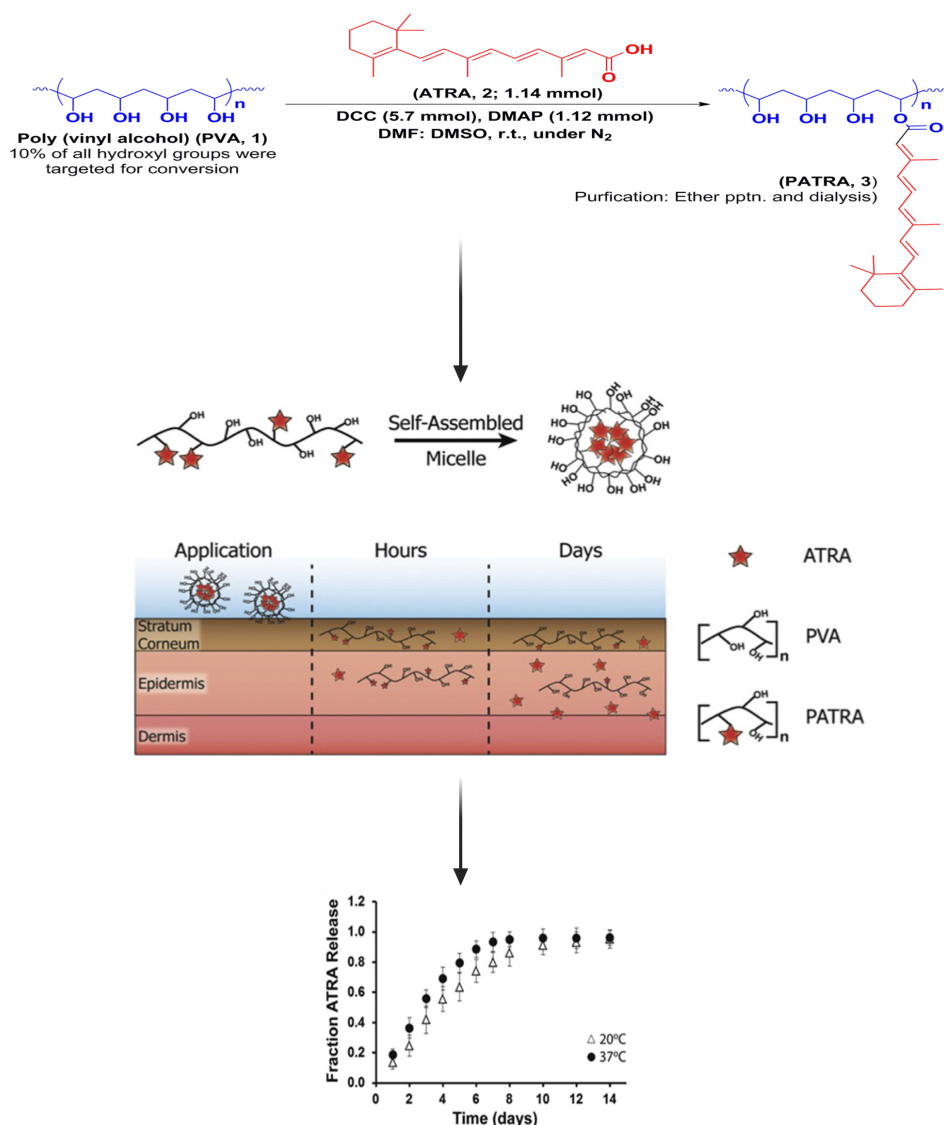
Figure 1.17. Figure showing the synthesis and the release profile of ATRA from the PDC (Castleberry et al., 2017)

Mycophenolic acid (MPA) is a potent anti-proliferative and immunosuppressant agent with anti-psoriatic action and is usually applied as a component of triple therapy involving a calcineurin inhibitor (ciclosporin) and prednisolone. Use of MPA for therapeutic purposes is restricted due to its poor oral bioavailability, and low aqueous solubility (Kelly and Butch, 2012). Supasena et al. (2020) reported conjugation of poloxamer 407 (P407) and MPA *via* an ester linkage resulting in a P407-MPA conjugate and was studied for micellization, particle size, size distribution, and antipsoriatic activity. ^{1}H-NMR implied that polymeric micelles formed from the P407-MPA conjugate showing its polyethylene oxide chain to the aqueous

environment while restricting the conjugated MPA within the inner core. Surprisingly, the conjugate had over 12-fold lower critical micelle concentration (CMC) compared to the polymer alone, *i.e.* P407. The conjugate showed an enzyme-dependent sustained-release and improved antiproliferation activity in an *in vitro* psoriasis model, *i.e.* tumour necrosis factor-α-induced HaCaT cells.

PDCs have also been evaluated for combination therapy. Mielanczyk et al. (2020) conjugated two hydrophobic anti-psoriatic agents, namely methotrexate (MTX) and acitretin (AC), with *N,N*-dimethylaminoethyl methacrylate (DMAEMA) repeating units in the polymethacrylic chains. These positively charged (+5 to +10 mV) nano- and microparticles were assessed for cytotoxicity *in vitro* using MTT and Annexin-V apoptosis assays on NHDF, Me45, HaCaT and BEAS-2B cell lines. The conjugates showed a novel cytostatic effect in Me45 cells and a pro-apoptotic effect in HaCaT cells. Epithelial BEAS-2B cells were the most sensitive to the polymer conjugates and gave responses *via* initiation of necrosis. Moreover, using an animal skin *in vitro* assay showed reduced side effects from these conjugates. Similarly, histopathological tests confirmed absence of irritation of the animal skin following dosing with these conjugates.

1.4.4. Polymer-Drug Conjugates for Treating Skin Infections

The increasing worldwide prevalence of bacterial infections, principally in persistent wounds, is an urgent priority and one in which novel treatments could be highly impactful. To this end, Shepherd et al. (2011) established a method where hyperbranched poly-(NIPAM) polymers were conjugated with the antibiotics Polymyxin-B and Vancomycin and were tested against bacteria in solution culture. Interestingly, attachment of bacteria to the polymers was reported which triggered conformational modification including disintegration of the polymer backbone and the establishment of polymer/bacteria complexes which upon removal also removed the attached bacteria and hence significantly reducing the bacterial load in the culture. The novel polymer was also evaluated using a "human burn" tissue engineered skin model infected with Gram-negative *Pseudomonas aeruginosa* and Gram-positive *Staphylococcus aureus;* significant decreases in the bacterial load was detected following use of the hyperbranched polymer in the form of polymer gel solution or hydrogel membrane.
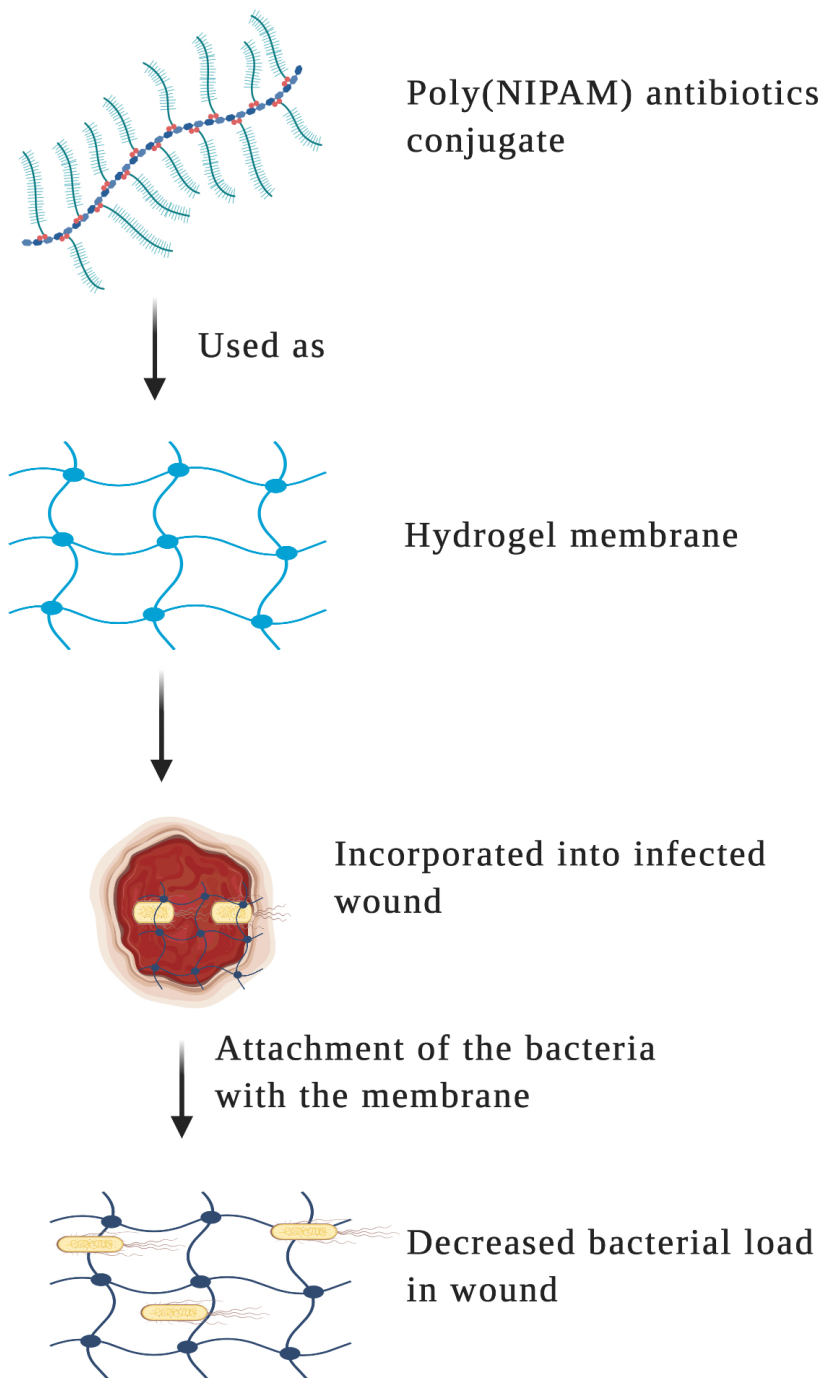
Figure 1.18. Illustration showing the use of a hydrogel membrane (made up of Poly(NIPAM)-Amb conjugate) onto the infected wound

Poly(N-isopropylacrylamide) (PNIPAM) is an extensively used temperature-reactive polymer produced originally in 1950s and is currently manufactured from industrially produced N-isopropylacrylamide. Swift et al. (2019) showed that highly branched poly-(*N*-isopropylacrylamide) (HB-PNIPAM), with a chain having solvato-chromic (different colours due to a solute when that solute is dissolved in dissimilar solvents) dye Nile red (or Nile blue

oxazone), might offer a fluorescence indicator when end groups attach to a bacterium and consequently chain sections isolate. In this drug-polymer conjugate, vancomycin was attached to HB-PNIPAM chain ends or as suspended groups on linear polymers individually having Nile red or Nile blue oxazone. Analysis of both the fluorescence and calorimetric results revealed that branched polymers responded to attachment of both the peptide target (D-Ala-D-Aa) and bacteria in a divergent trend. Results of fluorescence spectroscopy indicated that only the outer domain segments of branched polymers reacted to binding of Gram positive bacteria *Staphylococcus aureus* with only a slight reaction when linear analogous polymer or branched polymer with Nile red or Nile blue oxazone in the innermost core was exposed to *Staphylococcus aureus* cultured *in vitro* in chocolate blood agar.

Chromobacterium violaceum a Gram-negative bacterium normally found in water and soil, infrequently produces severe pyogenic or septicemic infections in human skin, generally seen as skin abscesses. *Chromobacterium violaceum* is mainly recognized as a violacein (bis-indole pigment with anti-bacterial and anti-viral properties) producer and as a reporter for quorum sensing molecules discovery. Quorum sensing (QS) is intercellular messaging facilitating individual bacteria to modify their activities in response to the resident Gram-positive and Gram-negative bacterial inhabitants' density *via* molecules described as autoinducers (Batista et al., 2020). QS also plays a role in regulation of gene expression of a bacterial population in response to chemicals (nutrients and toxins) in an environment. Bacterial quorum detection has been associated with several pathogenic bacterial processes, for instance biofilm creation, rendering this as an important focus for generating materials with a novel antibiotic action. Shepherd et al. (2019) synthesized pol-(*N*-isopropyl acrylamide) that was covalently connected to numerous chain ends to homoserine lactone as a crucial messenger molecule participating in quorum sensing and was shown to have anti-QS activity in a *Chromobacterium violaceum* assay.

Turos et al. (2007) successfully conjugated penicillin with polyacrylate, which was then formulated into nanoparticles with anti-bacterial activity. These nanoparticles were prepared by free radical polymerization in which penicillin-acrylate monomer was dissolved in a 7:3 (w/w) mixture of butyl acrylate and styrene in the presence of sodium dodecyl sulphate (surfactant) and potassium persulphate (radical initiator). *In vitro* activity was tested against methicillin-resistant *Staphylococcus aureus* (MRSA) and showed encouraging results with no cytotoxicity towards human dermal fibroblast (HDF) cell line. Furthermore, the conjugate

demonstrated hydrolytic cleavage by bacterial penicillinases, thus expanding the drug's action with regard to drug resistant strains such as MRSA. Similarly, these conjugated polymeric particles also showed positive results *in vivo* against a murine model, again with decreased cytotoxicity. When applied topically to a dermal abrasion model *in vivo*, this emulsion enhanced wound healing by an average of 3 to 5 days. Thus, this study suggests that polyacrylate nanoparticle-containing emulsions may be a promising therapy for treating skin infections.

Jeong et al. (2008) synthesized a polymer-drug formulation using Poly(lactic-co-glycolic)-acid containing ciprofloxacin particle sizes of 100–300 nm. These drug carriers were evaluated for *in vitro* and *in vivo* antibacterial activity against an eczema infecting strain of *E. coli*. As ciprofloxacin was released from this polymer-drug nano-system over a period of 14 days, the system provided a lower but sustained antibacterial action than free drug. However, *in vivo* antibacterial action was greater than the free drug. Interestingly, the *in vitro* experiments were conducted for 24-hour time period only, while in the *in vivo* experiment, BALB/c mice were sacrificed after 72 hours demonstrating that studies of sustained release antibiotic formulations should use *in vitro* studies over a lengthy period. Such a study was also undertaken by Toti et al. (2011) for PLGA polymers linked to rifampicin and azithromycin and who showed significant antibacterial activity against reproductive tract and groin skin epithelial cells infecting *Chlamydia trachomatis*.

In immunocompromised patients, fungal infections are a significant cause of morbidity and death. Presently, three main classes of medicines (azoles, echinocandins and polyenes) are used as antifungal agents with distinct mechanisms of action. However, these medications can generate adverse reactions due to their minimal specificity, drug–drug interactions and limited range of activity. Some of these constraints could be overcome by modifying the properties of current drugs through physical and chemical alterations, for example the alteration of the polyene antibiotic amphotericin B (AmB), by making a micellar suspension in deoxycholic acid (Fungizone®), AmB colloidal dispersion (Amphocil™), non-covalent AmB lipid complexes (ABLC™) and most commonly liposomal AmB (AmBisome®) which are now used against cutaneous leishmaniasis. Each of these formulations modify and slow the release of AmB, reducing plasma levels and consequently reducing its nephrotoxicity. Polymer–drug

conjugates of antifungal medications enhance the aqueous solubility of water-unsolvable medications, extend shelf life and crucially can reduce the toxicity of these drugs and facilitate drug release at the target sites (Franquet et al., 2004; Low and Rotstein, 2011)

Gurudevan et al. (2018) conjugated AmB to bovine serum albumin (BSA) *via* amide bonding to provide 6 to 8 weight % drug load. Characterization of the resultant polymer-drug conjugate was performed using SDS-PAGE, UV–visible, FTIR and CD spectroscopy. Interestingly the resulting conjugate was water-soluble, non-toxic to HEK-293 T cells up to 500 μg/mL *i.e.,* ~30 μg AmB and demonstrated <5% haemolysis at 200 μg/mL (equivalent to ~12 μg AmB) against human RBCc *in vitro*. At 37 °C this conjugate provided steady release of up to 20% AmB from the conjugate *in vitro,* whereas three times this amount was released in human blood plasma over 72 hours. This conjugate gave anti-fungal activity against Candida albicans, *C. parapsilosis* and *C. neoformans* showing minimum inhibitory concentration (MIC) of 0.7 to 1.1 μg/mL of AmB, similar values to AmBisome® MIC's of 0.78-1.5 μg/mL. In this study the model protein BSA was used as an effective carrier and implies that human serum albumin (HSA) could act as an effective carrier in future PDCs design.

1.4.5. Polymer- drug Conjugates for Delivering Drugs to Hair Follicles

Polymer technology has developed rapidly over recent decades and has resulted in the expansion of polymer-drug conjugates with a broad array of designs and chemical properties. Traditional non-degradable polymeric drug delivery carriers such as N-2-hydroxypropyl methacrylamide (HPMA) and poly-ethylene glycol (PEG) copolymers have been widely used in formulations and clinical settings but a trend towards biodegradable, stimuli-responsive, and targeted drug delivery systems is also seen with recent drug-polymer conjugates (Larson and Ghandehari, 2012).

Hair loss also known as androgenetic alopecia (AGA) is a persistent problem seen in both males and females. AGA is most common phenomenon reported in 50% of middle-aged men and almost 95% of the men between 80-90 years. Hair loss can lead to lowering of self-confidence, and can contribute to poor mental health including depression (Ellis et al., 2002)

The hair follicles and pilo-sebaceous unit provides a site where micro-, submicron-, and nano-sized material can enter and accumulate (Figure 1.19). The diameter of the hair follicle openings varies between 175±75μm in terminal hair follicles while it is 85±36μm in vellus hair follicles. The interaction surface of hair follicle infundibulum (cup or siphon in which a hair follicle develops) is estimated to be roughly 0.69 cm^2 for empty and 0.069 cm^2 for full follicles (Vogt et al., 2007: Rancan et al., 2014) so the infundibulum offers not only a potential reservoir site but also a significant surface area where contact between collected material and skin might arise. If drug-polymer conjugates accumulate in the hair follicle canal and releases their drug then this can produce not only local acting effects but also a high drug concentration to drive delivery through the tissue and into the systemic circulation (Toll et al., 2004; Shah et al., 2012).
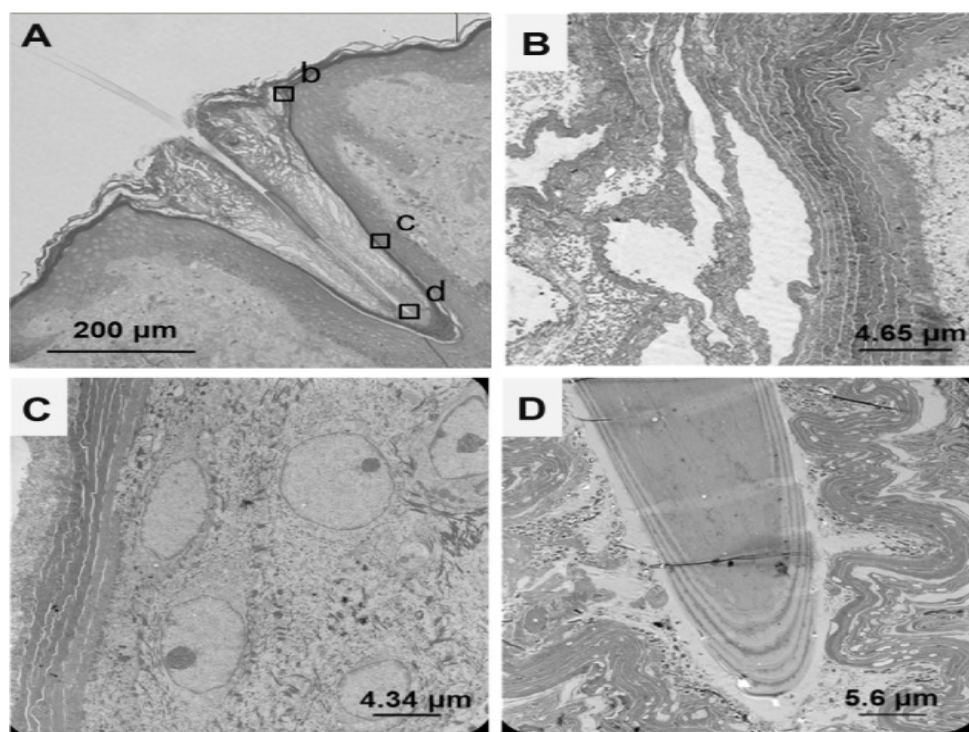
Figure 1.19. Photomicrograph of human terminal hair follicle. (A) Light micrograph of a longitudinal segment presenting the hair follicle hair shaft and infundibulum. The infundibulum is full of cell fragments and sebum. Enclosures (b–d) are areas of the hair follicle that were examined by using transmission electron microscope (B, C and D respectively) (Rancan et al., 2014).

Aljuffali et al. (2015) synthesized polymer lipid <u>nanocarriers</u>, termed "squarticles" conjugated with anti-platelet-derived growth factor (PDGF)-receptor β antibody to ascertain whether targeted minoxidil (MXD) (used for the male-pattern hair loss and an antihypertensive vasodilator) distributed to the hair follicles and papilla cells (DPCs). As the matrix of the squarticles, squalene and hexadecyl palmitate (HP, also called as cetyl palmitate) were employed. The resulting PDGF-squarticles had a mean diameter of 196 nm and zeta potential of − 47 mV. Encapsulation in the nanoparticle increased MXD swine skin accumulation from 0.12 to 0.25 μg/mg. The conjugation of antibody to the nanoparticles enhanced MXD hair follicular uptake by 3-fold as compared to that of the control solution in a BALB/c mouse *in vivo* model. Both upright and parallel sections of the porcine skin displayed a wide-ranging distribution of nanoparticles in the hair follicles, epidermis, and lower skin layers. This effective targeting of PDGF-squarticles to hair follicles might be beneficial better efficacy of minoxidil for alopecia or male pattern baldness.

Recently, Nagai et al. (2019) prepared polymer-drug formulations with minoxidil as nanoparticles (1% N-MXD) using p-hydroxyalkylbenzoates, methylcellulose and mannitol with a bead mill technique. N-MXD (90–300 nm) were applied to examine their impact on hair development using a common inbred mouse strain C57BL/6 (frequently termed "C57-black *6*"). Interestingly, minoxidil content in the hair bulbs was greater for N-MXD polymers than observed for commercially marketed MXD formulation which translated into greater drug efficiency. Notably, the levels of Insulin-like Growth Factor-1 (IGF-1) and vascular endothelial growth factor (VEGF) levels associated with hair growth were also more when N-MXD was delivered as compared to the commercial control.

1.4.6. Polymer-drug Conjugates for the Treatment of Cutaneous Leishmaniasis

Much of the focus has been on the use of PDCs for the treatment of visceral leishmaniasis (VL), and there are only very few studies reporting the use of PDCs for CL. One of such study has been reported by Silva-Carvalho et al. (2020), where he developed water-soluble Dextrin-Amphotericin-B (Dex-AmB) nanoparticulate-drug complexes with better therapeutic effectiveness and reduced toxicity. These nanocomplexes (214-347 nm) were synthesized by dissolving dextrin and Am-B in alkaline borate buffer, followed by dialysis, freeze-drying (FD) or nano spray-drying (SD). These nanocomplexes produced by relatively very simple technique were very effective against cutaneous leishmaniasis causing *Leishmania amazonensis* and *L. infantum* parasites respectively in axenic culture (IC$_{50}$ of 0.056 and 0.096μM for *L.*

amazonensis and 0.030 and 0.044µM for *L. infantum*, respectively). Interestingly, these polymer-drug nanocomplexes had significantly reduce cytotoxicity compared to Am-B alone when tested against macrophages using MTT assay. Thus dextran-amphotericin-B polymer-drug conjugates could be synthesized, so they can be delivered through mannose receptors into *Leishmania* infected macrophages.

Over the last two decades, the application of PDCs to diseases other than cancer has increased, including for topical delivery though this remains a relatively under researched area. As macromolecular constructs, passive diffusion through the intact stratum corneum barrier is not feasible and hence the focus is on targeting to the follicles or use in conditions where the skin barrier is damaged such as psoriasis or wound healing. Thus, opportunities exist for similar barrier dysfunctioning conditions such as atopic dermatitis, scabies or cutaneous leishmaniasis explained in Table 1.2 (Smith, 2007).

Table 1.2. Summary of the potential therapeutic targets for the application of PDCs to the skin

Challenge	Barrier to overcome	Target	Possible polymeric carrier/s
Scabies	NA	Lower SC	HA,Polypeptides
Cutaneous leishmaniasis	NA	Macrophages	Polysaccharides,*e.g.* arabinoglycan, chitosan
Insect repellent	NA	Insects	Film forming polymers without being topically absorbed *e.g.,* PAA
Fungal or bacterial infections	SC	Target cells	HA, polypeptide
Eczema	NA	To inhibit the inflammatory mediators, *e.g.* TNF α, IL-1 *etc*	Any non-irritant polymer *e.g.* HA, chitosan, PAA.
Winter Xerosis	SC	To overcome skin dryness	Polymers that can penetrate the skin whilst hydrating it as well, *e.g.* low molecular--weight HA
Acne	SC	To reach hair follicles	Lyso phosphatidylcholine, cyclodextrin and gel forming polymers like PAA

1.5. Insect Repellents

Various infectious and parasitic diseases, *i.e.* malaria, leishmaniasis, dengue fever *etc* are transferred to humans by the bite of insects and hence are called as insect-borne diseases,

causing thousands of mortalities every year. To prevent that, insect repellents are frequently used. Insect repellent is a substance that is usually applied to the skin to protect against the biting insects like mosquitos, ticks, chiggers *etc* (Fradin and Day, 2002).

Common insect repellents are broadly classified into two categories, *i.e.* natural insect repellents and synthetic insect repellents. Some of the commonly used insect repellents are DEET (N, N-diethyl-m-toluamide), p-menthane-3,8-diol (PMD), picaridin, nepetalactone, neem oil, permethrin. These are briefly discussed in the following.

DEET is a synthetic compound that is considered to be the most effective and commonly used in the world. It is a yellowish oil that can be applied onto the skin. Upon topical application, it has been reported that it can permeate through the skin into the bloodstream. In one of the study serum samples of the people using the DEET (lotion containing 25% of the DEET) on their skin as an insect repellent was taken in such a way that it was observed the serum had 1.82 to 18.84 ng/g of the DEET during the first 8 hours of the skin application (Chen-Hussey et al., 2014).

Similarly, picaridin is another synthetic repellent which was first made in the 1980s. Picaridin has been commonly used in different parts of the world but has only been available in the United States since 2005. When applied to the skin of rats, 60% of it was absorbed through the skin. In clinical trials it was found that less than 6% of the picaridin applied to the skin was absorbed. Picaridin may be broken into various metabolites (Van Roey et al., 2014).

 Similarly, another commonly used insect repellent is nepetalactone, first isolated from the plant catnip (Nepeta cataria). It is a bicyclic monoterpenoid, *i.e.* it is a ten-carbon compound. It is a very potent insect repellent and is having ten times higher activity than that of the commonly used insect repellent DEET (Birkett et al., 2011).

Permethrin is a broad-spectrum insecticide that has been used for a variety of purposes like agricultural and commercial/residential applications. It is also used to control termites, ectoparasites on the animals, and head lice or scabies in humans. It is also used for treating the

soldier's uniforms in the United States, thus helping to reduce outbreaks of insect-borne diseases (Young and Evans, 1998)

Among natural insect repellents, neem oil is a widely used insect repellent an alternative to DEET, and it has been tested for repellence against a range of arthropods that are of medical importance. It can provide up to 7.2 hours mean protection time against a dengue vector and irritating biting mosquitoes (Jilani and Saxena, 1990).

1.5.1. p-menthane-3,8-diol (PMD)

PMD is a naturally occurring compound that usually exists in two isomeric forms, *i.e.* cis and trans. In 2005, the centre for disease control (CDC) endorsed the use of topical repellent products containing para-menthane-3,8-diol (PMD) naturally obtained from a plant called the Eucalyptus citriodora (Lee et al., 2018). Chemically PMD is a monoterpene and can be obtained from both sources, *i.e.* synthetically and naturally. Naturally, it can be obtained from the distillation of the leaves of Eucalyptus citriodora (Carroll and Loye, 2006). On the other hand, it can be synthesised in the lab by the cyclisation of citronellal with excellent yield and purity (Yuasa et al., 2000). Similarly, in order to see the permeation of PMD into the skin, a study was performed in such a way that the pigskin was taken to which PMD lotion was applied. After 24 hours they saw that around 3.5% of PMD was able to penetrate the dermis of the skin, whilst the remaining dose was found to be evaporated off from the skin (Reifenrath et al., 2009).

A)   B)
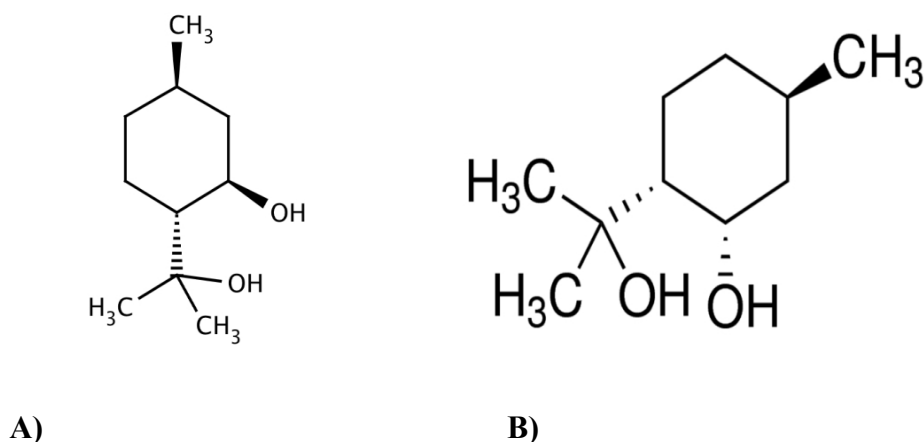
Figure 1.20. Structure of PMD A) trans isomeric form, B) cis isomeric form

1.5.2. Polymeric Carriers for Insect Repellents

For an effective insect repellent formulation, it is important that the concentration of the active compound should remain same over a sufficiently long time period. However, the efficacy of an insect repellent can be rendered by various reasons like, volatility and the permeation of the compound (Barradas et al., 2016). In order to tackle those, polymeric formulations have been developed. Various studies have reported the use of polymeric carriers for the insect repellents. Most of these studies have reported polymeric micro or nano capsules to encapsulate the insect repellents, *e.g.* DEET, PMD, citronella oil, picaridin and others (Katz et al., 2008; Salafsky et al., 1999). It has been shown that as a result of encapsulation physicochemical properties of the repellent like vapour pressure and partition coefficient can be modified. The polymers used for the preparation of these micro or nano capsules include chitosan, collagen and gelatine, it is because of forming covalent or ionic interactions with the encapsulating drugs beside their good safety profile. Similarly other polymers used for this purpose were carboxy methyl cellulose and cyclodextrins (Jing et al., 2014; Solomon et al., 2012).

1.6. Aim and Objectives of the Thesis

The aim of this project was to explore and develop a PDC for extended release and decreased permeation of an insect repellent, *i.e.,* p-menthane 3,8 diol.

The objectives of this project were:

a) Synthesis of a PDC having a hydrolysable ester bond
b) To characterise the PDC for its structure and properties by ^{1}H-NMR, IR spectroscopy, thermal analysis (TGA and DSC), molecular weight, drug loading and effect of pH on the aqueous solubility of the PDC
c) *In vitro* hydrolysis study by using porcine liver esterases (PLEs)
d) To evaluate the skin penetration and permeation of the free drug as well as the PDC
e) To test the irritation potential of the synthesised PDC.
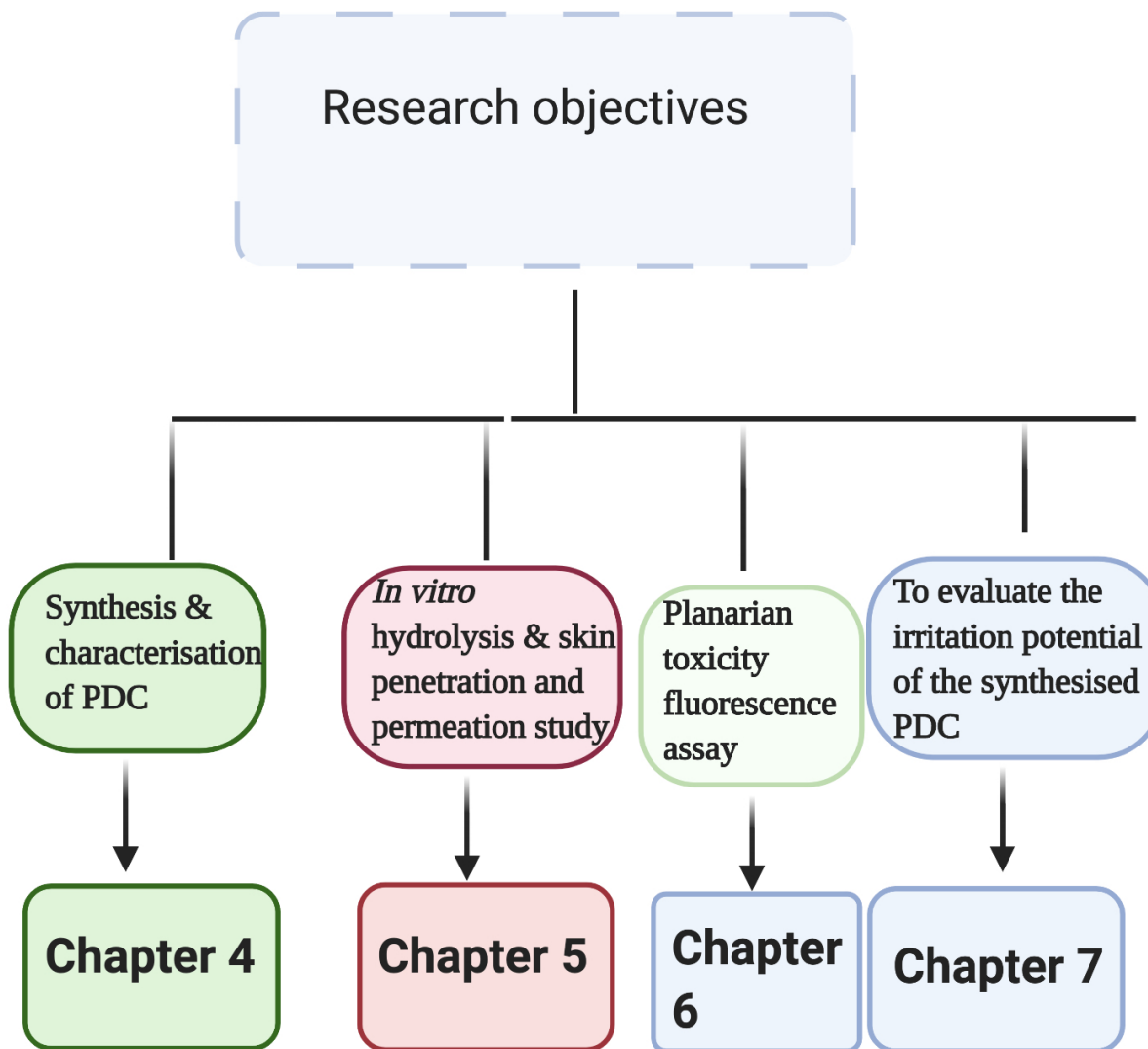
Figure 1.21. Illustration showing the linkage of main objectives with the thesis chapters

References

Abdo, J.M., Sopko, N.A., Milner, S.M., 2020. The applied anatomy of human skin: A model for regeneration. Wound Med. 28, 100179. https://doi.org/https://doi.org/10.1016/j.wndm.2020.100179

Abduljabbar, M.H., Basendwh, M.A., 2016. Complications of hyaluronic acid fillers and their managements. J. Dermatology Dermatologic Surg. 20, 100–106. https://doi.org/https://doi.org/10.1016/j.jdds.2016.01.001

Alberti, I., Kalia, Y.N., Naik, A., Guy, R.H., 2001. Assessment and Prediction of the Cutaneous Bioavailability of Topical Terbinafine, In Vivo, in Man. Pharm. Res. 18, 1472–1475. https://doi.org/10.1023/A:1012217209228

Alkilani, A.Z., McCrudden, M.T.C., Donnelly, R.F., 2015. Transdermal Drug Delivery: Innovative Pharmaceutical Developments Based on Disruption of the Barrier Properties of the stratum corneum. Pharmaceutics 7, 438–470. https://doi.org/10.3390/pharmaceutics7040438

Baek, S.-H., Kwon, E.Y., Bae, S.-J., Cho, B.-R., Kim, S.-Y., Hahn, J.-S., 2017. Improvement of d-Lactic Acid Production in Saccharomyces cerevisiae Under Acidic Conditions by Evolutionary and Rational Metabolic Engineering. Biotechnol. J. 12, 1700015. https://doi.org/10.1002/biot.201700015

Barcaui, E. de O., Carvalho, A.C.P., Piñeiro-Maceira, J., Barcaui, C.B., Moraes, H., 2015. Study of the skin anatomy with high-frequency (22 MHz) ultrasonography and histological correlation. Radiol. Bras. 48, 324–329. https://doi.org/10.1590/0100-3984.2014.0028

Barradas, T.N., Senna, J.P., Ricci, E.J., Mansur, C.R.E., 2016. Polymer-based Drug Delivery Systems Applied to Insects Repellents Devices: A Review. Curr. Drug Deliv. 13, 221–235. https://doi.org/10.2174/1567201813666151207110515

Barrientos, S., Stojadinovic, O., Golinko, M.S., Brem, H., Tomic-Canic, M., 2008. Growth factors and cytokines in wound healing. Wound repair Regen. Off. Publ. Wound Heal. Soc. [and] Eur. Tissue Repair Soc. 16, 585–601. https://doi.org/10.1111/j.1524-475X.2008.00410.x

Batista, J.H., Leal, F.C., Fukuda, T.T.H., Alcoforado Diniz, J., Almeida, F., Pupo, M.T., da

Silva Neto, J.F., 2020. Interplay between two quorum sensing-regulated pathways, violacein biosynthesis and VacJ/Yrb, dictates outer membrane vesicle biogenesis in Chromobacterium violaceum. Environ. Microbiol. n/a. https://doi.org/10.1111/1462-2920.15033

Becker, D.E., Reed, K.L., 2012. Local anesthetics: review of pharmacological considerations. Anesth. Prog. 59, 90–93. https://doi.org/10.2344/0003-3006-59.2.90

Benson, H.A.E., 2012. Skin structure, function, and permeation. Top. Transdermal Drug Deliv. 1–22.

Borke, T., Najberg, M., Ilina, P., Bhattacharya, M., Urtti, A., Tenhu, H., Hietala, S., 2018. Hyaluronic Acid Graft Copolymers with Cleavable Arms as Potential Intravitreal Drug Delivery Vehicles. Macromol. Biosci. 18, 1700200. https://doi.org/10.1002/mabi.201700200

Boulanger, B.L., 2007. Cellulitis, in: Garfunkel, L.C., Kaczorowski, J.M., Christy, C.B.T.-P.C.A. (Second E. (Eds.), . Mosby, Philadelphia, pp. 99–101. https://doi.org/https://doi.org/10.1016/B978-032303506-4.10057-4

Carrasquillo, O.Y., Pabón-Cartagena, G., Falto-Aizpurua, L.A., Santiago-Vázquez, M., Cancel-Artau, K.J., Arias-Berrios, G., Martín-García, R.F., 2020. Treatment of erythrodermic psoriasis with biologics: A systematic review. J. Am. Acad. Dermatol. https://doi.org/https://doi.org/10.1016/j.jaad.2020.03.073

Castleberry, S.A., Quadir, M.A., Sharkh, M.A., Shopsowitz, K.E., Hammond, P.T., 2017. Polymer conjugated retinoids for controlled transdermal delivery. J. Control. Release 262, 1–9. https://doi.org/https://doi.org/10.1016/j.jconrel.2017.07.003

Chen, H.-Y., Hou, J., Zhang, S., Liang, Y., Yang, G., Yang, Y., Yu, L., Wu, Y., Li, G., 2009. Polymer solar cells with enhanced open-circuit voltage and efficiency. Nat. Photonics 3, 649–653.

Choi, J.K., Jang, J.-H., Jang, W.-H., Kim, J., Bae, I.-H., Bae, J., Park, Y.-H., Kim, B.J., Lim, K.-M., Park, J.W., 2012. The effect of epidermal growth factor (EGF) conjugated with low-molecular-weight protamine (LMWP) on wound healing of the skin. Biomaterials 33, 8579–8590. https://doi.org/https://doi.org/10.1016/j.biomaterials.2012.07.061

Delgado-Charro, M.B., 2013. Richard Guy and his collaborators: "crackling" the skin code.

Skin Pharmacol. Physiol. 26, 302–312. https://doi.org/10.1159/000351937

Dolz-Pérez, I., Sallam, M.A., Masiá, E., Morelló-Bolumar, D., Pérez del Caz, M.D., Graff, P., Abdelmonsif, D., Hedtrich, S., Nebot, V.J., Vicent, M.J., 2020. Polypeptide-corticosteroid conjugates as a topical treatment approach to psoriasis. J. Control. Release 318, 210–222. https://doi.org/https://doi.org/10.1016/j.jconrel.2019.12.016

Duracher, L., Blasco, L., Hubaud, J.-C., Vian, L., Marti-Mestres, G., 2009. The influence of alcohol, propylene glycol and 1,2-pentanediol on the permeability of hydrophilic model drug through excised pig skin. Int. J. Pharm. 374, 39–45. https://doi.org/https://doi.org/10.1016/j.ijpharm.2009.02.021

Edlich, R.F., Winters, K.L., Britt, L.D., Long, W.B., 2005. Bacterial diseases of the skin. J. Long. Term. Eff. Med. Implants. https://doi.org/10.1615/JLongTermEffMedImplants.v15.i5.40

Ekladious, I., Colson, Y.L., Grinstaff, M.W., 2019. Polymer–drug conjugate therapeutics: advances, insights and prospects. Nat. Rev. Drug Discov. 18, 273–294. https://doi.org/10.1038/s41573-018-0005-0

Ellis, J.A., Sinclair, R., Harrap, S.B., 2002. Androgenetic alopecia: pathogenesis and potential for therapy. Expert Rev. Mol. Med. 4, 1–11. https://doi.org/10.1017/S1462399402005112

Etrych, T., Mrkvan, T., Chytil, P., Koňák, Č., Říhová, B., Ulbrich, K., 2008. N-(2-hydroxypropyl) methacrylamide-based polymer conjugates with pH-controlled activation of doxorubicin. I. New synthesis, physicochemical characterization and preliminary biological evaluation. J. Appl. Polym. Sci. 109, 3050–3061.

Feng, J., Lepetre-Mouelhi, S., Gautier, A., Mura, S., Cailleau, C., Coudore, F., Hamon, M., Couvreur, P., 2019. A new painkiller nanomedicine to bypass the blood-brain barrier and the use of morphine. Sci. Adv. 5, eaau5148–eaau5148. https://doi.org/10.1126/sciadv.aau5148

Feng, Q., Tong, R., 2016. Anticancer nanoparticulate polymer-drug conjugate. Bioeng. Transl. Med. 1, 277–296. https://doi.org/10.1002/btm2.10033

Franquet, T., Giménez, A., Hidalgo, A., 2004. Imaging of opportunistic fungal infections in immunocompromised patient. Eur. J. Radiol. 51, 130–138.

https://doi.org/https://doi.org/10.1016/j.ejrad.2004.03.007

Gianolio, D.A., Philbrook, M., Avila, L.Z., MacGregor, H., Duan, S.X., Bernasconi, R., Slavsky, M., Dethlefsen, S., Jarrett, P.K., Miller, R.J., 2005. Synthesis and evaluation of hydrolyzable hyaluronan-tethered bupivacaine delivery systems. Bioconjug. Chem. 16, 1512–1518. https://doi.org/10.1021/bc050239a

Greenwald, R.B., Zhao, H., Xia, J., Martinez, A., 2003. Poly(ethylene glycol) Transport Forms of Vancomycin: A Long-Lived Continuous Release Delivery System. J. Med. Chem. 46, 5021–5030. https://doi.org/10.1021/jm030202g

Hadgraft, J., Valenta, C., 2000. pH, pK(a) and dermal delivery. Int. J. Pharm. 200, 243–247. https://doi.org/10.1016/s0378-5173(00)00402-6

Hatanaka, T., Saito, T., Fukushima, T., Todo, H., Sugibayashi, K., Umehara, S., Takeuchi, T., Okamura, Y., 2019. Potential of biocompatible polymeric ultra-thin films, nanosheets, as topical and transdermal drug delivery devices. Int. J. Pharm. 565, 41–49. https://doi.org/10.1016/j.ijpharm.2019.04.059

Honari, G., Maibach, H., 2014. Chapter 1 - Skin Structure and Function, in: Maibach, H., Honari, G.B.T.-A.D. (Eds.), . Academic Press, Boston, pp. 1–10. https://doi.org/https://doi.org/10.1016/B978-0-12-420130-9.00001-3

Huang, Z., Wang, H., Lu, M., Sun, C., Wu, X., Tan, Y., Ye, C., Zhu, G., Wang, X., Cai, L., Li, X., 2011. A Better Anti-Diabetic Recombinant Human Fibroblast Growth Factor 21 (rhFGF21) Modified with Polyethylene Glycol. PLoS One 6, e20669.

Jing, H., Weijun, D., Liqin, L., Zuobing, X., 2014. Synthesis and application of polyacrylate nanocapsules loaded with lilial. J. Appl. Polym. Sci. 131. https://doi.org/10.1002/app.40182

Joralemon, M.J., Murthy, K.S., Remsen, E.E., Becker, M.L., Wooley, K.L., 2004. Synthesis, Characterization, and Bioavailability of Mannosylated Shell Cross-Linked Nanoparticles. Biomacromolecules 5, 903–913. https://doi.org/10.1021/bm0344710

Katz, T.M., Miller, J.H., Hebert, A.A., 2008. Insect repellents: historical perspectives and new developments. J. Am. Acad. Dermatol. 58, 865–871. https://doi.org/10.1016/j.jaad.2007.10.005

Kelly, K.A., Butch, A.W., 2012. Chapter 15 - Immunosuppressive Drug Monitoring:

Limitations of Immunoassays and the Application of Liquid Chromatography Mass Spectrometry, in: Dasgupta, A.B.T.-T.D.M. (Ed.), . Academic Press, Boston, pp. 323–348. https://doi.org/https://doi.org/10.1016/B978-0-12-385467-4.00015-4

Kim, J.H., Li, Y., Kim, M.S., Kang, S.W., Jeong, J.H., Lee, D.S., 2012. Synthesis and evaluation of biotin-conjugated pH-responsive polymeric micelles as drug carriers. Int. J. Pharm. 427, 435–442. https://doi.org/https://doi.org/10.1016/j.ijpharm.2012.01.034

Kim, P.-H., Sohn, J.-H., Choi, J.-W., Jung, Y., Kim, S.W., Haam, S., Yun, C.-O., 2011. Active targeting and safety profile of PEG-modified adenovirus conjugated with herceptin. Biomaterials 32, 2314–2326.

Kolarsick, P.A.J., Kolarsick, M.A., Goodwin, C., 2006. Anatomy and Physiology of the Skin.

Kopeček, J., 2013. Polymer-drug conjugates: origins, progress to date and future directions. Adv. Drug Deliv. Rev. 65, 49–59. https://doi.org/10.1016/j.addr.2012.10.014

Korkmaz, E., Friedrich, E.E., Ramadan, M.H., Erdos, G., Mathers, A.R., Ozdoganlar, O.B., Washburn, N.R., Falo, L.D., 2016. Tip-Loaded Dissolvable Microneedle Arrays Effectively Deliver Polymer-Conjugated Antibody Inhibitors of Tumor-Necrosis-Factor-Alpha Into Human Skin. J. Pharm. Sci. 105, 3453–3457. https://doi.org/https://doi.org/10.1016/j.xphs.2016.07.008

Larson, N., Ghandehari, H., 2012. Polymeric Conjugates for Drug Delivery. Chem. Mater. 24, 840–853. https://doi.org/10.1021/cm2031569

Lau, W.M., Ng, K.W., Sakenyte, K., Heard, C.M., 2012. Distribution of esterase activity in porcine ear skin, and the effects of freezing and heat separation. Int. J. Pharm. 433, 10–15. https://doi.org/https://doi.org/10.1016/j.ijpharm.2012.04.079

Lebwohl, M., Phelps, R., Gordon, M., Fleischmajer, R., 1990. Disease of the dermis. J. Am. Acad. Dermatol. 23, 295–299. https://doi.org/https://doi.org/10.1016/S0190-9622(08)81239-X

Lett, J.A., Sundareswari, M., Ravichandran, K., Latha, B., Sagadevan, S., 2019. Fabrication and characterization of porous scaffolds for bone replacements using gum tragacanth. Mater. Sci. Eng. C 96, 487–495.

Low, C.-Y., Rotstein, C., 2011. Emerging fungal infections in immunocompromised patients. F1000 Med. Rep. 3, 14. https://doi.org/10.3410/M3-14

Maeda, H., Sawa, T., Konno, T., 2001. Mechanism of tumor-targeted delivery of macromolecular drugs, including the EPR effect in solid tumor and clinical overview of the prototype polymeric drug SMANCS. J. Control. Release 74, 47–61. https://doi.org/https://doi.org/10.1016/S0168-3659(01)00309-1

Mao, K.-L., Fan, Z.-L., Yuan, J.-D., Chen, P.-P., Yang, J.-J., Xu, J., ZhuGe, D.-L., Jin, B.-H., Zhu, Q.-Y., Shen, B.-X., Sohawon, Y., Zhao, Y.-Z., Xu, H.-L., 2017. Skin-penetrating polymeric nanoparticles incorporated in silk fibroin hydrogel for topical delivery of curcumin to improve its therapeutic effect on psoriasis mouse model. Colloids Surfaces B Biointerfaces 160, 704–714. https://doi.org/https://doi.org/10.1016/j.colsurfb.2017.10.029

Marschütz, M.K., Bernkop-Schnürch, A., 2000. Oral peptide drug delivery: polymer–inhibitor conjugates protecting insulin from enzymatic degradation in vitro. Biomaterials 21, 1499–1507. https://doi.org/https://doi.org/10.1016/S0142-9612(00)00039-9

Mielanczyk, A., Mrowiec, K., Kupczak, M., Mielanczyk, Ł., Scieglinska, D., Gogler-Piglowska, A., Michalski, M., Gabriel, A., Neugebauer, D., Skonieczna, M., 2020. Synthesis and in vitro cytotoxicity evaluation of star-shaped polymethacrylic conjugates with methotrexate or acitretin as potential antipsoriatic prodrugs. Eur. J. Pharmacol. 866, 172804. https://doi.org/https://doi.org/10.1016/j.ejphar.2019.172804

Mizukami, S., Kashibe, M., Matsumoto, K., Hori, Y., Kikuchi, K., 2017. Enzyme-triggered compound release using functionalized antimicrobial peptide derivatives. Chem. Sci. 8, 3047–3053. https://doi.org/10.1039/c6sc04435b

Mogoşanu, G.D., Grumezescu, A.M., Bejenaru, C., Bejenaru, L.E., 2016. Polymeric protective agents for nanoparticles in drug delivery and targeting. Int. J. Pharm. 510, 419–429.

Mueller, R.S., Bettenay, S. V, Shipstone, M., 2002. Cutaneous candidiasis in a dog caused by Candida guilliermondii Vet. Rec. 150, 728 LP – 730. https://doi.org/10.1136/vr.150.23.728

N'Da, D.D., 2014. Prodrug Strategies for Enhancing the Percutaneous Absorption of Drugs. Mol. . https://doi.org/10.3390/molecules191220780

Nan, A., Nanayakkara, N.P.D., Walker, L.A., Yardley, V., Croft, S.L., Ghandehari, H., 2001.

N-(2-hydroxypropyl)methacrylamide (HPMA) copolymers for targeted delivery of 8-aminoquinoline antileishmanial drugs. J. Control. Release 77, 233–243. https://doi.org/https://doi.org/10.1016/S0168-3659(01)00514-4

Natfji, A.A., Nikitin, D.O., Semina, I.I., Moustafine, R.I., Khutoryanskiy, V. V, Lin, H., Stephens, G.J., Watson, K.A., Osborn, H.M.I., Greco, F., 2020. Conjugation of haloperidol to PEG allows peripheral localisation of haloperidol and eliminates CNS extrapyramidal effects. J. Control. Release 322, 227–235. https://doi.org/https://doi.org/10.1016/j.jconrel.2020.02.037

Natfji, A.A., Osborn, H.M.I., Greco, F., 2017. Feasibility of polymer-drug conjugates for non-cancer applications. Curr. Opin. Colloid Interface Sci. 31, 51–66. https://doi.org/https://doi.org/10.1016/j.cocis.2017.07.004

Nestle, F.O., Kaplan, D.H., Barker, J., 2009. Psoriasis. N. Engl. J. Med. 361, 496–509. https://doi.org/10.1056/NEJMra0804595

Pan, D., she, W., Guo, C., Luo, K., Yi, Q., Gu, Z., 2014. PEGylated dendritic diaminocyclohexyl-platinum (II) conjugates as pH-responsive drug delivery vehicles with enhanced tumor accumulation and antitumor efficacy. Biomaterials 35, 10080–10092. https://doi.org/https://doi.org/10.1016/j.biomaterials.2014.09.006

Pang, X., Du, H.-L., Zhang, H.-Q., Zhai, Y.-J., Zhai, G.-X., 2013. Polymer–drug conjugates: present state of play and future perspectives. Drug Discov. Today 18, 1316–1322. https://doi.org/https://doi.org/10.1016/j.drudis.2013.09.007

Pang, X., Jiang, Y., Xiao, Q., Leung, A.W., Hua, H., Xu, C., 2016. pH-responsive polymer–drug conjugates: Design and progress. J. Control. Release 222, 116–129. https://doi.org/https://doi.org/10.1016/j.jconrel.2015.12.024

Pang, X., Yang, X., Zhai, G., 2014. Polymer-drug conjugates: recent progress on administration routes. Expert Opin. Drug Deliv. 11, 1075–1086. https://doi.org/10.1517/17425247.2014.912779

Papanas, N., Maltezos, E., 2007. THE DIABETIC FOOT: ESTABLISHED AND EMERGING TREATMENTS. Acta Clin. Belg. 62, 230–238. https://doi.org/10.1179/acb.2007.037

Park, J.-H., Allen, M.G., Prausnitz, M.R., 2005. Biodegradable polymer microneedles:

Fabrication, mechanics and transdermal drug delivery. J. Control. Release 104, 51–66. https://doi.org/https://doi.org/10.1016/j.jconrel.2005.02.002

Patzelt, A., Lademann, J., 2013. Drug delivery to hair follicles. Expert Opin. Drug Deliv. 10, 787–797. https://doi.org/10.1517/17425247.2013.776038

Paul, M., 2020. Hypodermis.

Piérard, G.E., Uhoda, I., Piérard-Franchimont, C., 2003. From skin microrelief to wrinkles. An area ripe for investigation. J. Cosmet. Dermatol. 2, 21–28. https://doi.org/10.1111/j.1473-2130.2003.00012.x

Prausnitz, M.R., Langer, R., 2008. Transdermal drug delivery. Nat. Biotechnol. 26, 1261–1268. https://doi.org/10.1038/nbt.1504

Prow, T.W., Grice, J.E., Lin, L.L., Faye, R., Butler, M., Becker, W., Wurm, E.M.T., Yoong, C., Robertson, T.A., Soyer, H.P., Roberts, M.S., 2011. Nanoparticles and microparticles for skin drug delivery. Adv. Drug Deliv. Rev. 63, 470–491. https://doi.org/https://doi.org/10.1016/j.addr.2011.01.012

Pyo, S.M., Maibach, H.I., 2019. Skin Metabolism: Relevance of Skin Enzymes for Rational Drug Design. Skin Pharmacol. Physiol. 32, 283–294. https://doi.org/10.1159/000501732

Rădulescu, M., Holban, A.M., Mogoantă, L., Bălşeanu, T.-A., Mogoşanu, G.D., Savu, D., Popescu, R.C., Fufă, O., Grumezescu, A.M., Bezirtzoglou, E., 2016. Fabrication, characterization, and evaluation of bionanocomposites based on natural polymers and antibiotics for wound healing applications. Molecules 21, 761.

Raychaudhuri, S.K., Maverakis, E., Raychaudhuri, S.P., 2014. Diagnosis and classification of psoriasis. Autoimmun. Rev. 13, 490–495. https://doi.org/10.1016/j.autrev.2014.01.008

Rendon, A., Schäkel, K., 2019. Psoriasis Pathogenesis and Treatment. Int. J. Mol. Sci. 20, 1475. https://doi.org/10.3390/ijms20061475

Requejo-Aguilar, R., Alastrue-Agudo, A., Cases-Villar, M., Lopez-Mocholi, E., England, R., Vicent, M.J., Moreno-Manzano, V., 2017. Combined polymer-curcumin conjugate and ependymal progenitor/stem cell treatment enhances spinal cord injury functional recovery. Biomaterials 113, 18–30. https://doi.org/https://doi.org/10.1016/j.biomaterials.2016.10.032

Ringsdorf, H., 2007. Structure and properties of pharmacologically active polymers. J. Polym. Sci. Polym. Symp. 51, 135–153. https://doi.org/10.1002/polc.5070510111

Ringsdorf, H., 1975. Structure and properties of pharmacologically active polymers, in: Journal of Polymer Science: Polymer Symposia. Wiley Online Library, pp. 135–153.

Rossi, M., Carpi, A., Di Maria, C., Franzoni, F., Galetta, F., Santoro, G., 2009. Skin blood flowmotion and microvascular reactivity investigation in hypercholesterolemic patients without clinically manifest arterial diseases. Physiol. Res. 58.

Sahle, F.F., Gebre-Mariam, T., Dobner, B., Wohlrab, J., Neubert, R.H.H., 2015. Skin Diseases Associated with the Depletion of Stratum Corneum Lipids and Stratum Corneum Lipid Substitution Therapy. Skin Pharmacol. Physiol. 28, 42–55. https://doi.org/10.1159/000360009

Salafsky, B., Ramaswamy, K., He, Y.X., Li, J., Shibuya, T., 1999. Development and evaluation of LIPODEET, a new long-acting formulation of N, N-diethyl-m-toluamide (DEET) for the prevention of schistosomiasis. Am. J. Trop. Med. Hyg. 61, 743–750. https://doi.org/10.4269/ajtmh.1999.61.743

Seifu, M.F., Nath, L.K., 2019. Polymer-Drug Conjugates: Novel Carriers for Cancer Chemotherapy. Polym. Technol. Mater. 58, 158–171. https://doi.org/10.1080/03602559.2018.1466172

Shepherd, J., Sarker, P., Rimmer, S., Swanson, L., MacNeil, S., Douglas, I., 2011. Hyperbranched poly(NIPAM) polymers modified with antibiotics for the reduction of bacterial burden in infected human tissue engineered skin. Biomaterials 32, 258–267. https://doi.org/10.1016/j.biomaterials.2010.08.084

Singer, A.J., Clark, R.A., 1999. Cutaneous wound healing. N. Engl. J. Med. 341, 738–746. https://doi.org/10.1056/NEJM199909023411006

Solomon, B., Sahle, F.F., Gebre-Mariam, T., Asres, K., Neubert, R.H.H., 2012. Microencapsulation of citronella oil for mosquito-repellent application: formulation and in vitro permeation studies. Eur. J. Pharm. Biopharm. Off. J. Arbeitsgemeinschaft fur Pharm. Verfahrenstechnik e.V 80, 61–66. https://doi.org/10.1016/j.ejpb.2011.08.003

Staudinger, H., 1920. Über polymerisation. Berichte der Dtsch. Chem. Gesellschaft (A B Ser. 53, 1073–1085.

Supasena, W., Muangnoi, C., Thaweesest, W., Songkram, C., Ueda, K., Higashi, K., Moribe, K., Tanasupawat, S., Rojsitthisak, P., 2020. Enhanced Antipsoriatic Activity of Mycophenolic Acid Against the TNF-α-Induced HaCaT Cell Proliferation by Conjugated Poloxamer Micelles. J. Pharm. Sci. 109, 1153–1160. https://doi.org/https://doi.org/10.1016/j.xphs.2019.11.010

Swift, T., Katsikogianni, M., Hoskins, R., Teratarantorn, P., Douglas, I., MacNeil, S., Rimmer, S., 2019. Highly-branched poly(N-isopropyl acrylamide) functionalised with pendant Nile red and chain end vancomycin for the detection of Gram-positive bacteria. Acta Biomater. 87, 197–206. https://doi.org/https://doi.org/10.1016/j.actbio.2019.01.066

Turos, E., Shim, J.-Y., Wang, Y., Greenhalgh, K., Reddy, G.S.K., Dickey, S., Lim, D. V, 2007. Antibiotic-conjugated polyacrylate nanoparticles: new opportunities for development of anti-MRSA agents. Bioorg. Med. Chem. Lett. 17, 53–56. https://doi.org/10.1016/j.bmcl.2006.09.098

Valenta, C., Auner, B.G., 2004. The use of polymers for dermal and transdermal delivery. Eur. J. Pharm. Biopharm. 58, 279–289. https://doi.org/https://doi.org/10.1016/j.ejpb.2004.02.017

van der Maaden, K., Luttge, R., Vos, P.J., Bouwstra, J., Kersten, G., Ploemen, I., 2015. Microneedle-based drug and vaccine delivery via nanoporous microneedle arrays. Drug Deliv. Transl. Res. 5, 397–406. https://doi.org/10.1007/s13346-015-0238-y

Vicent, M.J., Duncan, R., 2006. Polymer conjugates: nanosized medicines for treating cancer. Trends Biotechnol. 24, 39–47. https://doi.org/https://doi.org/10.1016/j.tibtech.2005.11.006

Wang, Y., Su, W., Li, Q., Li, C., Wang, H., Li, Y., Cao, Y., Chang, J., Zhang, L., 2013. Preparation and evaluation of lidocaine hydrochloride-loaded TAT-conjugated polymeric liposomes for transdermal delivery. Int. J. Pharm. 441, 748–756. https://doi.org/https://doi.org/10.1016/j.ijpharm.2012.10.019

Webber, M.J., Appel, E.A., Meijer, E.W., Langer, R., 2016. Supramolecular biomaterials. Nat. Mater. 15, 13–26.

Williams, A., 2003. Transdermal and Topical Drug Delivery from Theory to Clinical Practice. Pharmaceutical Press.

Yang, J.-A., Kim, E.-S., Kwon, J.H., Kim, H., Shin, J.H., Yun, S.H., Choi, K.Y., Hahn, S.K., 2012. Transdermal delivery of hyaluronic acid – Human growth hormone conjugate. Biomaterials 33, 5947–5954. https://doi.org/https://doi.org/10.1016/j.biomaterials.2012.05.003

Yu, Y., Chen, C.-K., Law, W.-C., Mok, J., Zou, J., Prasad, P.N., Cheng, C., 2013. Well-defined degradable brush polymer–drug conjugates for sustained delivery of paclitaxel. Mol. Pharm. 10, 867–874.

Zhu, X., Anquillare, E.L.B., Farokhzad, O.C., Shi, J., 2014. Chapter 22 - Polymer- and Protein-Based Nanotechnologies for Cancer Theranostics, in: Chen, X., Wong, S.B.T.-C.T. (Eds.), . Academic Press, Oxford, pp. 419–436. https://doi.org/https://doi.org/10.1016/B978-0-12-407722-5.00022-0

.

Chapter 2. Materials and Methods

2.1. Materials

Material	Supplier
Hyaluronic acid (sodium salt) (MW 1.6 MDa, Batch# 070815-E1)	Contipro., Czech Republic
Citronellal (Lot# 10202671)	Fischer Scientific., UK
n-Heptane (Lot# 1697988)	Acros Organics., UK
(Benzotriazol-1-yloxy)tripyrrolidinophosphonium hexafluorophosphate (PyBOP) (Lot# A0374488)	Acros Organics., UK
N,N Diisopropyletylamine (DIPEA)(Lot# STBF9469V)	Sigma-Aldrich Co., UK
Dimethylsulfoxide (DMSO) (Lot# 1670195)	Fischer Scientific., UK
Sodium Chloride (Lot# 1557449)	Fischer Scientific., UK
Sodium carbonate anhydrous (CAS# 497-19-18)	Fischer Scientific., UK
Hydrochloric acid (CAS# 7647-01-0)	Fischer Scientific., UK
Dowex ion exchange resin (CAS# 217492, mesh size 50-100)	Sigma-Aldrich Co., UK
4, Dimethylamino pyridine (CAS#1122-58-3)	Acros Organics., UK
Polyacrylic acid (18,00 Da) (LOT#SLBS6469)	Sigma Aldrich Co.,UK
Polyacrylic acid (1.25 MDa) (LOT#MKBT3043V,CAS# 89-83-8)	Sigma-Aldrich Co., UK
Thionyl chloride (LOT#A0372214, CAS#7719-09-7)	Acros Organics., UK
N,N-Dicyclohexylcarbodiimide (LOT#A0385375)	Acros Organics., UK
Thymol (LOT#A0382019)	Fischer Scientific., UK
Triisobutylamine (CAS# 1116-40-1)	Sigma-Aldrich Co., Uk
Polyethyleneglycol dimethylether (dmPEG) (CAS# 24991-55-7)	Sigma-Aldrich Co., UK

Porcine liver esterases (CAS#39346-81-1)	Sigma-Aldrich Co., UK
Agarose low gelling temperature (LOT#SLBW7267)	Sigma-Aldrich Co., UK
Pur-A-lyzer Mega 1000 Dialysis kit (LOT# g01/17443)	Sigma-Aldrich Co., UK
p-Menthane 3,8 diol (CAS#42822-86-6, LOT#BS18U05312, BV18ZJ01182)	BOC sciences, USA
Acryloyl chloride (LOT# STBG5526V, STBF9634V)	Sigma-Aldrich Co., UK
Acrylic acid (CAS# 79-10-7)	Sigma-Aldrich Co., UK
2,2-Azobis(2-methyl-propionitrile) (LOT# STBC6554V)	Sigma-Aldrich Co., UK
Triethylamine (CAS# 121-44-8)	Sigma-Aldrich Co., UK
Porcine liver esterases (CAS# 9018-16-1)	Sigma-Aldrich Co., UK
Triisobutylphosphate (CAS# 126-71-6)	Acros Organics, Uk
Glycerol (CAS# 56-81-5)	Sigma-Aldrich Co., Uk
Polyethylene glycol-400 (PEG-400) (CAS# 25322-68-3)	Sigma-Aldrich Co., UK
Tween-20 (CAS# 9005-64-5)	Sigma-Aldrich Co., UK
Toulene (CAS# 108-88-3)	Sigma-Aldrich Co., UK
Ethyl acetate (CAS# 141-78-6)	Fischer scientific Co., UK
Parafluoroaniline (CAS# 371-40-4)	Sigma-Aldrich Co., UK
Benzalkonium chloride (CAS# 63449-41-2)	Sigma-Aldrich Co., UK
Dipropylene glycol (CAS# 25265-71-8)	Sigma-Aldrich Co., UK
Terpinyl acetate (CAS# 80-26-2)	Sigma-Aldrich Co., UK
Linalyl acetate (CAS# 499-75-2)	Fischer scientific Co., UK
Carvacrol (CAS# 115-95-7)	Sigma-Aldrich Co., UK

Silica gel (CAS# 112926-00-8)	Sigma-Aldrich Co., Uk

2.2 Methods

2.2.1 Chromatographic methods

2.2.1.1 TLC

Thin-layer chromatography (TLC) is a procedure applied in organic chemistry to separate compounds in a mixture based on variations in their polarity. In this work, the stationary phase was a thin layer of polar silica gel and various mobile phases were employed, typically organic solvents. Studies used Merck TLC Silica gel 60 F254 aluminum backed plates (Sigma-Aldrich). Initially, a line was drawn on the bottom of the TLC plate and mixtures were then spotted at this origin using thin capillaries before the bottom of the plate was submerged in an organic solvent, *i.e.* hexane:ethylacetate (4:1); the solvent travelled up the plate by capillary action, carrying and separating solutes by their lipophilicity and molecular weights. The TLC plates were then visualised using p-anisaldehyde (as an indicator). The p-anisaldehyde stain was prepared by mixing 5 mL of concentrated sulfuric acid into 135 mL of absolute ethanol and then adding 1.5 mL of glacial acetic acid dropwise in a round bottom flask placed over ice. Finally, 3.7 mL of p-anisaldehyde (also known as 4-methoxybenzaldehyde, analytical grade, Sigma-Aldrich) was added, and the solution was stirred to ensure homogeneity. The solution was refrigerated at 4-7 °C and was wrapped in an aluminum foil until use.

2.2.1.2 Column Chromatography

Column chromatography was carried out using silica gel. The column was prepared by taking a cylindrical glass column and plugging in with a small piece of cotton and then packing the column by a wet packing method; for every 1g of test material, the equivalent of 70g of fresh silica gel (60 mesh size) was used. Silica was added to a beaker and sufficient hexane was added to produce a slurry. The slurry was then poured into the column. After packing of the

column, the material was dissolved in ethyl acetate and was then put into the column with a final ratio of hexane:ethylacetate of 4:1. Fractions were collected in the tubes (15 mL) and were then analysed by TLC for the purpose of identification. At the end, the solvent system was evaporated by using rotary drier.

2.2.2 Infrared Spectroscopy

Infrared (IR) spectroscopy is widely used to verify chemical structures and to aid identification of compounds. IR is a region of electromagnetic radiation ranging between 400 cm^{-1} and 4000 cm^{-1}. The principle on which IR spectroscopy is based on is that the molecules that tend to absorb (by the bonds) electromagnetic radiation result in the transition between molecular vibrational or rational energy levels. The wavelength of the radiation absorbed is the characteristic of the bond (including environment) absorbing it. Thus, based upon the nature of these bonds (in the molecules) and their surrounding environment different wavelengths are absorbed and then emitted by different parts of molecules (Bates, 1976; Gillie et al., 2000).

The intensity by which a molecule (bond) absorbs radiation depends upon its dipole moment, *i.e.* the order of intensity of absorption will be OH>NH>CH. Similarly, there are different factors responsible to predict that where (wavenumber) these peaks can be seen. These include bond strength (stiffness of the bond), as a general rule greater the stiffness of the bond higher will be the wavenumber. Similarly, other factor is the mass effect, as mass on bond increases the wavenumber decreases (McDonald, 1986; Wellner, 2013).
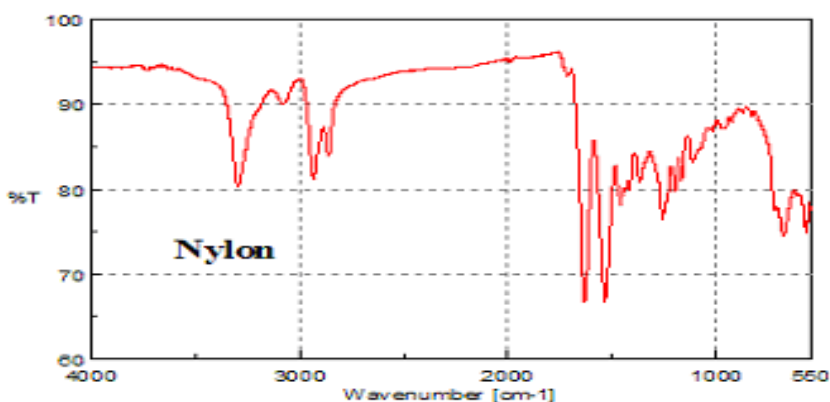
Figure 2.1. Exemplar IR spectra of Nylon (FTIR-Graph- www.microanalysis.com.au)

Infrared spectra were recorded using the ATR (attenuated total reflectance) technique on a Perkin Elmer (Spectrum 100) FT-IR spectrometer (Perkin Elmer Ltd., UK) from 4000 to 400 cm^{-1} with 16 scans averaged and collected at 4 cm^{-1} resolution. The absorption was obtained in wavenumbers [cm^{-1}]. The symbols ν and δ denote stretching and bending molecular modes respectively and peak intensities are categorized as s, strong; m, medium and w, weak, while br denotes broad peaks.

2.2.3 Nuclear Magnetic Resonance Spectroscopy

Nuclear magnetic resonance (NMR) spectroscopy is a highly sensitive and precise analytical technique for structural elucidation and material purity. It exploits the principle that when radiation in the radiofrequency region is used to excite atoms usually protons or carbon-13 atoms in such a way that their spin switches from being aligned with to being aligned against an applied magnetic field, thus giving a typical NMR spectrum. The spinning of the nuclei of certain atoms give them the properties of magnetic vector. Examples of such nuclei are ^{1}H, ^{13}C, ^{15}N, ^{19}F,^{29}Si and ^{31}P. Now when these nuclei are placed in a magnetic field they will try to align with the applied field. The greater the field strength the greater the energy difference (Watson and Pgce, 2020)

There are two types of NMR's, proton NMR and ^{13}C NMR. Proton NMR is the most commonly used form of NMR as it's a sensitive technique and can yield large amount of structural information. NMR spectra is represented in the form of chemical shifts. A chemical shift assigned to a proton is determined in relation to the proton of the tetramethyl silane. Here the chemical shift assigned to a compound is represented in the form of ppm. Value of 1ppm in Hertz (Hz) depends upon the strength of the applied magnetic field. For example, at a field strength of 100mHz a shift of 1ppm=100 Hz (Watson and Pgce, 2020).

In our experiments, we used Bruker DPX 400 (400 MHz) spectrometer to record ^{1}H-NMR spectra in either deuterated chloroform (CDCl$_3$) or deuterated dimethyl sulfoxide (DMSO-d6). ^{13}C- NMR spectra were recorded either in deuterated chloroform (CDCl$_3$) or in deuterated dimethyl sulfoxide (DMSO-d6). Chemical shifts (δ) are given in parts per million (ppm) using the subsequent abbreviations for splitting patterns: s, singlet; d, doublet; t, triplet; app. t, apparent triplet; dd, doublet of doublets; dt, doublet of triplets; q, quartet; m, multiplet.

2.2.4 Mass Spectroscopy

Mass spectrometry works on the principle of detecting the molecular weight of a molecule in such a way that it works by generating charged molecules or molecular fragments either in high vacuum or immediately before the sample enters the high vacuum. The most common source of generating these charged molecules is the electrospray ionisation (ESI). Upon the generation of these charged or fragmented molecules they are then detected by a detector (Glish and Vachet, 2003).

Mass spectrometry data were recorded on a Thermo Fisher LTQ Orbitrap XL instrument using ESI. Where possible, high-resolution mass spectroscopy (HR-MS) data are provided for the molecular ion or appropriate adduct, fragmentation patterns are also provided.

2.2.5 Melting Point

Melting points were determined using an Electrothermal Digital Melting Point apparatus (A-9000, Electrothermal Ltd, UK) with samples held in a capillary tube.

2.2.6 Thermogravimetric Analysis (TGA)

TGA is a thermal analysis technique in which the change of mass loss is measured concerning changing temperature. TGA uses a temperature ramp, shows weight loss that can provide information related to certain physical (evaporation) and chemical (decomposition or oxidative degradation) phenomena. The results from a thermogravimetric run may be presented by weight *versus* temperature (or time) curve, referred to as the thermogravimetric curve or rate of loss of weight *versus* temperature curve, referred to as the differential thermogravimetric curve. Depending upon the nature of the material (to be analysed) a thermogravimetric curve may undergo solvent evaporation followed by the decomposition or degradation (nature of which depends upon the type of the material) (Carrier et al., 2011).

TGA experiments were conducted with a Q50 thermogravimetric analyser (TA Instruments, UK). The TGA's temperature calibration was established with reference samples of nickel, zinc and iron. The weight calibration was established with certified Troemner 100 mg standard weight. TGA was conducted in an inert nitrogen atmosphere with a flow rate of 30 mL min^{-1}. All temperature transitions were assessed at a constant temperature ramp of 5°C min^{-1}. Samples weighing between 2-9 mg were placed in aluminium pans. The samples were subjected to these

conditions and heated at 5°C min^{-1} from 35°C to 590°C (depending upon the material, *e.g.* for PMD the maximum temperature was 100°C), and then cooled from 590°C to 35°C. Then the data were analysed by using the universal analysis thermal software.

2.2.7 Differential Scanning Calorimetry (DSC)

DSC is primarily method used for determining the energetics of the phase transitions within a macromolecule. It works on the principle of measuring the heat capacity of thermally induced events as a function of temperature. Though there are multiple applications of DSC ranging from determining the melting point, purity and the temperature of crystallisation but in polymers its mostly used to determine the glass transition temperature (Tg) (Chiu and Prenner, 2011).

DSC analysis of the samples used a DSC Q1000 (TA, Instrument, UK). The instrument was calibrated with indium (156.6°C). Experiments were carried out in an inert nitrogen atmosphere with a flow rate of 50 ml min^{-1}. Samples were subjected to different heating rates ranging from 10-50°C min^{-1}. Samples weighing between 3-9 mg were sealed (having a small hole to prevent the explosion of the volatile compounds). The samples were generally subjected to two cycles of heating and cooling: (i) samples were held at 35°C for 5 minutes, (ii) ramped from 35°C to 200°C, (iii) held at 200°C for 5 minutes, (iv) gradually cooled down from 200°C (at the rate of 10-50°C min^{-1}) to 35°C. Thermograms were analysed for melting events and for glass transition temperatures (Tg).

2.2.8 Elemental Analysis

CHN elemental analyses were obtained from MEDAC LTD, analytical and consultancy services. An elemental analyser (FLASH EA 1112 series, Thermo-Finnigan, Italy) was used for C (carbon) elemental analysis. For the analysis, combustion and reduction tubes (PerkinElmer) were used. The combustion reaction was run at 975°C in the presence of pure helium and oxygen as a carrier gas. For the determination of the carbon content, carbon in our samples was converted to carbon dioxide (CO_2) through combustion reaction followed by its quantification.

2.2.9 Liquid Chromatography-mass spectroscopy (LC-MS)

LC-MS analysis used an LC system coupled to an Apex-Q FTICR mass spectrometer (Bruker Daltonics) with a phenyl column (0.25 mm thickness). Spectra were obtained by electron ionization at 70 eV. 2μL of the sample was injected. Compounds (PMD and acryloyl-PMD (APMD) were quantified by using the external standards of the same compound, *i.e.* PMD and APMD at different concentrations. Five to six concentrations of the compounds were prepared from a stock solution of 1mg/mL (r^2=0.98).

2.2.10 Culturing *Dugesia lugubris (*Planarian) in the Laboratory

Dugesia lugubris (Schmidt, 1861) a planarian species is a useful organism in various laboratories for studying neurological development to toxicology. Planarians are freshwater flatworms which are inexpensive and simple to grow and maintain in the laboratory. *Dugesia lugubris* (catalogue LZC-030) was purchased from Blades Biological Limited (Cowden, Edenbridge, Kent TN8 7DX, UK).

2.2.10.1 Materials for the Culture

Materials used to culture and maintain planaria included glass beakers, large Petri dishes (26 cm × 15 cm × 8 cm), sterile plastic transfer pipettes, paper wipes, waste storage containers containing acetone:ethanol (1:1 v/v) (to store the dead or used planaria), chicken meat to feed the planaria, disposable gloves, ice, blender/food grinder, steel strainers and scalpels.

2.2.10.2 Culture Expansion

Planaria (*Dugesia lugubris*) (Figure 2.2) were retained in artificial pond water (APW) made by adding 0.5 g of instant ocean salt in 1000 mL of Milli-Q water (having 18.2 MΩ/cm resistivity) at ambient temperature. They were fed with uncooked chicken meat that was finely chopped at a quantity sufficient for nourishing planaria once a week. The APW was changed every 48 hours. The planaria were kept in a large beaker at a density of 50-100 worms with 3–15 mm body length in 2500 mL of prepared APW. It was important to ensure that the container had no residual chemical waste as planaria are extremely sensitive to chemical contamination.

Figure 2.2. Swimming *Dugesia lugubris* in APW. Scale bar is 2mm

Planaria were cultured in a dark room (to avoid algal growth in pond water and the natural light reluctance (negative phototaxis) of planaria) at room temperature. The culture was regularly examined to monitor the condition of the planaria. For culture development and expansion, planaria were fed once per week. Any mucus or residues accumulated inside surface of the beakers were wiped off by using a paper towel, especially in the regions where the worms were located. In cases where the culture generated a foul smell, colour changes or water degradation (worms twisting, wriggling and spinning in a corkscrew-like fashion was an indicator of culture contamination) it was immediately replaced with fresh APW in a new clean beaker.

References

Bates, J.B., 1976. Fourier transform infrared spectroscopy. Science (80-.). 191, 31–37.

Carrier, M., Loppinet-Serani, A., Denux, D., Lasnier, J.-M., Ham-Pichavant, F., Cansell, F., Aymonier, C., 2011. Thermogravimetric analysis as a new method to determine the lignocellulosic composition of biomass. Biomass and bioenergy 35, 298–307.

Chiu, M.H., Prenner, E.J., 2011. Differential scanning calorimetry: An invaluable tool for a detailed thermodynamic characterization of macromolecules and their interactions. J. Pharm. Bioallied Sci. 3, 39–59. https://doi.org/10.4103/0975-7406.76463

Gillie, J.K., Hochlowski, J., Arbuckle-Keil, G.A., 2000. Infrared spectroscopy. Anal. Chem. 72, 71–80.

Glish, G.L., Vachet, R.W., 2003. The basics of mass spectrometry in the twenty-first century. Nat. Rev. Drug Discov. 2, 140–150. https://doi.org/10.1038/nrd1011

McDonald, R.S., 1986. Review: infrared spectrometry. Anal. Chem. 58, 1906–1925. https://doi.org/10.1021/ac00122a003

Watson, D.G., Pgce, B.S.C.P., 2020. Pharmaceutical analysis E-book: a textbook for pharmacy students and pharmaceutical chemists. Elsevier.

Wellner, N., 2013. 6 - Fourier transform infrared (FTIR) and Raman microscopy: principles and applications to food microstructures, in: Morris, V.J., Groves, K.B.T.-F.M. (Eds.), Woodhead Publishing Series in Food Science, Technology and Nutrition. Woodhead Publishing, pp. 163–191. https://doi.org/https://doi.org/10.1533/9780857098894.1.163

https://www.microanalysis.com.au//wp-content/uploads/2015/10/FTIR-Graph.png

Chapter 3. Synthesis of p-menthane-3,8-diol (PMD) and Preliminary Attempts to Synthesise a Polymer-Drug Conjugate

3.1. Introduction

p-Menthane-3,8-diol (PMD) was synthesised in order to develop a polymer-drug conjugate. The rationale for the synthesis of conjugate was; primarily to develop a system for prolonged drug release as compared to the conventional use of free PMD. The hypothesis was that the drug (PMD) would conjugate with the polymer through an ester bond. Then, under the action of naturally occurring esterase enzymes on the skin, the drug would be released over an extended period. Numerous studies have reported the use of enzymes to cleave the ester bond, followed by the release of the drug (*e.g.,*Natfji et al., 2017). Secondly this approach would minimize drug uptake into and absorption through the skin and hence reduce systemic PMD uptake. The hypothesis for this was that the molecular weight of the polymer would prevent (or certainly minimise) absorption since in general, molecules with relatively low molecular weights (<500 Da), and that are lipophilic tend to permeate through skin as evidenced by drugs such as oestradiol, nicotine and fentanyl which are successfully administered from patches (Bos and Meinardi, 2000). Various studies raise specific concerns over the systemic absorption of insect repellents such as N,N-Diethyl-meta-Toluamide (DEET) and consequent side effects, especially regarding their use in pregnant women and the neonates (Tavares et al., 2018).

PMD, also ascribed as 1-(2-Hydroxy-4-methylcyclohexyl)-1-methylethanol and P-Menthane-3,8-diol, is a biochemical pesticide derived in small amounts from the essential oil of an Australian plant *Corymbia citriodora* (*Eucalyptus citriodora)* leaves. This active ingredient is used to make products that are applied to human skin and clothing to repel insects, such as mosquitoes and sandflies (Pandey et al., 2009). It is used in two types of consumer insecticide products: a spray and a lotion. It is a monoterpenoid alcohol with a formula of $(CH_3)_2CHC_6H_{10}CH_3$. It is a colourless liquid with a fragrant fennel-like odour. It occurs naturally, especially in exudates of *Eucalyptus* fruits. The molecular weight of the PMD is 172.27 g/mol, whilst its water solubility is poor having a logP value of 1.88 showing its high lipophilicity. The compound is generally encountered as a mixture of two cis and trans isomers, which have similar properties (Maia and Moore, 2011).

Polymer-drug conjugates have been extensively researched for more than 40 years (Elvira et al., 2005). There are various means to link the polymer with the drug covalently; the work presented here is focused on polymer-drug ester conjugates. Various examples have been reported in the literature for the successful conjugation of the polymers with the drugs through

esters bond (Larson and Ghandehari, 2012), using different chemical strategies (Avendaño and Menéndez, 2008; Halpern et al., 2014). Some of these are coupling through N,N-dicyclohexylcarbodiimide (DCC) or 1-ethyl-3-(3-dimethylaminopropyl)carbodiimide (EDC), making polymer or drug/ammino acid a better leaving group (Jung and Theato, 2013).

This chapter will focus on the synthesis of PMD followed by the chemical challenges involved in the synthesis (preliminary attempts), which lead to the final approach resulting in successful conjugation and characterization (described in chapter 4). Though PMD is commercially available, however, for this project the materials were synthesised in house to ensure purity and minimise batch-to-batch variability.

3.2. Materials

Hyaluronic acid (sodium salt) (MW 1.6MDa) was obtained from Contipro, Dolní Dobrouč, Czech Republic (Contipro obtains hyaluronic acid from cell walls of *Streptococcus zooepidemicus* bacterial culture), citronellal, dimethylsulfoxide (DMSO), sodium chloride, sodium carbonate anhydrous, Hcl and thymol were obtained from Fischer Scientific Co., UK. n-Heptane, (benzotriazol-1-yloxy)-tripyrrolidinophosphonium hexafluorophosphate (PyBOP) 4-dimethylamino pyridine, thionyl chloride and N,N-dicyclohexylcarbodiimide were obtained from Acros Organics., UK. N,N diisopropyletylamine (DIPEA), dowex ion exchange resin (mesh size 50-100), poly (acrylic acid) (1,800 Da and 1.2 MDa), polyethyleneglycol dimethylether (dmPEG), tertrabutylamine (TBA) were obtained from Sigma-Aldrich Co., UK.

3.3. Methods

3.3.1. Synthesis of PMD

PMD was synthesized by the method described by Yuasa et al. (2000). Briefly, 116g of sulphuric acid aqueous solution 0.25% (w/w) was first heated at 55°C with stirring. Then to this 100g of citronellal (the starting material) was added slowly and was stirred at the same temperature for the next 11 hours. Then 1.4 g of sodium hydroxide aqueous 25% (w/w) solution was added to it. After this, 120 mL of n-heptane was added in such a way that two layers, *i.e.,* an organic and an aqueous layer, were created. The reaction was monitored by TLC analysis using formaldehyde solution (4:1 v/v, hexane: ethyl acetate, used as mobile phase). The organic layer was collected and distilled to remove any water. The organic solution was then cooled to -50°C with continuous stirring for 20 h. After 20 h time period, transparent crystalline material was filtered. The yield was 38%.

3.3.1.1. Choice of Polymer for the Selection of Conjugation

The selection of the polymer was based upon two main criteria, one was that polymer should be non-immunogenic and should not have any adverse reactions such as irritation on skin and the other was presence of suitable group, *i.e.,* COOH to form an ester bond. The first polymer selected based on these criteria was hyaluronic acid (HA). HA is a natural polymer that acts as a skin emollient and is used in various dermatological products (Huang and Huang, 2018). HA is a naturally occurring glycosaminoglycan found all through the connective tissues. It is a nonimmunogenic and biodegradable polymer (Alaniz et al., 2002). Various research papers have reported successful conjugation of HA with drugs (Chen et al., 2014), including paclitaxel, Oncofid-S, biphosphonates, doxorubicin and cisplatin (Arpicco et al., 2014). Based on these reasons, it provided us with a base for the selection of hyaluronic acid as a first choice for the conjugation.

Another critical parameter for the selection of the polymer was to prevent absorption of the drug through the skin. Since in general, molecules that have relatively low molecular weight (< 500 Da) and that are lipophilic tend to permeate through the skin. Thus, based on this we selected the polymers with high molecular weight to prevent topical absorption, hence initially, we choose the HA with high molecular weight (Essendoubi et al., 2016). Additionally, HA is humectant, and retains water molecules onto the exterior of skin to maintain it pleasant and hydrated state.

3.3.2. Preliminary Attempts for the Conjugation

3.3.2.1. Synthesis Using the Method of Sahoo et al. (2008)

Several attempts were made to conjugate HA with PMD. The first method used was the one reported by Sahoo et al. (2008) with some modifications. Briefly, Dowex ion exchange resin (12.5g) was washed three times with 250 mL of water and then treated with 25 mL of TBA and left to react at room temperature for 1 hour. The resin was then filtered and collected. Then 1g of hyaluronic acid was dissolved in 100 mL of distilled water to which 10g of the Dowex-TBA resin was added, and the reaction was allowed to proceed at room temperature for 18 hours. The reaction mixture was filtered through a 0.45 μm sterile filter, the supernatant collected and freeze-dried for three days to yield HA-TBA mixture (Figure 3.1-a). Almost 500 mg of this mixture was dissolved in 60 mL of anhydrous DMSO, to this HA-TBA mixture, 0.5 mL of DIPEA and 0.9g of PyBop were added and left stirring at room temperature for 1 h. Finally, 1g of PMD was added, and the mixture was left stirring for another 24 h at room temperature.

3.3.3.2. Synthesis Using Fischer Esterification Reaction

The Fischer esterification theory and use of this theory on some polymers/compounds have been reported previously (Kantlehner, 1991; Wassei et al., 2011). Based upon this theory the first step was to convert the supplied HA into free HA which was then followed by the conversion of the hyaluronic acid to a hyaluronic acid chloride and then reacting it with PMD (Figure 3.1). For this, the following protocol was used. Firstly, sodium hyaluronate was dissolved in water to make a solution (1% w/v). To this, 1.0 mL of an acid (HCl, 4M) was added to generate a pH of 2.0. Then this solution was enclosed in a dialysis membrane (Medicell International Ltd., UK) having a molecular cut off value of 12-14,000 Da. The medium (distilled water) was changed periodically until the pH stabilized at 5.0. After this, it was subjected to freeze-drying for 3 days to obtain free hyaluronic acid. After the production of free hyaluronic acid, it was then refluxed with thionyl chloride at 75°C for 3 h, after which thionyl chloride was evaporated, and the obtained material was subjected to NMR.
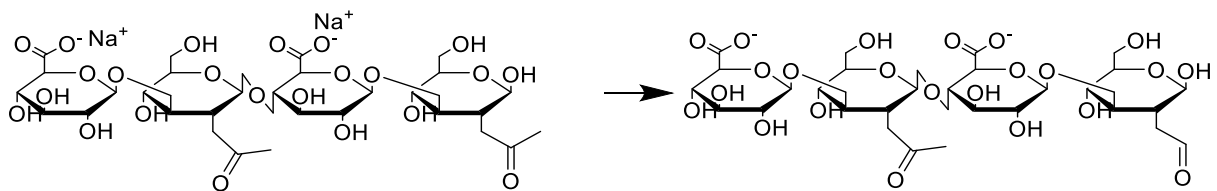
a) Conversion of HA to acid chloride form making it a better leaving group
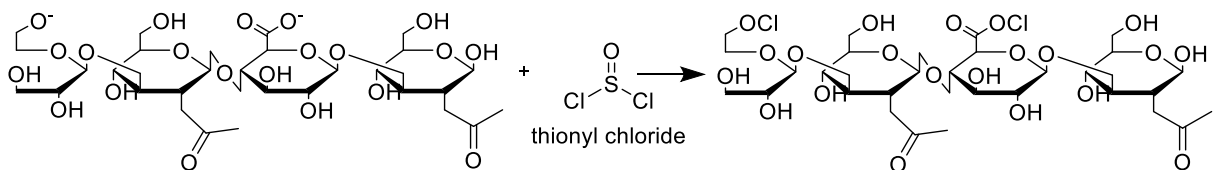
Figure 3.1. Steps used in Fischer Esterification Reaction for the generation of HA.

3.3.3.3. Synthesis Using the Method of Lee et al. (2008)

In this technique, the authors successfully reported conjugation of HA with paclitaxel (PX) through an ester bond by using dicyclohexylcarbodiimide (DCC) an activating agent for the carboxylic groups of HA (Lee et al., 2008). Briefly, for a desalting process, 1.0 g of HA (1.6 MDa) was dissolved in 100mL of deionized water, dialyzed (MWCO: 10-12k Da) for 24 h, and lyophilized. A blended mixture of desalted HA and dmPEG was added in 25mL of deionized water. The solution was well-stirred and lyophilized to obtain a dry HA/dmPEG complex powder. A total of 300mg of lyophilized HA/dmPEG complex was added in 5mL of anhydrous DMSO under an inert environment (using argon) with vigorous stirring at 80°C for 2 h. To this then DCC and DMAP were added and the solution was stirred for 1.0 h to activate carboxylic groups of HA. To the above solution, a solution of PMD (prepared by dissolving 100 g of PMD in 5mL of anhydrous DMSO) was slowly added using a syringe under an inert environment. The mixture was then stirred for 2 days at 40°C. The resultant solution was dialyzed against DMSO for one day and deionized water for three days using a dialysis membrane (MWCO: 10-12 kDa) to remove unreacted PMD and dmPEG.

3.3.4. Changing the Approach: From High Molecular Weight to Low Molecular Weight

The main aim of this study was to convert the high molecular weight HA into low molecular weight in an attempt to increase the reactivity of the polymer. For this purpose, the method reported by Tømmeraas and Melander, (2008) was applied (Tømmeraas and Melander, 2008). Briefly, 1g of HA was dissolved overnight at room temperature in 100 mL of deionized water. The solution was prewarmed to 60°C before adding 1.0 M HCl under vigorous stirring for 1 minute to give an acid concentration of 0.10 M. The total HA concentration was adjusted to 10 mg/mL. The mixture was left without agitation at 60°C (in an oil-filled thermostatic water bath) for a total of 52 h. Samples (5 mL each) were withdrawn over 52 h time. Each sample was immediately cooled on an ice-bath and neutralized with equimolar amounts of NaOH (1.0 M solution) before freezing and lyophilization.

3.3.4.1. Use of Poly(Acrylic Acid) as a Polymer

Due to the failure of the above methods, as an alternative approach, HA was replaced by another polymer, namely poly(acrylic acid) (PAA). PAA is a hydrophilic polymer, commercially available with an excellent safety profile (Ritthidej, 2011). PAA is used in topical formulations, *i.e.,* Lubrizol's Carbopol® applied in pharmaceutical industry as rheology convertors, suspension solidifiers, mucoadhesive facilitators, pill binders, extended release polymers, and bio-accessibility garnisher. PAA has suitable groups, *i.e.,* COOH to form an ester bond between the polymer and the PMD (Ritthidej, 2011). For the reasons mentioned above, a high molecular weight PAA was selected.

3.3.5. Synthesis Using the Method of Shin et al. (2014)

In this technique, the authors productively reported the conjugation of hyaluronic acid with methotrexate through an ester bond by using dicyclohexylcarbodiimide (DCC) as an activating agent for the carboxylic groups of hyaluronic acid. The basic principle of this method was first the activation of the carboxylic group (by making it a better leaving group) and then reaction with an alcohol to form a polymer-drug conjugate. The reaction was performed according to the basic scheme as outlined in the article (Shin et al., 2014). In brief, 100 mg of PAA (1.2 MDa; 0.083 micromoles) was dissolved in 33.33 mL of formamide to give a concentration of 3 mg/mL. Then, the solution was further diluted with 25 mL of dimethyl sulfoxide (DMSO) and allowed to stir at room temperature. To this DCC (15 mg) and DMAP (9 mg) were added

and stirred for a further 30 mins to activate the carboxyl group of PAA. Then to this an excess amount of the alcohol (10mg of PMD, to increase the chances of esterification) was added and the resulting solution was mixed under vigorous stirring at room temperature for 24 h, in the dark (by wrapping an aluminium foil around the flask). After that, the product was centrifuged at 3000 rpm for 5 min to remove any unreacted dicyclohexylurea residue, followed by purification using a dialysis membrane (MW cut-off = 12,000 ~14,000) against deionized water for two days, and lyophilization.

3.3.6. Synthesis Using the Procedure of Madgey et al. (2012)

The authors successfully reported conjugation of poly(acrylic acid) with salicylic acid. In this method, first of all, poly(acrylic acid) (both high molecular weight and low molecular weight were used) was converted into poly(acryloyl chloride) by using thionyl chloride (to provide a better leaving group) before attempting conjugation with PMD. Briefly, about 1.4 mole of thionyl chloride was added dropwise to 1.0 mole of polyacrylic acid in a round-bottom flask. The reaction mixture was stirred for 1 h at 60°C and left to cool at room temperature. The unreacted thionyl chloride was collected by filtration. The obtained product (PAA reacted with thionyl chloride) was washed with anhydrous methylene chloride and dried overnight in a vacuum at 40°C. A solution of 0.25 mole of PMD and 0.75 moles of triethylamine in 300 mL acetonitrile was added dropwise to 0.3 moles of poly(acryloyl chloride) pre-soaked in 100 mL acetonitrile for 6 h. After complete addition, the reaction mixture was stirred further for 6 hours at 25°C. The product was filtered off and washed with methanol, 1M HCl and distilled water one after another to remove the formed triethylamine hydrochloride and finally with diethyl ether. The obtained product was dried overnight under vacuum at 40°C.

3.3.7. Change of the Drug

It is well known that secondary and tertiary alcohols (PMD) are sterically more hindered hence tend to be less reactive than primary alcohols (Watile et al., 2019). So, to increase the reactivity of the compound towards the polymer a primary alcohol with somewhat structural similarities with PMD as well as some insect repellent properties was selected, specifically thymol (Pandey et al., 2009; Sharma and Anand, 1997). Both of the above approaches in 3.3.6 and 3.3.7 were

repeated with thymol (of converting the polymer into an acyl halide and then reacting with alcohol and DCC coupling) and PAA but in neither case products could be produced.

3.4. Results and Discussions

3.4.1. Transformation of Citronellal to PMD

The preparation of para-menthane-3,8-diol isomers from (+)-citronellal uses an acidic medium, as shown in Figure 3.2. The acidic medium acts as a catalyst for the cyclization of (+)-citronellal into para-menthane-3,8 diol (primary step in the synthesis of the said compound). Here HCl acted as an acidic medium in order to carry out the desired reaction.
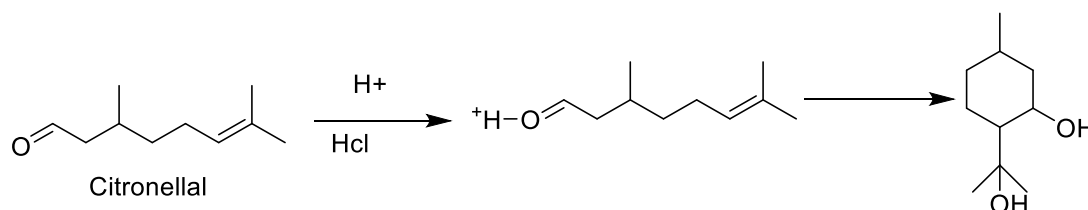
Figure 3.2. Schematic presentation of acid-catalysed cyclisation of (+)-citronellal into para-menthane-3,8-diol.

In this study, we evaluated different parameters as reported by Yuasa. et al. (2000) namely the acid concentration, the temperature of the medium and the reaction time. All these parameters were optimized and contributed to improving the conversion of citronellal to generate the highest yield of PMD during the reaction. The parameter with the highest yield was selected for the synthesis of PMD. The results are displayed in the Table 3.1.

Table 3.1. The effect of Various Parameters Upon the Final Conversion of (+)-Citronellal into PMD.

Run	Acid concentration (%)	Temperature (°C)	Time (hours)	Conversion of (+)- citronellal into PMD (mol %)
1	0.25%	50°C	24	44.8
2	0.5%	55°C	20	42.3
3	1%	60°C	16	43.1
4	1.5%	65°C	12	44.6
5	2%	70°C	8	43.5
6	2.5%	75°C	4	41.9

Table 3.1 shows clearly the change in the conversion of (+)-citronellal as a function of different parameters. The period for the conversion changed significantly by varying the acid concentration (acidity). It was necessary to stir it in a 50°C bath for 15 h, which is conceivable for a mass production perspective. The synthesis was reproducible (with a mean value of yield = 44 ± 5.2 %, n=6). Conversion of citronellal was calculated as:

Conversion (%) = citronellal$_{t=0}$ - citronellal$_{t=t}$ /mol citronellal$_{t=0}$

Reaction progress was monitored by using thin layer chromatography (TLC) analysis, which provided two clear spots (citronellal and PMD) using 20% ethyl acetate in an 80% hexane v/v solvent system. Purification was done on a silica gel column (230 − 240 mesh) using the same eluent system as above. NMR analysis was done to identify the final product (Figure 3.4). It is clear from ^{1}H-NMR spectra of PMD, giving characteristics peaks for CH$_3$ and for the secondary and tertiary OH groups (Figure 3.4-A and 3.4-B) signifies the IR spectra for PMD**.**

From the TLC chromatogram indicated in Figure 3.3, it can be observed that over the period of time the side products are diminishing, and the final product (PMD) is obtained. The TLC chromatogram clearly indicate the starting materials, intermediate product and the final product that is PMD.
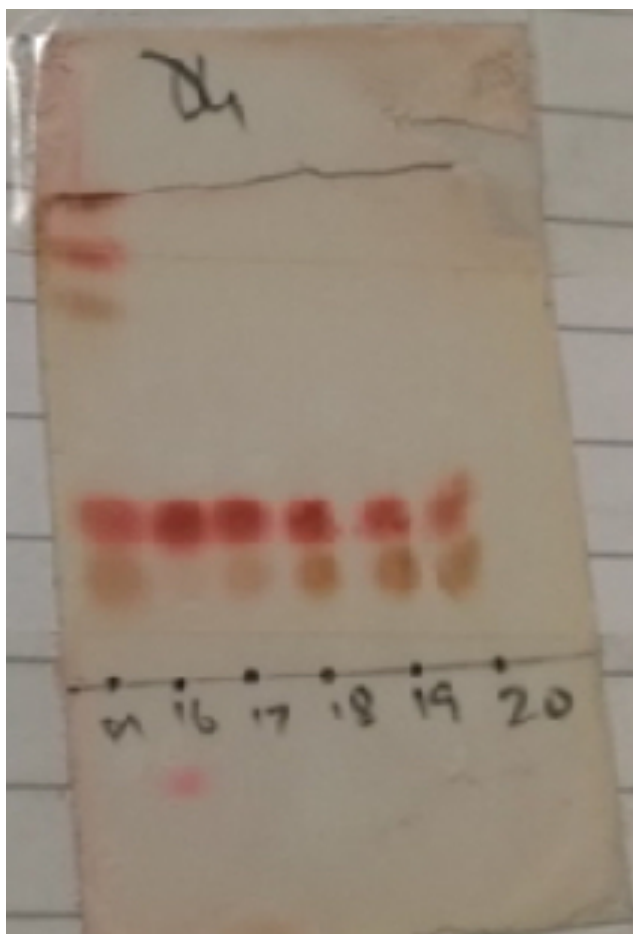
Figure 3.3. TLC chromatogram showing the gradual conversion of the citronellal into PMD as reaction proceeds

A)
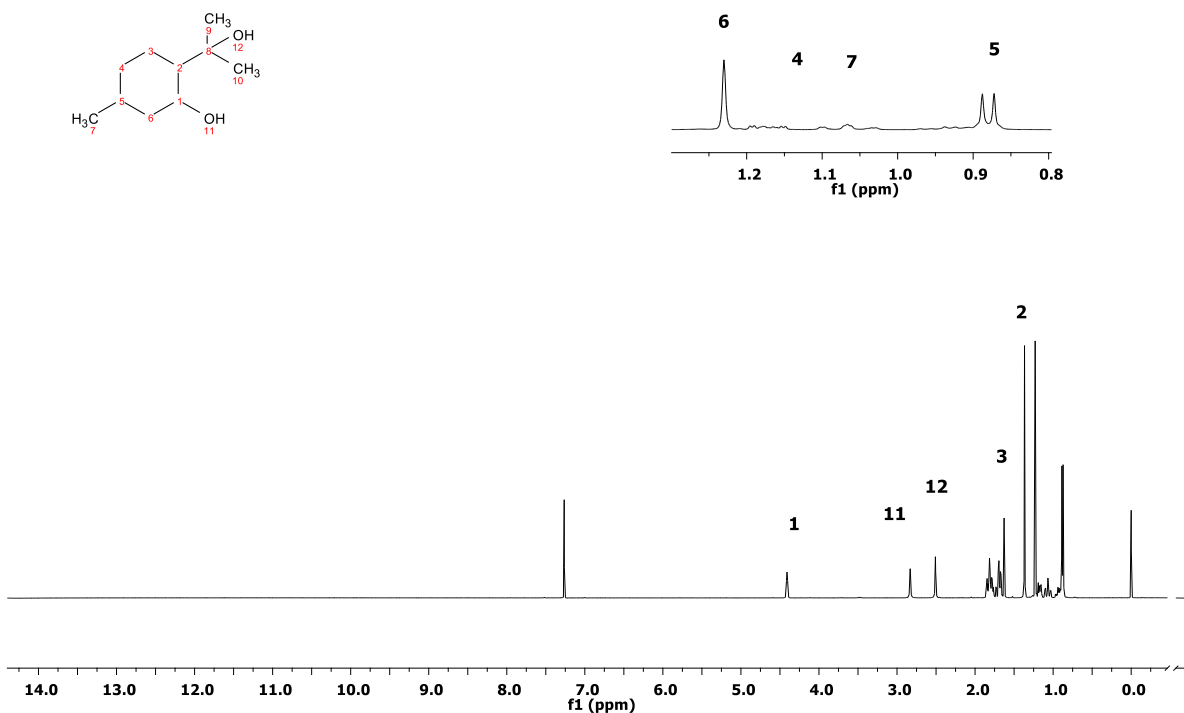
B)
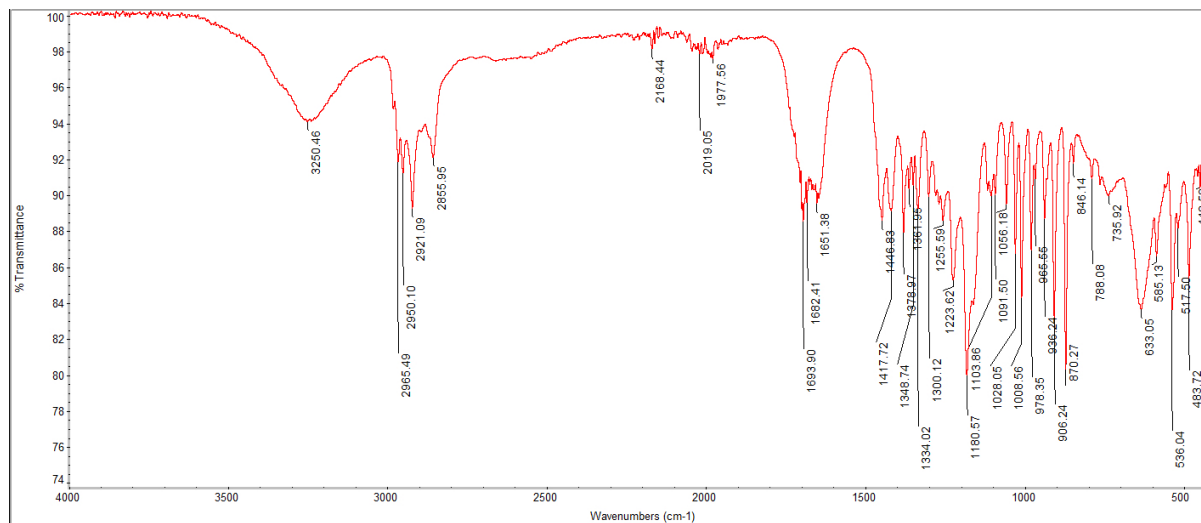
Figure 3.4. ^{1}H-NMR spectrum of (A) PMD, having characteristics peaks for CH$_3$ and for the secondary and tertiary OH groups (B) IR spectrum of PMD.

3.4.2. Preliminary Attempts to Synthesise a Polymer-Drug Conjugate Following

Sahoo et al. (2008)

The preparation of polymer-drug ester conjugates was not as straightforward as expected. Although the majority of reported polymer-drug conjugates (with HA or PAA) are largely prepared through amide bonds, a limited number of ester drug conjugates have also been reported. The published synthetic methods failed to produce desired polymer-drug ester conjugate.

The first method used for the conjugation between HA and PMD was described by Sahoo et al. (2008). PyBop is a phosphonium salt derivative. There have been reports suggesting the use of PyBop (a coupling agent) for the conjugation reaction between the carboxyl group and the amine group of peptides. The principle involved in this reaction is the activation of the carboxyl group by the PyBop coupling agent (Al-Warhi et al., 2012). Thus, based upon this, in this experiment, we used PyBop as a coupling agent between the COOH group of HA and OH group of the PMD. The first step in this reaction was the exchange of hyaluronan sodium salt to tert-butyl ammonium salt (TBA) in order to increase its solubility in DMSO. For the attachment of TBA with HA, first Dowex ion exchange resin was used (which facilitated the exchange of sodium ions from the HA with TBA) (Cerroni et al., 2015). The last step in this reaction was the addition of diisopropylethylamine *(*DIPEA) which acts as a base and is an essential ingredient in PyBop based synthesis (Singh and Argade, 2012).

There could be various reasons for the failure of the above-used method. The first can be the problems associated with human handling; for this, the reaction was repeated several times with as much care as possible regarding the handling of the experiment. The second reason can be the HA unable to react with the TBA but as seen from the Figure 3.5-D there are peaks related to TBA hence indicating that both of these reacted. Other two possible parameters that could have affected the said reaction would be the duration and the temperature of the reaction allowing the mixing of PMD with the rest of the reaction medium, *i.e.,* the temperature we used was ambient temperature while the duration of the reaction for which it was allowed to react was 24 h. In order to rule out the temperature the reaction was carried out at 30°C and the reaction time was increased to 48 h, but still, after those modifications, the desired results were not obtained.

A)
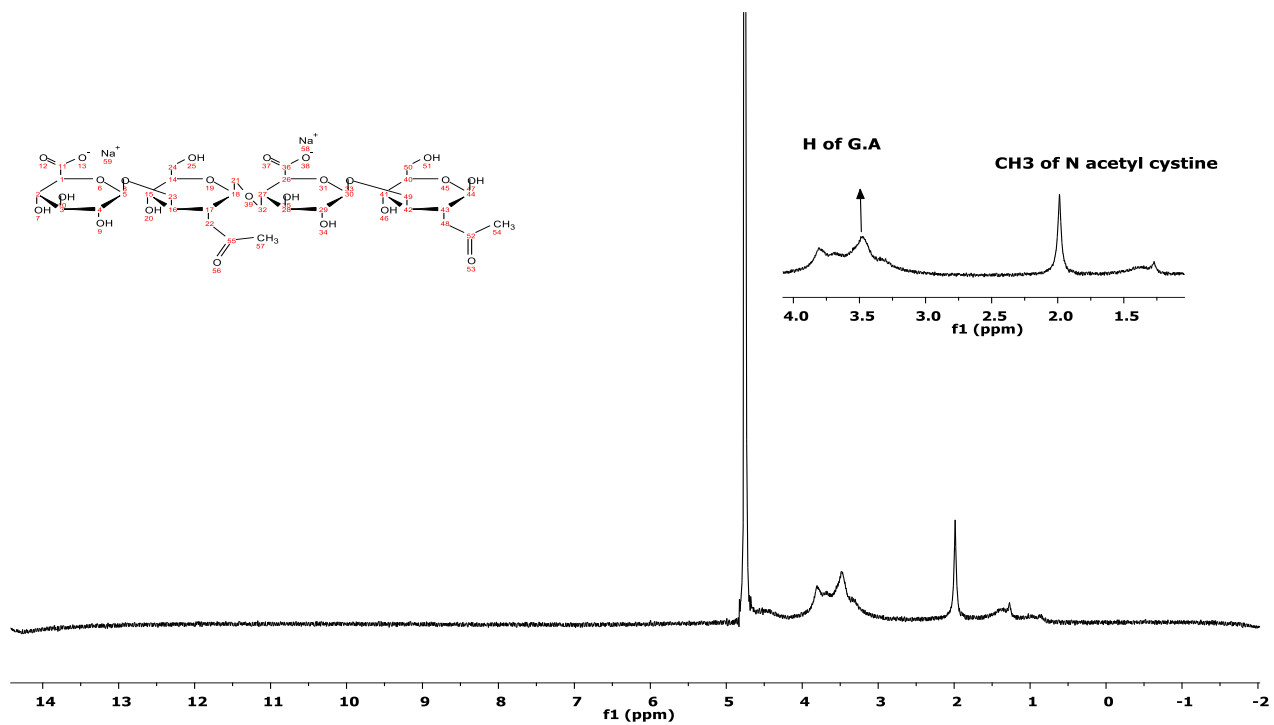
B)
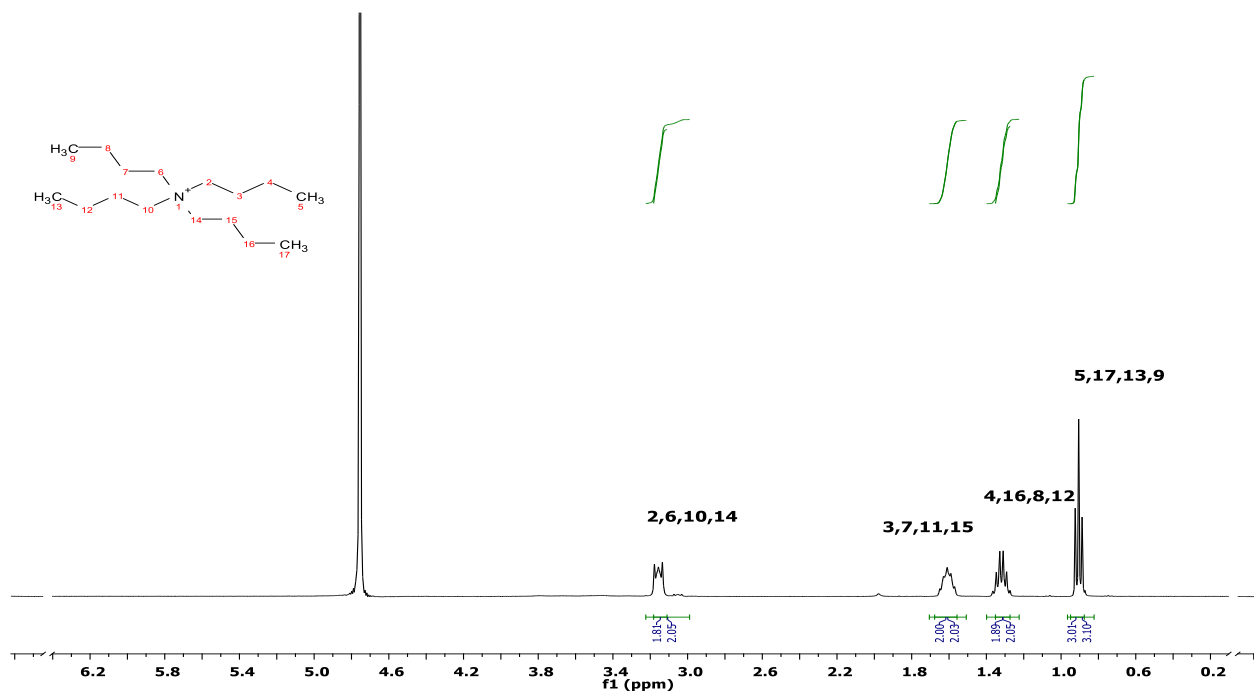
C)
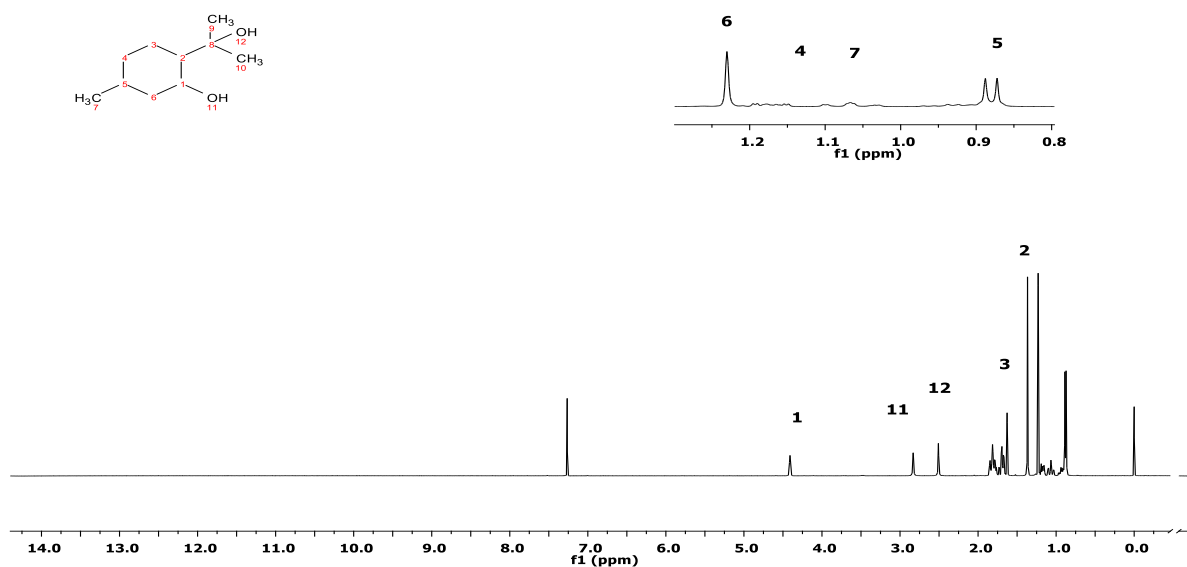
D)
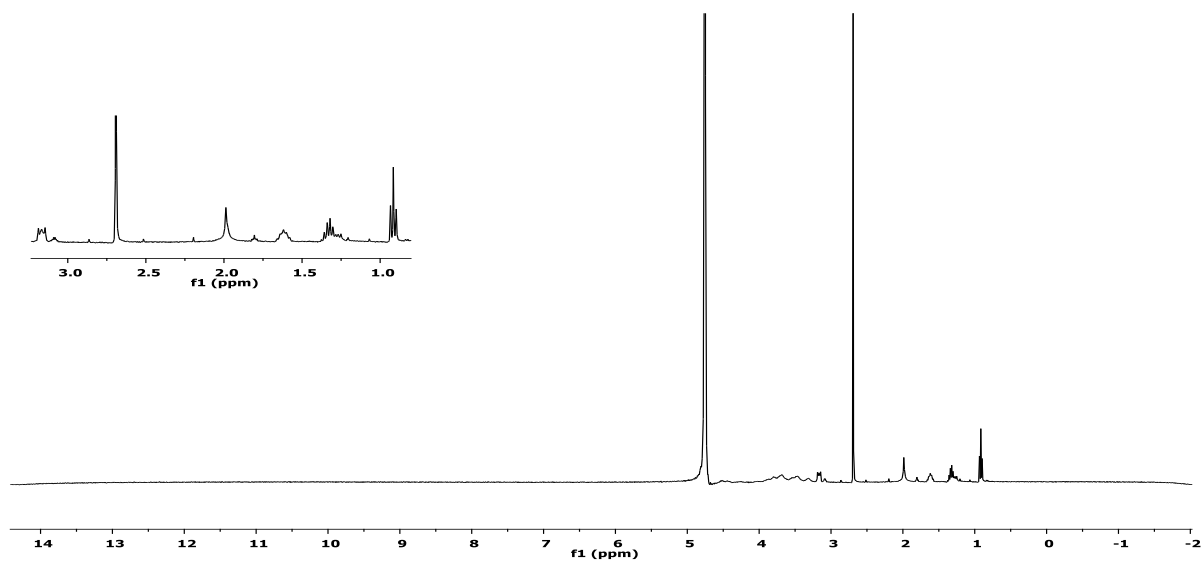
Figure 3.5. ^{1}H-NMR spectra collected from attempts to conjugate PMD with HA following the method of Sahoo et al., 2008. (A), spectrum of HA starting materials showing characteristic peaks for H of glucosamine and CH3 of N-acetylcysteine. (B), spectrum of TBA showing characteristic peak for NH2. (C), spectrum of PMD showing characteristic peaks for the secondary and tertiary OH groups. (D), spectrum of the final product indicating absence of PMD.

For the above outcomes, the most likely reason for this unsuccessful reaction may be a decreased affinity of the PyBop towards the hydroxyl groups of alcohol (PMD), though as indicated above, there are few examples of the successful conjugation. However, most of them account for the formation of the amide bond (between the carboxy and the amine groups) rather than the ester bond (Al-Warhi et al., 2012). Similarly, another possibility can be the formation of the side products during the chemical reaction that may hinder the conjugation of the said polymer and drug (Valeur and Bradley, 2009).

3.4.3. Synthesis Using Fischer Esterification Reactions

Another method that has been reported for the conjugation *via* an ester bond is to react an acyl halide with alcohol. In this method first, the carboxylic acid is reacted with a better leaving group, *i.e.,* chloride, *etc*. which is then reacted with alcohol in the presence of a base to form an ester (Ouellette and Rawn, 2014). Here, firstly we needed to attach a better leaving group, *i.e.,* chloride with the polymer. For this purpose, here, we have used thionyl chloride, which is a standard reagent used for the introduction of the chloride group (a leaving group) as shown previously by Petten et al. (2015).

There are several potential reasons for the failure of this reaction. The first could be the inability of the hyaluronic acid sodium salt to convert into free hyaluronic acid. Moreover, as it has been reported that the above certain temperatures there is a significant degradation/denaturation of HA (Mondek et al., 2015) which in our case was indicated by the change of colour of the HA solution (possibly indicating the degradation of HA). Consequently, instead of refluxing the reaction mixture at 65°C it was reacted at 50°C for 4 h. After changing the temperature, though there were no signs of the degradation of the polymer at the same time, there was also no conjugation between the HA (polymer) and the PMD (drug) as indicated in Figure 3.6-C. Thus, it can be concluded that although this decrease of the temperature was important to prevent the degradation of the polymer, it appears likely that this temperature was insufficient to cause the reaction between the HA and the PMD and hence can be the key factor in the unsuccessfulness of the said reaction.

A)

H of G.A

CH3 of N acetyl cystine
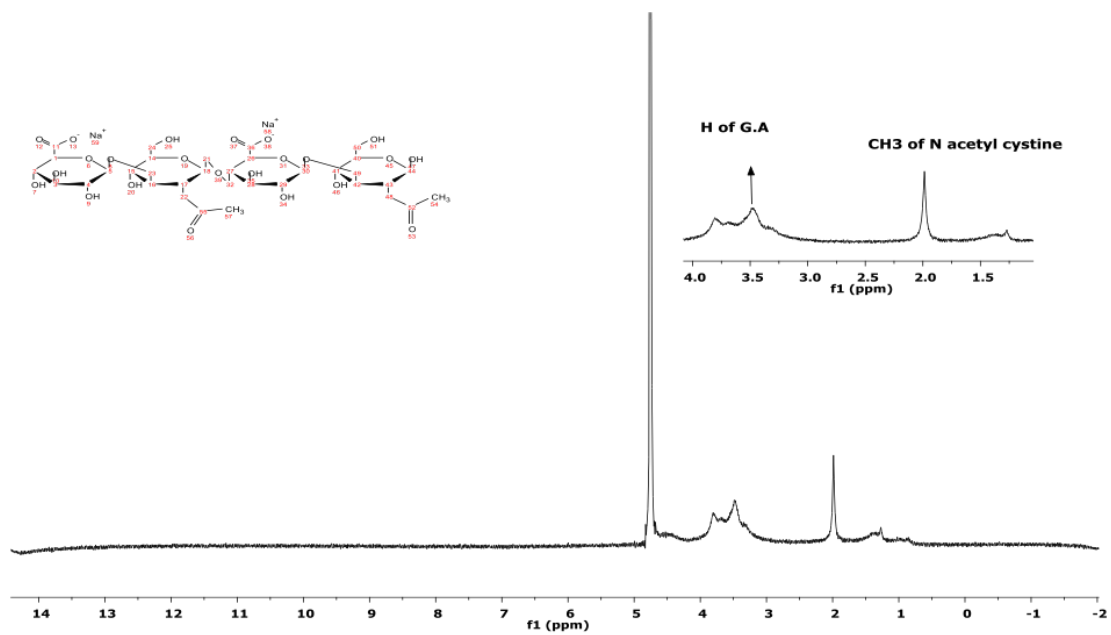
B)
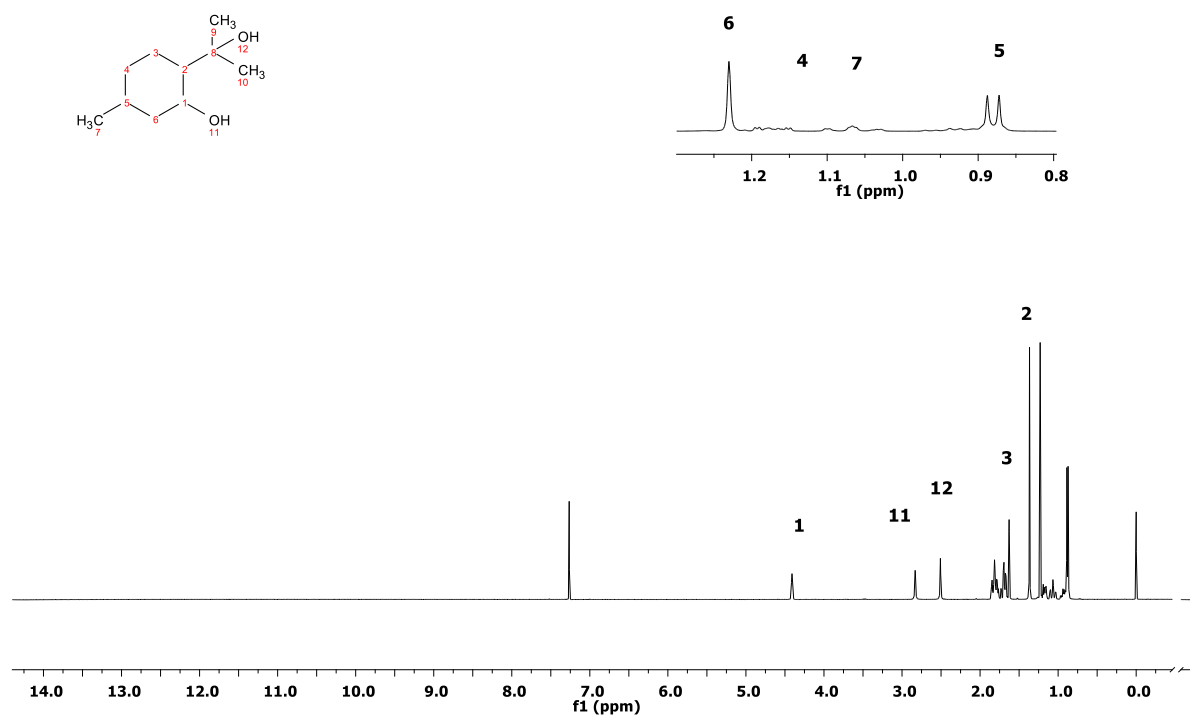
C)
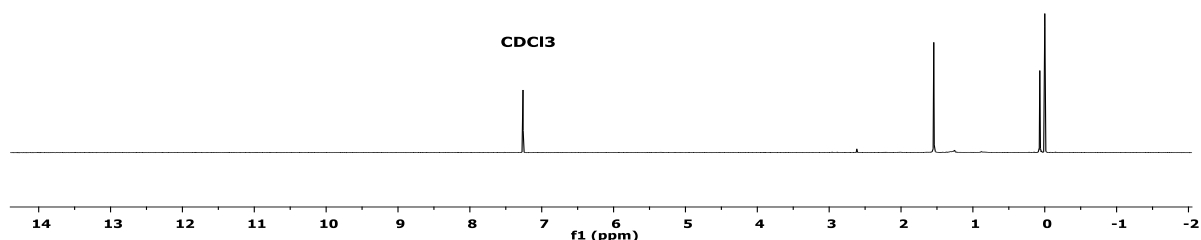
Fig 3.6. ^{1}H-NMR spectra collected from attempts to conjugate PMD with HA following the Fischer esterification method. (A), spectrum of HA starting materials showing characteristic peaks for H of glucosamine and CH$_3$ of N-acetylcysteine. (B), spectrum of PMD showing characteristic peaks for the secondary and tertiary OH groups. (C), spectrum of the final product indicating absence of PMD.

Synthesis Using the Method of Lee et al. (2008)

An alternative method to conjugate a polymer with the drug is by using DCC coupling. This method is based upon the activation of the carboxyl group (COOH) and then the subsequent conjugation with the drug. The first step for this reaction was converting the sodium hyaluronate into a free acid form. After that, in order to dissolve the free acid form of HA in DMSO, it was conjugated to polyethene glycol (dimethyl ether), for this reaction, DMAP added, which is required at 5 mol % for the efficient formation of esters ("Stiglich-esterification @ www.organic-chemistry.org," n.d.). From the results presented in Figure 3.8, it can be seen that the conjugation did not occur.

Again, there are several potential reasons for the unsuccessful reaction; the first one can be the unsuccessful reaction of dmPEG and the free HA. This was unlikely since the HA was able to dissolve in DMSO, as the solubility of free HA is very low in DMSO. Another possibility can be the unavailability of the dry conditions in the reaction as this reaction is very moisture

sensitive. Whilst the reaction uses dry conditions it is feasible that moisture could have entered the said reaction. Another reason for the failure of the reaction could be the not all of the carboxy groups of the HA were activated which may be due to the use of the very high molecular weight of HA; the high molecular weight could have hindered the access to all of the carboxy groups within the polymer which coupled with the sterically hindered hydroxy groups of the PMD may would have resulted in the unsuccessful outcome.

A)
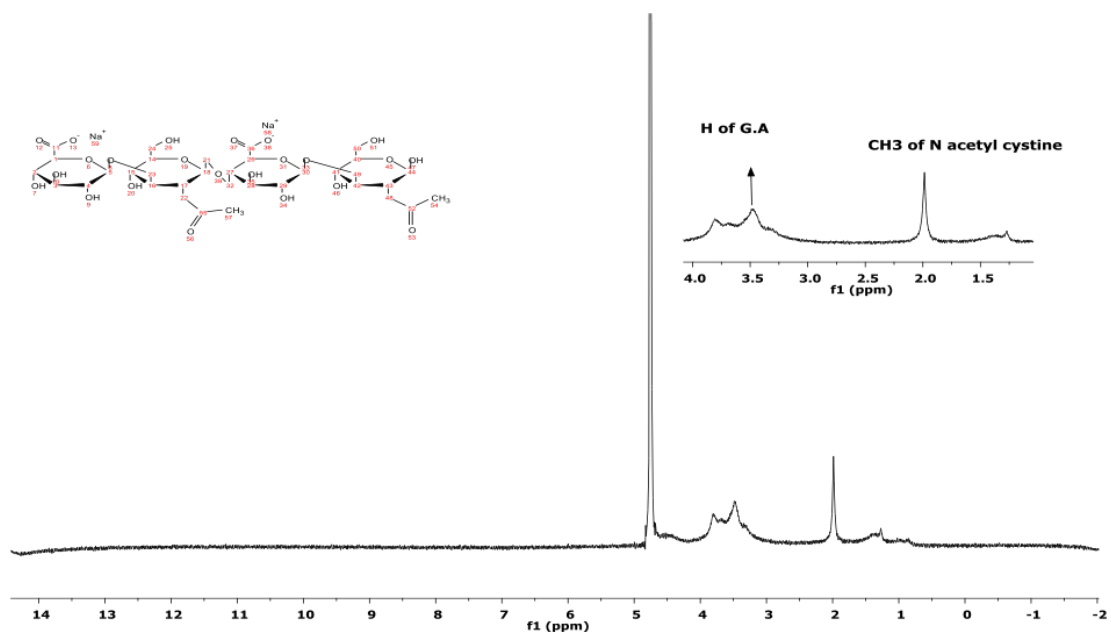
B)
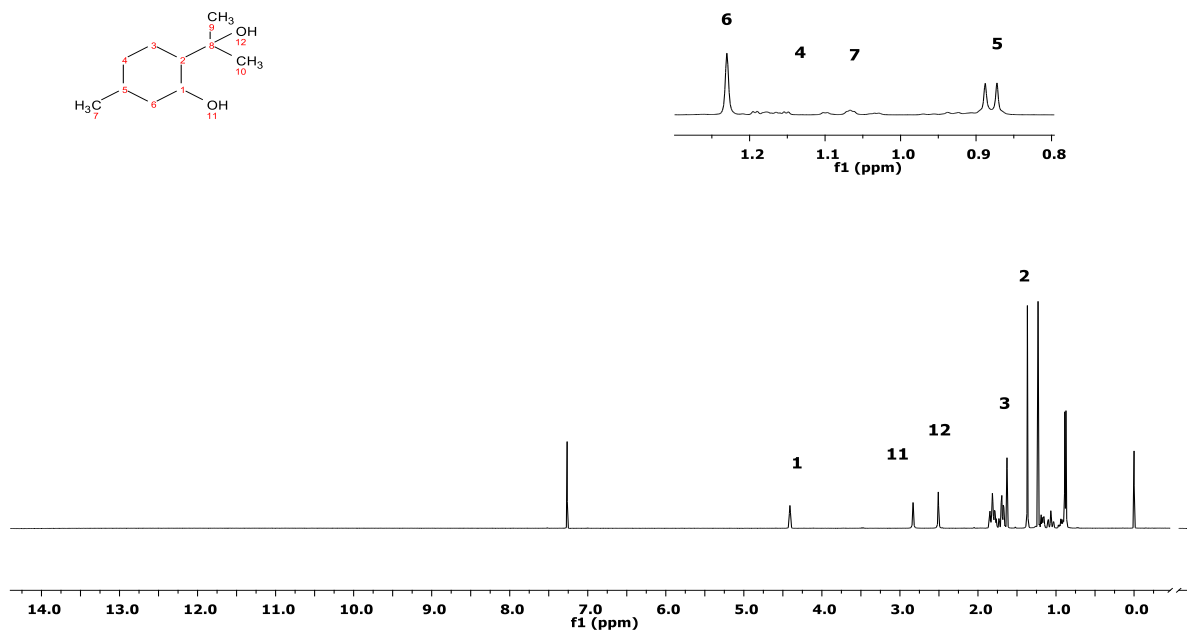
C)
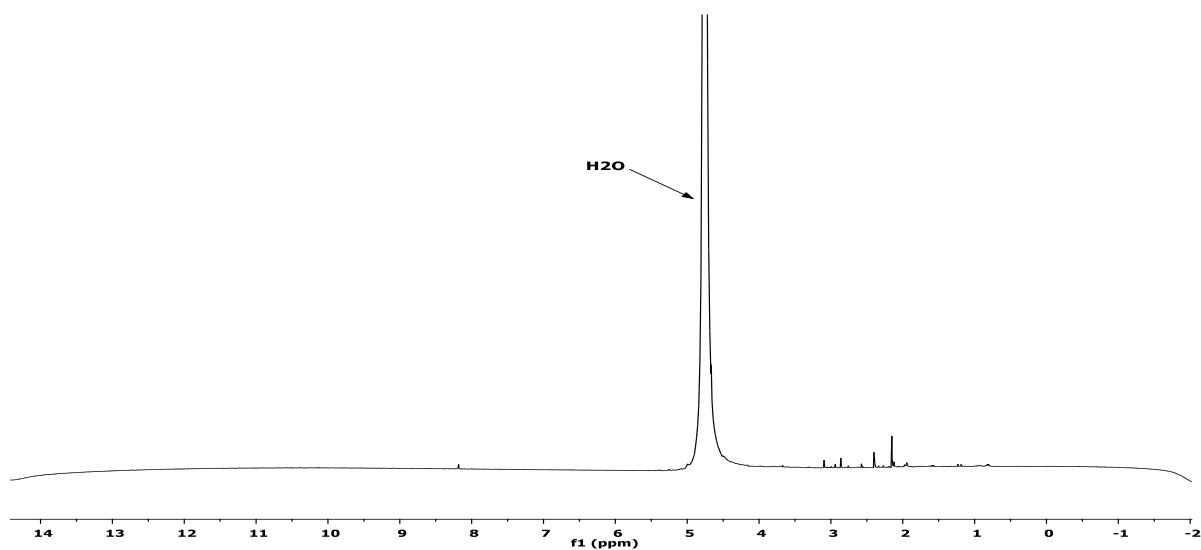
Figure 3.7. ^{1}H-NMR spectra collected from attempts to conjugate PMD with HA following Lee et al. (2008) (A), spectrum of HA starting materials showing characteristic peaks for H of glucosamine and CH$_3$ of N-acetylcysteine. (B), spectrum of PMD showing characteristic peaks for the secondary and tertiary OH groups. (C), spectrum of the final product indicating absence of PMD.

3.4.4. Changing the Approach: From High Molecular Weight to Low Molecular Weight

Initially, the HA that was used had a molecular weight of 1.6 MDa. As it has been reported that by decreasing the molecular weight, the reactivity of the polymer can be increased (Bernal et al., 2003), so to break the long chains of the polymer harsh conditions in the form of high temperature (60°C) and acidic environment (1M HCl) were provided. Upon following the indicated procedure (Bernal et al., 2003), the obtained solutions were subjected to gel permeation chromatography (GPC) in order to evaluate molecular weights. Results showed that various fractions of different molecular weights were found. To separate these fractions, they were passed through the dialysis membranes of various molecular weight cut-offs from 3000-12000 Daltons. After that, low molecular weight HA was reacted with that of PMD by using the DCC coupling method as described above, but it failed in the desired conjugation. Possible reasons for the failure may be the;

a) Degradation of the polymer during the procedure to form low molecular weight HA.

b) Inability of the HA to react with PMD.

The first potential reason was unlikely because there were no signs of the degradation of HA in the NMR spectra of the sample as the spectra was in accordance with the data of Tømmeraas and Melander (2008). Similarly, other reasons can be the inability of HA to react with the PMD, which may be due to the inability of the DCC to activate the carboxylic groups of the polymer; the most probable reason of the failure of the said reaction.

A)
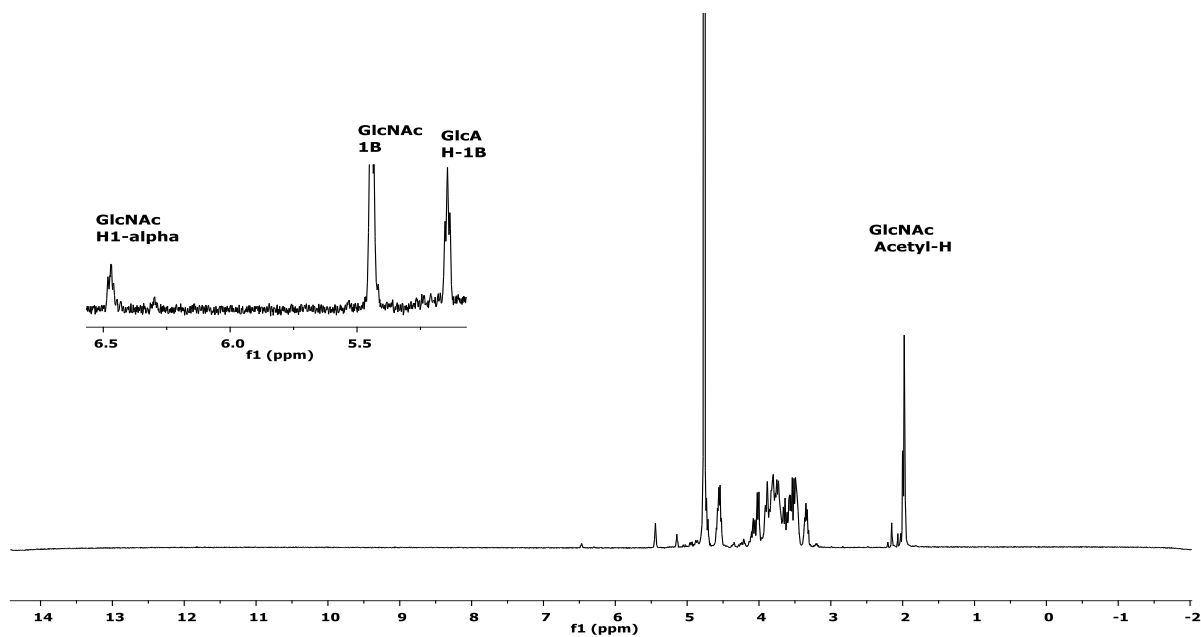
B)
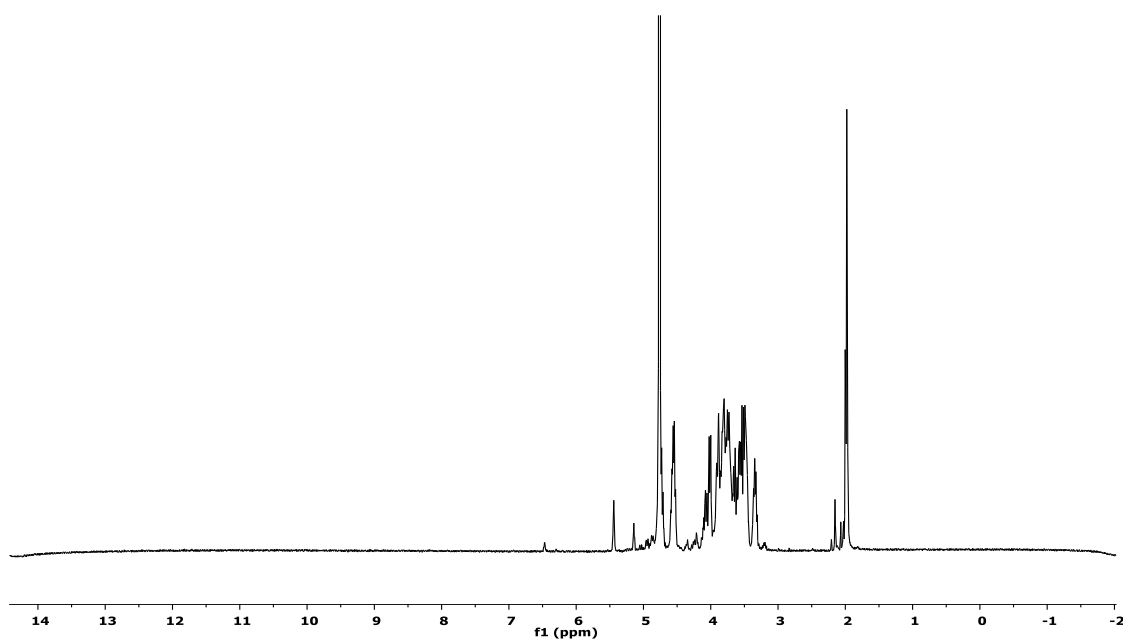
Figure 3.8. ^{1}H-NMR spectra collected from attempts to conjugate PMD with HA following the change of approach, using high to low molecular weight HA. A), spectrum of low molecular weight HA showing characteristic peaks for H of glucosamine and CH$_3$ of N-acetylcysteine. B), spectrum of the final product indicating absence of PMD.

3.4.5. Synthesis Using Procedure of Shin et al. (2014)

Given the lack of reactivity or conjugation with either high or low molecular weight HA, using varied synthetic routes, it appears that it is the polymeric carrier that was problematic. Consequently, attempts switched from HA to PAA, a polymer with excellent safety profile and has been used in topical formulations with the required chemical structure (possessing carboxylic groups) (Calixto et al., 2015). The technique opted here for the conjugation was as accomplished by Shin et al. (2014).

The main principle of this conjugation was based upon the formation of the ester bond by the DCC coupling method. However, this reaction also failed to produce the desired results. From experimental parameters possible reasons for this failure may be:

a) The amount of drug added
b) Reduced appropriate dark conditions to the solvent (formamide)
c) The temperature of the reaction
d) Unavailability of dry conditions

In order to ensure that the reaction did not fail because of the drug (PMD) availability, an excess amount of the drug was added. Similarly, it was ensured that during the reaction the round-bottomed flask (in which the reaction was taking place) was adequately covered with the aluminum foil. On the other hand, though in this case we did not further increased the temperature, but the possibility of the desired conjugation by increasing the temperature cannot be high, as previously described where HA did not give the desired results. Nevertheless, though this factor cannot be ruled out as there is possibility of the successful conjugation by increasing the temperature. Perhaps the most likely explanation was that there was some moisture ingress during the reaction since the solvent (DMSO) is highly hygroscopic.

A)
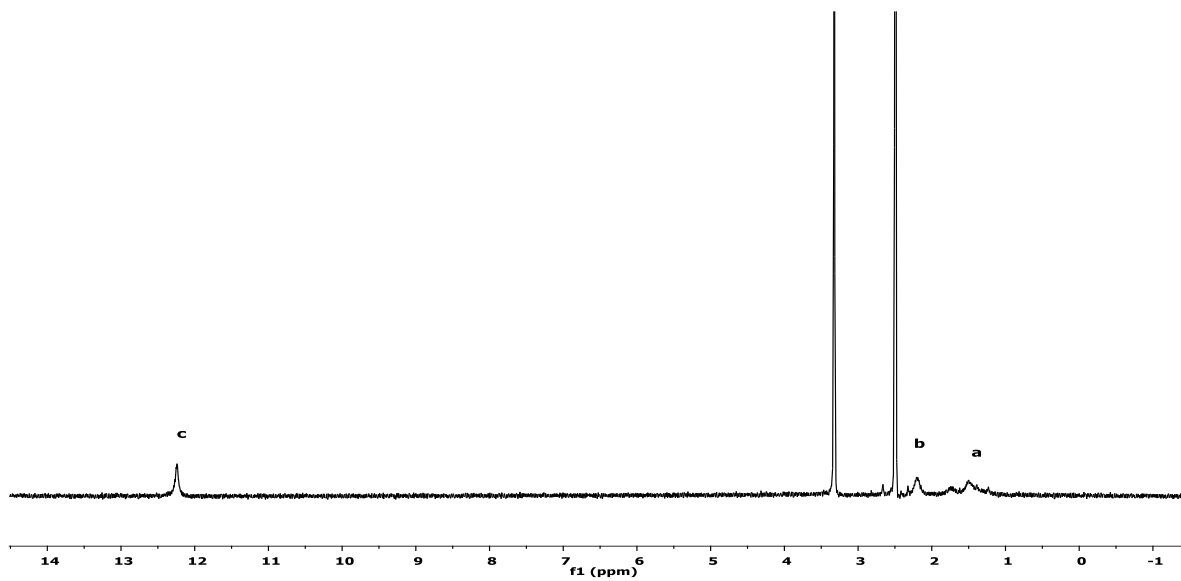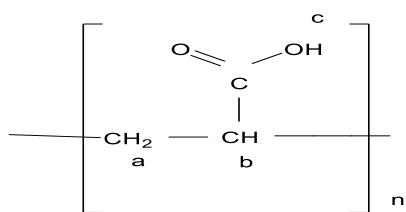
B)
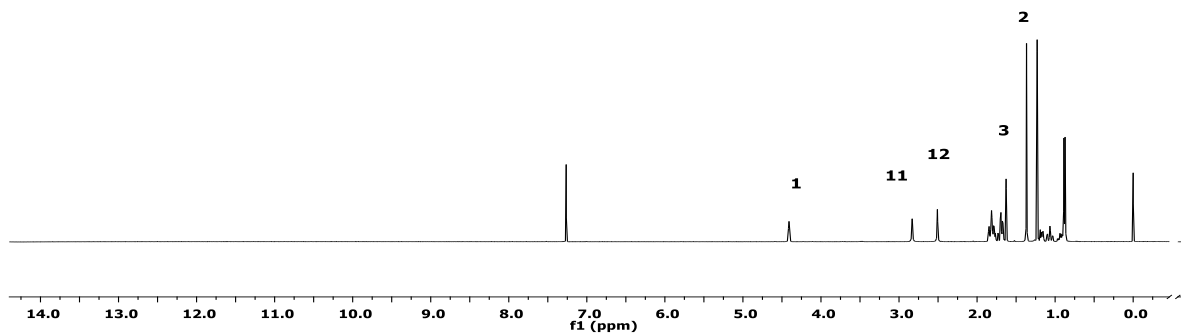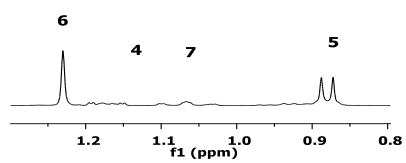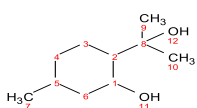
C)
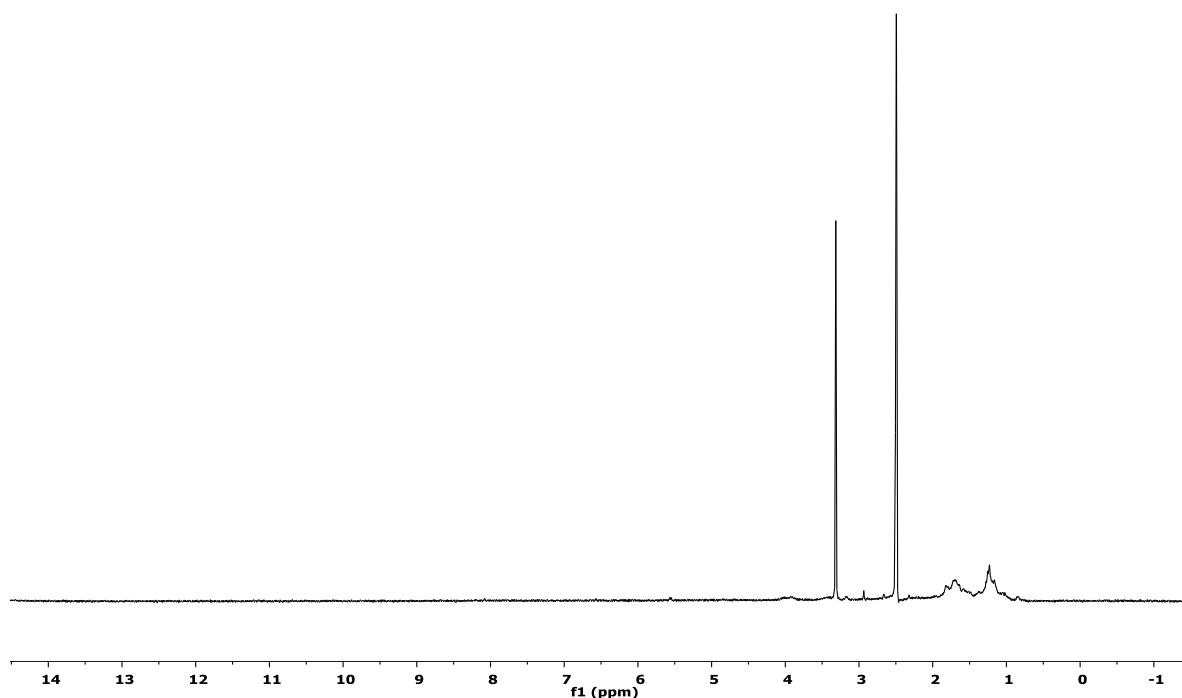
Figure 3.9. ¹H-NMR spectra collected from attempts to conjugate PMD with PAA following the method of Shin et al. 2008 (A), spectrum of PAA showing characteristic peak for COOH. (B), spectrum of PMD showing characteristic peaks for the secondary and tertiary OH groups. (C), spectrum of the final product indicating absence of PMD.

3.4.6. Synthesis Using the Method of Madgey et al. (2012)

Madgey et al. (2012) reported conjugation of PAA with salicylic acid through an ester bond by converting first PAA into poly(acryloyl chloride) and then subsequently reacting it with salicylic acid to form the said conjugate. Here, for the conversion of PAA into poly(acryloyl chloride), thionyl chloride was used, which after the required processing as outlined in the method was reacted with PMD. Though this method in the first attempt did produce good results but upon replicating the method was not reproducible. Possible reasons for the failure can be the inability of poly(acrylic acid) to be converted into poly(acryloyl chloride). The most probable reason for this failure can be as this method involved few steps after the reaction of PAA with thionyl chloride and during those steps most likely it was quite difficult to protect the converted polymer from the environmental moisture, hence, making it nearly impossible (even if the PAA was converted) to remain in poly(acryloyl chloride) form (Figure 3.10).

A)
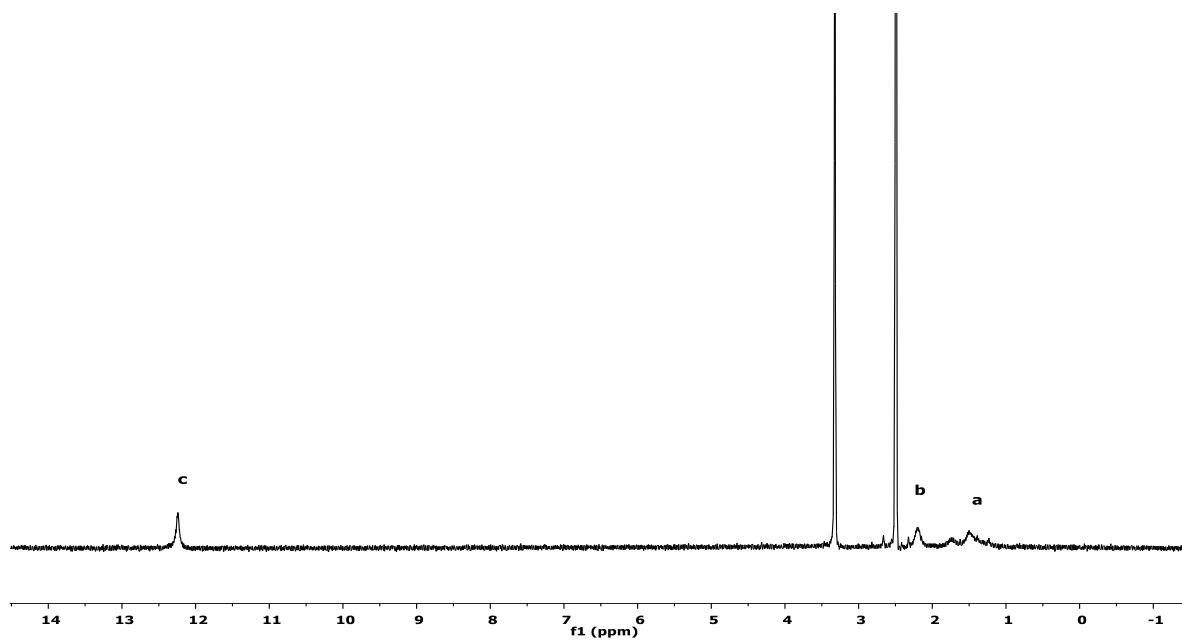
B)
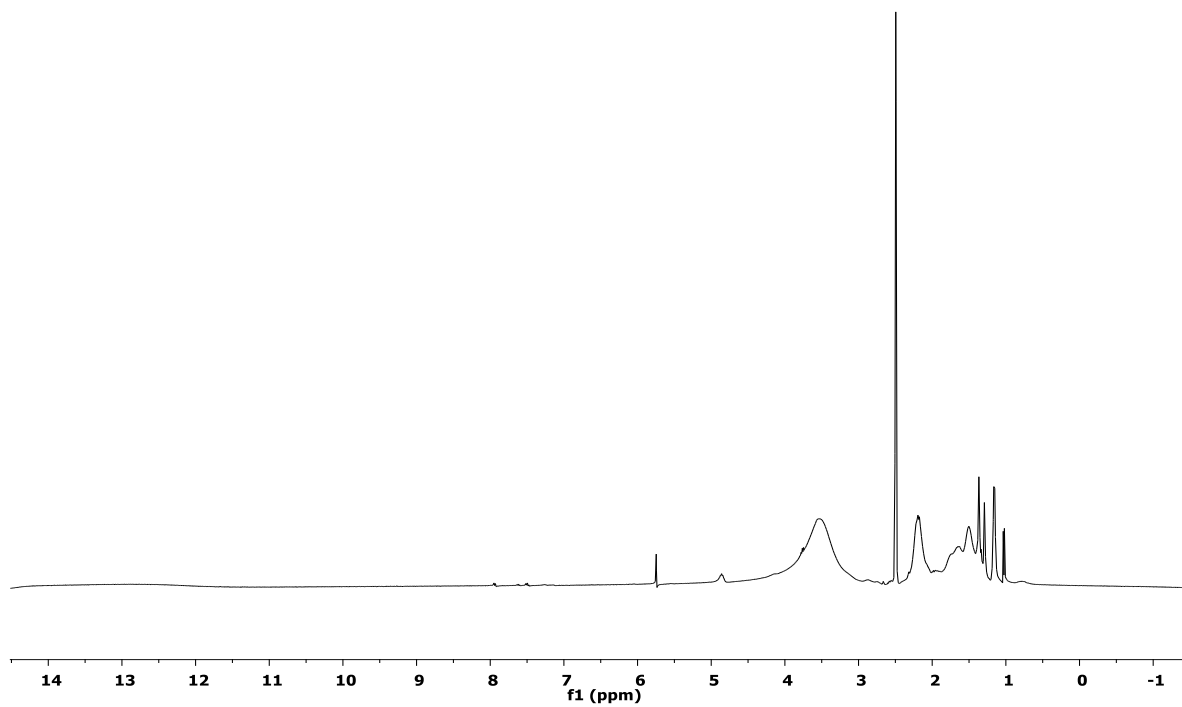
C)
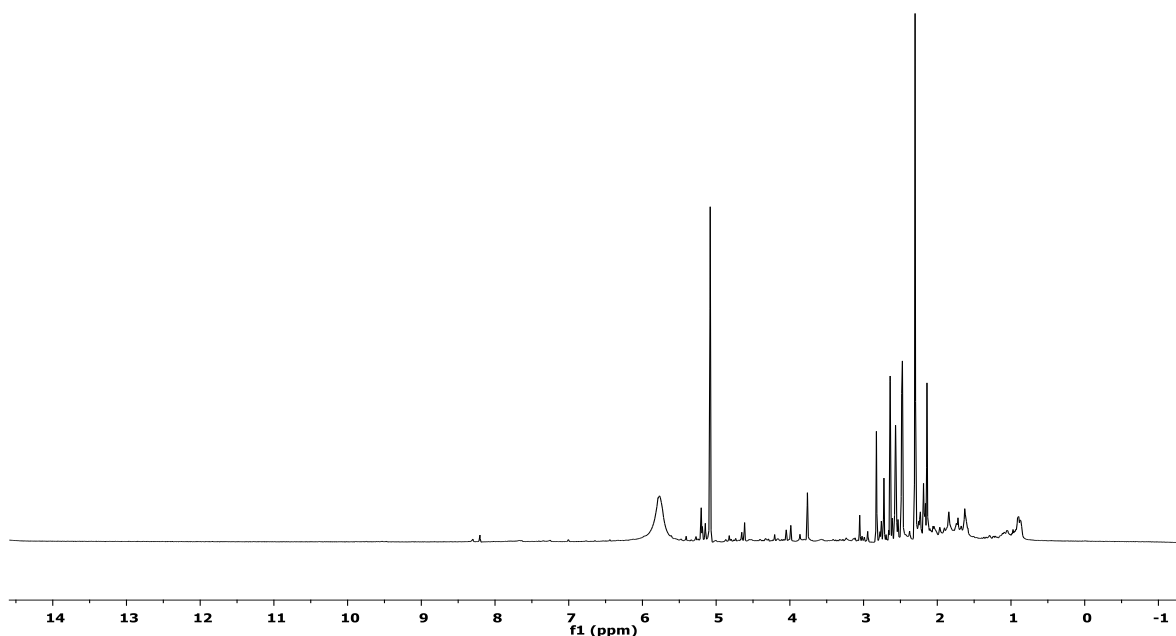
Figure 3.10. ^{1}H-NMR spectra for (A), PAA showing characteristic peak for COOH (B), PAA after treatment with thionyl chloride, showing reaction of COOH group of polyacrylic acid (C) PAA+PMD, having no signs of conjugation occurring

3.4.7. Change of the Drug

After these initial unsuccessful attempts, one of the proposed reasons for the failure of these reactions was the drug (PMD) has secondary and tertiary hydroxy groups making it difficult for them to react with the polymer. Based upon this, in order to see what will be the effect of the replacing PMD with a compound with the primary hydroxy group, we chose thymol. The reasons for choosing this compound was that it has a maximum resemblance to the PMD (in the structure) and also belongs to the same class of the compounds as that of PMD, *i.e.,* both are terpenoids, and also it has got some insect repellent properties (Pandey et al., 2009).

After selecting the new drug, *i.e.,* thymol, we employed the most commonly used methods in the literature for the formation of an ester bond, *i.e.,* conversion into an acyl halide. For this purpose, we followed previously described methods. The first in this list was by first converting poly(acrylic acid) into poly(acryloyl chloride) and then the reaction with thymol to form the

conjugate. In the first step, poly(acrylic acid) was successfully converted to poly(acryloyl chloride) which was indicated by the loss of the hydrogen for the carboxy group of poly(acrylic acid) which further indicated the presence of the Cl (Figure 3.11 C) after that conjugation was tried with the thymol. In this case, there was the appearance of one peak that was related to the drug, but the results were not reproducible (though being tried thrice under the same conditions). Moreover, the peak was for the OH group of thymol that in case of successful conjugation should have not been there (Figure 3.11 C).

In the second step as described before based on activation of the carboxylic group (by making it a better leaving group) and then reacting it with an alcohol to form a polymer-drug conjugate, DCC coupling method was employed which again failed to produce the desired results.

(A)

93
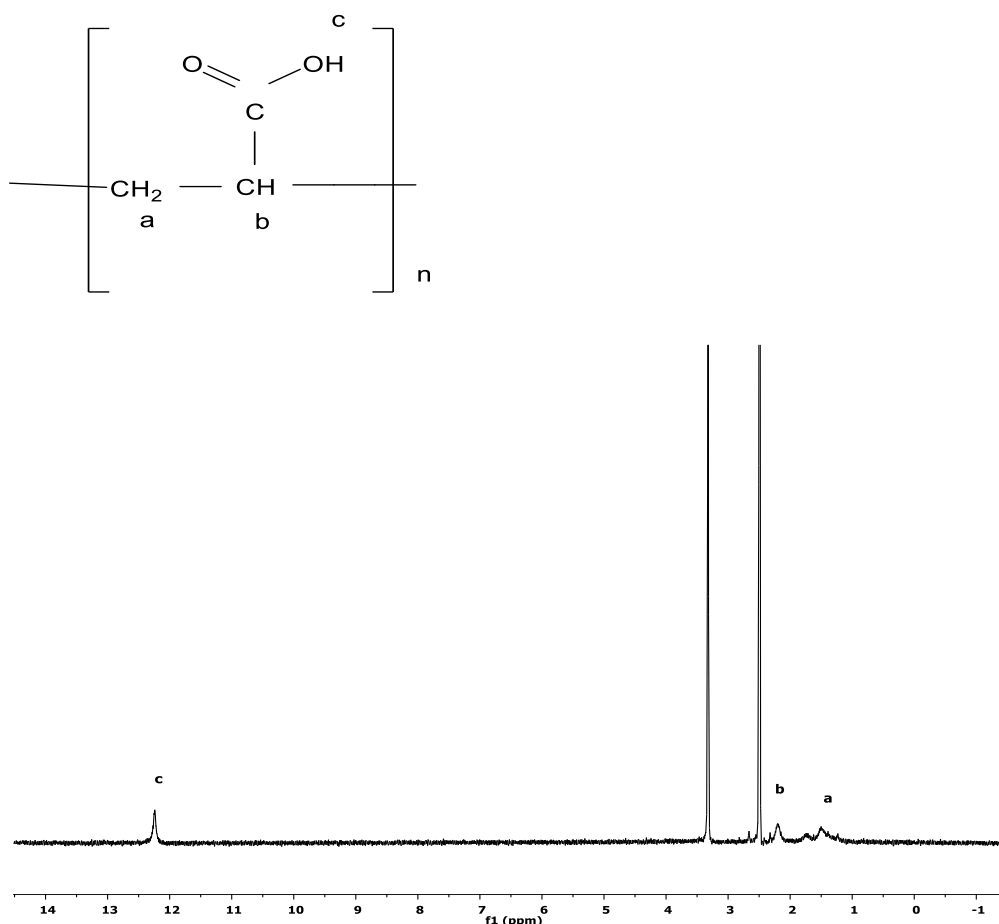
(B)
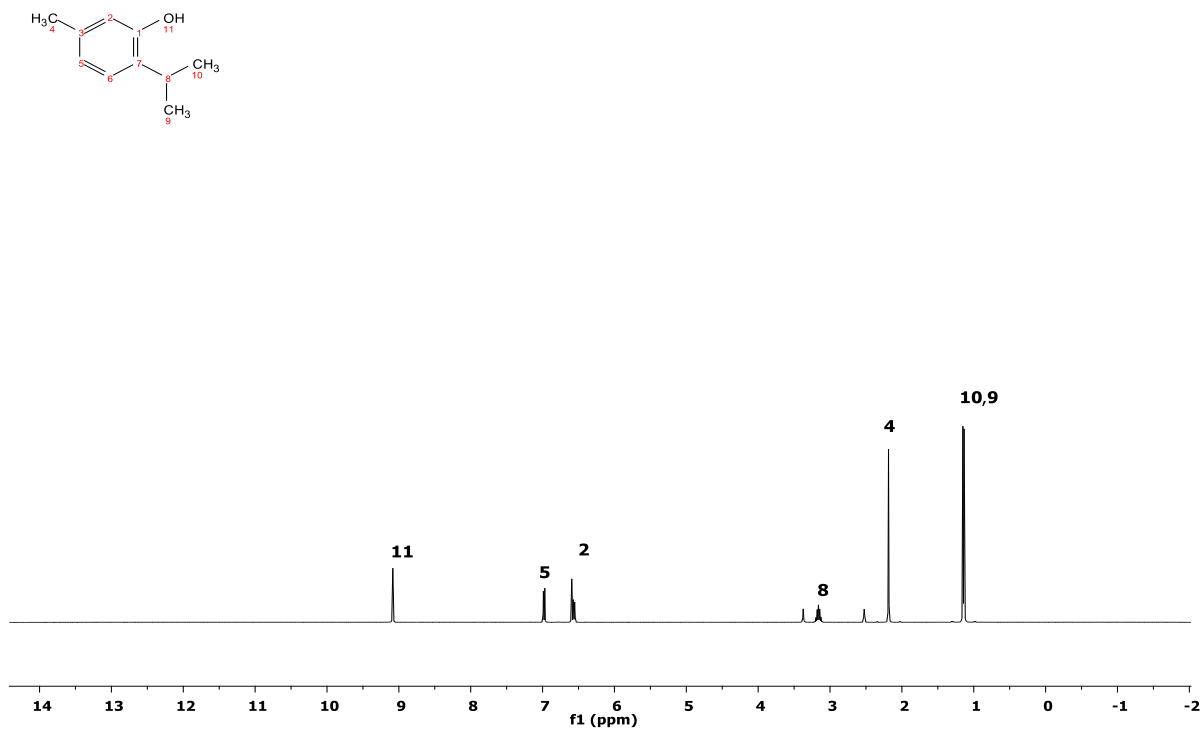
(C)
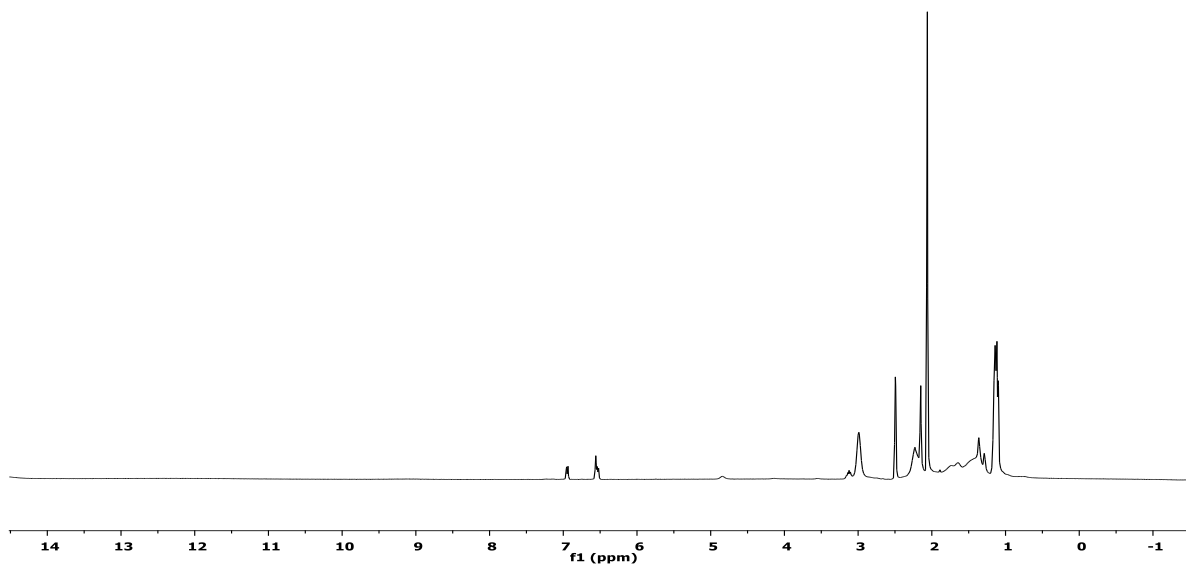
Figure 3.11. ¹H-NMR spectra for (A), PAA spectrum of PAA showing characteristic peak for COOH (B), Thymol, having a characteristic peak for primary OH group at 9.2 ppm (C) PAA+thymol showing no signs of conjugation

3.5. Conclusion

Due to the high molecular weight polymer initially used and the low reactivity of the PMD (because of secondary alcohol) the esterification of PMD was not that straightforward. The reported methods and our modifications to those procedures failed to yield the desired results. Despite changing the polymer, polymer molecular weight, solvents and the drug itself, the desired polymer-drug conjugate could not be synthesised. This led to the change of approach, *i.e.,* from polymer-drug conjugate to the monomer drug conjugate and then subsequent polymerisation of the said monomer drug conjugate to form a polymer with the incorporated drug (PMD).

References

Al-Warhi, T.I., Al-Hazimi, H.M.A., El-Faham, A., 2012. Recent development in peptide coupling reagents. J. Saudi Chem. Soc. 16, 97–116. https://doi.org /10. 1016/j.jscs.2010.12.006

Alaniz, L., Cabrera, P. V, Blanco, G., Ernst, G., Rimoldi, G., Alvarez, E., Hajos, S.E., 2002. Interaction of CD44 with Different Forms of Hyaluronic Acid. Its Role in Adhesion and Migration of Tumor Cells. Cell Commun. Adhes. 9, 117–130. https://doi.org/10.1080/15419060214522

Arpicco, S., Milla, P., Stella, B., Dosio, F., 2014. Hyaluronic acid conjugates as vectors for the active targeting of drugs, genes and nanocomposites in cancer treatment. Molecules 19, 3193–3230. https://doi.org/10.3390/molecules19033193

Avendaño, C., Menéndez, J.C., 2008. Chapter 11 - Drug Targeting in Anticancer Chemotherapy, in: Avendaño, C., Menéndez, J.C.B.T.-M.C. of A.D. (Eds.), . Elsevier, Amsterdam, pp. 351–385. /https://doi.org/ 10.1016/ B978-0-444-52824-7.00011-1

Bernal, D.P., Bedrossian, L., Collins, K., Fossum, E., 2003. Effect of Core Reactivity on the Molecular Weight, Polydispersity, and Degree of Branching of Hyperbranched Poly(arylene ether phosphine oxide)s. Macromolecules 36, 333–338. https://doi.org/10.1021/ma021510b

Bos, J.D., Meinardi, M.M.H.M., 2000. The 500 Dalton rule for the skin penetration of chemical compounds and drugs. Exp. Dermatol. 9, 165–169. https://doi.org/ 10. 1034/j.1600-0625.2000.009003165.x

Calixto, G., Yoshii, A.C., Rocha e Silva, H., Stringhetti Ferreira Cury, B., Chorilli, M., 2015. Polyacrylic acid polymers hydrogels intended to topical drug delivery: preparation and characterization. Pharm. Dev. Technol. 20, 490–496. https://doi.org/10.3109/10837450.2014.882941

Cerroni, B., Pasale, S.K., Mateescu, A., Domenici, F., Oddo, L., Bordi, F., Paradossi, G., 2015. Temperature-Tunable Nanoparticles for Selective Biointerface. Biomacromolecules

16, 1753–1760. https://doi.org/ 10.1021/ acs.biomac .5b00 268

Chen, B., Miller, R., Dhal, P., 2014. Hyaluronic Acid-Based Drug Conjugates: State-of-the-Art and Perspectives. J. Biomed. Nanotechnol. 10, 4–16. https://doi.org /10.1166/jbn.2014.1781

Elvira, C., Gallardo, A., Roman, J., Cifuentes, A., 2005. Covalent Polymer-Drug Conjugates. Mol. *10*(1*),* 114-125. https://doi.org /10.3390/10010114

Essendoubi, M., Gobinet, C., Reynaud, R., Angiboust, J.F., Manfait, M., Piot, O., 2016. Human skin penetration of hyaluronic acid of different molecular weights as probed by Raman spectroscopy. Ski. Res. Technol. 22, 55–62. https://doi. org / 10.1111/srt.12228

Halpern, J.M., Urbanski, R., Weinstock, A.K., Iwig, D.F., Mathers, R.T., von Recum, H.A., 2014. A biodegradable thermoset polymer made by esterification of citric acid and glycerol. J. Biomed. Mater. Res. Part A 102, 1467–1477. https://doi. org/10.1002/jbm.a.34821

Huang, G., Huang, H., 2018. Application of hyaluronic acid as carriers in drug delivery. Drug Deliv. 25, 766–772. https://doi.org/10.1080/10717544.2018.1450910

Jung, B., Theato, P., 2013. Chemical Strategies for the Synthesis of Protein–Polymer Conjugates BT - Bio-synthetic Polymer Conjugates, in: Schlaad, H. (Ed.), . Springer Berlin Heidelberg, Berlin, Heidelberg, pp. 37–70. https://doi.org / 10. 1007/12_2012_169

Kantlehner, W., 1991. 2.7 - Synthesis of Iminium Salts, Orthoesters and Related Compounds, in: Trost, B.M., Fleming, I.B.T.-C.O.S. (Eds.), . Pergamon, Oxford, pp. 485–599. https://doi.org/10.1016/B978-0-08-052349-1.00166-9

Larson, N., Ghandehari, H., 2012. Polymeric Conjugates for Drug Delivery. Chem. Mater. 24, 840–853. https://doi.org/10.1021/cm2031569

Lee, H., Lee, K., Park, T.G., 2008. Hyaluronic Acid−Paclitaxel Conjugate Micelles: Synthesis, Characterization, and Antitumor Activity. Bioconjug. Chem. 19, 1319–1325. https://doi.org/10.1021/bc8000485

Maia, M.F., Moore, S.J., 2011. Plant-based insect repellents: a review of their efficacy, development and testing. Malar. J. Malar. J. **10,** S11 https://doi.org/ 10.1186 /1475-2875-10-S1-S11

Mondek, J., Kalina, M., Simulescu, V., Pekař, M., 2015. Thermal degradation of high molar mass hyaluronan in solution and in powder; comparison with BSA. Polym. Degrad. Stab. 120, 107–113. https://doi.org/10.1016 /j.polymdegradstab .2015.06.012

Natfji, A.A., Osborn, H.M.I., Greco, F., 2017. Feasibility of polymer-drug conjugates for non-cancer applications. Curr. Opin. Colloid Interface Sci. 31, 51–66. https://doi.org/10.1016/j.cocis.2017.07.004

Ouellette, R.J., Rawn, J.D., 2014. 20 - Carboxylic Acids, in: Ouellette, R.J., Rawn, J.D.B.T.-O.C. (Eds.), . Elsevier, Boston, pp. 659–698. https://doi.org /10. 1016 /B978-0-12-800780-8.00020-6

Pandey, S.K., Upadhyay, S., Tripathi, A.K., 2009. Insecticidal and repellent activities of thymol from the essential oil of Trachyspermum ammi (Linn) Sprague seeds against Anopheles stephensi. Parasitol. Res. 105, 507–512. https://doi.org/10. 1007/s00436-009-1429-6

Petten, C.F., Kalviri, H.A., Kerton, F.M., 2015. Halodehydroxylation of alcohols to yield benzylic and alkyl halides in ionic liquids. Sustain. Chem. Process. 3, 16. https://doi.org/10.1186/s40508-015-0043-4

Ritthidej, G.C., 2011. Chapter 3 - Nasal Delivery of Peptides and Proteins with Chitosan and Related Mucoadhesive Polymers, in: Van Der Walle, C.B.T.-P. and P.D. (Ed.). Academic Press, Boston, pp. 47–68. https://doi.org/ 10. 1016 / B978-0-12-384935-9.10003-3

Sahoo, S., Chung, C., Khetan, S., Burdick, J.A., 2008. Hydrolytically degradable hyaluronic acid hydrogels with controlled temporal structures. Biomacromolecules 9, 1088–1092. https://doi.org/10.1021/bm800051m

Sharma, S., Anand, N., 1997. Chapter 3 - Natural Products, in: Sharma, S., Anand, N.B.T.-P.L. (Eds.), Approaches to Design and Synthesis of Antiparasitic Drugs. Elsevier, pp. 71–123. https://doi.org/10.1016/S0165-7208 (97) 80025-6

Shin, J.M., Kim, S.-H., Thambi, T., You, D.G., Jeon, J., Lee, J.O., Chung, B.Y., Jo, D.-G., Park, J.H., 2014. A hyaluronic acid–methotrexate conjugate for targeted therapy of rheumatoid arthritis. Chem. Commun. 50, 7632–7635. https://doi.org /10.1039/C4CC02595D

Singh, M., Argade, N.P., 2012. Synthetic Studies towards NG-121: Diastereoselective Synthesis of NG-121 Methyl Ether. Synthesis (Stuttg). 44, 3797–3804. https://doi.org/10.1055/s-0032-1317544

Steglich-esterification @ www.organic-chemistry.org, n.d. https://www.organic-chemistry.org/namedreactions/steglich-esterification.shtm

Tavares, M., da Silva, M.R.M., de Oliveira de Siqueira, L.B., Rodrigues, R.A.S., Bodjolle-d'Almeida, L., dos Santos, E.P., Ricci-Júnior, E., 2018. Trends in insect repellent formulations: A review. Int. J. Pharm. 539, 190–209. https://doi. org/10.1016/j.ijpharm.2018.01.046

Tømmeraas, K., Melander, C., 2008. Kinetics of Hyaluronan Hydrolysis in Acidic Solution at Various pH Values. Biomacromolecules 9, 1535–1540. https://doi. org/10.1021/bm701341y

Valeur, E., Bradley, M., 2009. Amide bond formation: beyond the myth of coupling reagents. Chem. Soc. Rev. 38, 606–631. https://doi.org/10.1039/B701677H

Wassei, J.K., Cha, K.C., Tung, V.C., Yang, Y., Kaner, R.B., 2011. The effects of thionyl chloride on the properties of graphene and graphene-carbon nanotube composites. J. Mater. Chem. 21, 3391–3396. https://doi.org/10.1039 / c0jm 029 10f

Watile, R.A., Bunrit, A., Margalef, J., Akkarasamiyo, S., Ayub, R., Lagerspets, E., Biswas, S., Repo, T., Samec, J.S.M., 2019. Intramolecular substitutions of secondary and tertiary alcohols with chirality transfer by an iron(III) catalyst. Nat. Commun. 10, 3826. https://doi.org/10.1038/s41467-019-11838-x

Yuasa, Yoshifumi, Tsuruta, H., Yuasa, Yoko, 2000. A Practical and Efficient Synthesis of p-Menthane-3,8-diols. Org. Process Res. Dev. 4, 159–161. https://doi.org / 10.1021/op9901036

Chapter 4. Synthesis and Characterisation of the Copolymer poly(AA-*co*-APMD)

4.1. Introduction

Paramenthane-3,8-diol (PMD) is a biochemical pesticide derived from eucalyptus plants. This active ingredient is used to make products that are applied to human skin and clothing to repel insects, such as mosquitoes (Pandey et al., 2009). There have been concerns over the use of insect repellents, notably in pregnant women as well as the infants; although there isn't sufficient data available on the use of PMD in these groups, nevertheless it is advised not to use it (for example "insect-repellent-usage @ www.infantrisk.com," n.d.).

Polymer-drug conjugates (PDCs) have been used as a tool for drug delivery and their usage is increasing because of enhanced drug solubility, targeted delivery of the drug and a decreased adverse effect profile (Malathi et al., 2020). There are various polymers that are commonly applied to the skin both in topical medicines and cosmetics, *e.g.* chitosan, hyaluronic acid, polyacrylates *etc* (Valenta and Auner, 2004). Selection of a polymer for topical drug delivery is based upon numerous parameters but the prime requirement is good safety profile, *i.e.* minimal irritation (Sugibayashi and Morimoto, 1994).

Polymers can be in the form of homo- or copolymers. Copolymers are systems in which macromolecules are obtained by the polymerisation of two different types of monomers (Hagiopol, 2016). Copolymers provide many advantages as compared to homopolymers, notably that copolymers have hybrid properties arising due to the individual monomers; these properties can then be tailored to meet the specific uses (Shukla, 2020). For example, poly (lactide-*co*-glycolide) uses poly(glycolide) which has a low glass transition temperature (Tg), and when combined with poly(lactide) (having higher Tg) the resulting copolymer has a stable Tg (Francois et al., 2015; Klein and Wojcik, 2001). Alongside the unique therapeutic properties (active targeting, enhanced stability *etc*) that copolymers may possess, copolymerisation also gives rise to tailored rheological and mechanical properties, *i.e.* flow, viscosity, softening point *etc* (Li et al., 2015).

Acrylic acid copolymers have been traditionally used for various purposes like ophthalmic drug delivery (Ma et al., 2008) whilst their application in topical and transdermal drug delivery is also well established (Don et al., 2008). As copolymers exhibit various physico-chemical

properties, it is important to characterise them fully (Contreras-López et al., 2013), commonly for thermal stability, Tg, molecular weight, composition of the polymer and reactivity ratio of the monomers (Srivastava and Kumar, 2013). Depending upon the usage, various specific tests can be performed, *e.g.* for hydrogels, copolymers are tested for their swelling properties (Shahzamani et al., 2020).

Here, a novel poly(acrylic-*co*-acryloylPMD) ester copolymer has been synthesised and characterised by ^{1}H NMR and IR spectroscopy. The copolymer thermal stability was assessed by thermogravimetric analysis (TGA), Tg by differential scanning calorimetry (DSC), molecular weight by gel permeation chromatography (GPC), reactivity ratio by liquid-chromatography mass-spectroscopy (LCMS), and drug loading by elemental and titration assay. Moreover, turbidimetric analysis was also performed to see the effect of pH on aqueous solubility of the copolymer.

4.2. Materials

PMD (p-Menthane-3,8-diol) was used as received (BOC, USA) (from this chapter onwards the PMD used was purchased commercially). Acrylic acid (AA) in liquid form (99%, Fisher Scientific, UK) was passed through the aluminium oxide column to remove the inhibitor prior to be used in copolymerization. Azobisisobutyronitrile (AIBN) was used as initiator and was recrystallized twice in methanol (Sigma-Aldrich, UK). Sodium hydroxide (Fisher Scientific, UK), acryloyl chloride and anhydrous triethylamine (Sigma-Aldrich, UK) were used as received. Poly(acrylic acid) (Mw=5000 Da) was purchased from Polysciences, Germany. All the solvents used were obtained from the Fisher Scientific, UK and were used as such without purification. TLC plates were obtained from Merck, Germany.

4.3. Methods

4.3.1. Synthesis of Monomer Drug Conjugate (APMD)

3.54 g of PMD was dissolved in 4 mL of anhydrous THF and stirred for 10-15 minutes until a clear solution was obtained. Then to this 3.44 mL of anhydrous triethylamine was added to de-protonate the PMD and was allowed to further stir for 5 minutes. Then, to this solution mixture,

1.8 mL of acryloyl chloride was added dropwise. As this is a highly exothermic reaction, the round bottom flask was placed over ice. Then this mixture was allowed to stir at room temperature for 4 h. After that, the solvent was evaporated under vacuum followed by silica column chromatography using mixtures of ethyl acetate and hexane (1:4) and the product determined by thin layer chromatography (TLC). The final product was a viscous oil (2.1 g). Yield (53%). The yield was calculated as: (Amount of pure product recovered/Amount of chemical used) *100)

^{1}H NMR, (DMSO, 400 MHz): δ 6.40 ppm (1H, d), 6.25 ppm (1H, q),5.90-6 ppm (1H, d), 5.30 ppm (1H, s), 4.20 ppm (1H, s), 0.90 ppm (6H, s), 0.80 ppm (3H, d). IR data 3221 cm^{-1}= OH of PMD, 2840-2970 cm^{-1}= C-H stretch, 1719 cm^{-1} = Ester linkage, 1017-1048 cm^{-1} =C-H bending. m/z = 242.19 Da which corresponds to $C_{13}H_{22}O_3Na$.

4.3.2. Synthesis of poly(AA-*co*-APMD) Copolymer

The poly(AA-*co*-APMD) copolymer was synthesised via free radical polymerisation (with varying molar ratios). All the magnetic stirrers and glassware used in the experiment were dried at 110 °C for 6-8 h prior to the experiment. Briefly, (depending upon the molar ratio of the monomers used) in a typical reaction (7:3 APMD:AA) APMD (300 mg), acrylic acid (285 mg) and azobis(isobutylronitrile)(AIBN) (0.005 mol/L) were added into a flask together with ethanol (5 mL) as a solvent. After degassing the solution with nitrogen for 20 mins, the mixture was stirred under the inert environment at 65 °C for 16 h. Then, the flask was cooled to quench the reaction and the product obtained was dialysed using a regenerated cellulose membrane (suitable for ethanol, Sigma Aldrich, UK, MWCO 2000 Da) against ethanol for 2 days with 6 times change of the solvent to remove unreacted monomers and oligomers. The final product poly(AA-*co*-APMD) was obtained by using a rotary vacuum for 20-30 mins at 50 °C. The yield of copolymer after the purification was 18-50% for different molar ratios except 1:9 (AA:APMD), where the yield was extremely low (2%), and attempts to obtain a homopolymer of APMD failed. Yield of the poly(AA-*co*-APMD) was calculated by:

% yield= Amount of copolymer made/Amount of monomers used*100

4.3.3. Turbidimetric Measurements

The turbidity of polymer solutions at different molar ratios, *i.e.* 9:1 and 3:7 (AA:APMD) was investigated at 1 mg/mL with a Shimadzu UV/VIS-2401 PC spectrophotometer (Japan) at 400 nm. For this experiment, poly(acrylic acid) (PAA) was used as a control. The experiment was performed at room temperature. The pH of the solutions was changed by adding 0.1 N sodium hydroxide (NaOH) and determined using a digital pH-meter (JenWay, UK). All the experiments were performed in triplicate.

4.3.4. Molecular Weight and Molecular Weight Distribution of the Polymers

Molecular weight of the copolymers and its distribution was determined using a gel permeation chromatography (GPC) instrument equipped with an Agilent 1100 series RI detector, quaternary pump and Waters Ultra hydrogel columns with pore sizes of 250, 500 and 1 000 A, respectively. The mobile phase consisted of THF with a flow rate of 0.75 mL /min. The eluent was DMF containing Bu_4NBr (0.1% w/v). In this experiment copolymers of varying ratios of acrylic acid (AA) and acryloyl PMD (APMD) were used ranging from 1:9, 3:7, 5:5, 7:3, 9:1 (AA:APMD). PAA was used as a control.

4.3.5. Reactivity Ratio Experiment

4.3.5.1. Method Development

The first step in the reactivity ratio experiment was to develop a method for the analysis of both AA and APMD. For this purpose, LCMS was used. Briefly, for the purpose of constructing a calibration curve for both AA and APMD, a stock solution of 1000 µg/mL (1mg/mL) was prepared by dissolving 14.2 mg of AA and 17.8 mg of APMD in 14.2 and 17.8 mL ethanol respectively. This was then serially diluted to make 200, 100, 50, 25, 10, 5 and 1 µg/mL dilutions (by using following formula):

Concentration $_{(start)}$ x Volume $_{(start)}$ = Concentration $_{(final)}$ x Volume$_{(final)}$

(abbreviated as $C_1V_1 = C_2V_2$)

4.3.5.2. Reactivity Ratio Experiment

Monomer mixtures of AA and APMD were dissolved in ethanol. Five monomer mixtures were investigated with the AIBN concentration was kept constant in all cases (0.005 mol/L). The polymerization, carried out at 60 °C, was allowed to proceed to low conversions (below 10%). For this purpose, reactions were stopped before 2 h. The obtained product was subjected to liquid chromatography mass-spectroscopy (LCMS) for analysis. The analysis was performed for both AA and APMD

4.3.6. Drug Loading

Two methods were used for the calculation of drug loading, *i.e.* titration method and elemental analysis.

4.3.6.1. Titration Method

In this method, firstly PAA (5,000 Da, Polysciences, Germany) was used and 5 different solutions of PAA in water:ethanol (7:3 v/v) were prepared (1,2,3,4 and 5 mg/mL). All solutions were flushed with nitrogen to remove any dissolved carbon dioxide (as during the reaction it may form carbonic acid which may give false results). Then, 3mL of PAA solution from each of the stock (1, 2, 3, 4 and 5 mg/mL) was taken and to this 3 drops of phenolphthalein indicator was added. Then 0.1M NaOH solution was added dropwise until a faint pink colour appeared (at this point the reaction was stopped) and the volume of NaOH used was recorded. Similar data obtained from the copolymer system (volume of 0.1M NaOH used) was correlated with the data obtained from the PAA. For example, in the case of 5 mg/mL of copolymer solution, the volume of 0.1M NaOH used was 3mL and the % of PAA was calculated as:

Volume of NaOH used in PAA-volume of NaoH used in copolymer/ Volume of NaoH used in PAA*100 (Soto et al., 2014)

4.3.6.2. Elemental Analysis

An elemental analyser (FLASH EA 1112 series, Thermo-Finnigan, Italy) was used for C (carbon) elemental analysis. Samples were prepared by the method as described earlier at four

different molar ratios, *i.e.* 3:7, 5:5, 7:3 and 1:9 (AA:APMD). After the product was obtained, it was dried overnight in a vacuum oven (Thermo Fischer, UK) at 40 °C to ensure complete removal of the moisture. A total of 2-3 mg samples was sealed in HPLC vials (Thermo Fischer, UK) and were subjected to analysis. For the analysis, combustion and reduction tubes (PerkinElmer) were used. The combustion reaction was run at 975 °C in the presence of pure helium and oxygen as carrier gas.

4.3.7. Thermal Analysis

Thermal analysis was performed by using two techniques, *i.e.* thermogravimetric analysis (TGA) and differential scanning calorimetry (DSC).

4.3.7.1. TGA

TGA was carried on copolymer poly(AA-*co*-APMD) samples of different molar ratios with PAA and PMD used as controls, as described in chapter 2. In this experiment we used non-Hermetic pans.

4.3.7.2. DSC Study

In order to determine the glass transition temperature (Tg) of the copolymers (of varying molar ratios) and the PAA (as a control). Procedure described in chapter 2 was followed. Here we used Hermetic pans. Moreover, this experiment was carried out by the technician.

4.4. Results and Discussion

4.4.1. Synthesis of Monomer Drug Conjugate (APMD)

After the initial failed attempts to synthesise a polymer-drug conjugate, an alternative route of conjugating PMD with a monomer (that can be polymerised) was explored, *i.e.* producing an acryloyl-PMD monomer (APMD) and then subsequently polymerising this conjugate alone (homopolymer) or with another monomer (in our case acrylic acid) to form a copolymer. This synthesis route for copolymers has been reported previously in various studies (Chytil et al.,

2010; Liu et al., 2015) and is considered to be a good alternative if the conventional polymer-drug conjugation approach is unsuccessful. There are various advantages of this method, notably in drug loading as in this method the percentage of drug loading is typically higher than for conventional PDCs whilst the drawbacks include that the approach often involves more synthetic steps and depending upon the monomer used, water solubility may be decreased, *e.g.* if the methacrylic acid monomers are used there are reports of a decrease in the water solubility of the obtained product (Bozorg et al., 2020).

Here we chose acryloyl chloride as a precursor for the conjugation due to two reasons; the first was that the chloride group provides a platform for the formation of an ester bond between the PMD and the acryloyl chloride. The other was the acrylic acid itself, as it is the precursor of the poly(acrylic acid)-based polymers, which are commonly used in topical drug delivery and have an excellent safety profile (Ritthidej, 2011).

A typical nucleophilic reaction synthesised the monomer drug conjugate (acryloyl-PMD). This involves a nucleophilic attack by alcohol, *i.e.* OH, followed by the removal of the leaving group, *i.e.* Cl. Triethylamine (TEA) was used as a base to convert the HCl (formed during the reaction) into a salt (triethylamine hydrochloride, a by-product). The chemical structure of the APMD was verified by ^{1}H NMR, shown in Figure 4.1. By comparing the NMR spectra of the PMD alone and acryloyl chloride alone, we identified two main parameters for the verification of successful conjugation. First was the loss of one (δ 3.38 or 4.42 ppm) of the OH groups from PMD (due to the formation of an ester bond between the PMD and the acryloyl chloride) and the other was the appearance of the peaks indicating the presence of CH_2 and CH groups of the acryloyl chloride at around δ6 ppm. From the ^{1}H NMR spectra of the APMD (Figure 4.1) it can be seen that both of these criteria were fulfilled such that the peak indicating the presence of one of the OH group in PMD, was lost. Moreover, new peaks were found in the region of δ6 ppm, indicating the presence of acryloyl moiety and, hence indicating a successful reaction. Further confirmation was from mass spectroscopy that showed the presence of a strong peak corresponding to a mass of 242 Da, which is in agreement with the molecular formula $C_{13}H_{22}O_3Na$. Thus, from these, we can conclude that the synthesis of APMD was successfully achieved.
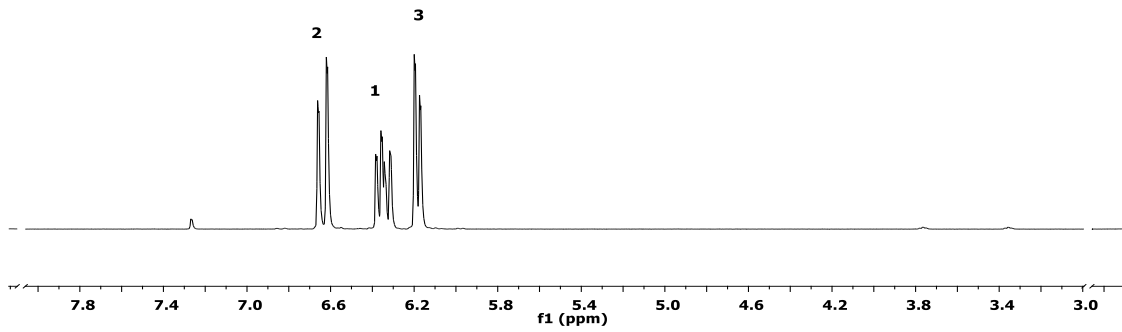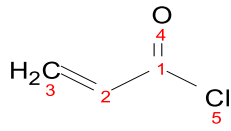
A
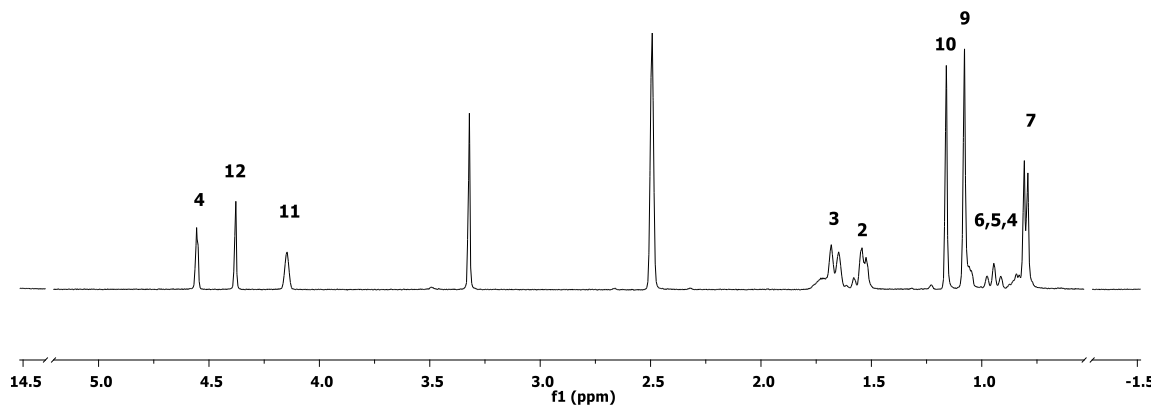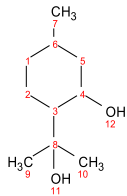
B
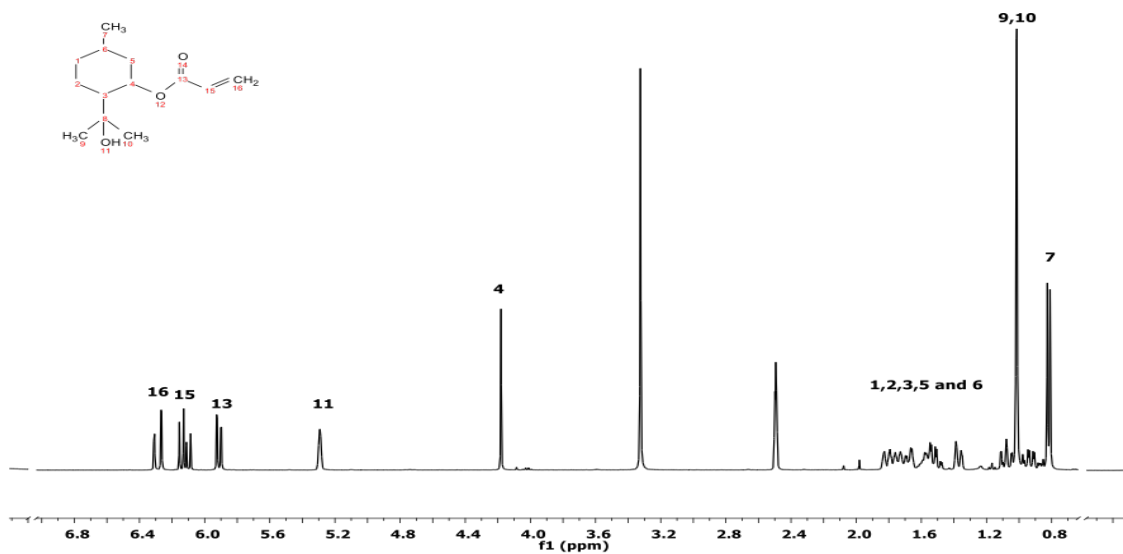
C
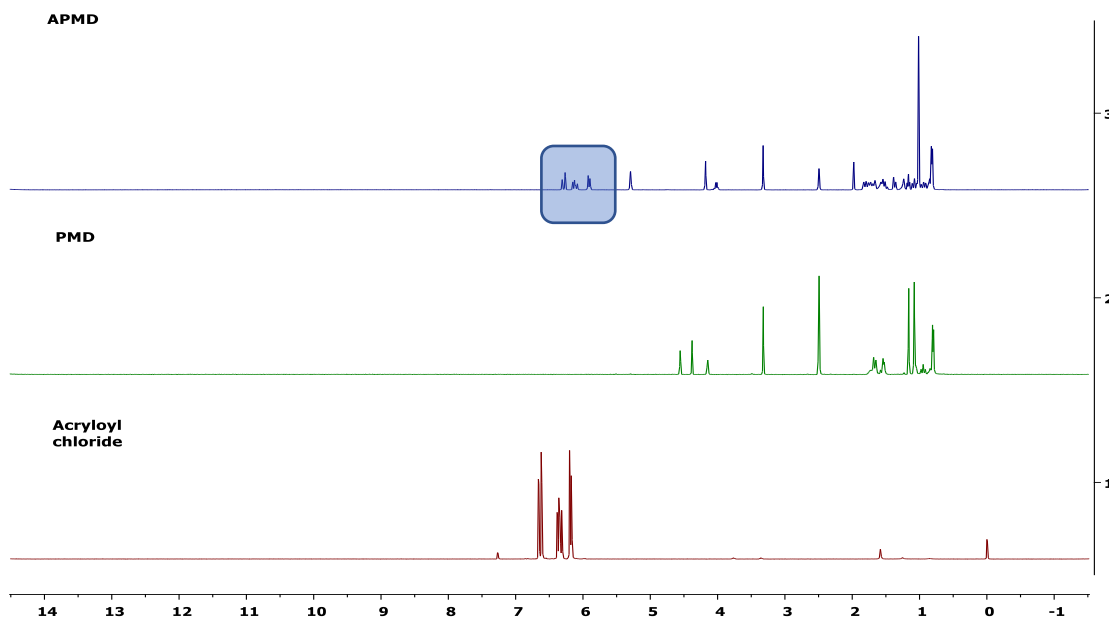
D

Figure 4.1 ^{1}H-NMR spectra of (A) Acryloyl chloride, having characteristics peaks for CH$_2$ and CH groups at around δ6 ppm. (B) PMD, having characteristics peaks for CH$_3$ and

for the secondary and tertiary OH groups. **(C) Acryloyl PMD, showing successful conjugation indicated by the appearance of characteristic peaks for acryloyl chloride. (D) Comparative spectra of acryloyl chloride, PMD and APMD.**

4.4.2. Synthesis of Poly(AA-*co*-APMD)

In this study, a novel hydrolysable (by esterases) copolymer poly(AA-*co*-APMD) was synthesised through free radical polymerisation. Briefly, the copolymer was synthesised by free radical polymerisation of two monomers, *i.e.* acrylic acid (AA) and acryloyl PMD (APMD) using AIBN as a free radical initiator. The ^{1}H NMR confirmed chemical structure of the copolymer. Verification of the polymerisation was affirmed (Figure 4.2) by the loss of the peaks corresponding to the double bonds of the acryloyl moiety of APMD, as these double bonds are the point of attack by the initiator (AIBN) during free radical polymerisation (Mota-Morales et al., 2018).

Along with this, another indicator was the broadening of NMR peaks, as ^{1}H NMR peaks of the copolymer are usually broader (due to the repetitive units) and a common phenomenon observed with the macromolecules (Paulsen et al., 2017). Moreover, GPC analysis showed a peak with a polydispersity index (PI) of 2.9. The Mw of the copolymer was 6,200 Da. In order to prove the presence of the ester bond, C NMR and infra-red (IR) spectroscopy were used. In C NMR, we expected to have a peak between 170-190 ppm (indicating the presence of carbonyl carbon). In Figure 4.2, the C NMR spectra showed a faint peak at 175 ppm that could be related to the carbonyl carbon. Moreover, the IR spectra showed the presence of the ester bond in both APMD and the poly(AA-*co*-APMD).
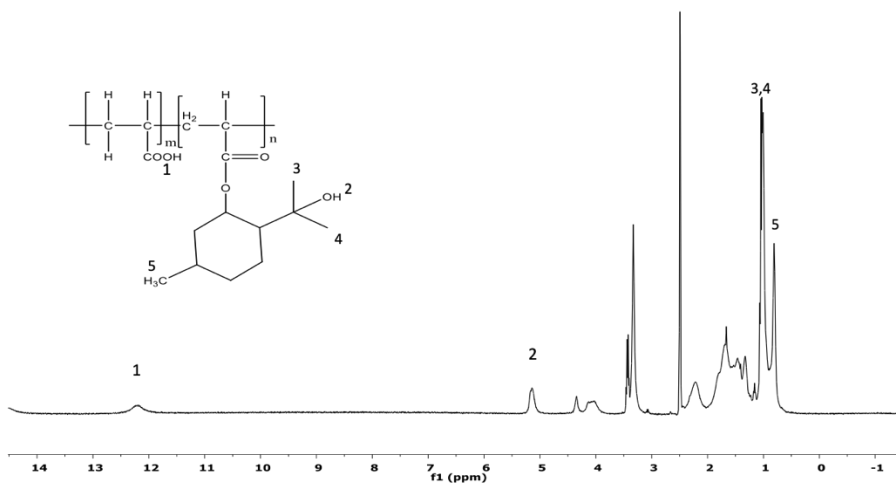
A
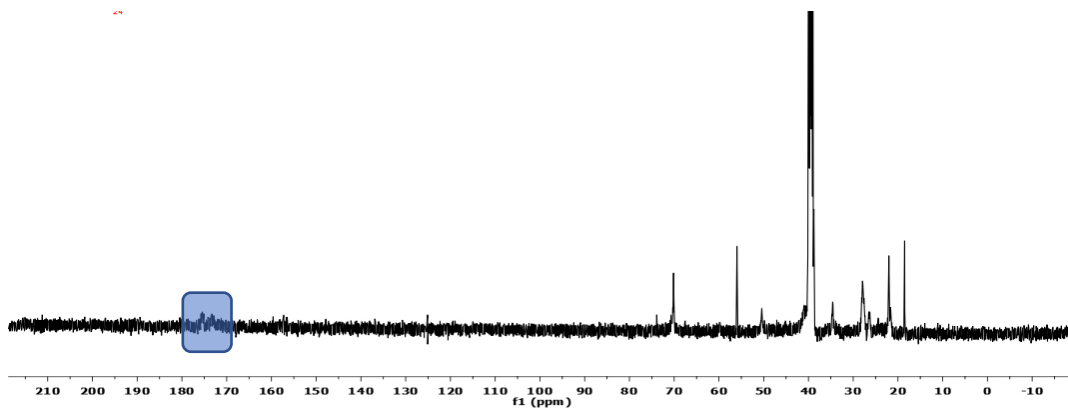
B
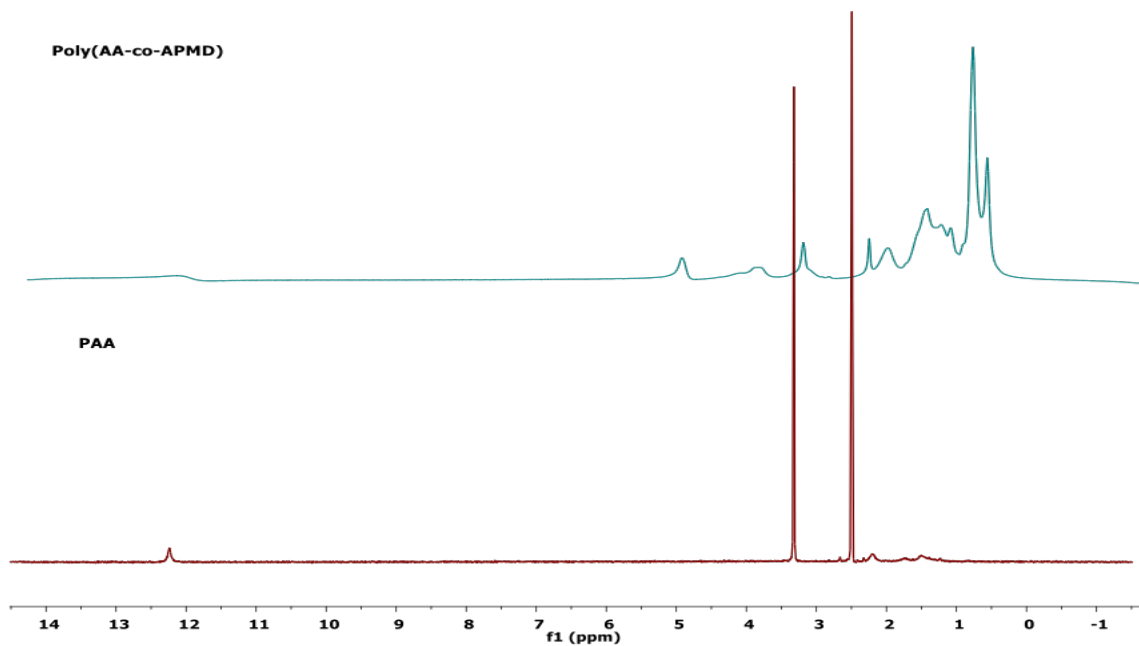
C
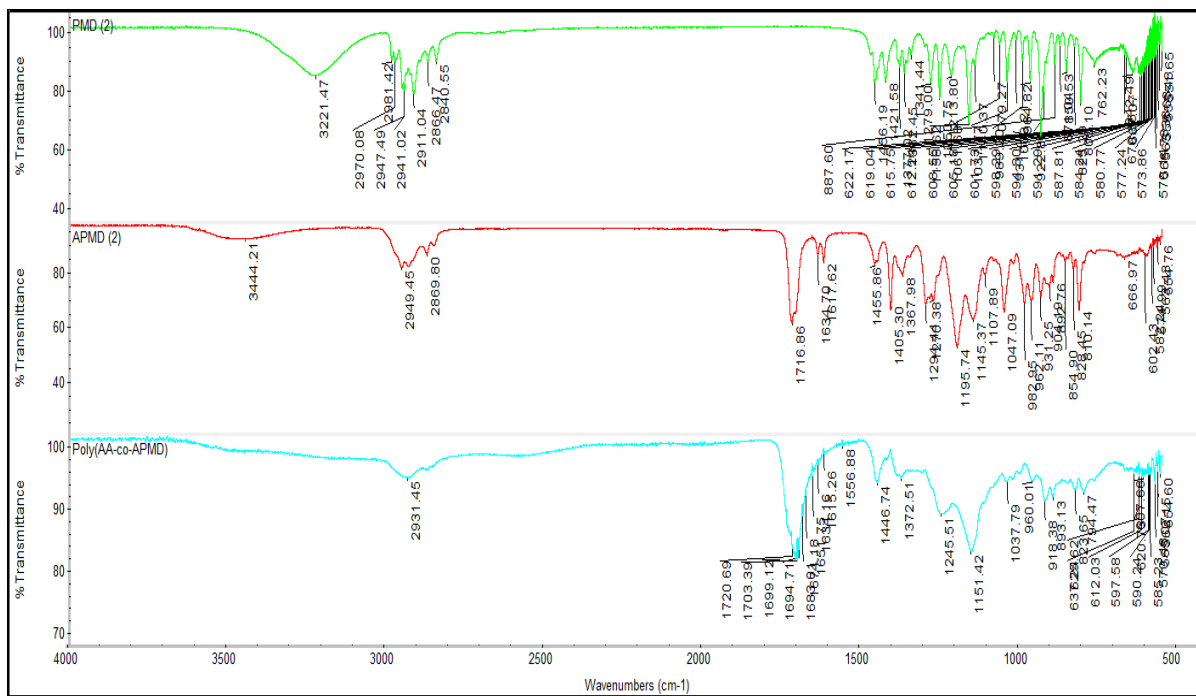
D

Figure 4.2 ^{1}H-NMR spectra of (A) Poly(AA-co-APMD) showing peaks for COOH group of the AA, OH, CH and CH$_2$ groups of APMD. (B) ^{13}C-NMR spectra of Poly(AA-*co*-APMD) showing a faint peak for carbonyl carbon. (C) Comparative spectra of PAA and Poly(AA-*co*-APMD) showing the presence of extra peaks in the copolymer corresponding to APMD. (D) IR spectra (overlapped), showing PMD with characteristic peaks for OH

(3217 cm^{-1}), CH stretching (2840-2970 cm^{-1} region), APMD showing a prominent peak at 1716 cm^{-1} indicating formation of ester bond and the copolymer, poly(AA-*co*-APMD).

4.4.3. Copolymer Composition

The first step to calculate reactivity ratios is to know the composition of the copolymer. For this purpose, it is essential to have an analytical method that can detect the monomer(s) concentration. In our case, we had two monomers, *i.e.* acrylic acid (AA) and acryloylPMD (APMD). The most commonly used method for the detection of a monomer during a polymerisation reaction is ^{1}HNMR, but due to the overlapping peaks from the acrylic groups, it was not possible to use this method. Further, due to the absence of a chromophore, we could not use the HPLC or UV spectroscopy. Therefore, we used LCMS to detect the monomers during the polymerisation. Here, we were only able to detect APMD and could not detect the acrylic acid (most probably due to the volatile nature of the monomer).

The first step in the validation of a method (LCMS) is to assess whether it can quantitatively detect a compound or not and how accurate the detection is. For this purpose, a calibration curve was constructed, shown below.
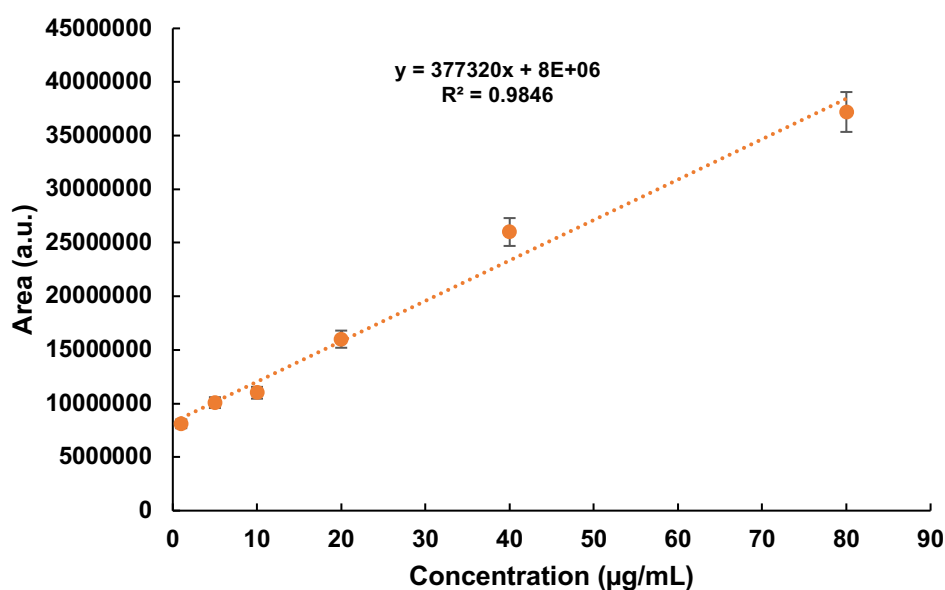
Figure 4.3 Calibration curve for the APMD by using LCMS (n=3)
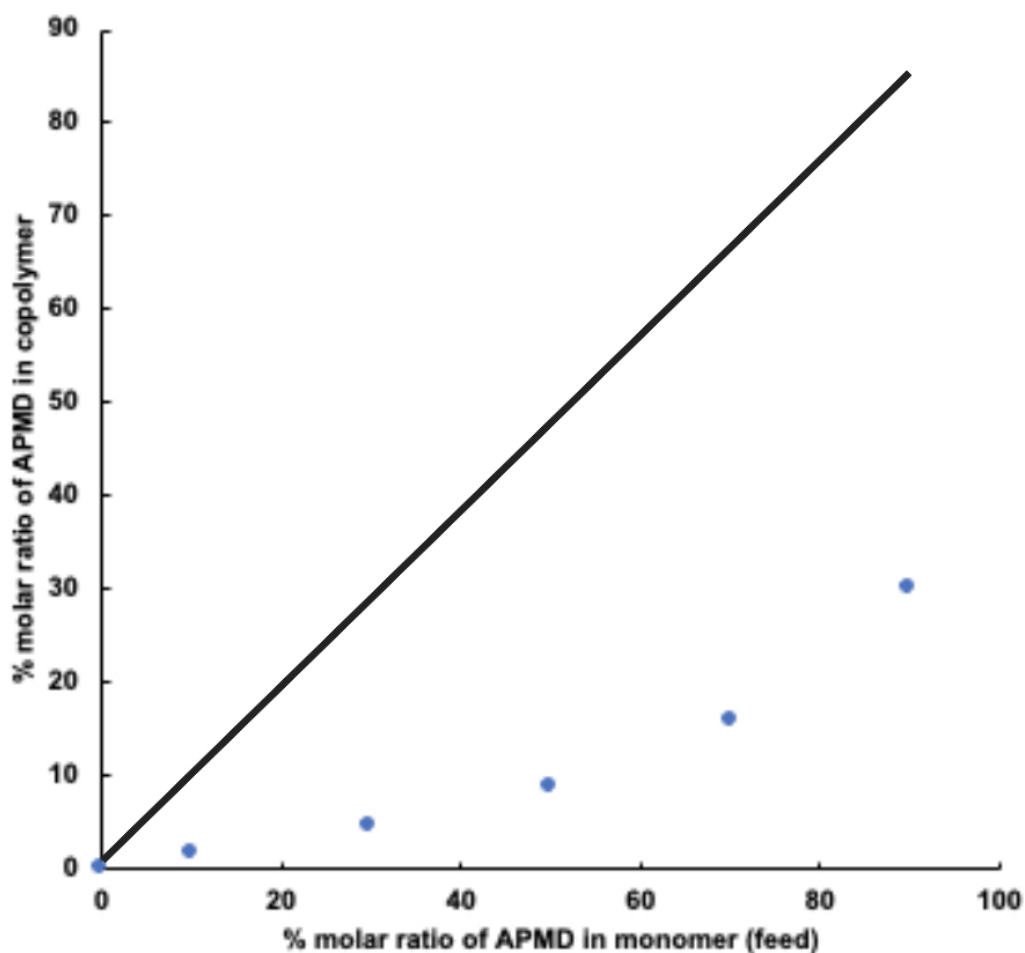
Figure 4.4 Composition of the copolymers as the function of the feed mixtures (APMD). Black line indicates the partition between the lower and upper halves of the graph.

4.4.4. Calculation of Reactivity Ratio

During the synthesis of a copolymer, usually, one monomer is more reactive than the other monomer or (rarely) both the monomers may have same reactivity towards each other. Thus, in order to know the reactivity of one monomer towards another, the reactivity ratio is calculated. A reactivity ratio can be defined as the difference between the ratio of the monomers in the copolymer system to the ratio of feed mixture (Ebnesajjad, 2003).

In order to calculate the reactivity ratio various parameters, need to be calculated, including monomer feed ratio composition, monomer copolymer composition and conversion of the monomer. The mole fractions (in mol%) of APMD in the feed as well as the copolymers (at

five different molar ratios) were calculated by using LCMS. The data is presented in Table 4.2. Reactivity ratios of APMD and AA were determined by the application of conventional linearization methods such as the Finemann–Ross (FR) and Kelen–Tüdós (KT) methods. The Finemann–Ross (FR) method is one of the commonly used method for determining reactivity ratios, where G and H (numerical values obtained through the initial feed and final copolymer composition of that monomer, in our case APMD) have a linear relationship with each other according to the following equation:

$G = r_{APMD}H - r_{AA}$ (Erbil et al., 2009).

The FR plot obtained by linear regression analysis for APMD/AA copolymers is in Figure 4.5. For obtaining the FR plot certain parameters needs to be calculated which are summarised in Table 4.1.

Table 4.1. Compositional FR Parameters for Poly(AA-*co*-APMD) Copolymer System

F	f	f^2/F (H)	$f(1-F/f)$ (G)
0.11	0.063	0.036	0.5
0.42	0.176	0.073.	0.24
1	0.449	0.201	0
2.33	1.38	0.81	-0.78
9	8.09	7.27	-7.19

Where F=%APMD in monomer mixture/total %APMD, i.e. 1/9=0.11, 3/7=0.42

And f= %APMD in copolymer mixture/total %APMD, i.e. 0.6/0.94=0.063, 0.15/0.85=0.176
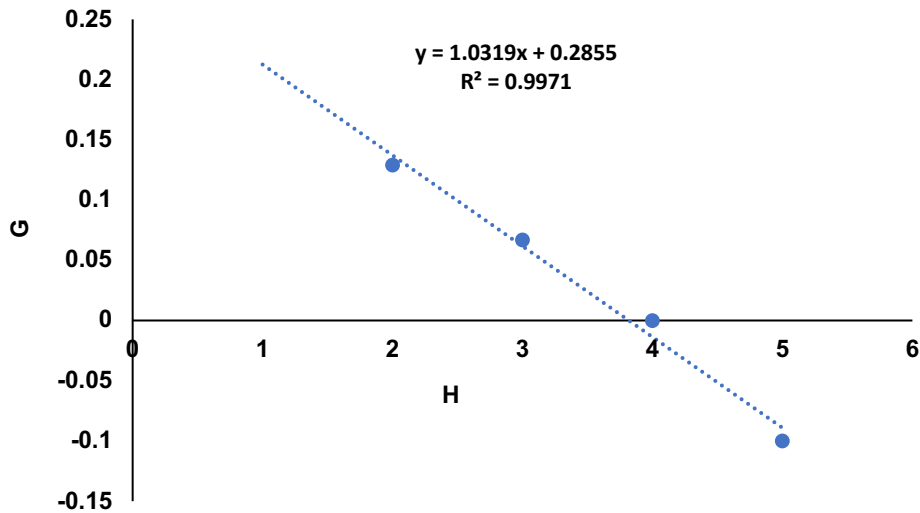
Figure 4.5. FR method for determining monomer reactivity ratios in the copolymerisation of APMD and AA by using LCMS data (for APMD).

Kelen and Tüdós (KT) applied these two parameters, *i.e.* G and H in the linearized copolymerization equation, along with new parameters such as α, η and ζ. The intercepts at $\zeta = 0$ and $\zeta = 1$ of the η versus ζ plots yield $-r_{APMD}/\alpha$ and r_{AA}, respectively (Erbil et al., 2009).

Table 4.2. Compositional KT Parameters for Poly(AA-*co*-APMD) Copolymer System

F	f	f²/F (H)	f(1-F/f)(G)	η	Ξ
0.11	0.063	0.036	0.5	0.89	0.06
0.42	0.176	0.073	0.24	0.40	0.12
1	0.449	0.201	0.	0	0.27
2.33	1.38	0.81	-0.78	-0.58	0.60
9	8.09	7.27	-7.19	-0.92	0.93

Where $\alpha = 0.52$

$\eta = G/(\alpha+H)$ and $\xi = H(\alpha+H)$

The plot shows data points with the trend line equation:

$$y = -1.9165x + 0.7169$$
$$R^2 = 0.9186$$

The x-axis is labeled ξ ranging from 0 to 1, and the y-axis is labeled η ranging from -1.5 to 1.
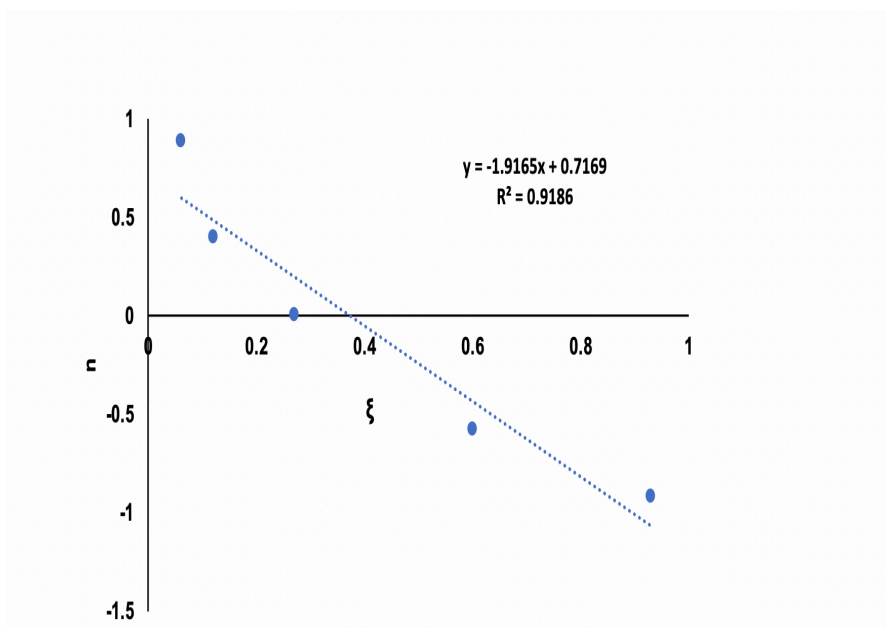
Figure 4.6 KT method for determining monomer reactivity ratios in the copolymerisation of APMD and AA by using LCMS data (for APMD).

Table 4.3. Comparison of reactivity ratios by various methods for AA/APMD copolymers

	r_1 (AA)	r_2 (APMD)
FR method	1.03	0.28
KT method	1.9	0.71

Various studies have reported that as a monomer becomes bulkier the reactivity of it decreases, for example when acrylic acid was copolymerised with methyl methacrylate the reactivity ratio of the acrylic acid was found to be 1.5 and for the methyl methacrylate it was 0.48 (Ekpenyong, 1985).

From the values summarised in Table 4.3 (for the reactivity ratios of both monomers, *i.e.* AA and APMD) it can be seen that reactivity ratio values are different by the two methods, *i.e.* FR and KT method. As discussed earlier in FR method a plot of *G* as ordinate and *H* as abscissa is plotted resulting in a straight line whose slope is r_1 and intercept is r_2. The slope of the line of best fit is influenced greatly by the points which are closer to the origin, hence giving a non-uniform weightage to the points and thus errors in the results are produced. The validity is only

qualitative and the estimates of r_1 and r_2 can change with each experiment by analysing the data in different ways. Moreover, the high and low experimental composition data are unequally weighed, which produces large effects on the calculated values of r_1 and r_2. To overcome these issues KT introduced refinement of linearization by adding an arbitrary constant '' α'' into FR equation, which helps the data to spread more evenly over the entire composition range ultimately giving equal weightage to all the data. Thus, we suggest that the inclusion of the '' α'' accounts for different values.

However, in both calculations it is clear that AA is more reactive than APMD, and interestingly by 1.03/0.28 = 3.7 times by FR method and 1.9/0.71 = 2.7 times by KT method so in both cases showing AA about 3 x more reactive than APMD. Thus, it is expected that copolymers will contain greater levels of AA than APMD than anticipated, simply from their feed composition. So, loading of PMD on the copolymer will be lower than anticipated, as discussed in section 4.4.9.

4.4.5. Turbidimetric Study:

In the present work, we studied the turbidity of poly(AA-*co*-APMD) copolymers with varying monomer ratios. The main aim of this was to study the effects of adding APMD (non-ionic) monomers into the copolymer system on the aqueous solubility at different pH's by observing changes in opacity. Here PAA was used as a control. For such copolymer systems, a term called critical pH of complexation pH(crit) is used below which the solution becomes turbid which is an indication of the phase separation in the system due to the formation of insoluble complexes (Khutoryanskiy et al., 2004). Hydrogen bonded interpolymer complexes (IPC) are formed between the proton donor (weak polyacids like PAA) and proton acceptor (non-ionic polybases like polyethylene glycol) polymers in the aqueous solution. An important limitation of such polymer systems is that they are usually soluble only within a narrow pH window. Normally, at pH values higher than 4-5, interpolymer complexation via hydrogen bonding is not possible due to the increase of ionised sites (carboxylate groups) in the polyacids chain, whilst on the other hand, at pH values lower than 3-3.5, the hydrogen bonded IPC precipitates (forming a turbid solution) because the fraction of the carboxylate anions in the polyacid chains (responsible for the solubility of the complex) decreases significantly (Khutoryanskiy and Staikos, 2009; Mun et al., 2003). From the results (Figure 4.7) it can be seen that the copolymer, *i.e.* poly(AA-*co*-APMD) mixture turns very turbid at lower pH, whilst it remains clear at higher

pH, this behaviour can be best explained by the formation of the hydrogen bonded IPC in between the AA and the APMD chains. Moreover, the PAA solution (control) remains practically transparent throughout the pH region. This behaviour can be attributed to the negative charge of the PAA (due to AA units), implying that either no interpolymer complexation is formed due to the negatively charged AA units or the IPCs formed are more hydrophilic and soluble in water.
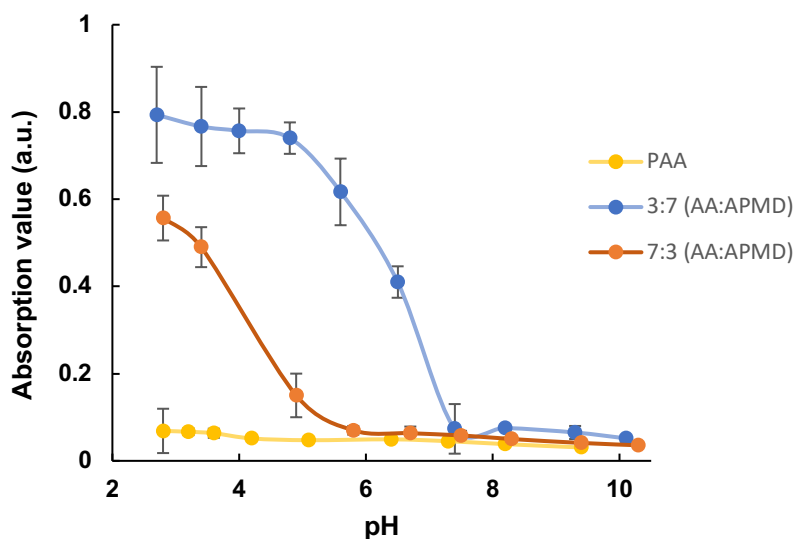
Figure 4.7. Effect of pH on the turbidity of the solution of PAA and the copolymers with varying molar ratios (of AA:APMD)

4.4.6. Molecular Weight Characterisation

 GPC analysis results demonstrated that poly(AA-*co*-APMD) copolymer with a relatively high molecular weight distribution (Mw/Mn >3.5) was obtained. Table 4.4 shows the molecular weight, PDI and molar percentage of monomers in the feed. Based on the results, it can be seen that increasing incorporation of AA units into the copolymer system resulted in higher molecular weights. This confirms the earlier findings that (from the reactivity ratio data) that AA is more reactive than APMD since higher reactivity's of monomers produce high molecular weight polymers (Abbasi et al., 2020). A further factor affecting polymer molecular weight is the kinetic chain length which is (in the case of free radical polymerisation) the approximate number of monomers that are consumed by each radical; the greater the kinetic chain length, the larger will be the molecular weight. The kinetic chain length depends upon the initiation and termination rate of the polymerisation reaction (Principles of Polymerization,4th Edition @

www.wiley.com), and bulky cyclic groups tend to terminate polymerisation (Tüdo and Földes-Berezsnich, 1989) resulting in the decrease kinetic chain length and ultimately decrease molecular weight.   Given the large discrepancies in molecular weight with addition of increasing amounts of APMD, it is likely that both the reactivity ratio (approximately three-fold higher for AA) and the kinetic chain length affects the molecular weight of the resulting copolymers. The PDI (Mw/Mn) is relatively high (quite common for free radical polymerisation) and could be controlled by the terminating the polymerisation reaction at low conversion rates (Krivorotova et al., 2015).

Table 4.4. Molecular Weight Data for Copolymer Poly(AA-*co*-APMD) System

Molar feed ratio (AA:APMD)	Mw	Mw/Mn
1:9	1800	2.1
3:7	6200	2.9
5:5	11500	3.1
7:3	29200	3.3
9:1	53100	3.4
PAA (10:0)	252000	3.45

4.4.7. Thermal Study

4.4.7.1.Thermogravimetric Analysis (TGA)

TGA investigated thermal stability of the copolymer poly(AA-*co*-PMD) at different molar ratios and PAA along with the PMD (both as controls). The primary purpose of this experiment was to explore the stability of the poly(AA-*co*-APMD) copolymer and monitor thermal events. From Figure 4.8, it can be seen that the control, *i.e.* PMD, the weight loss starts at 40 °C and the material is essentially lost at 60°C, which is according to the literature. Moreover, this loss

in weight is attributed to high vapour pressure rather than the degradation of the material itself (Drapeau et al., 2011). Purpose of making it into a copolymer was to slow and extend the release, as the Figure 4.8 shows that it is rapidly lost when applied as a single compound to the skin. PAA is a widely used and suitably stable polymer showing minimal weight loss up to ~150 °C, with perhaps the slight decrease due to loss of surface adsorbed water. Beyond this it starts to degrade. From the Figure 4.8, it can be seen that there two significant stages of the degradation in PAA; one at 190 °C and the other at 336 °C, whilst there is an initial weight loss below 100 °C which can be attributed to the loss of moisture. The first stage of the degradation (in PAA) till 336 °C accounts for most of the weight loss (70%), whilst the second stage after 336 °C accounts for remaining of the overall weight loss, *i.e.* almost 91% at 590 °C. The data obtained for PAA is in correspondence with the literature. However, there are few deviations which can be attributed to the impurities within the polymer sample (McNeill and Sadeghi, 1990). Complexing PMD in the copolymers clearly stabilises the weight loss. With 3AA:7APMD, some weight loss (approx. 3.2%) at 40 degrees is seen but is likely the adsorbed moisture or the PMD from the relative smaller APMD chains (oligomers) within the copolymer. Weight loss at about 250 °C, can be attributed to decarboxylation (release of CO_2) process. Similarly, above 350 °C the weight loss can be due to the chain scission, as at high temperature, the release of fragments within the acrylic acid sequence is possible (Maurer et al., 1987).
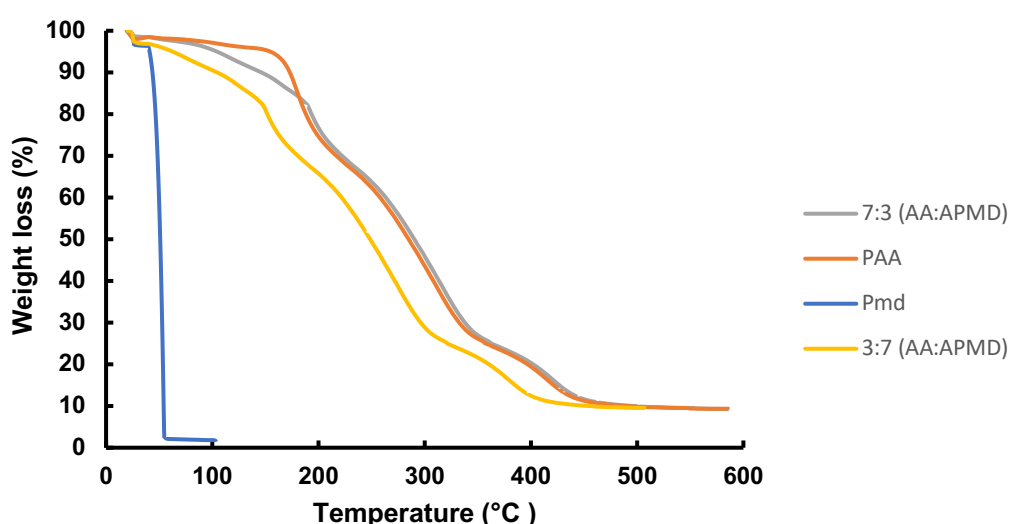
Figure 4.8. Thermal gravimetric analysis of the materials

4.7.2. DSC Analysis

DSC analysis was performed on PAA alone followed by the copolymer poly(AA-*co*-APMD) at different molar ratios to determine the glass transition temperature (Tg) - the temperature below which a polymer's physical properties change to those of a glassy state (Ebnesajjad, 2016). DSC determined the Tg of the copolymers (at two molar ratios) under a nitrogen atmosphere (at 40 °C /min). For synthesised PAA, the Tg value was around 101°C which is in agreement with the literature (Wong et al., 2007), whilst the copolymers poly(AA-*co*-APMD) showed Tg's varying from 48-59 °C for different molar ratios. It was found that increasing the amount of APMD in the copolymers results in decreased Tg, *i.e.* for 7:3 (AA: APMD), the Tg onset was at 51.9 °C, whilst for 3:7 (AA: APMD) it was 48.2 °C. Two main parameters can affect the Tg, firstly the strength of the bond between the molecules, and secondly the stiffness of the polymer chain (Hobson, 2001). The results, showing PAA has a higher Tg than the copolymers, can be best explained by the higher polarity of PAA due to which there is increase dipole interaction between the molecules hence it has rigid chains, whilst the addition of the APMD monomer decreases the polarity and the dipole interactions leading to decreased intermolecular interactions which ultimately makes the structure less rigid.
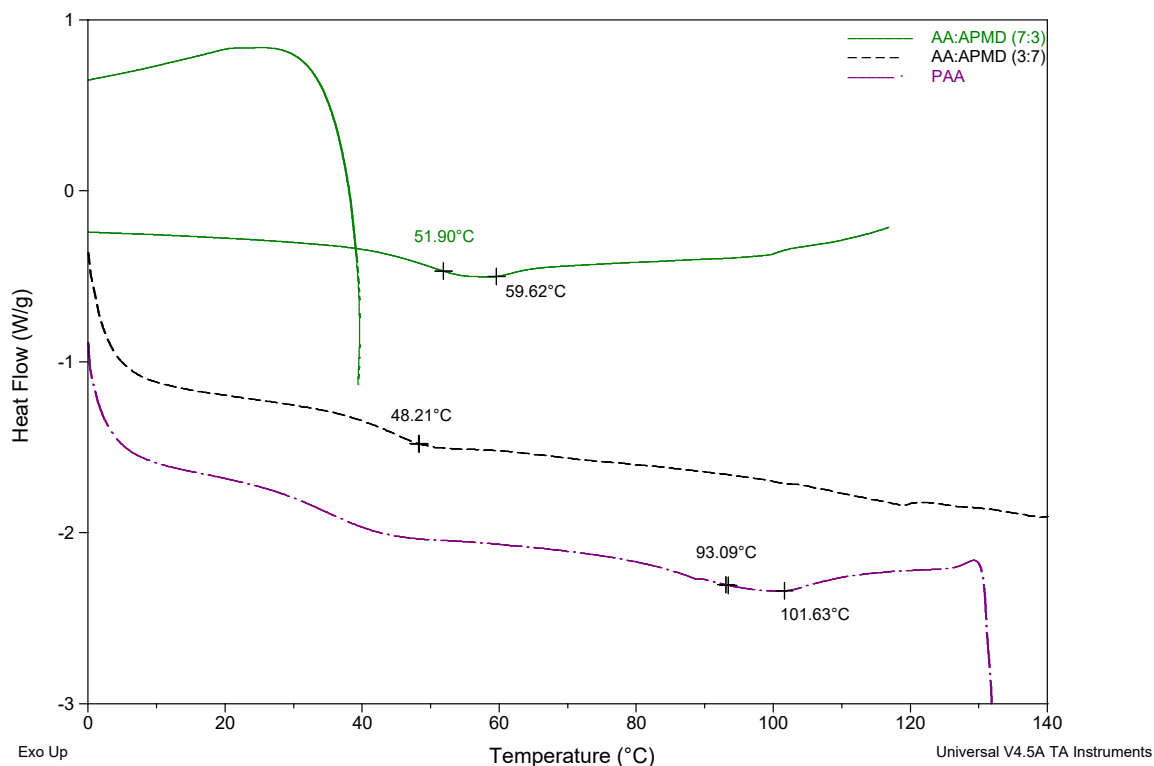
Figure 4.9. DSC thermograms of poly(AA-*co*-APMD) at two different monomer ratios and PAA

4.4.8. Drug Loading Study

The most commonly used technique for determining drug loading in polymer-drug conjugates is ^{1}H NMR (Zhang et al., 2004). Unfortunately, due to the overlapping of the peaks of CH_2 and CH groups of both the drug (PMD) in the APMD monomer and the AA it was not feasible to use this method. Therefore, in order to determine the amount of drug-loaded in the copolymer system, other methods were explored; two methods were used namely the titration method (for determining free carboxylic groups) hence indirectly showing the amount of PMD present while the second technique used was the elemental analysis in which the percent carbon content data was obtained to determine the PMD concentration.

4.4.8.1. Titration Study

Different types of the complexometric titration methods have been used to quantify certain functional groups, including carboxylic groups (Fras et al., 2004). Most titration methods use spectrophotometric analysis and commonly employ solvents in which our copolymer was insoluble or use conditions that might result in the breakage of the ester bond in the copolymer (van Houwelingen et al., 1980). Therefore, a conventional method was used by titrating the copolymer against an excess amount of base (NaOH) in the presence of a pH indicator (phenolphthalein). The prime concern during this process was to ensure that the ester bond of the copolymer do not hydrolyse. For this purpose, the whole reaction was performed over ice in order to prevent the hydrolysis of the ester bond in the copolymer as the hydrolysis of an ester is slower at a lower temperature than the neutralisation reaction.

The titration calibration curve for the PAA control showed an excellent correlation (r^2=0.99) between the concentration of the PAA and the volume of the NaOH (0.1 M) used for neutralisation, thus indicating the suitability of this method for quantification of the free carboxylic groups. Moreover, previous studies have also reported the titration of PAA by the same method (Bensacia and Moulay, 2012) thus giving confidence in the approach.
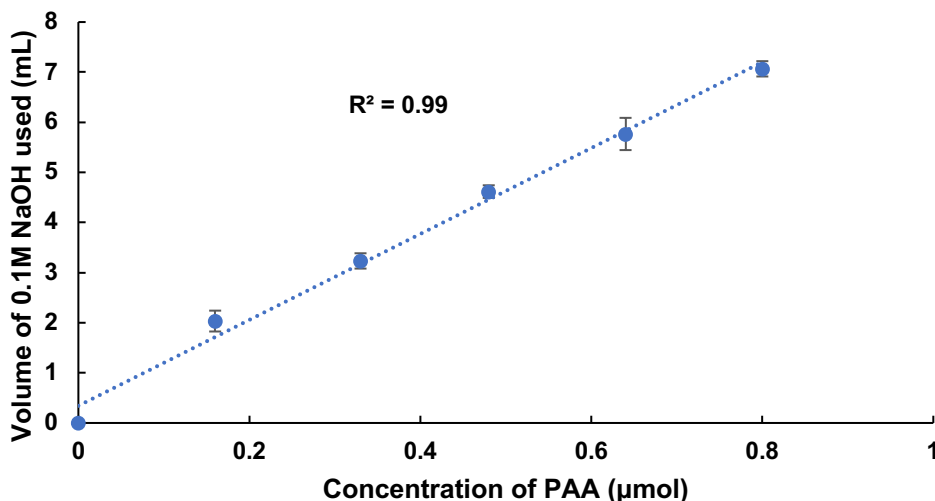
Figure 4.10. Calibration curve for PAA by using titration method. Data are represented as mean ± standard deviation (n=3).

From this calibration curve, the volume of 0.1M NaOH used to neutralise the copolymer systems was used to assess the PAA content. For example, for 0.8. μmol of copolymer (3:7, AA:APMD) solution was neutralised by 8.9 mL of 0.1M NaOH. From this the percentage of free carboxylic groups were calculated by using the following formula:

$$\text{Volume}_{(\text{NaOH used in PAA})}-\text{Volume}_{(\text{NaOH used in copolymer})}/\text{ Volume}_{(\text{NaoH used in PAA})}*100.$$

From the above equation the amount of free carboxylic groups (AA,) was 89.8% and so the assumption is that the remainder of the material (10.2%) was APMD

Table 4.5. Drug loading calculation at various molar ratios of the monomers by the titration method

Monomer ratio	Volume of 0.1M NaOH	%AA content	%APMD content
3:7 (AA:APMD)	8.9 mL	89.8	10.2
5:5 (AA:APMD)	9.25 mL	92.5	7.5
7:3 (AA:APMD)	9.62 mL	96.2	3.8

4.4.8.2. Elemental Analysis

Elemental analysis is a technique that provides information on the composition of any chemical entity at an elemental level, *i.e.* C, N, H *etc*. This technique is commonly employed to determine the composition of polymers (Hu et al., 2019). Here, the amount of PMD (drug) within the copolymer was determined through elemental analysis. The drug percentage was calculated by using carbon (%) via the carbon (content) analysis. The rationale for using carbon content was that both APMD and AA have carbon atoms in their structures. For calculating the amount of drug-loaded, first it was necessary to determine the percentage of carbon in PMD alone and PAA alone. It is understood that by changing the molar ratio of the copolymer will have different carbon content (%C) in the final product. The drug content was calculated through the following equation.

Weight (%) Drug= $\%C_{(\text{copolymer})}-\%C_{(\text{PAA})}/\%C_{(\text{PMD})}-\%C_{(\text{PAA})}*100$ (Hu et al., 2019).

For the copolymer 3:7 (AA:APMD), the total weight(%) of the APMD was calculated to be 9.7%, in close agreement with the titrimetric value of 10.2%.

Table 4.6. Drug loading calculation at various molar ratios of the monomers by the elemental analysis method

Monomer ratio	%AA content	%APMD content
3:7 (AA:APMD)	91.3	9.7
5:5 (AA:APMD)	92.9	7.1
7:3 (AA:APMD)	96.8	3.2

4.4.9. Correlation of Drug Loading with Reactivity Ratio

The composition of a copolymer is usually different from the composition of the monomer feed from which copolymer is synthesised because different monomers have different reactivities to undergo copolymerisation (Ayranci et al., 2016). Here it can be seen that initially, APMD concentration in the mixture feed during the 3:7 (AA:APMD) synthesis was 70% whilst acrylic acid was 30%. However, after the synthesis of the copolymer, the percentage of incorporated acrylic acid is 85-88% (obtained from titration and elemental analysis), far higher than the initial composition, *i.e.* 30%. This indicates that APMD is far less reactive than the AA. This observation is in agreement with the data obtained from the reactivity ratio experiment. It can be due to the bulky nature of the APMD as there have been reports that when the structure is bulky, it can lead to decrease in reactivity ratio because bulky groups promote termination of the reaction hence inhibiting polymerisation of that particular monomer (Elias, 1977).

4.5.   Conclusion

Free radical polymerisation of AA and APMD resulted in the formation of poly(AA-*co*-APMD) ester copolymer with low to medium molecular weight (depending upon the monomer ratios).The reactivity ratio study revealed that the AA is much reactive than the APMD, probably due to the presence of bulky cyclohexane ring in the APMD. The properties of the copolymer were dependent upon the monomer ratios in the feed mixtures. Higher content of APMD in the monomer mixture results in the formation of a turbid solution in water. Thermal analysis revealed the thermal stability of the copolymer as compared to the free drug (PMD) whilst the DSC study revealed a decrease in the Tg by the addition of APMD into the mixture feed, most probably due to the decrease in the rigidity of the polymer chain. Drug loading was calculated by two methods; titration method and elemental analysis. Both were showing comparable results. These results were in accordance with the reactivity ratio studies.
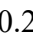
References

Abbasi, R., Nodehi, A., Atai, M., 2020. Synthesis of poly(acrylic-co-itaconic acid) through precipitation photopolymerization for glass-ionomer cements: Characterization and properties of the cements. Dent. Mater. https://doi.org/https://doi.org/10.1016/j.dental.2020.03.006

Ayranci, R., Ak, M., Karakus, M., Cetisli, H., 2016. The effect of the monomer feed ratio and applied potential on copolymerization: investigation of the copolymer formation of ferrocene-functionalized metallopolymer and EDOT. Des. Monomers Polym. 19, 545–552. https://doi.org/10.1080/15685551.2016.1187438

Bensacia, N., Moulay, S., 2012. Functionalization of Polyacrylic Acid with Tetrahydroxybenzene via a Homolytic Pathway: Application to Metallic Adsorption. Int. J. Polym. Mater. Polym. Biomater. 61, 699–722. https://doi.org/10.1080/00914037.2011.617343

Bozorg, M., Hankiewicz, B., Abetz, V., 2020. Solubility behaviour of random and gradient copolymers of di- and oligo(ethylene oxide) methacrylate in water: effect of various additives. Soft Matter 16, 1066–1081. https://doi.org/10.1039/C9SM02032B

Chytil, P., Etrych, T., Kříž, J., Šubr, V., Ulbrich, K., 2010. N-(2-Hydroxypropyl)methacrylamide-based polymer conjugates with pH-controlled activation of doxorubicin for cell-specific or passive tumour targeting. Synthesis by RAFT polymerisation and physicochemical characterisation. Eur. J. Pharm. Sci. 41, 473–482. https://doi.org/https://doi.org/10.1016/j.ejps.2010.08.003

Contreras-López, D., Saldívar-Guerra, E., Luna-Bárcenas, G., 2013. Copolymerization of isoprene with polar vinyl monomers: Reactivity ratios, characterization and thermal properties. Eur. Polym. J. 49, 1760–1772. https://doi.org/https://doi.org/10.1016/j.eurpolymj.2013.03.030

Don, T.-M., Huang, M.-L., Chiu, A.-C., Kuo, K.-H., Chiu, W.-Y., Chiu, L.-H., 2008. Preparation of thermo-responsive acrylic hydrogels useful for the application in transdermal drug delivery systems. Mater. Chem. Phys. 107, 266–273. https://doi.org/https://doi.org/10.1016/j.matchemphys.2007.07.009

Drapeau, J., Rossano, M., Touraud, D., Obermayr, U., Geier, M., Rose, A., Kunz, W., 2011. Green synthesis of para-Menthane-3,8-diol from Eucalyptus citriodora: Application for repellent products. Comptes Rendus Chim. 14, 629–635. https://doi.org/https://doi.org/10.1016/j.crci.2011.02.008

Ebnesajjad, S., 2016. Introduction to Plastics, in: Baur, E., Ruhrberg, K., Woishnis, W.B.T.-C.R. of E.T. (Eds.), Plastics Design Library. William Andrew Publishing, pp. xiii–xxv. https://doi.org/https://doi.org/10.1016/B978-0-323-47357-6.00021-0

Ebnesajjad, S., 2003. 5 - Polymerization and Finishing Melt Processible Fluoropolymers, in: Ebnesajjad, S.B.T.-M.P.F. (Ed.), . William Andrew Publishing, Norwich, NY, pp. 41–122. https://doi.org/https://doi.org/10.1016/B978-188420796-9.50008-4

Ekpenyong, K.I., 1985. Monomer reactivity ratios: Acrylic acid-methylmethacrylate copolymerization in dimethylsulfoxide. J. Chem. Educ. 62, 173.

Elias, H.-G., 1977. Copolymerization BT - Macromolecules: Volume 1 · Structure and Properties, in: Elias, H.-G. (Ed.), . Springer US, Boston, MA, pp. 761–798. https://doi.org/10.1007/978-1-4615-7364-7_22

Erbil, C., Terlan, B., Akdemir, Ö., Gökçeören, A.T., 2009. Monomer reactivity ratios of N-isopropylacrylamide–itaconic acid copolymers at low and high conversions. Eur. Polym. J. 45, 1728–1737. https://doi.org/https://doi.org/10.1016/j.eurpolymj.2009.02.023

Francois, E., Dorcemus, D., Nukavarapu, S., 2015. 1 - Biomaterials and scaffolds for musculoskeletal tissue engineering, in: Nukavarapu, S.P., Freeman, J.W., Laurencin, C.T.B.T.-R.E. of M.T. and I. (Eds.), . Woodhead Publishing, pp. 3–23. https://doi.org/https://doi.org/10.1016/B978-1-78242-301-0.00001-X

Fras, L., Stana-Kleinschek, K., Ribitsch, V., Sfiligoj-Smole, M., Kreze, T., 2004. Quantitative Determination Of Carboxyl Groups In Cellulose Polymers Utilizing Their Ion Exchange Capacity And Using A Complexometric Titration. Mater. Res. Innov. 8, 145–146. https://doi.org/10.1080/14328917.2004.11784850

Hagiopol, C.B.T.-R.M. in M.S. and M.E., 2016. Copolymers. Elsevier. https://doi.org/https://doi.org/10.1016/B978-0-12-803581-8.01126-7

Hobson, R., 2001. Glass Formation and Sub-Tg Transitions in Polymers: Influence of Carbon Chemistry, in: Buschow, K.H.J., Cahn, R.W., Flemings, M.C., Ilschner, B., Kramer, E.J.,

Mahajan, S., Veyssière, P.B.T.-E. of M.S. and T. (Eds.), . Elsevier, Oxford, pp. 3545–3550. https://doi.org/https://doi.org/10.1016/B0-08-043152-6/00631-8

Hu, Y., Stevens, D.M., Man, S., Crist, R.M., Clogston, J.D., 2019. Total drug quantification in prodrugs using an automated elemental analyzer. Drug Deliv. Transl. Res. 9, 1057–1066. https://doi.org/10.1007/s13346-019-00649-8

insect-repellent-usage @ www.infantrisk.com, n.d.

Khutoryanskiy, V. V, Dubolazov, A. V, Nurkeeva, Z.S., Mun, G.A., 2004. pH Effects in the Complex Formation and Blending of Poly(acrylic acid) with Poly(ethylene oxide). Langmuir 20, 3785–3790. https://doi.org/10.1021/la049807l

Khutoryanskiy, V. V, Staikos, G., 2009. Hydrogen-bonded interpolymer complexes: formation, structure and applications. World Scientific.

Klein, L.C., Wojcik, A.B., 2001. Polymer–Ceramic Nanocomposites: Polymer Overview, in: Buschow, K.H.J., Cahn, R.W., Flemings, M.C., Ilschner, B., Kramer, E.J., Mahajan, S., Veyssière, P.B.T.-E. of M.S. and T. (Eds.), . Elsevier, Oxford, pp. 7577–7584. https://doi.org/https://doi.org/10.1016/B0-08-043152-6/01357-7

Krivorotova, T., Radzevicius, P., Makuska, R., 2015. Synthesis and characterization of anionic pentablock brush copolymers bearing poly(acrylic acid) side chains on the brush blocks separated by linear poly(butyl methacrylate) blocks. Eur. Polym. J. 66, 543–557. https://doi.org/https://doi.org/10.1016/j.eurpolymj.2015.02.027

Li, X., Ouyang, C., Yuan, Y., Gao, Q., Zheng, K., Yan, J., 2015. Evaluation of ethylene–acrylic acid copolymer (EAA)-modified asphalt: Fundamental investigations on mechanical and rheological properties. Constr. Build. Mater. 90, 44–52. https://doi.org/https://doi.org/10.1016/j.conbuildmat.2015.04.049

Liu, J., Liu, W., Weitzhandler, I., Bhattacharyya, J., Li, X., Wang, J., Qi, Y., Bhattacharjee, S., Chilkoti, A., 2015. Ring-Opening Polymerization of Prodrugs: A Versatile Approach to Prepare Well-Defined Drug-Loaded Nanoparticles. Angew. Chemie Int. Ed. 54, 1002–1006. https://doi.org/10.1002/anie.201409293

Ma, W.-D., Xu, H., Wang, C., Nie, S.-F., Pan, W.-S., 2008. Pluronic F127-g-poly(acrylic acid) copolymers as in situ gelling vehicle for ophthalmic drug delivery system. Int. J. Pharm. 350, 247–256. https://doi.org/10.1016/j.ijpharm.2007.09.005

Malathi, M., Vedha Hari, B.N., Ramyadevi, D., 2020. Chapter 6 - Polymeric nanocarriers for topical drug delivery in skin cream, in: Nanda, A., Nanda, S., Nguyen, T.A., Rajendran, S., Slimani, Y.B.T.-N. (Eds.), Micro and Nano Technologies. Elsevier, pp. 109–126. https://doi.org/https://doi.org/10.1016/B978-0-12-822286-7.00006-1

Maurer, J.J., Eustace, D.J., Ratcliffe, C.T., 1987. Thermal characterization of poly(acrylic acid). Macromolecules 20, 196–202. https://doi.org/10.1021/ma00167a035

McNeill, I.C., Sadeghi, S.M.T., 1990. Thermal stability and degradation mechanisms of poly(acrylic acid) and its salts: Part 1—Poly(acrylic acid). Polym. Degrad. Stab. 29, 233–246. https://doi.org/https://doi.org/10.1016/0141-3910(90)90034-5

Mota-Morales, J.D., Sánchez-Leija, R.J., Carranza, A., Pojman, J.A., del Monte, F., Luna-Bárcenas, G., 2018. Free-radical polymerizations of and in deep eutectic solvents: Green synthesis of functional materials. Prog. Polym. Sci. 78, 139–153. https://doi.org/https://doi.org/10.1016/j.progpolymsci.2017.09.005

Mun, G.A., Nurkeeva, Z.S., Khutoryanskiy, V. V, Sarybayeva, G.S., Dubolazov, A. V, 2003. pH-effects in the complex formation of polymers I. Interaction of poly(acrylic acid) with poly(acrylamide). Eur. Polym. J. 39, 1687–1691. https://doi.org/https://doi.org/10.1016/S0014-3057(03)00065-X

Pandey, S.K., Upadhyay, S., Tripathi, A.K., 2009. Insecticidal and repellent activities of thymol from the essential oil of Trachyspermum ammi (Linn) Sprague seeds against Anopheles stephensi. Parasitol. Res. 105, 507–512. https://doi.org/10.1007/s00436-009-1429-6

Paulsen, K., Frasco, D., Scientific, T.F., 2017. Qualitative and quantitative analysis of the polymerization of PS- b -P t BA block copolymer using picoSpin 80 NMR.

Principles+of+Polymerization,+4th+Edition-p-9780471274001 @ www.wiley.com, n.d.

Ritthidej, G.C., 2011. Chapter 3 - Nasal Delivery of Peptides and Proteins with Chitosan and Related Mucoadhesive Polymers, in: Van Der Walle, C.B.T.-P. and P.D. (Ed.), . Academic Press, Boston, pp. 47–68. https://doi.org/https://doi.org/10.1016/B978-0-12-384935-9.10003-3

Shahzamani, M., Taheri, S., Roghanizad, A., Naseri, N., Dinari, M., 2020. Preparation and characterization of hydrogel nanocomposite based on nanocellulose and acrylic acid in

the presence of urea. Int. J. Biol. Macromol. 147, 187–193. https://doi.org/https://doi.org/10.1016/j.ijbiomac.2020.01.038

Shukla, S., 2020. Synthesis, kinetics and characterization of environment friendly waterborne acrylate copolymers. Mater. Today Proc. https://doi.org/https://doi.org/10.1016/j.matpr.2020.04.164

Soto, D., Urdaneta, J., Pernia, K., 2014. Characterization of Native and Modified Starches by Potentiometric Titration. J. Appl. Chem. 2014, 162480. https://doi.org/10.1155/2014/162480

Srivastava, A., Kumar, R., 2013. Synthesis and Characterization of Acrylic Acid-g-(Carrageenan) Copolymer and Study of Its Application. Int. J. Carbohydr. Chem. 2013, 892615. https://doi.org/10.1155/2013/892615

Sugibayashi, K., Morimoto, Y., 1994. Polymers for transdermal drug delivery systems. J. Control. Release 29, 177–185. https://doi.org/https://doi.org/10.1016/0168-3659(94)90134-1

Tüdős, F., Földes-Berezsnich, T., 1989. Free-radical polymerization: Inhibition and retardation. Prog. Polym. Sci. 14, 717–761. https://doi.org/https://doi.org/10.1016/0079-6700(89)90008-7

Valenta, C., Auner, B.G., 2004. The use of polymers for dermal and transdermal delivery. Eur. J. Pharm. Biopharm. 58, 279–289. https://doi.org/https://doi.org/10.1016/j.ejpb.2004.02.017

van Houwelingen, G.D.B., Aalbers, J.G.M., de Hoog, A.J., 1980. Determination of amino- and carboxyl end-groups in poly(paraphenylene terephthalamide). Fresenius' Zeitschrift für Anal. Chemie 300, 112–120. https://doi.org/10.1007/BF00517828

Wong, C.L.H., Kim, J., Torkelson, J.M., 2007. Breadth of glass transition temperature in styrene/acrylic acid block, random, and gradient copolymers: Unusual sequence distribution effects. J. Polym. Sci. Part B Polym. Phys. 45, 2842–2849.

https://doi.org/10.1002/polb.21296

Zhang, X.-M., Patel, A.B., de Graaf, R.A., Behar, K.L., 2004. Determination of liposomal encapsulation efficiency using proton NMR spectroscopy. Chem. Phys. Lipids 127, 113–120. https://doi.org/https://doi.org/10.1016/j.chemphyslip.2003.09.013

Chapter 5. *In vitro* Hydrolysis and Skin Penetration and Permeation Study of the Copolymer poly(AA-*co*-APMD)

5.1. Introduction

Insect repellents are widely applied to prevent bites and associated rash that are caused by insect bites. They are also commonly used as a protective measure against insect-borne diseases. Current insect repellent formulations have various shortcomings, thus requiring strategies to improve their performance (Maia and Moore, 2011; Rodriguez et al., 2015).

Polymers are widely used in pharmaceutical dosage form including covalently attaching the drug with the polymer backbone (D'Souza and Topp, 2004). Therapeutically, PDCs have been used for various purposes that include cancer (Greco and Vicent, 2008) and for other diseases. One (of various) reason for attaching the drug to a polymeric backbone is to enable long-lasting drug delivery (Zhu et al., 2014); for this purpose, they are conjugated *via* various degradable linkages (Dong et al., 2019; Lau et al., 2013). There are several mechanisms for the release of the drug from degradable linkages, including pH mediated drug release, enzymatic drug release and temperature-mediated drug release *etc* (de la Rica et al., 2012; Deng et al., 2009). Among enzymatic drug release, various enzyme sensitive linkages have been synthesised, one of which is the ester linkage that can be hydrolysed by the addition of esterases (Zhang et al., 2017). Human skin contains naturally occurring esterases, which can hydrolyse the ester compounds (Findlay, 1955). Pigs have multiple forms of carboxylesterases, with the highest levels being in the liver. These enzymes are readily available as porcine liver esterases (PLEs) whereas human skin esterases have limited and expensive commercial availability and so PLEs are widely used in enzymatic drug release studies (Zhou et al., 2019).

As discussed earlier in chapter 3, various studies raise specific concerns over the systemic absorption of insect repellents such as diethyltoluamide (DEET) and subsequent side effects, especially regarding their use in pregnant women and the neonates (Tavares et al., 2018). Therefore, it is important to minimise the systemic absorption of the repellent, for which we have employed the conjugation of the drug to the polymer backbone. To achieve this objective, a Franz diffusion cell approach was used to assess the penetration and permeation of the active ingredients (Wiechers, 2005) using pig ear skin which is a common skin model to study topical penetration and permeation of compounds (Abd et al., 2016). This chapter examines the hydrolysis of the copolymer poly(AA-*co*-APMD) with the addition of porcine liver esterases followed by studies into the penetration and permeation of the copolymer and PMD alone into

the pig ear skin. In order to monitor penetration and permeation, *in vitro* experimental conditions mimicked *in vivo* use as closely as possible

5.2. Materials

 p-menthane-3,8-diol (PMD) was purchased from BOC Sciences (USA), D-Squame tapes were obtained from Clinical & Derm, USA. Parafilm ® (Bemis Flexible Packaging (AMCOR), USA), porcine liver esterases (PLEs), acryloyl chloride and ammonium acetate were acquired from Sigma-Aldrich (Merck, UK), acetonitrile (ACN), ethanol and all other solvents used were of LCMS grade and were procured from Fischer Scientific, UK.

5.3. Methods

5.3.1. Method Development for the Analysis of PMD

Certification of an analytic technique used throughout the drug development and drug production is required to prove that the procedures are appropriate for their proposed objective. Consequently, for the analysis of PMD, liquid chromatography-mass spectroscopy (LC-MS) was used. The sensitivity of the method was tested by determining the limit of detection (LOD) and limit of quantification (LOQ) for PMD. For accomplishing this objective, the following method was used:

Device calibration is a critical stage in most measurement processes. It is a set of procedures that determine the correlation between the yield of the measurement system (*e.g.,* the reaction of an apparatus) and the recognized values of the calibration requirements (*e.g.,* the quantity of analyte present). The first step in the analysis of PMD was to construct a calibration curve. In order to prepare a sample for the calibration curve, a stock solution of 1000 µg/mL (1mg/mL) was prepared by dissolving 10 mg of PMD in 10 mL of acetonitrile.   This was then serially diluted to make 200, 100, 50, 25, 10, 5 and 1 µg/mL dilutions (by using the following):

Concentration $_{(start)}$ x Volume $_{(start)}$ = Concentration $_{(final)}$ x Volume$_{(final)}$

(abbreviated as $C_1V_1 = C_2V_2$)

with solutions prepared in water: acetonitrile ratio of 4:6 v/v. The main reason for using water: acetonitrile (4:6 v/v) was to have equivalence with the final solution (with or without enzymes) after adding acetonitrile to quench the aqueous enzyme hydrolysis solution.

5.3.2. *In vitro* Hydrolysis of the Copolymer by Using Porcine Liver Esterases (PLEs)

For these experiments, 5mg/mL of copolymer containing 3:7 (AA:APMD) was dissolved in water: acetonitrile mixture (9:1 v/v) and the pH was adjusted to 7 by ammonium acetate buffer (10 mM of the buffer was prepared by dissolving 77 mg of ammonium acetate in 100 mL of LCMS grade water). Then, 35 mg of PLEs (1 unit of enzyme per μM of the copolymer) was added and the solution was stirred at 32±1°C (to mimic the skin temperature). Experimental samples (0.75 mL) were systematically withdrawn and quenched with equivolume of acetonitrile (0.75 mL). They were then subjected to centrifugation (Sanyo MSE Micro Centaur MSB010.CX2.5) at 13000 rpm for 12 minutes; the supernatant was collected and was analysed by LCMS. In this study, the control used was of the same copolymer but without PLEs. All experiments were performed in triplicate, and representative data are shown. The concentration for the unknown samples was calculated as:

Concentration (μg/mL) of unknown= Peak area*Dilution factor.

Dilution factor was calculated as Df= Vf/Vi where Df stands for dilution factor, Vf for final volume and Vi for initial (original) volume.

5.3.3. *In vitro* Hydrolysis of Monomer Drug Conjugate (APMD) by Using PLEs

Initially, 1.2 mg/mL of monomer drug conjugate (APMD) was dissolved in acetonitrile (ACN) followed by the dropwise addition of water with continuous stirring until a clear solution was obtained with a final proportion of water: acetonitrile of 9:1 (v/v). The pH of the solution was adjusted to 7 by adding ammonium acetate buffer (10 mM of the buffer was prepared by dissolving 77 mg of ammonium acetate in 100 mL of LCMS grade water). Then to this, 54.3 mg of PLEs (1 unit of enzyme per micromole of APMD) were added, and the solution was stirred at 32 ± 1°C (corresponding to the skin temperature). Experimental samples (0.75 mL each) were regularly taken and quenched with an equivolume of ACN (0.75 mL) and were then subjected to centrifugation at 13000 rpm for 12 minutes, after which the supernatant was

collected and was subjected to analysis by LCMS. In this study, the control used was of APMD without PLEs. All experiments were completed in triplicate, and representative numbers are displayed. The concentration for the unknown samples was assessed by using the following calculation:

Concentration (µg/mL) of unknown= Peak area*Dilution factor

Dilution factor was calculated as Df= Vf/Vi where, Df stands for dilution factor, Vf for final volume and Vi for initial (original) volume.

5.3.4. *In vitro* Hydrolysis by Adding Continuous Supply of PLEs

In order to assess long term release of PMD from the copolymer, a continuous (replenished) supply of the enzyme was provided. Briefly, the same procedure as reported earlier (5.3.2) was followed but with a minor modification, *i.e.,* after every 24 h, a fresh aliquot of the enzyme was added (at the above concentration). In this study, the control used was copolymer without PLEs. The experiment was performed in triplicate. The concentration of the liberated PMD was calculated as:

Concentration (µg/mL) of unknown= Peak area*Dilution factor

Dilution factor was calculated as: Df= V_f/V_i where, Df stands for dilution factor, V_f for final volume and V_i for initial (original) volume.

5.3.5. Evaluation of the PMD Release Profile

Evaluation of the PMD release profile was done by using

Zero-order kinetics F=K_0 t where *F* is the fraction of drug release at time *t* and K_0 is the zero-order release constant.

First-order kinetics Ln (1−F) = −K_1t where K_1 is the first order release constant.

 Higuchi model F=−K_2t1/2 where K_2 is the Higuchi constant.

Korsmeyer-Peppas Model MtM∞=K_3tn where MtM∞ is the fraction of drug release at time *t*, K_3 is the release rate constant, and *n* is the release exponent. The different release mechanisms were characterized using the calculated *n* value. When *n* < 0.5, the diffusion

mechanism is quasi-Fickian, $n = 0.5$ is Fickian diffusion, $0.45 < n < 1$ refers to non-Fickian diffusion, $n = 1$ is case-II transport, and $n > 1$ refers to super case-II transport (Wong and Dodou, 2017).

5.3.6. *In vitro* Skin Penetration and Permeation Study

5.3.6.1. Preparation of Skin Membranes

Although human skin is the most relevant membrane for percutaneous drug absorption, due to its limited availability for experimental use, a wide range of animal models has been investigated as a replacement. Porcine skin was found to be a good alternative for human skin in several *in vitro* studies (Lau et al., 2010; Rizi et al., 2011). Pig ears obtained from a local slaughterhouse (within 6 h of animal sacrifice) were kept at -20°C before membrane preparation (frozen skin was used within two months). The ears were defrosted before preparation and cleaned under cold running tap water. Hair was trimmed with a trimmer (Panasonic, Japan). Full-thickness skin containing dermis and epidermis was harvested from the underlying cartilage by using a scalpel (Swann-Morton, UK).

5.3.6.2. Skin Permeation Study

The permeation of PMD and the copolymer were compared to determine the amount of each that may potentially be taken up by the systemic circulation. For this, firstly the integrity of the skin was checked by physical inspection of the skin. The skin was then mounted on six glass Franz-type diffusion cells, with nominal diffusion area of 3.14 cm^2 and the receptor volume of 15 mL. Thickness of the skin was 70μm. Skin samples were positioned between the donor and receptor chambers of the cell, with the dermis in contact with the receptor medium. Finite doses (15mg/5 mL, 3mg/mL) of each PMD and the copolymer prepared in water: ethanol (8:2 v/v) were applied to the donor chamber. For the preparation of solutions, the volume of ethanol was kept at 20% (v/v) to prevent the increase in permeation by the ethanol itself as per Williams and Barry (2004). The Franz-cells were placed in an incubator set at 32±1°C. The permeation studies were performed under occlusion with Parafilm to ensure hydration and equilibration of the stratum corneum. Samples (1 mL) were taken periodically from the receptor compartment at 0.25, 0.5, 1, 1.5, 3, 6, 12, 24,48 and 72 h and were replaced with

equivolume of the water: ethanol (8:2 v/v) receptor medium. For each PMD and copolymer, six replicates were used.

5.3.6.3. Skin Penetration Study

At the end of the permeation study, *i.e.,* 72 h, a skin penetration study was performed. For this, a tape stripping method was used to collect the test compound from the skin in such a way that twenty tape strips were used. The first two tape strips were assumed to account for the solution remaining on the skin surface of each donor chamber, tape strips 3-10 accounted for the upper stratum corneum, while from 11-20 accounted for the lower stratum corneum. The strips of adhesive tapes were cautiously attached to the marked skin location to prevent wrinkles, with continuous weight application. For the extraction process, the tape strips were immersed in ethanol and were subjected to sonication for 15 minutes at room temperature. Any remaining skin particulates were removed *via* filtration using 0.45μm filter (ThermoFischer, UK) and the extraction liquid was subjected to analysis by gel permeation chromatography (GPC). For GPC, we used THF as a solvent with an injection volume of 100 μL and a flow rate of 1mL/min. Here, PMD was used as control and was analysed through LCMS.

5.3.6.4. Data Analysis for Skin Permeation and Penetration Study

Permeation was evaluated by plotting the cumulative amount (Q_A) of the PMD or copolymer permeated per unit surface area of the membrane against the collection time for each diffusion cell. For this study, a steady state flux (J_{SS}) was calculated by linear regression using Microsoft Excel software within the first two hours.

5.3.6.5. Statistical analysis

Statistical analysis was carried out using MS Excel 2016 Data Analysis Add-In programme. Significant differences and comparisons of the means were made using ANOVA (single factor).

5.4. Results and Discussion

5.4.1. Analysis of PMD

5.4.1.1. Method Development for the Analysis of PMD

One of the major concerns for this study was to develop an accurate and sensitive method to detect PMD. Commonly used methods for the detection of a drug are HPLC and UV. Here, these methods were not suitable as PMD does not have a chromophore to be detected and a synthetic approach to attach a chromophore risks loss of this volatile analyte. Thus, a mass spectroscopy related technique was sought. Previously gas chromatography-mass spectroscopy (GCMS) has been used as an analytical method to analyse PMD (Tian et al., 2005), but we were unable to accurately quantify low levels of PMD through this method. Thus, liquid chromatography-mass spectroscopy (LC-MS) was used to analyse and quantify PMD. The first step (to develop a method for the detection and quantification of PMD) was to optimise conditions/setting (selection of column as well as the other parameters such as the amount of acid to be used). Initially, we used a C-4 column with 1% formic acid, but this gave excessive tailing. Likewise, a cyano column (CN columns with cyanopropyl groups) with 1% formic acid also resulted in excessive tailing as well as poor peak separation. The chromatogram for this is shown in Figure 5.1.

Subsequently, a phenyl column with 2% formic acid gave better peak separation (Figure 5.2) and no significant tailing was found in the peaks as compared to the preliminary attempts; the shape of the peak is important because if the baseline of the peak or overall shape of the peak is distorted, the calibration curve can be compromised since the software calculates the concentration by overall area of the peak. The best possible explanation for the success of 2% formic acid and phenyl column can be that the formic acid ''buffers'' the eluent system well away from the pka of the analyte leaving the analyte in the ion suppressed form. Moreover, phenyl column has got affinity towards the OH groups thus leading to a good retention and better separation of the peak (Ge and Sem, 2012).
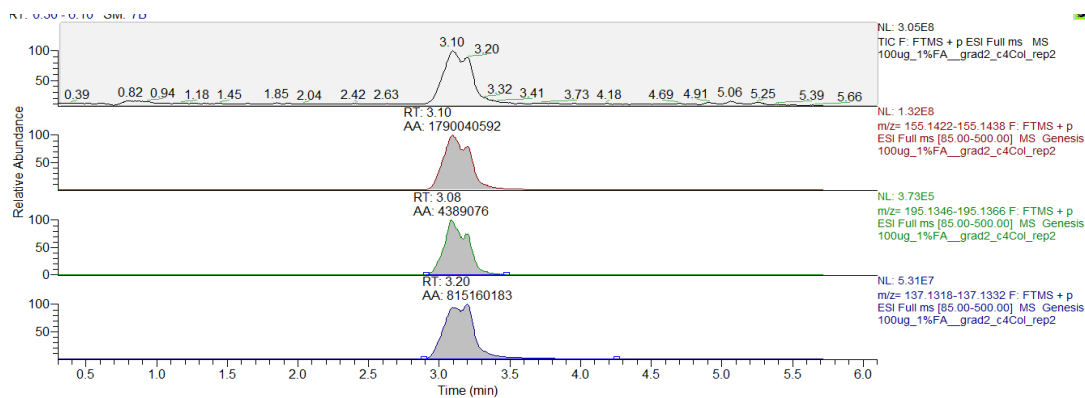
A
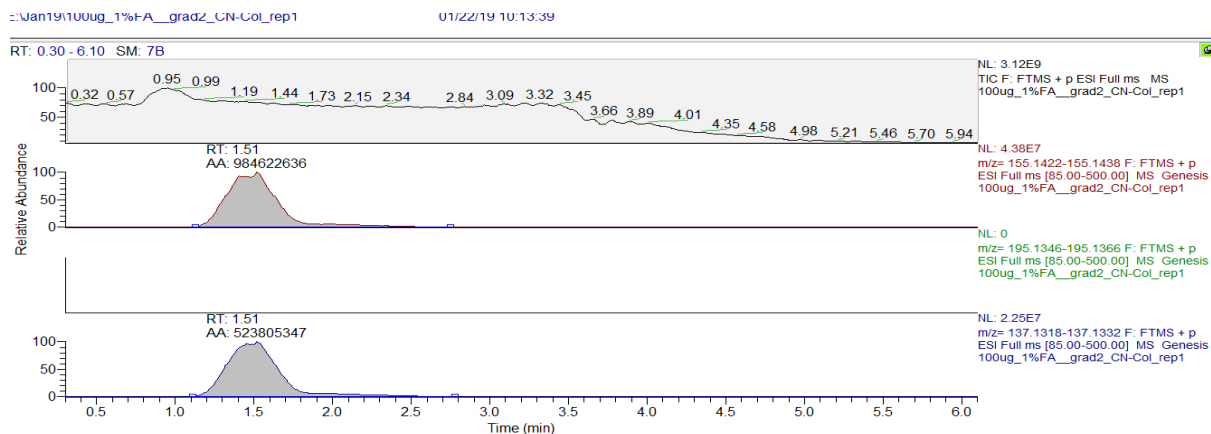
B

Figure 5.1. Preliminary attempts for the method development to analyse PMD, showing chromatogram A (using C-4 column) & B (using cyano column).
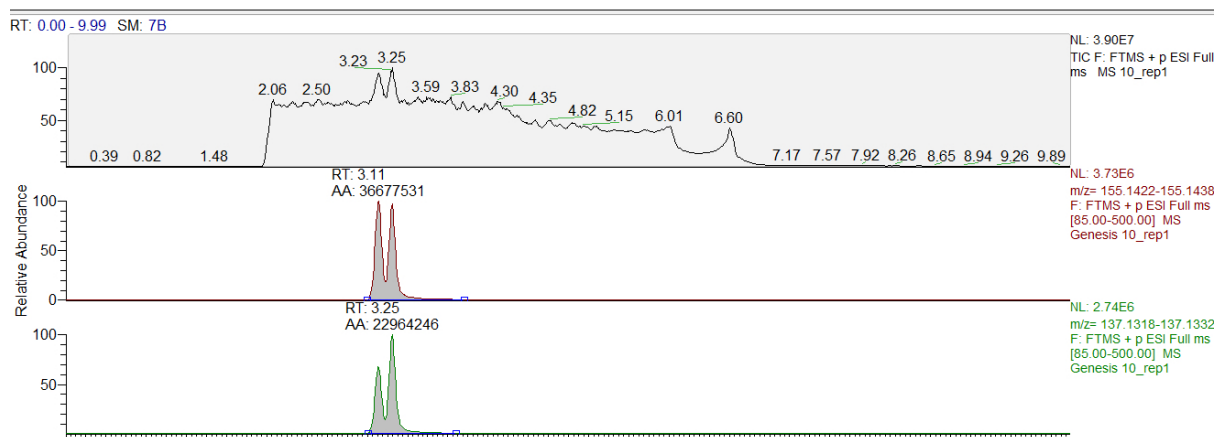
Figure 5.2. Chromatogram showing two separate peaks for PMD corresponding to 155 and 137 Da using the phenyl column with 2% formic acid

The chromatogram obtained showed two peaks that accounted for PMD, one with molecular mass of 155 Da at the retention time of 3.11 mins and the other with molecular mass of 137 Da at 3.25 mins. The one with the molecular mass of 155 Da indicated removal of one OH group from the PMD and other with the molecular mass of 137 Da indicated removal of two OH groups from the PMD plus a negative charge due to the loss of an electron. Data can be analysed by considering either of these two peaks (depending upon the calibration curve). The selection of the peak (corresponding to a particular molecular mass) was done on the basis of best regression value obtained. In our case, the peak corresponding to 155 Da gave best results and hence was used for the analysis. Moreover, this phenomenon (removal of OH groups from the PMD) can be possibly explained by the fact that in mass spectroscopy due to the electron impact ionisation conditions homolytic cleavage of the hetero atoms like oxygen, nitrogen and sulphur is very common and often leads to the loss of the largest possible radical, in this case a hydroxyl (OH) group (Conda-Sheridan et al., 2014).
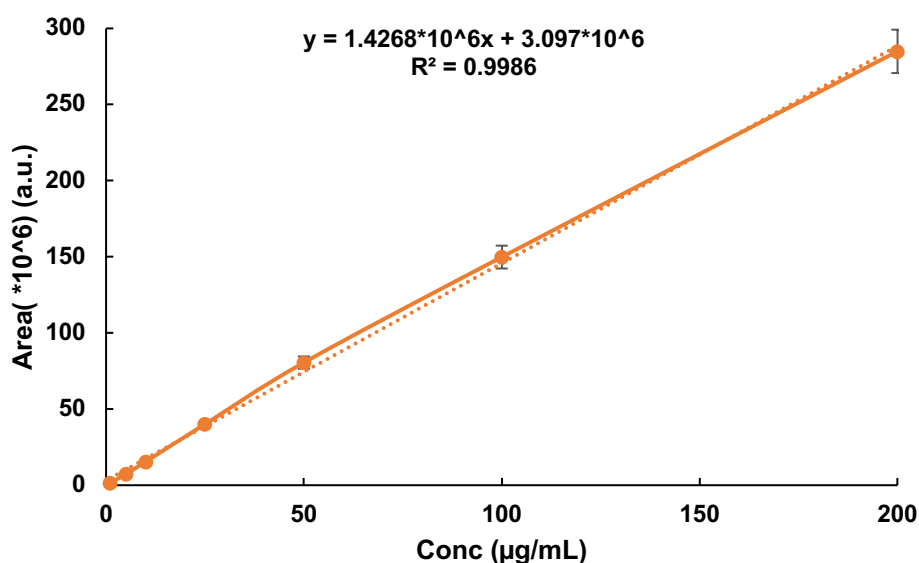
Figure 5.3. Calibration curve for different concentrations of PMD using the peak at 155 Da, due to the loss of one -OH group. Data are represented as mean ± standard deviation (n = 3).

144

5.4.1.2. Limit of Detection (LOD) and Limit of Quantification (LOQ) for the Analysis of PMD

LOD and LOQ provides a measure of sensitivity and precision of an analytical method. Several methodologies can be used to calculate the LOD and LOQ. One of such method is to estimate LOD and LOQ from the signal to noise ratio (S/N) of the lowest calibrator. This method was not selected owing to the variability in its reproducibility (as S/N ratio varies during different experiments). Values were thus determined by testing various concentrations and to experimentally see that what LOD and LOQ an instrument can detect, and how reproducible the data is (Conda-Sheridan et al., 2014). So, based on this experiment we found the limit of detection (LOD) for PMD at 1μg /mL, while limit of quantification (LOQ) for PMD was 5μg /mL.

5.4.1.3. Inter-day and Intraday Precision

Inter and intraday precision is an important parameter used to determine the accuracy and exactness of the method. In this case, inter and intraday assay accuracies were expressed as the percent difference between the measured concentration and the nominal concentration. The percentage accuracy of the method was expressed by the following formula:

% Accuracy = (Measured concentration)/(Nominal concentration)x100 (Bhadra et al., 2011).

The intra-day assay used replicate (n=3) determinations for each concentration of a sample during each analytical run while inter-day assay was carried out by using replicate (n=3) determination of each concentration made on three separate days.

By using the above formula, it was found that percentage accuracy for the intraday results were 91% (Table 5.1) while for the inter day results it was found to be 94.3% (Table 5.2). ICH guidelines require an analytical method to have a linearity (R^2) of >0.999 (here was found to be 0.9986) with an accuracy of 100 +/- 2% and intra- and inter-day precision of ≤2% as residual standard deviation. Whilst the assay developed only partially met these criteria, given the challenging nature of the analyte and that this was used for a developmental rather than a commercial project, the method was suitable for use without further extensive refinements.

Table 5.1. Intraday Assay for the Determination of Accuracy (n=3)

Nominal concentration (µg /mL)	Measured Concentration (µg /mL)			Mean (µg /mL)	SD
	1	2	3		
5.0	2.9	2.8	3.5	3.06	0.37
10.0	9.6	8.1	7.9	8.5	0.92
25.0	25.0	25.0	25.0	25.0	0
50.0	50.0	48.7	49.0	49.2	0.68
100.0	100.0	98.0	99.0	99.0	1.0
200.0	200.0	198.0	199.0	199.0	1.0

Table 5.2. Inter-day Assay for the Determination of Accuracy (n=3)

Nominal concentration (µg /mL)	Measured concentration (µg /mL)			Mean (µg /mL)	SD
	1	2	3		
5.0	3.06	5.8	1.4	3.4	2.1
10.0	8.53	11.6	8.6	9.5	1.7
25.0	25.0	22.6	26.6	24.7	2.0
50.0	49.23	47.4	55.3	50.6	4.1
100.0	99.0	101.5	113.6	104.7	7.8
200.0	199.0	196.8	191.3	195.7	3.9

5.4.2. *In vitro* Hydrolysis Study of the Copolymer

Conjugation of the acryloyl chloride with PMD to form acryloyl-PMD (APMD) was through an ester bond in such a way that the APMD was subsequently copolymerised with acrylic acid (AA) to form the final copolymer. Hydrolysis of the ester bond was investigated by incubating with PLEs to confirm that the copolymer was indeed a substrate for the enzyme. Thus, the copolymer and PLEs were incubated at $32\pm1°C$ (to mimic the skin temperature) with the control copolymer incubated without PLEs (and to evaluate the stability of the ester bond). The results were plotted from the data obtained by using the following equation

Concentration (µg/mL) of unknown= Peak area*Dilution factor

Dilution factor was calculated as shown previously:

$Df = V_f/V_i$

$Df = 1.5/0.75 = 2$

From the equation of the calibration curve (for 155 Da) shown below, we were able to calculate the unknown concentration.

$x = (y - 3E+06)/1E+06$

where x= Concentration and y=Area

By putting the value of area (y) for unknown samples (collected at different time intervals) into the above equation and then multiplying the obtained results with the dilution factor, *i.e.* 2, the following results were obtained which were plotted as a cumulative concentration (µg /mL) vs time (Figure 5.4).
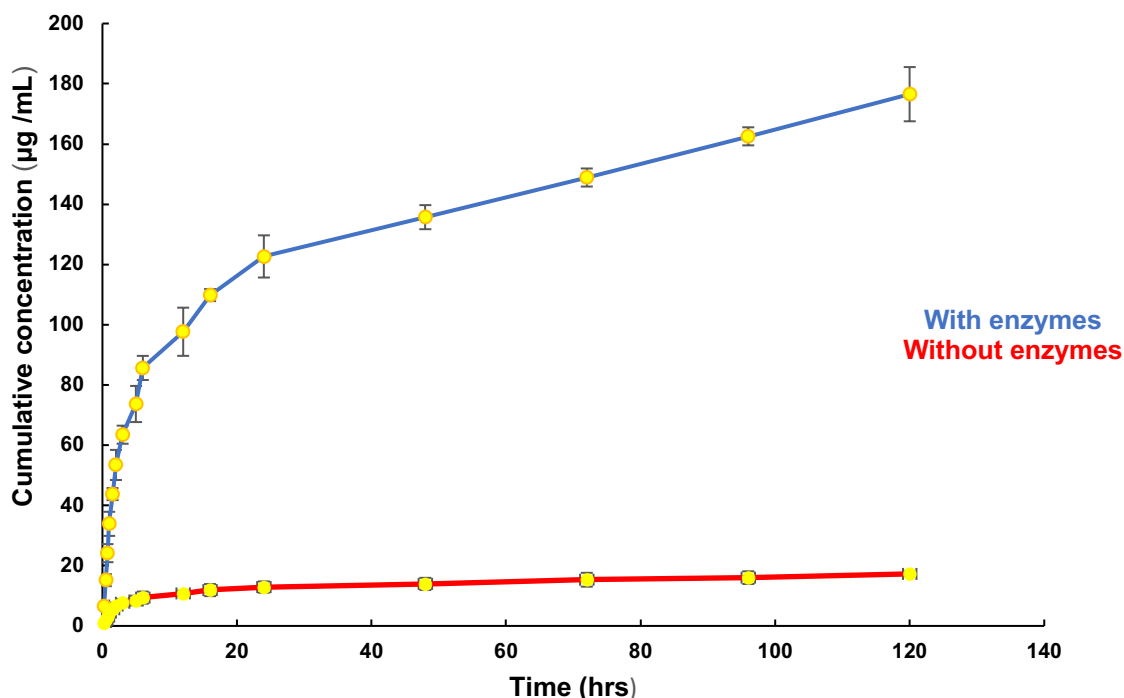
Figure 5.4. Release profile of PMD from the co-polymer with or without PLEs. Data are represented as mean ± standard deviation (n = 3).

In this experiment 5mg/mL of the polymer containing approximately 0.4 mg of PMD was used (calculated from titration study and elemental analysis). From the Figure 5.4 it can clearly be observed that as compared to control (without enzyme) there has been a significant hydrolytic release of the drug indicating that the copolymer is a substrate for PLEs. Moreover, it can also be seen that during the initial 6 h there is rapid release of the drug (showing that the enzymes are still binding to the substrates) followed by a slower sustained release (shown by the plateau in the graph) although this remains above that when no enzymes are present. The initial release phase liberated 85 µg /mL of the PMD, almost which was almost 50% of the total amount of drug released over 5 days (176 µg /mL). Total release at the end of the experiment accounted for around 45% of the total drug load. There can be several explanations for this relatively low amount of drug release. Drug release from the polymeric backbone is governed by multiple factors, *i.e.,* molecular weight, hydration of a polymeric prodrug, steric hindrance and distribution of the drug along the polymeric chain (D'Souza and Topp, 2004). It has been reported by Tallury et al. (2008) that drug release rates decrease with increasing molecular weight, due to chain entanglements which increase with increasing molecular weight and impede the diffusion of drug molecules (or the enzymes) through polymer matrix leading to a decrease in drug release. Likewise hydration of the polymeric prodrug also plays an important

role in drug release in such a way that greater the extent of hydration then greater will be the drug release; as a general rule, the greater the hydrophilicity of a polymer then the greater will be the hydration and vice versa (Pitt and Shah, 1996). Another reason for this relatively low drug release can be steric hindrance; which basically indicates the ability of an enzyme/compound to access the centre of a target compound (Larsen, 1989; Seeman et al., 1984). Moreover, distribution of the drug along the polymeric chain also plays an important role such that PDCs having pendant drugs distributed uniformly along the backbone release faster than those that have them in clustered blocks (Shah et al., 1990). Interestingly, with the control experiment and no enzymes then there is also an initial burst release over the first 6 hours with approximately 10 µg of the PMD released (approximately 2.5% of the loaded drug) followed by a slow but sustained minor release of a further 7 µg over the following 114 hours (approximately 0.015% release per hour over this period). Again, the burst release is approximately half that of the total release and could be attributed to rapid release of accessible "surface exposed" PMD after which the ester linked repellent is stable for extended periods.

From the above, two different hypotheses were tested to assess the relatively low PMD release; (a) measuring release from a lower molecular weight (monomer-drug conjugate, *i.e.* APMD) to determine if steric constraints or chain entanglement was the prime reason and (b) by periodically adding more enzymes to the co-polymer after every 24 h to determine if the enzyme was inactive after a period of time (Wang et al., 2002).

5.4.3. *In vitro* Hydrolysis of Monomer-drug Conjugate (APMD) by Using PLEs

To determine the effects of molecular weight in our system and the role of chain entanglement or steric constraints on drug release, the monomer drug conjugate (APMD) having a molecular weight of 224 Da was used (1.2 mg/mL) in a hydrolysis study.
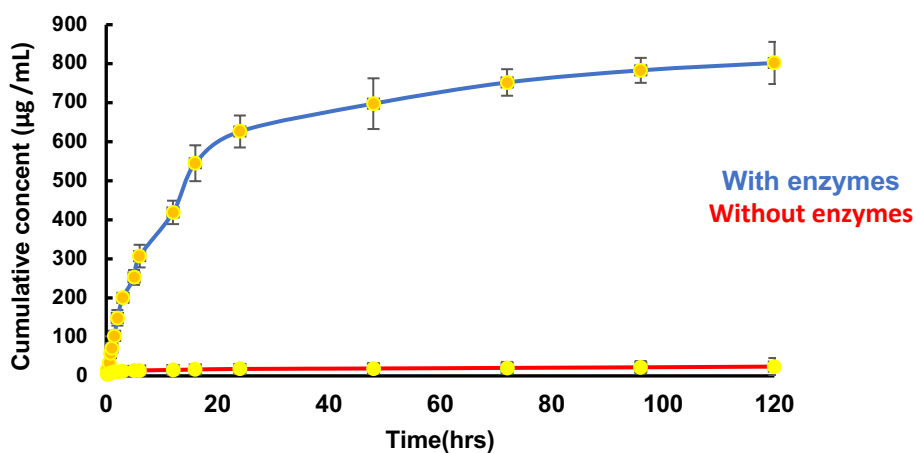
Figure 5.5. Release of the drug over 5 days from the monomer-drug conjugate (APMD) by using PLEs. Data are represented as mean ± standard deviation (n = 3).

Figure 5.4 confirms that molecular weight plays an important role in the release of the PMD from the copolymer. Over five days, almost 90% of the drug was released and it is clear that the initial burst phase extends to 24 hours by which time nearly 80% of the release has occurred. There are several reasons for molecular weight to affect drug release, the most likely of which is chain entanglements, which hamper the diffusion of drug molecules and enzymes through the polymer matrix leading to a decrease in drug release (Tallury et al., 2008). The above results strongly suggest that restricted access of the enzyme to the ester bond in the copolymer resulted in the relatively low drug release seen in Figure 5.4.

5.4.4. *In vitro* Hydrolysis of the Copolymer by Adding Additional PLEs

One of the other possible reasons for the relatively low drug release from the copolymer could have been exhaustion of the enzymes decreasing drug release. In order to test this hypothesis, we choose to constantly add additional enzymes to the system to assess the impact on drug release. For this purpose, fresh enzymes were added after every 24 h over the five days period.

From Figure 5.6, and in comparison, to the original study (Figure 5.4), it is clear that the release of PMD has not been significantly improved by the addition of further fresh enzyme. In the initial study, following 5 days treatment with PLE's 178 µg of PMD was released whereas when fresh enzyme was added daily, 180 µg of PMD was released. Thus, lack of, or loss of,

enzymatic activity was not a factor in the modest release profiles. Consequently, the most probable reason for the observed release profile is that all conjugated PMD molecules are not readily accessible for the enzymes to hydrolyse as there are reports suggesting that the orientation of the polymer chain plays an important role in the accessibility of the enzymes to hydrolyse the bond and release the drug (Kawai et al., 2019).
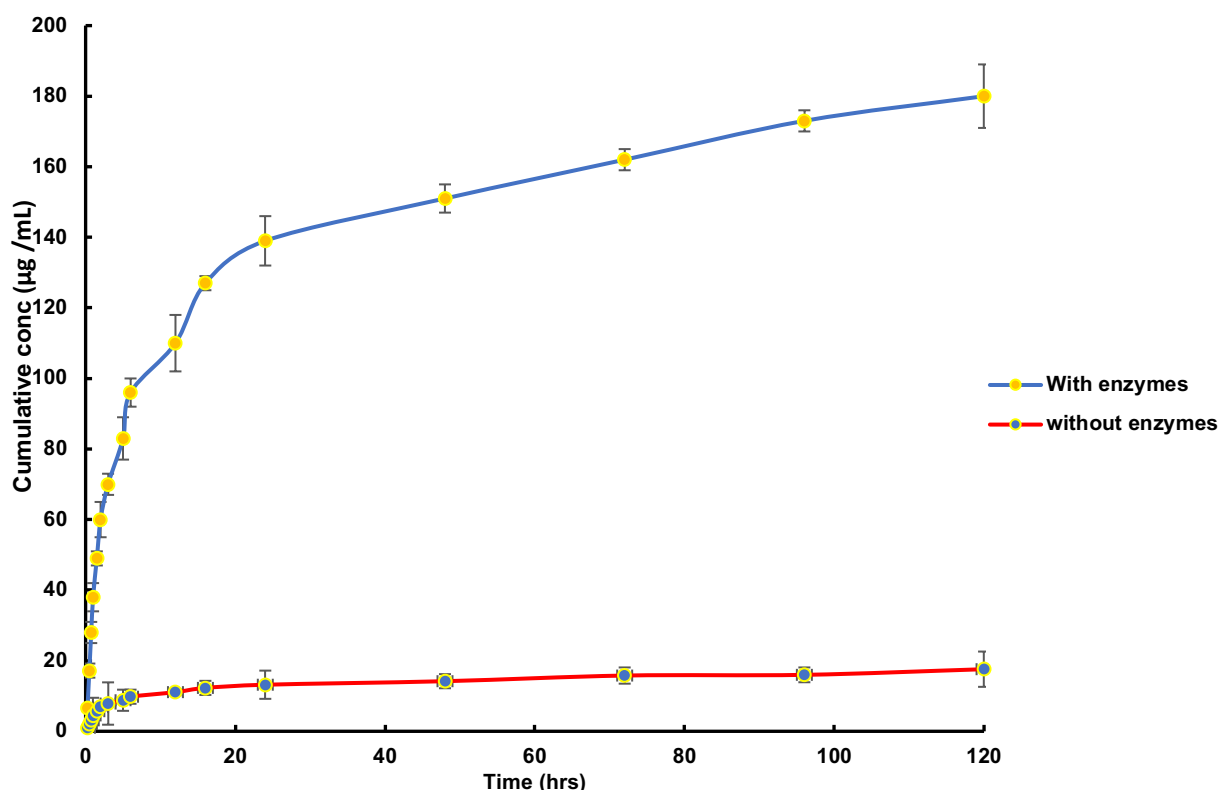
Figure 5.6. Release of the drug over 5 days time from the copolymer by adding PLEs. Data are represented as mean ± standard deviation (n = 3).

5.4.5. Study of Kinetics and Mechanism of Drug Release

In order to distinguish which type of mechanism is followed by the release of drug from the polymer matrix, the kinetics of drug release study can be assessed (Fu and Kao, 2010). To study the kinetics of the drug release, initial 2 h drug release data from the initial enzyme experiment (Figure 5.4) was used. The release constants were calculated from the slope of appropriate plots, and the correlation coefficient (R^2) by linear regression analysis using Microsoft Excel 2016. The representative drug release kinetics plots were plotted for zero order, first order, Higuchi and Korsmeyer-Peppas kinetics for our synthesised copolymer. The

correlation coefficient was selected as a criterion to evaluate the appropriate kinetic model and the corresponding release kinetic data for the synthesized copolymer. The value of R^2 closest to 1 (0.98 for zero order, 0.83 for first order, 0.91 for Korsmeyer-Peppas model and 1.0 for Higuchi model) indicated the best fit of drug release data. Though the zero-order model gave a very high best fit correlation, it can be clearly seen from Figure 5.10 that the best linearity (r^2 = 1.0) was detected in Higuchi's equation plot signifying the release of drug from polymer follows the square root of time.

Different factors controlling the release of drug include the material matrix (composition, structure, swelling and degradation), release medium (pH, enzymes) and nature of the drug (solubility, stability and interaction with matrix) (Costa and Sousa Lobo, 2001). According to the Higuchi model, and inherent assumptions, it was concluded that the polymer upon contact with the water does not swell (indicating dissolution of the matrix is negligible) suggesting the release of drug from an insoluble matrix by a time-dependent diffusion process based on Fick's law.

The data of initial 60% drug release was incorporated to Korsmeyer-Peppas model to determine the mechanism of drug release from the Poly (AA-*co*- APMD) copolymer. In this model "n" is the release exponent, indicative of the mechanism of drug release. The values of "n" (calculated from the slope of the graph) for the polymer was found to be 0.655 indicating non-Fickian or anomalous diffusion mechanism.
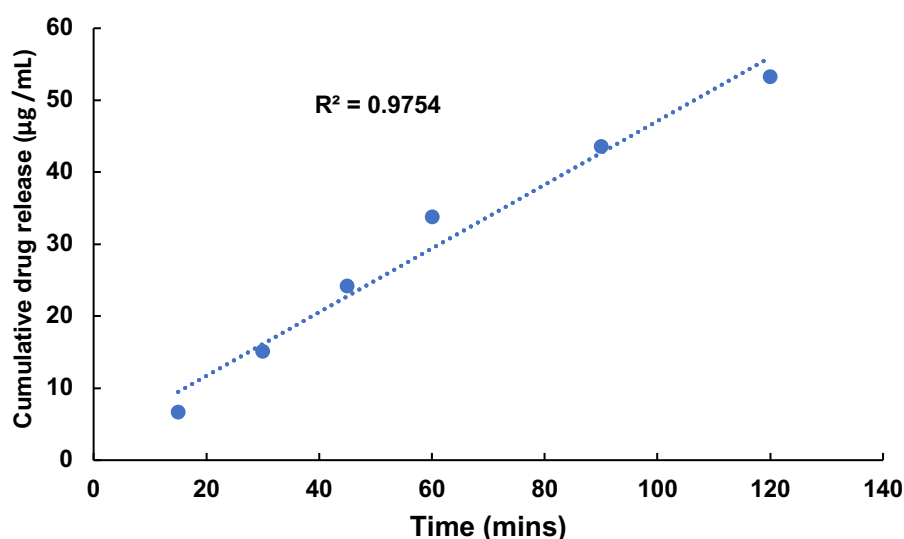
Figure 5.7. Zero order release plot derived from a PLEs hydrolysis experiment with copolymer as substrate (n=3)
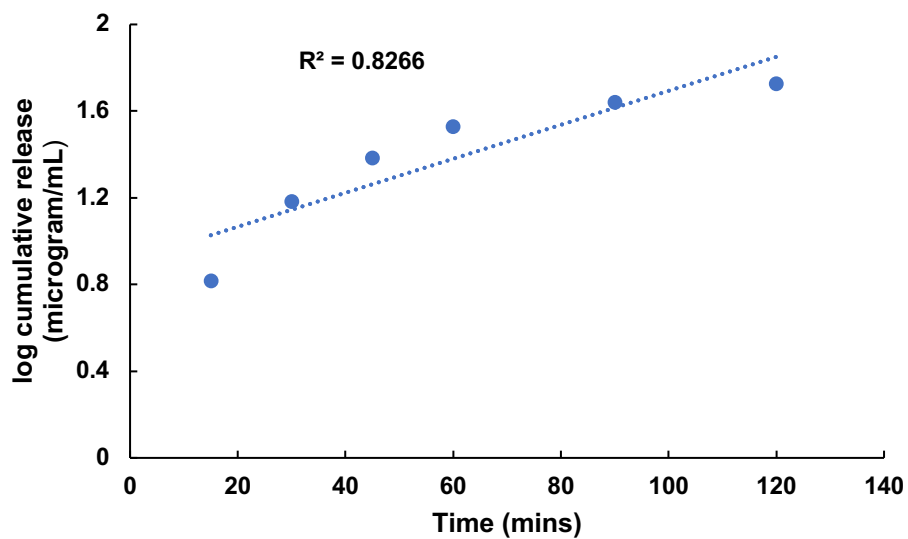
Figure 5.8. First order release plot derived from a PLEs hydrolysis experiment with copolymer as substrate (n=3)
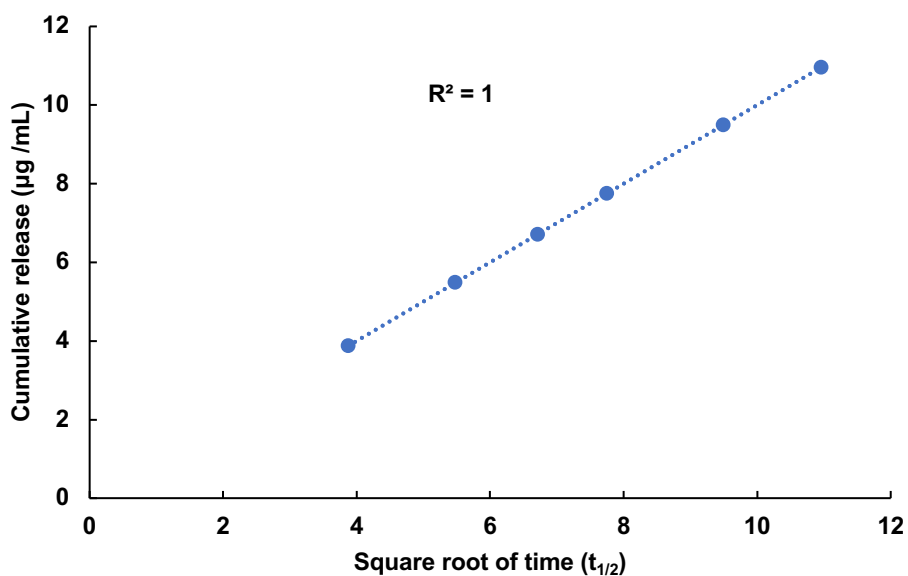
Figure 5.9. Higuchi's release plot derived from a PLEs hydrolysis experiment with copolymer as substrate (n=3)
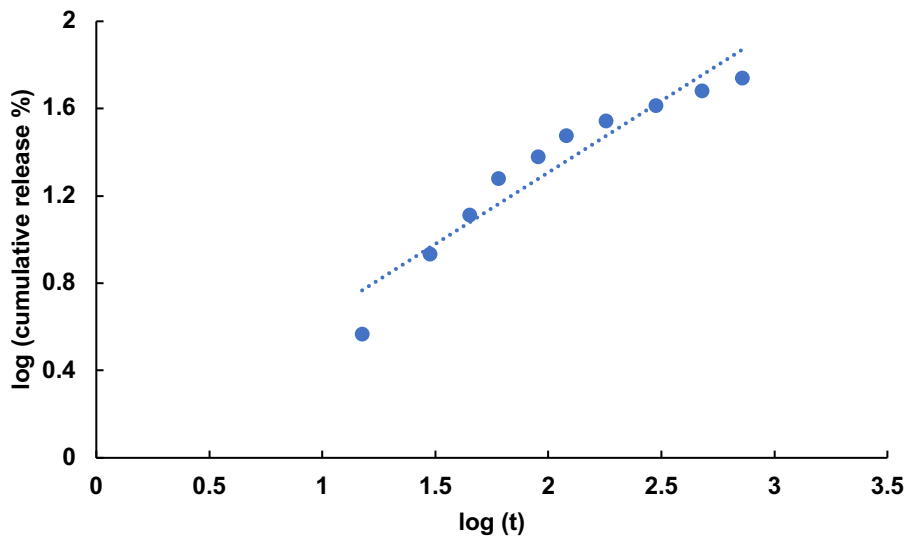
Figure 5.10. Korsmeyer-Peppas release plot derived from a PLEs hydrolysis experiment with copolymer as substrate (n=3)

Table 5.3. The r^2 and k values for the copolymer by applying different drug release models (k was obtained through the slope of the individual graph).

Drug Release Model	r^2 value	k value (h^{-1})
Zero order	0.97	0.4426
First order	0.82	0.0078
Higuchi's model	1.00	1.00
Korsmeyer-Peppas model	0.91	n=0.655

5.4.6. *In vitro* Skin Penetration and Permeation Study

5.4.6.1. Method Development

Before performing any study, one of the prerequisites is to identify an analytical technique for the laboratory analysis of the compound of interest. Therefore, the main challenge here was to develop an appropriate technique for the analysis of the copolymer. As described above, due to the lack of a chromophore in our compound, we were unable to use methods such as HPLC and UV, hence the alternative was to use mass spectroscopy-based techniques. For this purpose, LC-MS was evaluated but unfortunately this did not give any definitive peaks. The most probable reason for this is the cut off molecular weight limit for this instrument was 5,000 Da, whereas the copolymer is 6,000 Da. An alternative approach that is commonly used in the analysis of polymers is matrix assisted laser desorption/ionization-time of flight (MALDI-TOF) (Schwarzinger et al., 2012). Again, this was tested here, to analyse and quantify our copolymer but regrettably this also did not give any reliable result. The most probable reason for this might be the presence of bulkier groups (PMD) in our copolymer and it is known that polymers with bulkier groups are difficult to be analysed by MALDI-TOF (Montaudo et al.*,* 2006). Another method evaluated was a calorimetric method based upon the previous results (described in previous chapter) but this method wasn't sufficiently sensitive to detect concentration changes at the micrograms level.

5.4.6.1.1. Use of Gel Permeation Chromatography (GPC)

After the initial attempts to develop an analytical method for the detection and quantification of the polymer, gel permeation chromatography **(**GPC) was selected as there are reports for this method to not only to identify polymers but also to quantify them (Chen et al.*,* 2003). Based upon this technique, a calibration curve (Figure 5.11) was prepared but unfortunately this method (GPC) also provided unreliable results due to a lack of sensitivity.
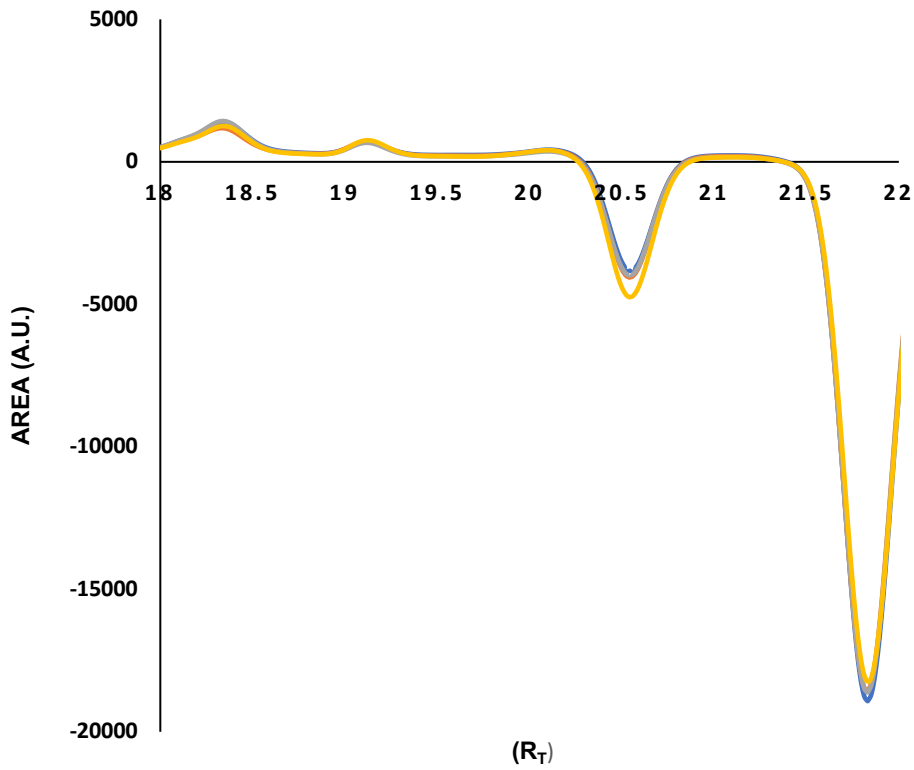
A)
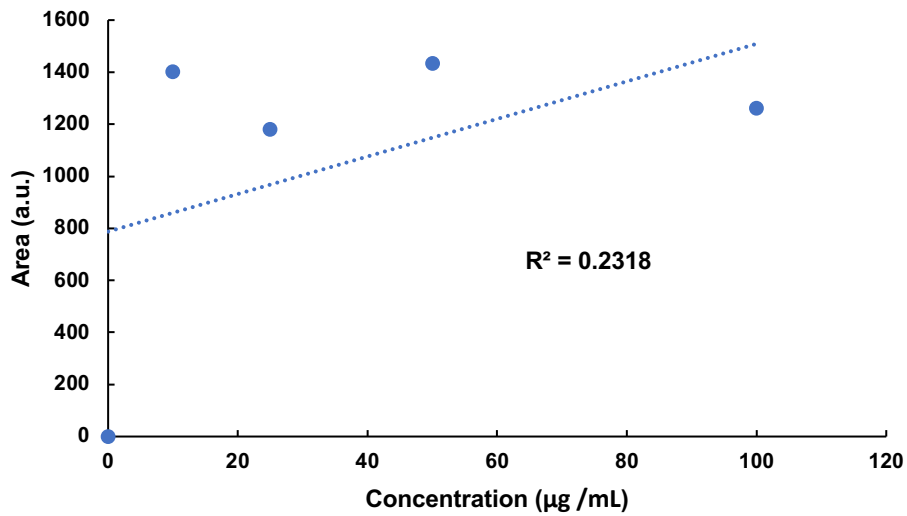
B)

Figure 5.11. A) GPC traces for the analysis of the copolymers. B) Calibration curve for the evaluation of the copolymers by using GPC.

Copolymer detection

Methods used

LCMS   Titration study   MALDI-TOF   GPC

Finally GPC was used
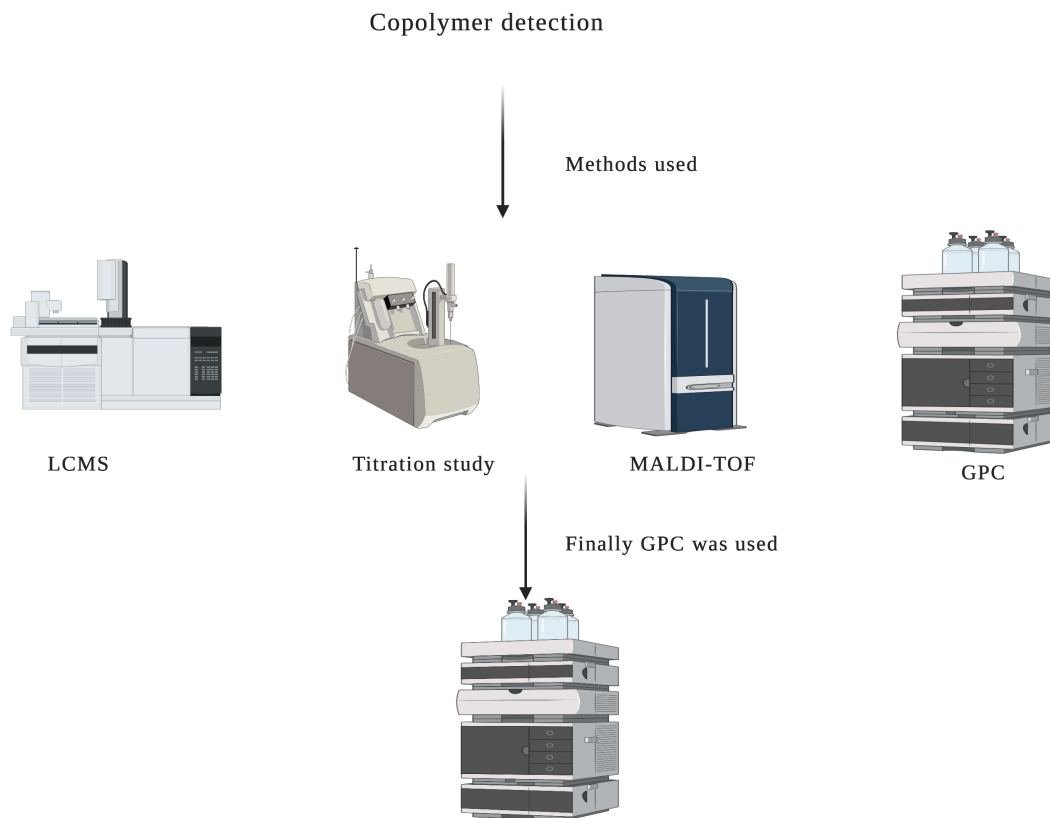
Figure 5.12. Various methods opted for the detection of the copolymer

5.4.6.1.2. Design of Experiments for Skin Penetration and Permeation

The design of this experiment sought to determine both the penetration and retention in the skin as well as permeation through the tissue for both the copolymer and PMD alone. For this purpose, two different sets of experiments (n=6), one for PMD and one for the copolymer were performed.
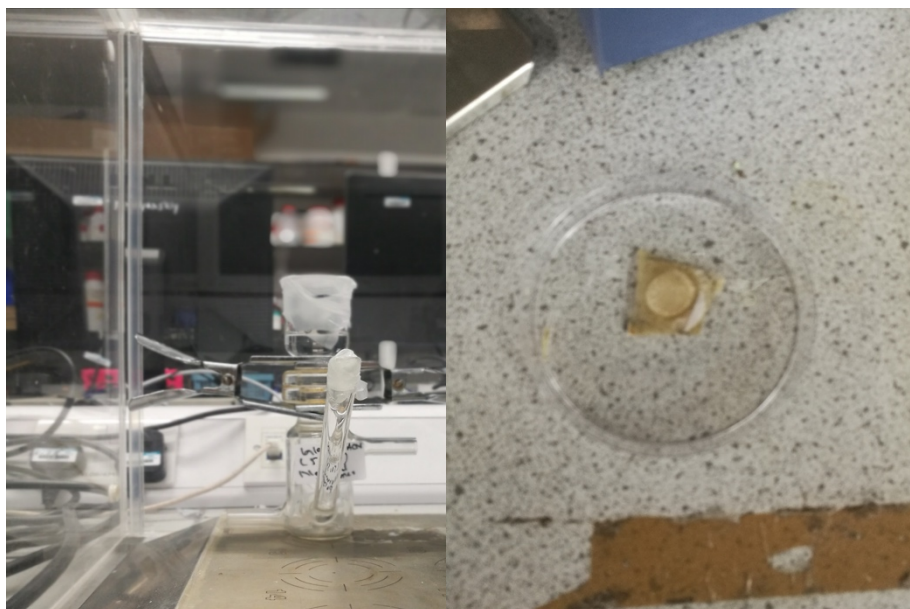
A)   **B)**

Figure 5.13.   Exemplar images representing the experimental set up of A) Permeation study; (B) Penetration study.

5.4.6.1.3. Solubility and Stability in Receptor Phases

Maintenance of sink conditions during the permeation study is crucial to maintain the maximal concentration gradient across the membrane throughout the experiment. The selection of an appropriate receptor solution was thus essential. As a rule, in order to maintain sink conditions throughout the experiment, the concentration of the penetrant in the receptor phase must not exceed 10% of its saturated solubility, and the receptor solution should not affect the membrane integrity (Williams and Barry, 2004).

5.4.6.1.4. Solubility and Stability of PMD and Copolymer in Water-Ethanol Mixture

Both copolymer and PMD were virtually insoluble in water. There are different means to improve the solubility of the test compounds, one of which is the addition of an organic solvent and so ethanol was added with a final ratio of 8:2 (v/v) for water:ethanol. The volume of ethanol was kept at 20% (v/v) in order to prevent ethanol itself from increasing the permeation according to Williams and Barry (2004) .

5.4.6.1.5. Solubility in Extraction Solvent

To extract compounds from skin samples and from tape strips, an extraction solvent is required to allow the test compounds to partition from the skin/strips into the solvent. For this purpose, the test compound should be stable within the solvent during the whole process (Weerheim and Ponec, 2001). Due to the stability and solubility of both the copolymer and PMD, ethanol was selected as the extraction solvent.

5.4.6.2. Permeation Study

A permeation study was carried out to investigate whether the copolymer could permeate the skin or not, in comparison with PMD alone. Due to the limited availability of fresh skin, frozen porcine ear skin (frozen for less than 2 months) was used in this study.

When applied alone to the skin, the permeation for PMD followed the typical profile for a finite dose application (Figure 5.13-a), with rapid initial permeation over the first 6 hours before the donor depletion. Over the first 6 hours, 246 μg /mL permeated accounting for 8% of the applied dose (3mg/mL) which is low; there might be two reasons for this low amount of the drug (PMD) permeating, first, can be the volatile nature of PMD (Lee et al., 2018) and the second reason can be the penetration of the drug into the skin (more than the permeation). Although PMD is volatile in nature and there is high probability of the evaporation of the drug but as we performed the experiments in an occluded environment (Franz cell), therefore, the probability of the analyte escaping out was low and hence this reason was ruled out. On the other hand, the possibility of the presence of the drug within the skin layers was confirmed from the results of the penetration study (Figure 5.15) indicating the presence of bulk of the PMD and thus indicating near steady state permeation throughout the stratum corneum after 72 h exposure.

On the other hand, in case of the copolymer, the concentration of the copolymer in the reservoir medium was below the limit of detection (Fig 5.14-b**)** which was expected due to higher molecular weight which is expected to hinder or indeed prevent permeation.

It was interesting to see that when the copolymer was dosed, PMD was also found to be below the LOD. Although we expected that there should be some PMD in the receptor phase (released as a result of the hydrolysis of the ester bond of the copolymer, though the concentration should be significantly less as compared to the same amount of PMD applied alone, *i.e.,* without being

conjugated to the polymer), this could be the result of the use of frozen skin in which the freeze-and-thaw process might have damaged the activity of the skin enzymes and other proteins, as explained by Kolarsick et al. (2006); others have shown frozen porcine ear skin to be metabolically active. However, there may not be enough enzymes to rapidly hydrolyse the copolymer for the parent compounds to be detected above LOD in this experiment (Jacobi et al., 2007).
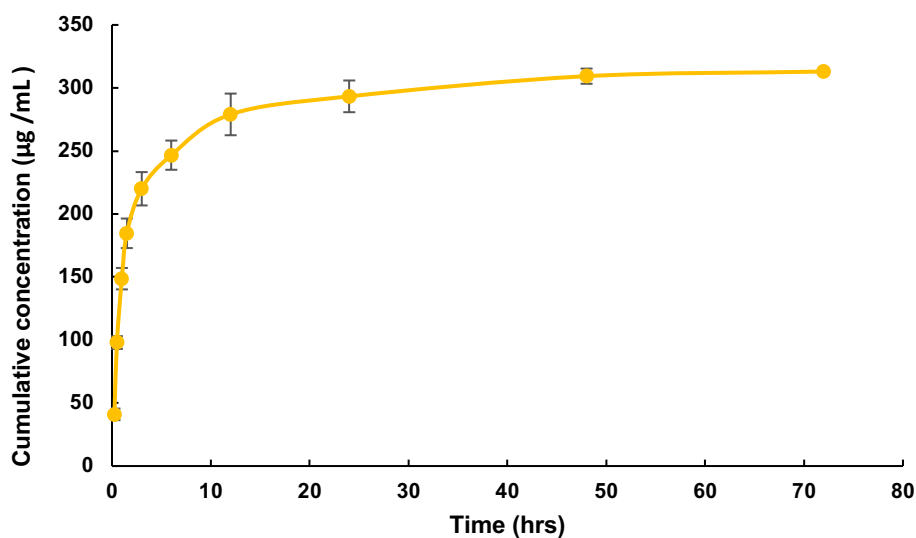
A)
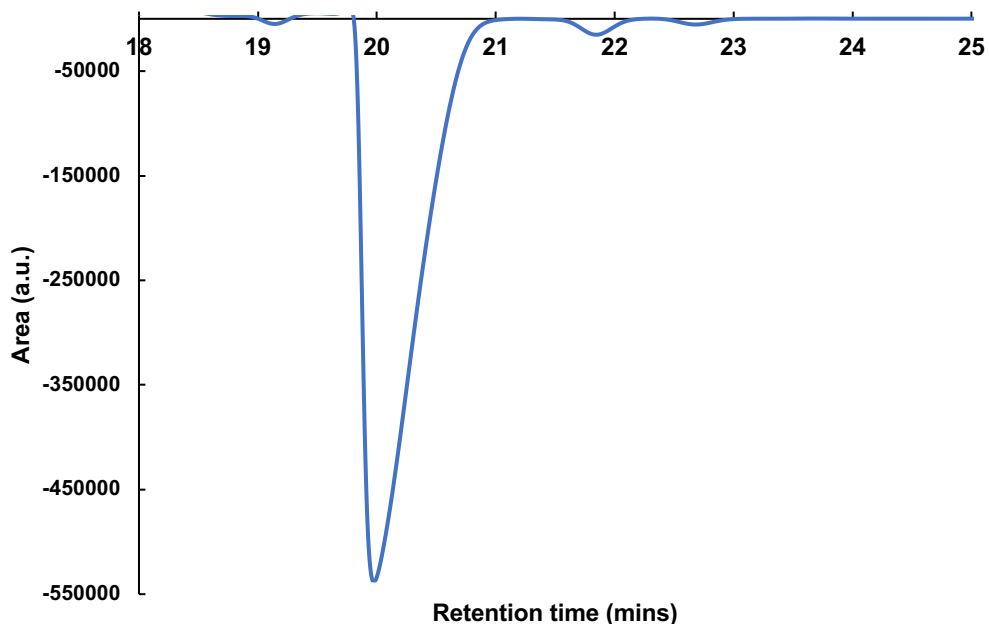
B)

Figure 5.14. **Permeation data for A) PMD and B) Exemplar retention peak showing absence of the copolymer. Data is expressed as mean ± SD (n=6).**

In short, the results show that PMD alone is able to permeate through porcine skin but that the amount of PMD (from the copolymer) and the copolymer itself permeating into the receptor phase was below the LOD. This could be advantageous as one of the aims of synthesising this system was to minimise side effects by minimising permeation through the skin and localising the copolymer to the outer skin layers. To investigate the distribution of the drug across the skin, a depth profile study was then carried out following the skin permeation study.

5.4.6.3 Skin Penetration Study

In this experiment, both PMD (as a control) and copolymer retention within the skin after the 72 h permeation study was assessed by removing the skin from the Franz cell and placing in a Petri dish. In order to determine the penetration of the drug (PMD) and the copolymer within the skin, a tape stripping technique was used. There are several factors *e.g.* tape stripping force, skin hydration and position of the tape, which can influence the quantity of stratum corneum (SC) that is removed by each tape-strip leading to high variation in the results. Thus, the tape stripping study is a technique to estimate the distribution of compounds in different layers of the SC and can be used comparatively.

From the results shown in Figure 5.15, it can be seen that in the case of the copolymer, tape 1-2 represents the surface adsorbed materials containing the highest amount of copolymer. 3-10 represents the outer stratum corneum of the skin with some copolymer detected. Tape strips 11-20 arise from the lower stratum corneum, and Figure 5.14 shows that no copolymer was detected in these lower layers. These results reinforce the permeation data showing that no copolymer could pass through the intact skin. Although quantitation is inexact due to assay difficulties, from figure 5.13, 93% of the total copolymer was detected in the surface adsorbed (strips 1-2) layer with only 7% in the outer stratum corneum (and likely towards the surface of the outer stratum corneum).

During the copolymer study, PMD release was also expected; due to the activity of naturally occurring esterases it was assumed that there would be hydrolysis of the ester bond and some of the PMD may penetrate the skin. However, analysis of the samples (extracted through the tape strips by ethanol, evaporated and then reconstituted by adding water: acetonitrile (4:6) (for the detection by LCMS) showed no evidence for the presence of PMD. This may be the result of the use of frozen skin in which the freeze-and-thaw processes might have a damaging effect on the skin enzymes and other proteins.

The control use of PMD alone showed that PMD was distributed throughout the different skin layers. Of the total PMD detected, 37% was in the superficial adsorbed sample (strips 1-2), 33% in strips 3-10 and 30% in strips 11-20. Near uniform distribution of PMD in the upper and lower stratum corneum implies that the PMD had, in fact, reached near steady state permeation throughout the stratum corneum after 72 h exposure.
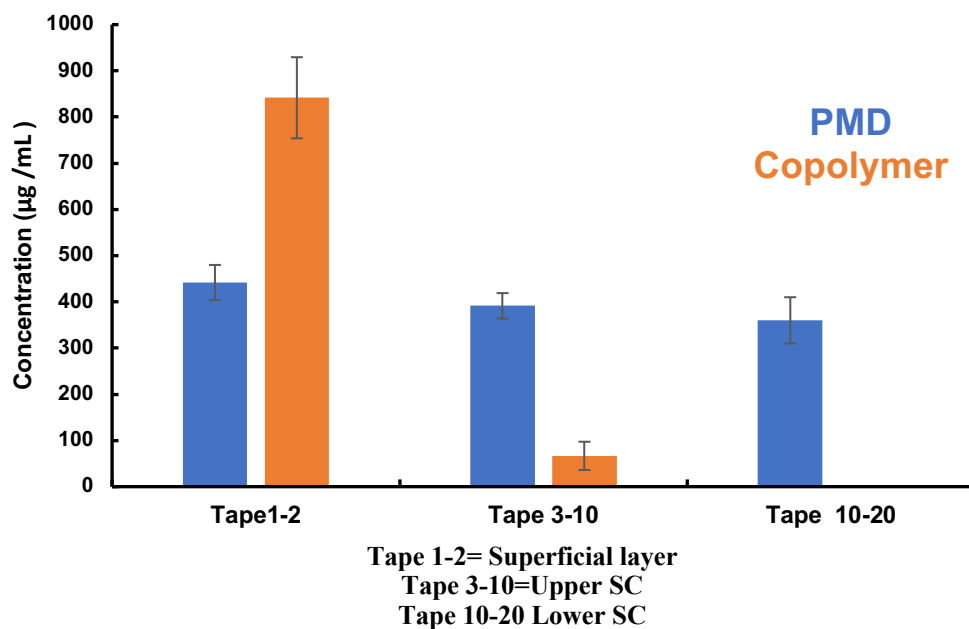
Figure 5.15. Skin penetration data for PMD (control) and copolymer in frozen-thawed porcine skin. Data is expressed as mean ± SD (n=6).

5.5. Conclusion

The results from the porcine liver esterases (PLEs) incubation suggest that the ester bond in copolymer is susceptible to hydrolysis by PLEs, so this can be a model for cutaneous esterases, under the conditions employed in the present experiments. The amount of the parent compound (PMD) liberated from the control experiments was approximately 45% of the loading, and thus it can be concluded that the hydrolysis of the copolymer was predominantly enzymatic with minor hydrolysis in water of the exposed PMD groups. The amount of the drug released from the copolymer was below expectations, therefore, in order to investigate the effect of various

parameters, *i.e.,* exhaustion of the enzymes and different molecular weights different experiments were performed, indicating that molecular weight does have an effect whilst adding of new/additional enzymes didn't have any effect on amount of PMD released.

Permeation of insect repellents into the systemic circulation is associated with side effects, thus, to assess the permeation and penetration profile of our copolymer and PMD alone (control), skin permeation and penetration experiments were undertaken. It was found that as compared to PMD, copolymer only penetrated the upper epidermal layer and did not permeate the skin (pig ear), indicating that this approach (polymer-drug conjugation) can be used to avoid permeation of the parent compound into the general circulation and hence the side effects associated with it can be overcome.

References

Abd, E., Yousef, S.A., Pastore, M.N., Telaprolu, K., Mohammed, Y.H., Namjoshi, S., Grice, J.E., Roberts, M.S., 2016. Skin models for the testing of transdermal drugs. Clin. Pharmacol. 8, 163–176. https://doi.org/10.2147/CPAA.S64788

Bhadra, S., Das, S.C., Roy, S., Arefeen, S., Rouf, A.S.S., 2011. Development and Validation of RP-HPLC Method for Quantitative Estimation of Vinpocetine in Pure and Pharmaceutical Dosage Forms. Chromatogr. Res. Int. 2011, 801656. https://doi.org/10.4061/2011/801656

Chen, J.-S., Liao, M.-C., Lin, C.-H., 2003. Determination of polymer content in modified bitumen. Mater. Struct. 36, 594–598. https://doi.org/10.1007/BF02483278

Conda-Sheridan, M., Lee, S.S., Preslar, A.T., Stupp, S.I., 2014. Esterase-activated release of naproxen from supramolecular nanofibres. Chem. Commun. 50, 13757–13760. https://doi.org/10.1039/C4CC06340F

Costa, P., Sousa Lobo, J.M., 2001. Modeling and comparison of dissolution profiles. Eur. J. Pharm. Sci. 13, 123–133. https://doi.org/https://doi.org/10.1016/S0928-0987(01)00095-1

D'Souza, A.J.M., Topp, E.M., 2004. Release from polymeric prodrugs: Linkages and their degradation. J. Pharm. Sci. 93, 1962–1979. https://doi.org/https://doi.org/10.1002/jps.20096

de la Rica, R., Aili, D., Stevens, M.M., 2012. Enzyme-responsive nanoparticles for drug release and diagnostics. Adv. Drug Deliv. Rev. 64, 967–978. https://doi.org/https://doi.org/10.1016/j.addr.2012.01.002

Deng, K., Zhang, P., Ren, X., Zhong, H., Gou, Y., Dong, L., Li, Q., 2009. Synthesis and characterization of a pH/temperature responsive glycine-mediated hydrogel for drug release. Front. Mater. Sci. China 3, 374. https://doi.org/10.1007/s11706-009-0069-1

Dong, H., Pang, L., Cong, H., Shen, Y., Yu, B., 2019. Application and design of esterase-responsive nanoparticles for cancer therapy. Drug Deliv. 26, 416–432. https://doi.org/10.1080/10717544.2019.1588424

FINDLAY, G.H., 1955. THE SIMPLE ESTERASES OF HUMAN SKIN. Br. J. Dermatol. 67,

83–91. https://doi.org/10.1111/j.1365-2133.1955.tb12696.x

Fu, Y., Kao, W.J., 2010. Drug release kinetics and transport mechanisms of non-degradable and degradable polymeric delivery systems. Expert Opin. Drug Deliv. 7, 429–444. https://doi.org/10.1517/17425241003602259

Ge, X., Sem, D.S., 2012. Affinity-based profiling of dehydrogenase subproteomes. Methods Mol. Biol. 803, 157–165. https://doi.org/10.1007/978-1-61779-364-6_11

Greco, F., Vicent, M., 2008. Polymer-drug conjugates: Current status and future trends. Front. Biosci. 13, 2744–2756. https://doi.org/10.2741/2882

Jacobi, U., Kaiser, M., Toll, R., Mangelsdorf, S., Audring, H., Otberg, N., Sterry, W., Lademann, J., 2007. Porcine ear skin: an in vitro model for human skin. Ski. Res. Technol. Off. J. Int. Soc. Bioeng. Ski. [and] Int. Soc. Digit. Imaging Ski. [and] Int. Soc. Ski. Imaging 13, 19–24. https://doi.org/10.1111/j.1600-0846.2006.00179.x

Kawai, F., Kawabata, T., Oda, M., 2019. Current knowledge on enzymatic PET degradation and its possible application to waste stream management and other fields. Appl. Microbiol. Biotechnol. 103, 4253–4268. https://doi.org/10.1007/s00253-019-09717-y

Kolarsick, P.A.J., Kolarsick, M.A., Goodwin, C., 2006. Anatomy and Physiology of the Skin.

Larsen, C., 1989. Macromolecular prodrugs. XII. Kinetics of release of naproxen from various polysaccharide ester prodrugs in neutral and alkaline solution. Int. J. Pharm. 51, 233–240. https://doi.org/https://doi.org/10.1016/0378-5173(89)90196-8

Lau, W.M., Heard, C.M., White, A.W., 2013. Design, synthesis and in vitro degradation of a novel co-drug for the treatment of psoriasis. Pharmaceutics 5, 232–245. https://doi.org/10.3390/pharmaceutics5020232

Lau, W.M., White, A.W., Heard, C.M., 2010. Topical Delivery of a Naproxen-Dithranol Co-drug: In Vitro Skin Penetration, Permeation, and Staining. Pharm. Res. 27, 2734–2742. https://doi.org/10.1007/s11095-010-0274-8

Lee, J., Choi, D.B., Liu, F., Grieco, J.P., Achee, N.L., 2018. Effect of the Topical Repellent para-Menthane-3,8-diol on Blood Feeding Behavior and Fecundity of the Dengue Virus Vector Aedes aegypti. Insects 9, 60. https://doi.org/10.3390/insects9020060

Maia, M.F., Moore, S.J., 2011. Plant-based insect repellents: a review of their efficacy,

development and testing. Malar. J. https://doi.org/10.1186/1475-2875-10-S1-S11

Montaudo, G., Samperi, F., Montaudo, M., 2006. Characterization of synthetic polymers by MALDI-MS. Prog. Polym. Sci. - PROG POLYM SCI 31, 277–357. https://doi.org/10.1016/j.progpolymsci.2005.12.001

Pitt, C.G., Shah, S.S., 1996. Manipulation of the rate of hydrolysis of polymer-drug conjugates: The secondary structure of the polymer. J. Control. Release 39, 221–229. https://doi.org/https://doi.org/10.1016/0168-3659(95)00156-5

Rizi, K., Green, R., Donaldson, M., Williams, A., 2011. Using pH Abnormalities in Diseased Skin to Trigger and Target Topical Therapy. Pharm. Res. 28, 2589–2598. https://doi.org/10.1007/s11095-011-0488-4

Rodriguez, S.D., Drake, L.L., Price, D.P., Hammond, J.I., Hansen, I.A., 2015. The Efficacy of Some Commercially Available Insect Repellents for Aedes aegypti (Diptera: Culicidae) and Aedes albopictus (Diptera: Culicidae) . J. Insect Sci. 15. https://doi.org/10.1093/jisesa/iev125

Schwarzinger, C., Gabriel, S., Beißmann, S., Buchberger, W., 2012. Quantitative Analysis of Polymer Additives with MALDI-TOF MS Using an Internal Standard Approach. J. Am. Soc. Mass Spectrom. 23, 1120–1125. https://doi.org/10.1007/s13361-012-0367-1

Seeman, J.I., Viers, J.W., Schug, J.C., Stovall, M.D., 1984. Correlation of nonadditive kinetic effects with molecular geometries. Structure and reactivity of alkyl- and cycloalkenylpyridines. J. Am. Chem. Soc. 106, 143–151. https://doi.org/10.1021/ja00313a030

Shah, S.S., Kulkarni, M.G., Mashelkar, R.A., 1990. Release kinetics of pendant substituted bioactive molecules from swellable hydrogels: role of chemical reaction and diffusive transport. J. Memb. Sci. 51, 83–104. https://doi.org/https://doi.org/10.1016/S0376-7388(00)80895-9

Tallury, P., Airrabeelli, R., Li, J., Paquette, D., Kalachandra, S., 2008. Release of antimicrobial and antiviral drugs from methacrylate copolymer system: Effect of copolymer molecular weight and drug loading on drug release. Dent. Mater. 24, 274–280. https://doi.org/https://doi.org/10.1016/j.dental.2007.05.008

Tavares, M., da Silva, M.R.M., de Oliveira de Siqueira, L.B., Rodrigues, R.A.S., Bodjolle-

d'Almeida, L., dos Santos, E.P., Ricci-Júnior, E., 2018. Trends in insect repellent formulations: A review. Int. J. Pharm. 539, 190–209. https://doi.org/https://doi.org/10.1016/j.ijpharm.2018.01.046

Tian, Y., Liu, X., Zhou, Y., Guo, Z., 2005. [Extraction and determination of volatile constituents in leaves of Eucalyptus citriodora]. Se pu = Chinese J. Chromatogr. 23, 651–654.

Wang, L.F., Chiang, H.N., Chen, W.B., 2002. Synthesis and properties of a naproxen polymeric prodrug. J. Pharm. Pharmacol. 54, 1129–1135. https://doi.org/10.1211/002235702320266307

Weerheim, A., Ponec, M., 2001. Determination of stratum corneum lipid profile by tape stripping in combination with high-performance thin-layer chromatography. Arch. Dermatol. Res. 293, 191–199. https://doi.org/10.1007/s004030100212

Wiechers, J.W., 2005. 20 - Optimizing Skin Delivery of Active Ingredients From Emulsions: From Theory To Practice, in: Rosen, M.R.B.T.-D.S.H. for P.C. and C.P. (Ed.), Personal Care & Cosmetic Technology. William Andrew Publishing, Norwich, NY, pp. 409–436. https://doi.org/https://doi.org/10.1016/B978-081551504-3.50025-0

Williams, A.C., Barry, B.W., 2004. Penetration enhancers. Adv. Drug Deliv. Rev. 56, 603–618. https://doi.org/https://doi.org/10.1016/j.addr.2003.10.025

Wong, R.S.H., Dodou, K., 2017. Effect of Drug Loading Method and Drug Physicochemical Properties on the Material and Drug Release Properties of Poly (Ethylene Oxide) Hydrogels for Transdermal Delivery. Polymers (Basel). 9, 286. https://doi.org/10.3390/polym9070286

Zhang, T., Chen, Xin, Xiao, C., Zhuang, X., Chen, Xuesi, 2017. Synthesis of a phenylboronic ester-linked PEG-lipid conjugate for ROS-responsive drug delivery. Polym. Chem. 8, 6209–6216. https://doi.org/10.1039/C7PY00915A

Zhou, Q., Xiao, Q., Zhang, Y., Wang, X., Xiao, Y., Shi, D., 2019. Pig liver esterases PLE1 and PLE6: heterologous expression, hydrolysis of common antibiotics and pharmacological consequences. Sci. Rep. 9, 15564. https://doi.org/10.1038/s41598-019-51580-4

Zhu, X., Anquillare, E.L.B., Farokhzad, O.C., Shi, J., 2014. Chapter 22 - Polymer- and Protein-Based Nanotechnologies for Cancer Theranostics, in: Chen, X., Wong, S.B.T.-C.T. (Eds.),

. Academic Press, Oxford, pp. 419–436. https://doi.org/https://doi.org/10.1016/B978-0-

Chapter 6. Planarian Toxicity Fluorescent Assay: A Rapid and Cheap Pre-screening Tool for Potential Skin Irritants

This chapter has been published as:

Syed Ibrahim Shah, Adrian C.Williams, Wing Man Lau, Vitaliy V.Khutoryanskiy.2020. Planarian toxicity fluorescent assay: A rapid and cheap pre-screening tool for potential skin irritants

6.1. Introduction

The design of formulations that contact human tissues requires toxicological testing and, in particular, topically applied formulations require skin irritation testing. Numerous methods have been used to evaluate the irritation potential of chemicals towards human tissues such as eyes, skin, nose or vagina. The classical Draize test used rabbits to assess the ocular and skin irritation of cosmetics and personal care products (Draize et al., 1944). Due to ethical as well as scientific concerns (Callens et al., 2001; Sharpe, 1985), alternative tests have been sought. For skin irritation testing, *in vitro* methods are available including the commercially available Episkin, Epiderm and Zenskin cell culture models (Ahn et al., 2010; Graham et al., 2018) although such tissue equivalents do not entirely recapitulate the in vivo tissue – for example lacking blood or lymph circulation or providing an incomplete tissue physiology. Numerous guidance documents exist for skin irritation testing, for example from the European Centre for the Validation of Alternative Methods (ECVAM) or the Organisation for Economic cooperation (OECD). Typically, the guidance specifies the skin equivalent to be used and its integrity testing, the numbers of replicates, duration of study *etc*., which requires specialist and relatively expensive laboratory services. Contrarily, planaria are readily available at a low cost and are easily cultured and maintained in a laboratory in artificial pond water (Gentile et al., 2011a) and thus may offer a low cost *in vivo* alternative model to rapidly screen potential skin irritants prior to undertaking extensive regulatory studies.

Alternative *in vivo* tests have been previously sought, typically employing lower order models. For example, Adriaens and Remon. (1999) reported a slug mucosa irritation test (SMIT) to characterise toxicological and irritation properties of various pharmaceutical materials and formulations for ocular, nasal and vaginal drug delivery, as well as some consumer products (Callens et al., 2001; Dhondt et al., 2005; Lenior et al. 2011, Lenior et al. 2013). The SMIT has also been adapted by others; for example, Forbes et al. (2011) tested silicone elastomer gels for vaginal drug delivery and in a series of studies; we have previously used a SMIT to evaluate the irritation potential of ocular formulations (Khutoryanskaya et al., 2014; Al Khateb et al,

2016), mucoadhesive polymers for nasal drug delivery (Porfiryeva, 2019) and mucoadhesive nanoparticles for intravesical drug delivery (Kaldybekov et al., 2019). Other invertebrate *in vivo* models used in toxicological testing include *Brachionus calyciflorus* rotifers for screening the toxicity of various penetration enhancers on ciliated epithelium (Adriaens et al., 1997) and *Caenorhabditis elegans* nematodes (Hunt, 2017). As with our present study, these models were proposed as a pre-screening tool prior to a time-consuming and relatively costly regulatory study.

Planaria are a freshwater-living flatworms commonly used as a model in developmental and regeneration research (Gentile et al., 2011b). As advanced invertebrates with a primitive brain having features similar to the vertebrate nervous system, planaria are used in neuropharmacology to predict the neurotoxicity of test substances (Hagstrom et al., 2016). They have a well-developed enzymatic system and so have been used to study organophosphorus pesticide toxicity (Hagstrom et al., 2018), the cytotoxic, genotoxic and mutagenic effects of metals (Pra et al., 2005) and for environmental toxicological studies (Li, 2008; Wu and Li, 2018). Importantly for the current work, planaria have a simple but well-characterised epidermal membrane (made of ciliated cells) that acts as the first point of contact between the worm and a foreign substance (Azimzadeh and Basquin, 2016).

The Globally Harmonised System (GHS) aims to consolidate global differences by classifying hazardous materials according to their health, environmental and physical hazards (Winder et al., 2005). For skin irritants, the GHS system draws on human experience, structure-activity models or the Primary Irritation Index (PII) caused by a chemical, derived from *in vivo* studies following OECD guidelines. The PII test applies 0.5mL or 0.5g of test substance to intact animal skin for up to 4 hours. For each animal, the dermal response scores (sum of the scores for erythema formation and oedema formation) at 24, 48, and 72 hours post exposure are recorded to generate a mean irritation score per time point (Bagley et al., 1996; Marzuki et al., 2019). PII scores < 1.5 are considered as non-irritant, PII $\geq 1.5 < 2.3$ corresponds to mild irritants, PII $\geq 2.3 < 4.0$ show moderate irritants whereas PII values ≥ 4 are seen with strong irritants.

The purpose of this study was to develop a rapid and cheap pre-screening tool to reduce the use of complex cell culture, organ and animal models. Here, we have used *Dugesia lugubris* as a model to predict human skin irritation of test substances by measuring the uptake of a fluorescent marker (sodium fluorescein) into the flatworms following exposure to various irritants; our hypothesis is that increasingly toxic substances will disrupt the barrier function of the planarian epidermis hence leading to greater accumulation of sodium fluorescein inside the worm.

6.2. Materials and Methods

6.2.1. Chemicals and Reagents

Benzalkonium chloride (BKC), glycerol, parafluoro aniline (PFA), polyethylene glycol-400 (PEG-400), carvacrol, isopropyl alcohol, decanol, tri-isobutyl phosphate, terpinyl acetate, sodium fluorescein and agarose were purchased from Sigma-Aldrich (UK). Benzyl alcohol, citronellal, linalyl acetate, 1-bromohexane and methyl palmitate were purchased from Fischer Scientific, UK. Instant ocean salt was from Aquarium Systems (UK).

Table 6.1. Test articles with CAS number, GHS classification and in order of PII values

Test article	CAS number	GHS classification	PII*
Polyethylene glycol-400 (PEG-400)	25322-68-3	Not classified (Non-Irritant)	0.0
Dipropylene glycol	25265-71-8	Not classified (Non-Irritant)	0.33
Isopropyl alcohol	67-63-0	Not classified (Non-Irritant)	0.78
Benzyl alcohol	100-51-6	Category 3 (Mild Irritant)	1.56
Terpinyl acetate	80-26-2	Category 3 (Mild Irritant)	2.0
Tri-isobutyl phosphate	126-71-6	Category 3 (Mild Irritant)	2.0
Decanol	112-30-1	Category 2 (Moderate irritant)	3.33
Parafluoro aniline (PFA)	371-40-4	Category 2 (Moderate irritant)	3.5
Linalyl acetate	499-75-2	Category 2 (Moderate irritant)	3.67
Citronellal	106-23-0	Category 1B (Strong irritant)	4.0

1-Bromohexane	111-25-1	Category H315 (Strong irritant)	4.0
Carvacrol	115-95-7	Category 1B (Strong irritant)	4.2
Methyl palmitate	112-39-0	Category H315 (Strong irritant)	4.56
Benzalkonium chloride (BKC)	63449-41-2	Category 1B (Strong irritant)	6.54

*PII < 1.5 = Non irritant, PII ≥ 1.5 < 2.3 = mild irritants, PII ≥ 2.3 < 4.0 = moderate irritants, PII ≥4 as strong irritants.

6.2.2. Test Organisms

Planaria (*Dugesia lugubris*) were purchased from Blades Biological Ltd (Kent, UK). The animals were maintained in artificial pond water (APW) (0.5 g of instant ocean salt in 1 L of Milli-Q water), prepared by the method of Cebrià and Newmark (2005) at room temperature. Animals were fed raw chicken (cut into small pieces), at a quantity sufficient to feed the planaria once a week. The pond water was changed every 48 hours.

6.2.3. Mobility Assay

Planarian mobility was assessed using the method previously described by Mei-Hui-Li (2012). Five concentrations of each test substance were prepared (0.1, 0.05, 0.025, 0.01 and 0.005 % w/v) by dissolving the test substance in APW. Where the irritants were not directly soluble, these compounds were first dissolved in dimethylsulphoxide (DMSO) before adding to APW followed by vigorous stirring until a clear solution was obtained. For these, the final volume of DMSO was maintained at 1% (v/v) to avoid irritation from the solvent itself (Pagán et al., 2009). An individual planarian was placed into a glass Petri dish containing 15 mL of the test solution or into APW or APW with 1% (v/v) DMSO as a control. The petri dish was placed over 1 cm grid graph paper and a video recorder was used from above. After 5 minutes' equilibration, planarian mobility was recorded as the number of times they crossed a grid line over the next 5 minutes. For each solution, mobility was assessed for 3 planaria and data are represented as the mean ± SD.

6.2.4. Acute Toxicity Assay

The toxicity of the test substances to planarian was assessed by the method previously described by Mei-Hui-Li (2012) with some modifications. Five concentrations of each test substance were prepared (0.1, 0.05, 0.025, 0.01 and 0.005 % w/v). For each concentration, five animals were added to a Petri dish containing 25 mL of the test solution and each study was conducted in triplicate. Acute toxicity was assessed over 96 hours with planaria inspected every 24 hours; those without detectable movement were assumed dead and removed from the test solution. Again, APW or APW with 1% (v/v) DMSO was used as a control.

6.2.5. Fluorescence Intensity (FI) Test

The protocol was informed by the mobility and toxicity studies and so test substances at 0.1% (w/v) were employed with planaria exposure of 1 min followed by washing with APW for a further 1 min. The planaria were then placed in a 0.1% (w/v) solution of sodium fluorescein in APW for 1 min. Finally, the planaria were washed with APW (15 mL) for 1 min to remove excess sodium fluorescein adsorbed to the outer worm surface. The test animal was then immobilised by embedding it in 2% agarose solution following the protocol of Shen et al. (2018) with minor modifications. In brief, a planarian was transferred onto a microscopic slide (VWR, UK), after which few drops of agarose solution were carefully added to cover the whole animal. The slide was immediately placed on ice leading to gelling of the agarose solution, immobilising the test animal. Fluorescence images of individual planaria were collected with a Leica MZ10F stereomicroscope (Leica Microsystems, UK) with Leica DFC3000G digital camera, 1.6× magnification with 160 ms exposure time (gain 2.6×), Gamma = 0.7 and wavelength=519 nm (excitation wavelength). The negative controls were planaria treated only with sodium fluorescein in APW for water-soluble test compounds and sodium fluorescein in 1% DMSO solution (v/v) in APW for the poorly water-soluble test compounds. To quantify sodium fluorescein inside a planarian, the fluorescence of the whole animal was measured using ImageJ (version 1.8.0_112) software and the value obtained normalised by dividing by the area (cm^2) of the individual planarian. All experiments were conducted in triplicate.

6.2.6. Statistical Analysis

Statistical significance for the fluorescence intensity test was determined using one-way analysis of variance (ANOVA), followed by Bonferroni correction using Graphpad Prism software (version 7.0). To correlate the experimental fluorescence intensity values with literature data for skin irritants, a Pearson correlation test was performed.

6.3. Results and Discussion

6.3.1. Mobility Assay

A planarian mobility assay has been previously used to assess neurotoxicity of several substances (Hagstrom et al., 2015) and hence we extrapolated the approach as a tool to assess skin irritants. For this purpose, a range of compounds was selected, spanning known non-, mild-, moderate- and strong-irritants along with control groups in APW alone (for water soluble compounds) or APW with 1% (v/v) DMSO (for poorly water-soluble compounds).

Locomotion was plotted as a function of the concentration of irritant (Figure 6.1). Planaria movement was invariant with increasing concentrations of the non-irritant PEG-400. Conversely, exposure to the strong irritant carvacrol stopped planaria mobility entirely and at the lowest tested concentration (0.005% w/v). The response to the mild irritant benzyl alcohol indicated some dose-response behaviour, but the locomotion inhibition was more pronounced and at lower concentrations for the other test materials. Indeed, the profiles for benzalkonium chloride (strong irritant) and linalyl acetate (moderate irritant) were indistinguishable over the selected concentration range, and the profiles for tri-isobutyl phosphate (mild) and parafluoro aniline (moderate) were contradictory. Given these confounding results, the mobility test appears unreliable for determining irritation from different classes of irritant and so was not developed further. However, given the sensitivity of planarian mobility to these agents, this approach could potentially identify chemicals that are non-irritant.
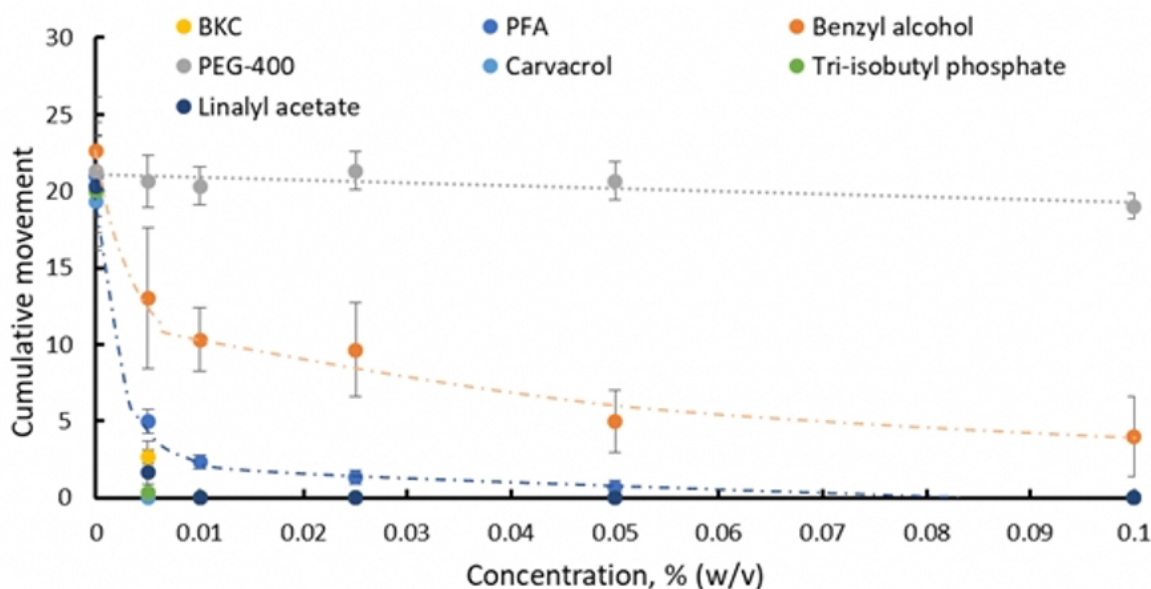
Figure 6.1. Effect of test compound concentrations on planaria locomotion. Cumulative movement = Number of times a planarian crossed the 1cm gridline during the 5-minute study. Data are represented as mean ± standard deviation (n = 3). The dashed/dotted lines are for the guidance of the eye only.

6.3.2. Acute Toxicity Assay

Acute toxicity was assessed every 24 hours for up to 96 hours of exposure to non-irritants (dipropylene glycol and PEG-400), a mild irritant (tri-isobutyl phosphate), a moderate irritant (linalyl acetate) and a strong irritant (carvacrol). Again, APW alone was used as a control for test compounds soluble in water while APW with 1% (v/v) DMSO was used as a control for those poorly soluble in water and the data was normalised against these; for both controls, all planaria survived the test. As with the mobility assay, the planaria showed no adverse effects on exposure to the non-irritants (dipropylene glycol and PEG-400) whereas exposure to the strong irritant carvacrol was lethal at the lowest dose (0.005% w/v). However, the data for the mild (tri-isobutyl phosphate) and moderate (linalyl acetate) irritants were confounding with planaria not surviving low dose exposure to the mild irritant but were more robust on exposure to higher concentrations of the moderate irritant. It was notable that the effects of exposure to the irritants did not change beyond the first 24-hour exposure period.

The above results illustrate a generic issue of seeking a lower order animal model to screen irritants for human use. Clearly the planarian membrane is extremely simple and fragile compared to, for example, human skin with its robust outer stratum corneum barrier. Whilst tri-isobutyl phosphate is a mild irritant on human skin, as an organophosphorus compound it is used in herbicides and fungicides and is listed by the European Chemicals Agency (ECHA) as "acutely harmful to aquatic organisms" (Eto, 1997; Hendriks et al., 1994). Indeed, an LC_{50} (96h) of 18-22 mg/L is reported for fish and an EC_{50} (48h) of 24 mg/L for aquatic invertebrates (as are planaria), equivalent to 0.0024% w/v and in a similar range to the results shown here in Figure 6.2. Linalyl acetate is a naturally occurring phytochemical and a principle component of lavender essential oil (Batool et al., 2020). Toxicity data towards marine invertebrates is limited as the compound is volatile (though our experiments were conducted under occlusion) and there is potential for hydrolysis of the ester to liberate some linalool. Notwithstanding these issues, an EC_{50} of 59 mg/L has been reported towards aquatic invertebrates (Daphnia) (Silver Registration Dossier ECHA @ www.echa.europa.eu) indicating that linalyl acetate would be expected to be less harmful to our test animal than tri-isobutyl phosphate, in accordance with the trend in Figure 6.2.
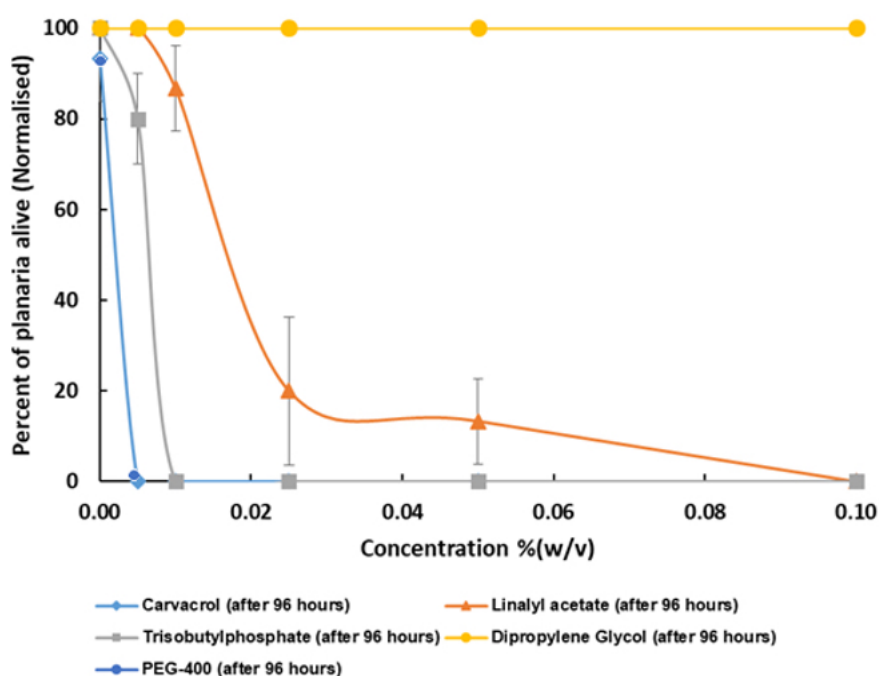
Figure 6.2. Acute toxicity study showing the effects of selected irritants on planaria survival. Data are represented as mean ± standard deviation (n = 15).

As with the mobility assay, the planaria acute toxicity assay was unsuitable to predict human skin irritation of our test compounds, other than to potentially identify chemicals that are non-irritant.

6.3.3. Fluorescence Study

The above results clearly demonstrate that both concentration and exposure time to irritants impact the viability of planaria (Hagstrom et al., 2015). Thus, a method was required that is simple, rapid and discriminating and hence short-term exposure (1 min) to low concentrations (0.1% w/v) of irritant followed by 1 min exposure to sodium fluorescein was selected. It is known that sodium fluorescein can penetrate damaged tissue and has been used to assess the extent of injury to human vaginal and eye tissues (Ayehunie et al., 2011; Morrison et al., 2017). Here, we assume that irritation to planaria causes damage to its outer membrane and that such damage will allow sodium fluorescein to enter the animal, with concentrations related to severity of damage from the irritant. To normalise the results, total fluorescence is expressed as per cm^2 of the planaria surface area. The protocol used to evaluate penetration of fluorescein into planaria is schematically shown in Figure 6.3 and Figure 6.4 shows exemplar fluorescent images.
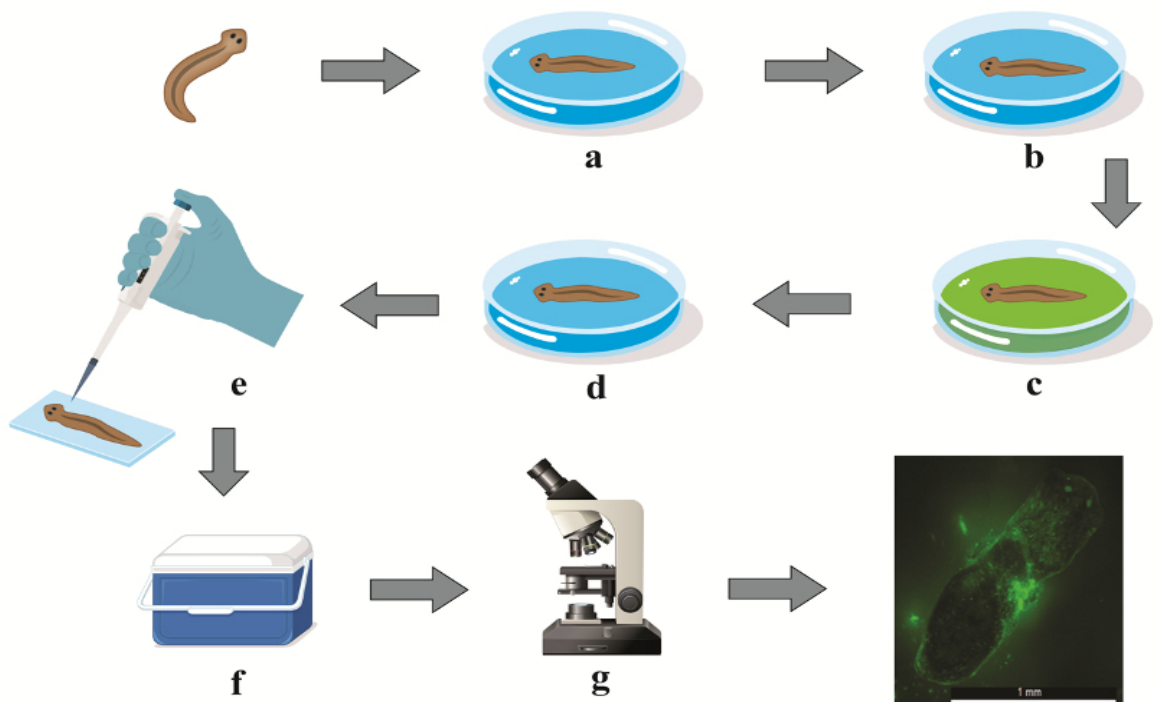
Figure 6.3. Illustrative diagram depicting the planaria fluorescence assay: (a) planarian in a solution of test substance (0.1 % w/v) for 1 min; (b) planarian washed in fresh APW for 1 min; (c) planarian in a solution of sodium fluorescein (0.1 % w/v) for 1 min; (d) planarian washed in fresh APW for 1 min to remove surface absorbed dye; (e) planarian placed on microscopy slide and covered with agarose sol; (f) slide placed on ice for 5-10 mins to allow agarose to solidify; (g) fluorescence assessed microscopically. Scale bar is 1mm (the scale bar represents the magnification of the microscope rather than the size of the object)
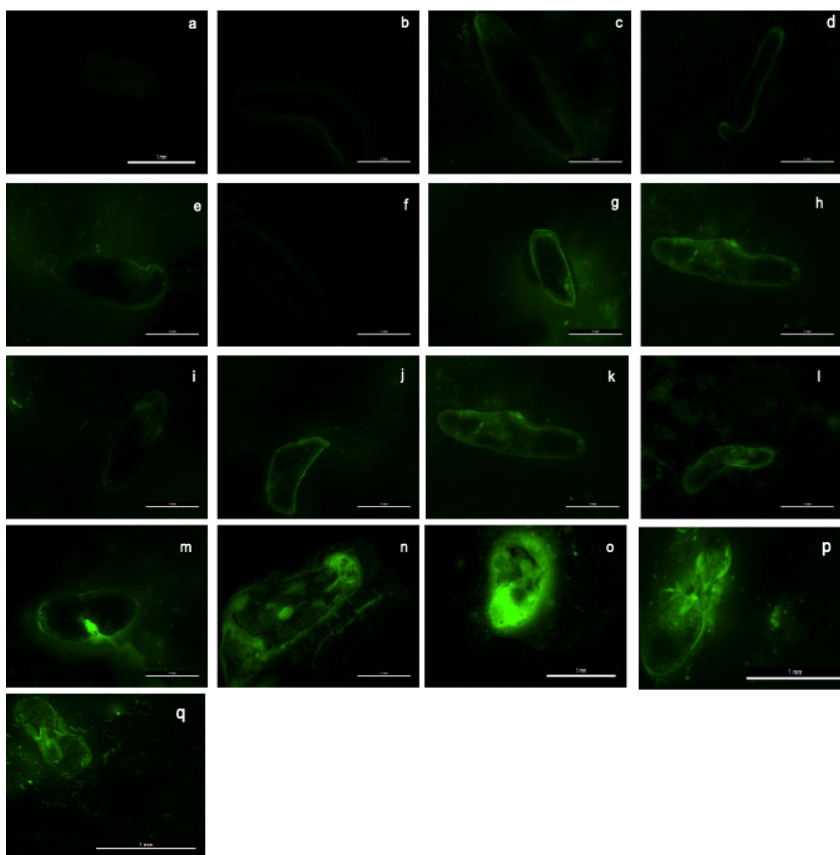
Figure. 6.4. Exemplar fluorescent images of auto fluorescence (a), negative control without and with DMSO in sodium fluorescein solution (b and c) and after planaria being exposed to PEG-400 (d), dipropylene glycol (e), isopropyl alcohol (f), terpinyl acetate (g), tri-isobutyl phosphate (h), benzyl alcohol (i), linalyl acetate (j), decanol (k), para-fluoroaniline (l), citronellal (m), carvacrol (showing disintegration of lower part of the planaria body) (n), benzalkonium chloride (also showing evidence for catastrophic membrane damage) (o), 1-bromohexane (p), and methyl palmitate (q). Scale bar is 1mm (the scale bar represents the magnification of the microscope rather than the size of the object)

Fourteen test substances were evaluated, five strong irritants and three from each class of moderate-, mild- or non-irritants, alongside controls of 1 minute exposure to APW with or without DMSO, and an untreated planarium to determine autofluorescence. Autofluorescence was negligible and fluorescence uptake into the control planaria was minimal following short term exposure to the dye; uptake of 4 a.u./cm^2 from APW with DMSO indicates no substantive damage to the outer membrane. Following exposure to the non-irritants, fluorescence was not signficantly different to that of the control animals, with greatest intensity seen for PEG-400 exposure at 5.0 ± 2.3 a.u./cm^2. Data for the mild-irritants was also not signficiantly different

to that of the controls, with benzyl alcohol causing fluorescence of 4.6 ± 3.9 a.u./cm^2 which rose to 10.0 ± 5.8 a.u./cm^2 with tri-isobutyl phosphate. The increasing trend in fluorescence intensity continiued with the moderate irritants, ranging from decanol (9.5 ± 3.2 a.u./cm^2) to linalyl acetate (20.0 ± 3.0 a.u./cm^2). It is notable that in our acute toxicity assay (Figure 6.2), linalyl acetate appeared less harmful to the planaira than expected from its GHS classification or PII value (Table 1) but in the fluorescence assay is shown to be a moderate irritant close to the borderline with the strong irritant classification. As a strong irritant, citronellal (18.0 ± 6.2 a.u./cm^2) gave similar fluorescence to linalyl acetate, whilst methyl palmitate and bromohexane showed similar F.I's, (24.8 ± 4.1 a.u./cm^2 and 22.6 ± 6 a.u./cm^2 respectively). Both benzalkonium chloride (53.0 ± 11.2 a.u./cm^2) and carvacrol (48.0 ± 12.5 a.u./cm^2) caused catastrophic damage to the membrane resulting in significantly higher fluorescence intensities than all other tests. The result show that all the strong irritants gave significantly greater fluorescence intensities (P at least <0.05) than the non irritants and controls.
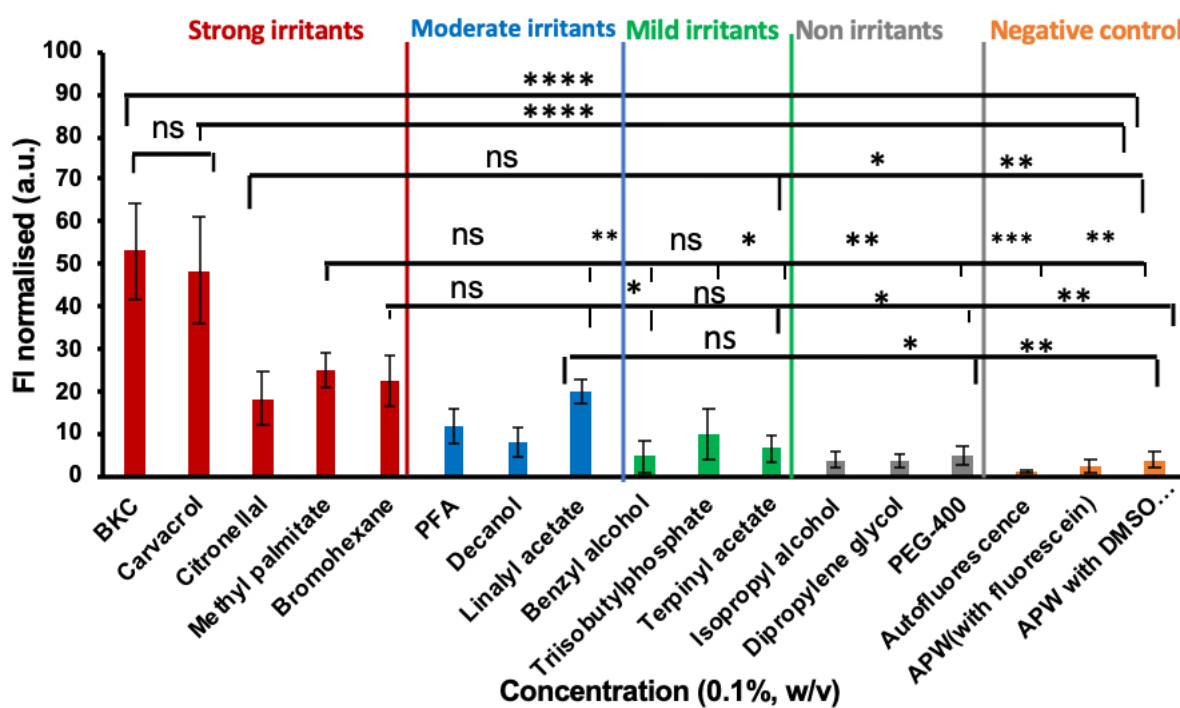
Figure 6.5. Fluorescence intensity (per cm^2) of individual planaria exposed to different test substances. Data are expressed as mean ± standard deviation (n = 3). Statistically significant differences are given *as: **** represents p<0.0001, *** p=0.0005, while ** and * p<0.05 and ns = not significant.*

6.3.3 Correlation Between Human Primary Irritation Index (PII) and Planaria Fluorescence Intensity (FI)

Despite the dissimilar membrane structures, we sought to correlate the membrane damage caused to planaria by the irritants with literature data that has been used in predictions of human skin irritation. The Primary Irritation Index (PII) is from a patch test on albino rabbit skin and is a composite score of the number and severity of erythema / oedema to a test substance (Chakrabarti et al., 2018). The literature data available for PII was correlated with our fluorescence results, as shown in Figure 6.6. Test substances whose PII values were available in the literature (n=12) were plotted against our experimental fluorescence intensities (per cm^2); due to catastrophic membrane damage (Figure 6.4), fluorescence values following treatment with BKC and carvacrol do not represent uptake of dye through a membrane and so were excluded. Clearly our fluorescence intensities within the planaria increase with increasing values of the primary irritation index. The Pearson's correlation (r) value (0.87) shows a statistically significant (p<0.005) positive correlation. This correlation suggests that this assay can serve as a rapid pre-screening tool to identify the likely category or irritation potential of compounds towards human skin. Though further study is merited using a broader library of compounds, the speed and simplicity of the assay provides an attractive alternative to tests using higher order vertebrates.
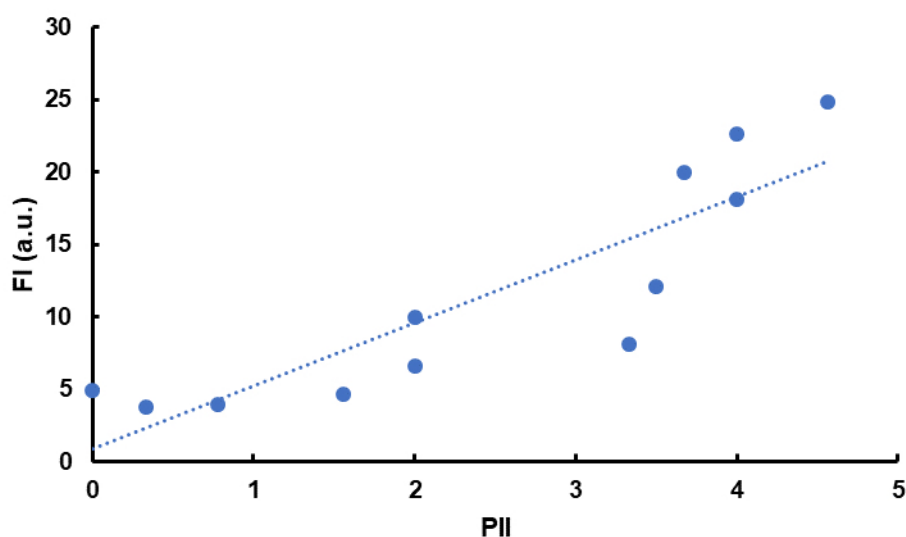
Figure 6.6. Correlation between the Primary Irritation Index of compounds (PII) and the Fluorescence Intensity (FI) values obtained in this study. Pearson's correlation value r = 0.87 (p<0.005)

6.4. Conclusion

Our studies demonstrate planaria mobility or acute toxicity testing poorly discriminate between categories of skin irritants but may demonstrate materials that are either non-irritating or act as very strong skin irritants. The planarian fluorescence assay is more discriminating with a direct correlation between fluorescence uptake into worms following short term exposure to irritants and literature reported irritation defined by their primary irritation index values. The fluorescence assay offers a rapid *in vivo* screening tool employing a model that is readily available and easy to maintain and which could act as a pre-screening method to inform subsequent sophisticated and costly assessments of skin irritants. Potentially this assay could be further extended to test irritation properties of various chemicals towards ocular, nasal and vaginal mucosa.

References

Adriaens, E., Voorspoels, J., Mertens, J., Remon, J.P., 1997. Effect of Absorption Enhancers on Ciliated Epithelium: A Novel In Vivo Toxicity Screening Method Using Rotifers. Pharm. Res. 14, 541–545. https://doi.org/10.1023/A:1012176322362

Adriaens, E., Remon, J.P., 1999. Gastropods as an Evaluation Tool for Screening the Irritating Potency of Absorption Enhancers and Drugs. Pharm. Res. 16, 1240–1244. https://doi.org/10.1023/A:1014801714590

Al Khateb, K., Ozhmukhametova, E.K., Mussin, M.N., Seilkhanov, S.K., Rakhypbekov, T.K., Lau, W.M., Khutoryanskiy, V.V., 2016. In situ gelling systems based on Pluronic F127/PluronicF68 formulations for ocular drug delivery. Int. J. Pharm. 502, 70–79.

https://doi.org/10.1016/j.ijpharm.2016.02.027

Ayehunie, S., Cannon, C., LaRosa, K., Pudney, J., Anderson, D.J., Klausner, M., 2011. Development of an in vitro alternative assay method for vaginal irritation. Toxicology 279, 130–138. https://doi.org/https://doi.org/10.1016/j.tox.2010.10.001

Ahn, J.-H., Eum, K.-H., Lee, M., 2010. Assessment of the dermal and ocular irritation potential of lomefloxacin by using in vitro methods. Toxicol. Res. 26, 9–14. https://doi.org/10.5487/TR.2010.26.1.009

Azimzadeh, J., Basquin, C., 2016. Basal bodies across eukaryotes series: basal bodies in the freshwater planarian Schmidtea mediterranea. Cilia 5, 15. https://doi.org/10.1186/s13630-016-0037-1

Bagley, D.M., Gardner, J.R., Holland, G., Lewis, R.W., Regnier, J.-F., Stringer, D.A., Walker, A.P., 1996. Skin irritation: Reference chemicals data bank. Toxicol. Vitr. 10, 1–6. https://doi.org/https://doi.org/10.1016/0887-2333(95)00099-2

Batool, S., Khera, R.A., Hanif, M.A., Ayub, M.A., Memon, S., 2020. Chapter 14 - Curry Leaf, in: Hanif, M.A., Nawaz, H., Khan, M.M., Byrne, H.J.B.T.-M.P. of S.A. (Eds.), . Elsevier, pp. 179–190. https://doi.org/https://doi.org/10.1016/B978-0-08-102659-5.00014-8

Botham, P., Osborne, R., Atkinson, K., Carr, G., Cottin, M., Van Buskirk, R.G., 1997. IRAG Working Group 3: Cell function-based assays. Food Chem. Toxicol. 35, 67–77. https://doi.org/https://doi.org/10.1016/S0278-6915(96)00106-8

Callens, C., Adriaens, E., Dierckens, K., Remon, J.P., 2001. Toxicological evaluation of a bioadhesive nasal powder containing a starch and Carbopol® 974 P on rabbit nasal mucosa and slug mucosa. J. Control. Release 76, 81–91. https://doi.org/https://doi.org/10.1016/S0168-3659(01)00419-9

Cebrià, F., Newmark, P.A., 2005. Planarian homologs of netrin and netrin receptor are required for proper regeneration of the central nervous system and the maintenance of nervous system architecture. Development 132, 3691 LP – 3703. https://doi.org/10.1242/dev.01941

Chakrabarti, S., Islam, J., Hazarika, H., Mazumder, B., Raju, P.S., Chattopadhyay, P., 2018. Safety profile of silver sulfadiazine-bFGF-loaded hydrogel for partial thickness burn wounds. Cutan. Ocul. Toxicol. 37, 258–266. https://doi.org/10.1080/15569527.2018.1442843

Dhondt, M.M.M., Adriaens, E., Van Roey, J., Remon, J.P., 2005. The evaluation of the local tolerance of vaginal formulations containing dapivirine using the Slug Mucosal Irritation test and the rabbit vaginal irritation test. Eur. J. Pharm. Biopharm. 60, 419-425.https://doi.org/10.1016/j.ejpb.2005.01.012

Eto, M., 1997. Functions of Phosphorus Moiety in Agrochemical Molecules. Biosci. Biotechnol. Biochem. 61, 1–11. https://doi.org/10.1271/bbb.61.1

Forbes, C.J., Lowry, D., Geer, L., Veazey, R.S., Shattock, R.J., Klasse, P.J., Mitchnick, M., Goldman, L., Doyle, L.A., Muldoon, B.C.O., Woolfson, A.D., Moore J.P., Malcolm, K., 2011. Non-aqueous silicone elastomer gels as a vaginal microbicide delivery system for the HIV-1 entry inhibitor maraviroc. J. Control. Release 156, 161-169.https://doi.org/10.1016/j.jconrel.2011.08.006.

Gentile, L., Cebrià, F., Bartscherer, K., 2011a. The planarian flatworm: an in vivo model for stem cell biology and nervous system regeneration. Dis. Model. Mech. 4, 12–19. https://doi.org/10.1242/DMM.006692

Gentile, L., Cebrià, F., Bartscherer, K., 2011b. The planarian flatworm: an in vivo model for stem cell biology and nervous system regeneration. Dis. Model. &amp; Mech. 4, 12 LP – 19. https://doi.org/10.1242/dmm.006692

Graham, J.C., Wilt, N., Costin, G.-E., Villano, C., Bader, J., Krawiec, L., Sly, E., Gould, J., 2018. Evaluation of a tiered in vitro testing strategy for assessing the ocular and dermal irritation/corrosion potential of pharmaceutical compounds for worker safety. Cutan. Ocul. Toxicol. 37, 380–390. https://doi.org/10.1080/15569527.2018.1483944

Hagstrom, D., Cochet-Escartin, O., Collins, E.-M.S., 2016. Planarian brain regeneration as a model system for developmental neurotoxicology. Regeneration 3, 65–77. https://doi.org/10.1002/reg2.52

Hagstrom, D., Cochet-Escartin, O., Zhang, S., Khuu, C., Collins, E.-M.S., 2015. Freshwater Planarians as an Alternative Animal Model for Neurotoxicology. Toxicol. Sci. 147, 270–285. https://doi.org/10.1093/toxsci/kfv129

Hagstrom, D., Zhang, S., Ho, A., Tsai, E.S., Radić, Z., Jahromi, A., Kaj, K.J., He, Y., Taylor, P., Collins, E.-M.S., 2018. Planarian cholinesterase: molecular and functional characterization of an evolutionarily ancient enzyme to study organophosphorus pesticide toxicity. Arch. Toxicol. 92, 1161–1176. https://doi.org/10.1007/s00204-017-2130-7

Hendriks, A.J., Maas-Diepeveen, J.L., Noordsij, A., Van der Gaag, M.A., 1994. Monitoring response of XAD-concentrated water in the rhine delta: A major part of the toxic compounds remains unidentified. Water Res. 28, 581–598. https://doi.org/https://doi.org/10.1016/0043-1354(94)90009-4

Hunt, P.R., 2017. The C. elegans model in toxicity testing. J. Appl. Toxicol. 37, 50-59. 10.1002/jat.3357. Epub 2016 Jul 22.

Kaldybekov, D.B., Filippov, S.K., Radulescu, A., Khutoryanskiy, V.V., 2019. Maleimide-functionalised PLGA-PEG nanoparticles as mucoadhesive carriers for intravesical drug delivery, Eur. J. Pharm. Biopharm. 143, 24-34.https://doi.org/10.1016/j.ejpb.2019.08.007

Khutoryanskaya, O. V, Morrison, P.W.J., Seilkhanov, S.K., Mussin, M.N., Ozhmukhametova, E.K., Rakhypbekov, T.K., Khutoryanskiy, V. V, 2014. Hydrogen-Bonded Complexes and Blends of Poly(acrylic acid) and Methylcellulose: Nanoparticles and Mucoadhesive Films for Ocular Delivery of Riboflavin. Macromol. Biosci. 14, 225–234. https://doi.org/10.1002/mabi.201300313

Lenoir, J., Claerhout, I., Kestelyn, P., Klomp, A., Remon, J.P., Adriaens E., 2011. The slug mucosal irritation (SMI) assay: Development of a screening tool for the evaluation of ocular

discomfort caused by shampoos. Toxicol. in Vitro. 25, 1919-1925.https://doi.org/10.1016/j.ijpharm.2019.03.027

Lenoir, J., Bachert, C., Remon, J.-P., Adriaens, E., 2013. The Slug Mucosal Irritation (SMI) assay: A tool for the evaluation of nasal discomfort. Toxicol. in Vitro. 27, 1954–1961. https://doi.org/https://doi.org/10.1016/j.tiv.2013.06.018

Liang, H., Brignole-Baudouin, F., Rabinovich-Guilatt, L., Mao, Z., Riancho, L., Faure, M.O., Warnet, J.M., Lambert, G., Baudouin, C., 2008. Reduction of quaternary ammonium-induced ocular surface toxicity by emulsions: an in vivo study in rabbits. Mol. Vis. 14, 204–216.

Li, M.-H., 2008. Effects of nonionic and ionic surfactants on survival, oxidative stress, and cholinesterase activity of planarian. Chemosphere 70, 1796–1803. https://doi.org/https://doi.org/10.1016/j.chemosphere.2007.08.032

Marzuki, A., Rahman, L., Mamada, S.S., 2019. Toxicity test of stem bark extract of banyuru (Pterospermum celebicum miq.) using BSLT (brine shrimp lethality test) and cream irritation test, in: Journal of Physics: Conference Series. IOP Publishing, p. 72018.

Morrison, P.W.J., Porfiryeva, N.N., Chahal, S., Salakhov, I.A., Lacourt, C., Semina, I.I., Moustafine, R.I., Khutoryanskiy, V. V, 2017. Crown Ethers: Novel Permeability Enhancers for Ocular Drug Delivery? Mol. Pharm. 14, 3528–3538. https://doi.org/10.1021/acs.molpharmaceut.7b00556

Pagán, O.R., Coudron, T., Kaneria, T., 2009. The flatworm planaria as a toxicology and behavioral pharmacology animal model in undergraduate research experiences. J. Undergrad. Neurosci. Educ. 7, A48–A52.

Porfiryeva, N.N., Nasibullin, S.F., Abdullina, S.G., Tukhbatullina, I.K., Moustafine, R.I., Khutoryanskiy, V.V., 2019. Acrylated Eudragit® E PO as a novel polymeric excipient with enhanced mucoadhesive properties for application in nasal drug delivery. Int. J. Pharm. 5621, 241-248.

Sharpe, R., 1985. The Draize test—Motivations for change. Food Chem. Toxicol. 23, 139–143. https://doi.org/https://doi.org/10.1016/0278-6915(85)90005-5

Shen W., Shen Y., Lam Y.W., Chan D. 2018. Live Imaging of Planaria. Rink J. (eds) Planarian Regeneration. Methods in Molecular Biology. 1774. https://doi.org/10.1007/978-1-4939-7802-1_22

Winder, C., Azzi, R., Wagner, D., 2005. The development of the globally harmonized system (GHS) of classification and labelling of hazardous chemicals. J. Hazard. Mater. 125, 29–44. https://doi.org/https://doi.org/10.1016/j.jhazmat.2005.05.035

Wu, J.-P., Li, M.-H., 2018. The use of freshwater planarians in environmental toxicology studies: Advantages and potential. Ecotoxicol. Environ. Saf. 161, 45–56. https://doi.org/https://doi.org/10.1016/j.ecoenv.2018.05.057

Silver Registration Dossier ECHA. 2011. https://echa.europa.eu/registration-dossier/-/registered-dossier/16155/6/2/1

Chapter 7. Toxicity Evaluation of the poly(AA-*co*-APMD) by Planarian Fluorescence Assay

7.1 Introduction

Any formulation that is used topically requires testing for its irritation potential (Madan and Levitt, 2014). For this purpose, numerous methods had been used for irritation screening, ranging from *in vivo* methods such as the Draize test to *in vitro* methods using cell cultures such as Episkin or Epiderm. There have also been various attempts by researchers to develop lower animal models to replace the higher order *in vivo* models (Parasuraman, 2011). The planaria fluorescence assay (described in chapter 6) is one such model to predict the skin irritation potential of a compound

p-menthane 3,8 diol (PMD) is a terpenoid and a naturally occurring insect repellent that is applied topically to repel insects (Drapeau et al., 2011). Polyacrylic acid (PAA) is an ionic polymer and is commonly employed in skin formulations, especially in hydrogels (Devine et al., 2006). Similarly, acrylic acid copolymers are widely used for drug delivery purpose (Ma et al., 2008). When testing the irritation potential of a compound towards the skin, acute toxicity testing is usually performed and essentially determines the effect of a single dose of a compound on a specific animal species. Studies have reported that PMD is safe to be applied on the skin at lower doses while at higher doses it did cause skin irritation whilst low molecular weight polyacrylic acid is described as a skin irritant (EPA safety document for PMD; polyacrylic safety www.polysciences.com).

Planaria are a freshwater-living worms commonly used as a model in developmental and regeneration research (Gentile et al., 2011a). Planaria, are advanced invertebrates with some similarities in nervous system to the vertebrates. They are frequently used in neuropharmacology to predict the neurotoxicity of test substances (Hagstrom et al., 2016). Based upon their well-developed enzymatic system, they are also used to study organophosphorus pesticide toxicity (Hagstrom et al., 2018). They have also been used to study the cytotoxic, genotoxic and mutagenic effects of metals (Pra et al., 2005) as well as environmental toxicological studies (Li, 2008; Wu and Li, 2018). Moreover, planaria have a simple but well-characterised epidermal membrane (made of ciliated cells) that act as the first point of contact between the worm and a foreign substance (Azimzadeh and Basquin, 2016). In this work, we investigated the irritation potential of the copolymer poly (AA-*co*-APMD) compared with PAA and PMD alone, by using the planaria fluorescence assay.

7.2 Materials

PMD was purchased from BOC sciences, USA. Benzalkonium chloride (BKC), sodium fluorescein and agarose were purchased from the Sigma-Aldrich, UK. PAA (Mw=5000 Da) was purchased from Polysciences, Germany and sodium hydroxide was from Fischer Scientific, UK. Instant ocean salt was from Aquarium Systems (UK).

7.3 Test Organisms

Planaria (*Dugesia lugubris*) were purchased from Blades Biological Ltd (Kent, UK). The animals were maintained in artificial pond water (APW) (0.5 g of instant ocean salt in 1L of Milli-Q water), prepared by the method of Cebrià and Newmark (2005) at room temperature. Animals were fed raw chicken (cut into small pieces), quantity sufficient for feeding planaria once a week. The pond water was changed every 48 h.

7.4 Methods

The protocol used was as described in chapter 6. Briefly a planarian was exposed to 0.1% (w/v) of the test substance for 1 min, followed by a washing with APW for a further 1 min. The planaria were then placed in a 0.1% (w/v) solution of sodium fluorescein in APW for 1 min. Finally, the planaria were washed with APW (15 mL) for 1 min to remove excess sodium fluorescein adsorbed to the outer worm surface. The test animal was then immobilised by embedding it in 2% agarose solution following the protocol of Shen et al. (2018) with minor modifications. In brief, a planarian was transferred onto a microscopic slide (VWR, UK), after which few drops of agarose solution were carefully added to cover the whole animal. The slide was immediately placed on ice leading to gelling of the agarose solution and immobilisation of the test animal. Fluorescence images of individual planaria were collected with a Leica MZ10F stereomicroscope (Leica Microsystems, UK) with Leica DFC3000G digital camera, 1.6× magnification with 160 ms exposure time (gain 2.6×), Gamma = 0.7 and wavelength=519 nm (excitation wavelength). The negative controls were planaria treated only with sodium fluorescein in APW for water- soluble test compounds and sodium fluorescein in 1% DMSO solution (v/v) in APW for the poorly water-soluble test compounds. To quantify sodium fluorescein inside a planarian, the fluorescence of the whole animal was measured using ImageJ (version 1.8.0_112) software and the value obtained normalised by dividing by the area (cm^2) of the individual planarian. All experiments were conducted in triplicate.

7.5 pH Study

In this study the pH of the medium (APW) was either increased or decreased by adding either 0.1 M HCl or NaOH. Briefly, APW was prepared by mixing 0.5g of instant ocean salt in 1L of Milli-Q water. The pH of the solution was measured by pH-meter (Thermo-Fischer, UK). To this 0.1M HCl or NaOH solution was added, and at each point, the pH of the solution was measured.

7.6 Statistical Analysis

Statistical significance for the fluorescence intensity test was determined using one-way analysis of variance (ANOVA), followed by Tukey's test using Graphpad Prism software (version 7.0).

7.7 Results and Discussions

7.7.1 Fluorescence Study

In this study, three test compounds were used namely PAA, PMD and the synthesised copolymer poly (AA-*co*-APMD). Benzalkonium chloride (BKC) was used as positive irritant control while APW with and without DMSO (1% v/v) was used as the negative control for water-insoluble and water-soluble compounds, respectively. The aim of this study was to evaluate the irritation potential of PMD alone, PAA alone and the irritation potential of the synthesised copolymer.

As with the study described in chapter 6, the fluorescence intensity of planaria exposed to artificial pond water before immersion in the fluorescent dye was minimal and indistinguishable from background fluorescence showing that the planarian membranes were intact. In either negative control (APW with or without DMSO) the FI values of 2.6 and 2.5 a.u. respectively were not significantly different showing that the addition of DMSO did not affect the worms membrane, which indeed is in accordance with chapter 6. With the positive control, BKC, FI was 52.6, again in good agreement with the earlier study and, together with the negative control data, shows that the assay is reproducible.

A study conducted by US-EPA (the United States Environmental Protection Agency) for the registration of PMD as an insect repellent shows that PMD is quite safe to be used on the skin,

as it caused only slight erythema on rabbit skin when a concentrated solution was applied (EPA safety document for PMD); based upon this study it was expected that the fluorescence intensity (FI) of the planaria following exposure to PMD would be comparable to that of other non-irritants. The results indeed showed that the FI of planaria exposed to 0.1% (w/v) PMD was similar to that following exposure to PEG-400 (5 a.u.). However, as shown in the planarian assay development work, irritation is often related to concentration and the mild erythema caused in the rabbit assay is likely attributed to a greater concentration of PMD being applied.

Similarly, according to the literature, low molecular weight PAA is a skin irritant while high molecular weight cross-linked PAA, such as Carbopol, has an excellent safety profile (polyacrylic safety www.polysciences.com). PAA (low molecular weight, *i.e.* 5000 Da), was found to be an irritant for the planaria, with FI of 14.6 comparable to para fluoro aniline (12.6 a.u.), a moderate irritant. In the copolymer, *i.e.* poly(AA-*co*-APMD), the FI value fell to 7.5, indicating a   good safety profile and comparable to mild irritants in chapter 6 such as terpinyl acetate (8.1 a.u.).
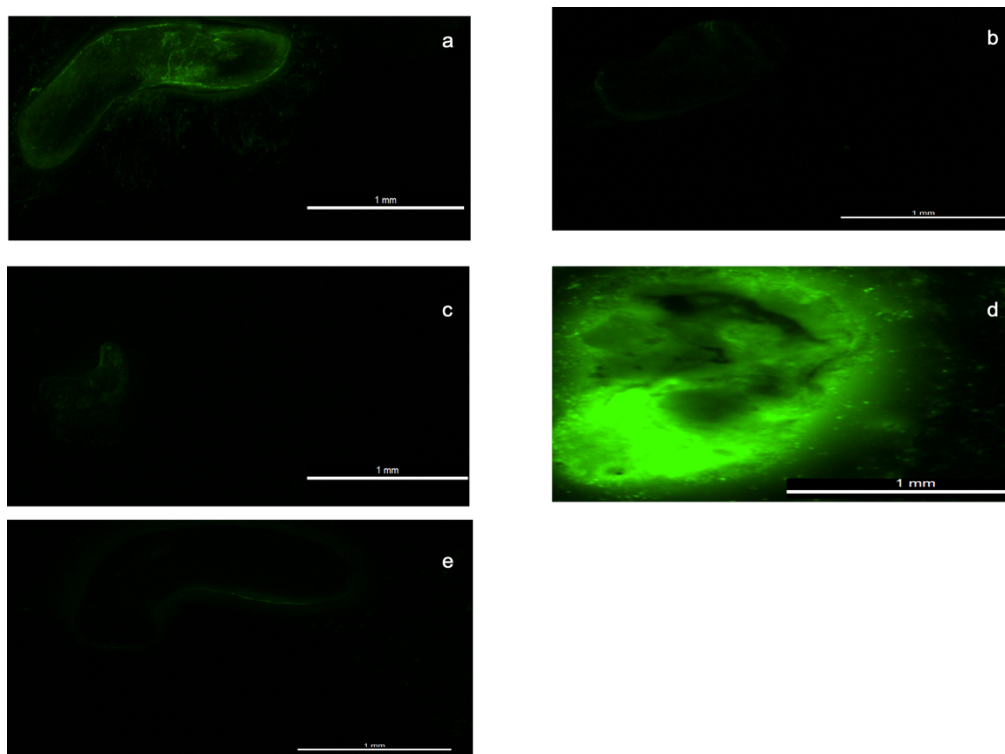
Figure 7.1. Exemplar fluorescent images of APW with fluorescein in DMSO (e), and after planaria being exposed to PAA (a), PMD (b), copolymer (c) and BKC (d).
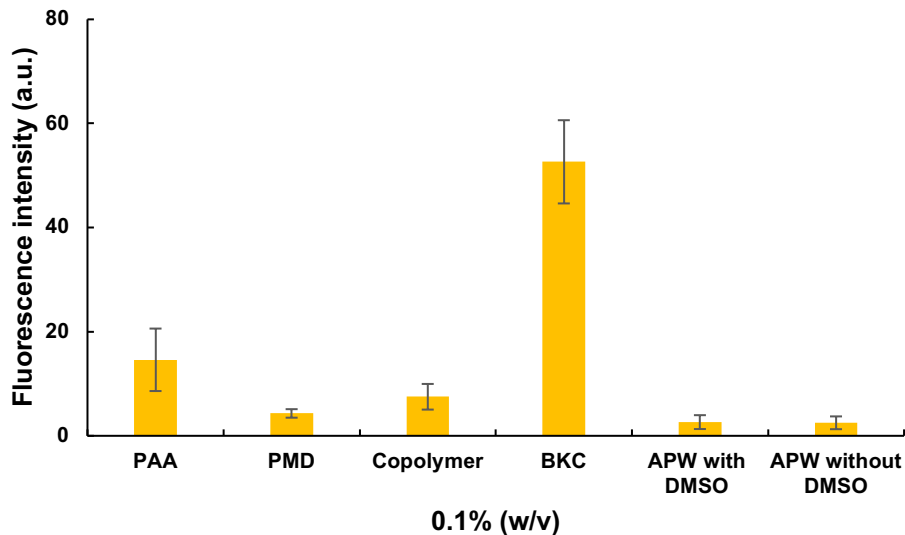
Figure 7.2. Fluorescence intensity (per cm^2) of individual planaria exposed to different test substances. Data are expressed as mean ± standard deviation (n = 3).

7.7.2 pH Study

To explore further the cause of irritation by PAA in planaria, the influence of pH on the worms' membrane was investigated. A series of solutions of artificial pond water were adjusted to pH: 2.8, 3.2, 3.6, 4.2, 4.9, 5.5, 6.3, 7.3, 8.2, 9.1 and 10.2. The planaria were exposed to the differing solutions for 1 min and then washed and exposed to the fluorescence for a further 1 min as above. The results showed that below pH 4.2 and above 8.2 there was a significant accumulation of sodium fluorescein within the planaria (hence indicating the toxicity). PAA has free carboxylic acid groups, and the presence of these cause a decrease in pH such that the pH of the PAA solution is 4.1. at which value there is significant damage seen to the planarian membrane. This result is in good agreement with the literature where extreme pH changes have been shown to lead to stagnation in the growth of flatworms colonies (de Oliveira et al., 2018)
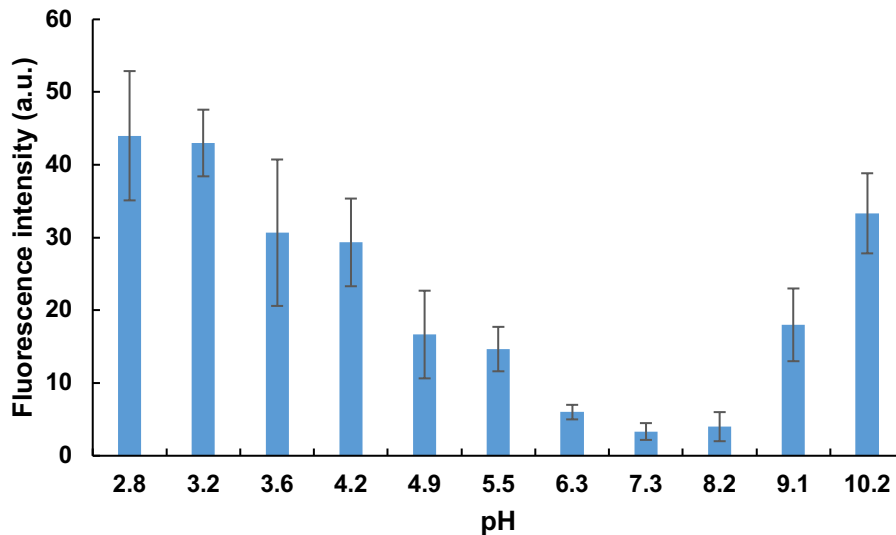
Figure 7.3. Fluorescence intensity (per cm^2) of individual planaria exposed to different pH. Data are expressed as mean ± standard deviation (n = 3).

7.8 Conclusion

This study has shown that, in our planarian assay, PMD is a non-irritant whereas the polymer PAA is a moderate irritant, in agreement with the existing literature. When prepared as a co-polymer, the poly (AA-*co*-APMD) is a mild irritant. This finding was expected and can be partially attributed to the pH changes seen when the worms are incubated with the free polymer which causes the solution pH to drop to a level where the worm membrane becomes damaged. On co-polymerisation, the free carboxylic acid content falls and hence the pH of the solution rises to nearer neutrality where membrane damage is minimal. Though for sure, this (pH) may not be the only reason for the decrease in the irritation potential of the copolymer and there must be other factors responsible for that.

References

Azimzadeh, J., Basquin, C., 2016. Basal bodies across eukaryotes series: basal bodies in the freshwater planarian Schmidtea mediterranea. Cilia 5, 15. https://doi.org/10.1186/s13630-016-0037-1

1fff54a3aa09f8fe4cc7d6bbba8bb7c2ac3186ee @ www.polysciences.com, n.d.

de Oliveira, M.S., Lopes, K.A.R., Leite, P.M.S.C.M., Morais, F.V., de Campos Velho, N.M.R., 2018. Physiological evaluation of the behavior and epidermis of freshwater planarians (Girardia tigrina and Girardia sp.) exposed to stressors. Biol. Open 7, bio029595. https://doi.org/10.1242/bio.029595

Cebrià, F., Newmark, P.A., 2005. Planarian homologs of netrin and netrin receptor are required for proper regeneration of the central nervous system and the maintenance of nervous system architecture. Development 132, 3691 LP – 3703. https://doi.org/10.1242/dev.01941

Devine, D.M., Devery, S.M., Lyons, J.G., Geever, L.M., Kennedy, J.E., Higginbotham, C.L., 2006. Multifunctional polyvinylpyrrolidinone-polyacrylic acid copolymer hydrogels for biomedical applications. Int. J. Pharm. 326, 50–59. https://doi.org/https://doi.org/10.1016/j.ijpharm.2006.07.008

Drapeau, J., Rossano, M., Touraud, D., Obermayr, U., Geier, M., Rose, A., Kunz, W., 2011. Green synthesis of para-Menthane-3,8-diol from Eucalyptus citriodora: Application for repellent products. Comptes Rendus Chim. 14, 629–635. https://doi.org/https://doi.org/10.1016/j.crci.2011.02.008

Gentile, L., Cebrià, F., Bartscherer, K., 2011a. The planarian flatworm: an in vivo model for stem cell biology and nervous system regeneration. Dis. Model. &amp; Mech. 4, 12 LP – 19. https://doi.org/10.1242/dmm.006692

Hagstrom, D., Cochet-Escartin, O., Collins, E.-M.S., 2016. Planarian brain regeneration as a model system for developmental neurotoxicology. Regeneration 3, 65–77. https://doi.org/10.1002/reg2.52

Hagstrom, D., Zhang, S., Ho, A., Tsai, E.S., Radić, Z., Jahromi, A., Kaj, K.J., He, Y., Taylor, P., Collins, E.-M.S., 2018. Planarian cholinesterase: molecular and functional characterization of an evolutionarily ancient enzyme to study organophosphorus pesticide

toxicity. Arch. Toxicol. 92, 1161–1176. https://doi.org/10.1007/s00204-017-2130-7

Ma, W.-D., Xu, H., Wang, C., Nie, S.-F., Pan, W.-S., 2008. Pluronic F127-g-poly(acrylic acid) copolymers as in situ gelling vehicle for ophthalmic drug delivery system. Int. J. Pharm. 350, 247–256. https://doi.org/10.1016/j.ijpharm.2007.09.005

Madan, R.K., Levitt, J., 2014. A review of toxicity from topical salicylic acid preparations. J. Am. Acad. Dermatol. 70, 788–792. https://doi.org/https://doi.org/10.1016/j.jaad.2013.12.005

Liang, H., Brignole-Baudouin, F., Rabinovich-Guilatt, L., Mao, Z., Riancho, L., Faure, M.O., Warnet, J.M., Lambert, G., Baudouin, C., 2008. Reduction of quaternary ammonium-induced ocular surface toxicity by emulsions: an in vivo study in rabbits. Mol. Vis. 14, 204–216.

Parasuraman, S., 2011. Toxicological screening. J. Pharmacol. Pharmacother. 2, 74–79. https://doi.org/10.4103/0976-500X.81895

Shen W., Shen Y., Lam Y.W., Chan D. 2018. Live Imaging of Planaria. Rink J. (eds) Planarian Regeneration. Methods in Molecular Biology. 1774. https://doi.org/10.1007/978-1-4939-7802-1_22

Skaer, R.J., 1965. The origin and continuous replacement of epidermal cells in the planarian Polycelis tenuis (Iijima). J. Embryol. Exp. Morphol. 13, 129 LP – 139.

Summary, I.E., Identity, A., Use, B., Assessment, C.R., n.d. Menthane-3,8-diol (011550) Biopesticide Registration Eligibility Document.

Vraka, C., Nics, L., Wagner, K.-H., Hacker, M., Wadsak, W., Mitterhauser, M., 2017. LogP, a yesterday's value? Nucl. Med. Biol. 50, 1–10. https://doi.org/https://doi.org/10.1016/j.nucmedbio.2017.03.003

Wu, J.-P., Li, M.-H., 2018. The use of freshwater planarians in environmental toxicology studies: Advantages and potential. Ecotoxicol. Environ. Saf. 161, 45–56. https://doi.org/https://doi.org/10.1016/j.ecoenv.2018.05.057

Chapter 8. General Conclusion and Future Work

8.1 General Conclusion

Insect borne diseases are a significant cause of mortality around the world (Zeller et al., 2013). Infections like malaria, dengue fever and leishmaniasis are transmitted to humans by the bite of an insect. In order to prevent this, insect repellents are frequently used (Fradin and Day, 2002). Various types of insect repellents are used for this purpose ranging from synthetic to natural insect repellents. Commonly used are DEET (N, N-diethyl-m-toluamide), p-menthane-3,8-diol (PMD), picaridin, nepetalactone, neem oil and permethrin (Chen-Hussey et al., 2014). PMD is a naturally occurring insect repellent but can also be synthesised in the laboratory (Carroll and Loye, 2006; Yuasa et al., 2000). However, use of PMD has some drawbacks including rapid evaporation and potential absorption of the repellent into the systemic circulation raising concerns over its use in pregnant women and infants. Thus, there is a need for a strategy to overcome these problems.

This PhD project focused on the development of a polymer-drug conjugate. The rationale for the synthesis of the conjugate was primarily to develop a system for prolonged drug release as compared to the conventional use of free PMD by exploiting the naturally occurring esterases enzymes on the skin, and secondly to minimise drug uptake into and absorption through the skin and hence reduce systemic PMD uptake as the molecular weight of the polymer would prevent (or certainly minimise) absorption. The first chapter provided an overview of skin as a potential site for drug delivery, described polymer-drug conjugates   and their advantages followed by a comprehensive discussion on the use of polymer-drug conjugates for drug delivery to diseased skin, *e.g.* eczema, wound healing, skin infections and cutaneous leishmaniasis. Most of these studies were promising in terms of efficacy and safety along with other parameters like the stability of the formulation and the drug loading. In some studies, issues that prevented the clinical translation of the conjugates were identified, which include difficulties with scaling up their synthesis followed by the disparity in the *in vitro* and *in vivo* results.

The second chapter provided an overview of the general methods and materials that were used during this project. The third chapter described preliminary attempts to synthesise a polymer-drug conjugate using high and low molecular weight hyaluronic and polyacrylic acid (PAA). Hyaluronic acid was chosen because of its excellent safety profile, the moisturising effect that

it has and the presence of suitable functional groups for the conjugation. Similarly, PAA was selected because of its good safety profile and the presence of suitable functional groups. Several methods followed by modifications in these methods were attempted to conjugate the polymers with PMD but failed to yield the desired results. Despite changing the polymer, polymer molecular weight, solvents and the drug itself, the desired polymer-drug conjugate could not be synthesised. The most probable reason for the unsuccessful reaction was steric hindrance of PMD and access to the reactive sites in the polymer themselves (as polymers are large molecules). This led to a change of approach, *i.e.* to develop a monomer drug conjugate and then subsequent polymerisation to form a polymer with the incorporated drug (PMD).

The fourth chapter focused on the synthesis and characterisation of the polymer-drug conjugate using free radical polymerisation of AA and APMD which resulted in the formation of poly(AA-*co*-APMD) ester copolymer with low to medium molecular weight (depending upon the monomer ratios). The synthesis was then followed by characterisation to determine the properties of the copolymer, *e.g.* glass transition temperature (Tg), reactivity ratio of the monomers, molecular weight and drug loading on the copolymers. The reactivity ratio study revealed that the AA is much reactive than the APMD, probably due to the presence of bulky cyclohexane ring in the APMD. The properties of the copolymer were dependent upon the monomer ratios in the feed mixtures and consequently the content of APMD in the polymer. Higher content of APMD results in the formation of a turbid solution in water. Thermal analysis revealed greater thermal stability of the PMD in the copolymer as compared to the free drug (PMD) whilst the DSC study revealed a decrease in the Tg by the addition of APMD into polyacrylic acid, most probably due to the decrease in the rigidity of the polymer chain. Drug loading was calculated by two methods; a titration method and elemental analysis both gave comparable results which were in agreement with the reactivity ratio studies.

The fifth chapter tested the hypothesis that esterases will hydrolyse the ester bond in the copolymer and thus will release the PMD over an extended period, and that the molecular weight of the copolymer will decrease the penetration and permeation of the PMD through the skin. For this purpose, porcine liver esterases (PLEs) were used to hydrolyse the ester bond in the copolymer. The results showed that the ester bond in the copolymer is susceptible to hydrolysis by PLEs. The amount of the parent compound (PMD) liberated from the control

experiments was approximately 45% of the loading. Thus, it was concluded that the hydrolysis of the copolymer was mostly if not purely enzymatic and no chemical hydrolysis and decomposition was involved, also evidence by the lack of PMD release in the absence of the enzyme. The amount of the drug released from the copolymer was below expectations the basis for which was investigated to test whether exhaustion of the enzymes or steric effects affected PMD release; molecular weight was shown to influence release whereas adding of new/additional enzymes did not have any effect on the amount of PMD released indicating that the enzymes had not been saturated. To assess the permeation and penetration profile of our copolymer and PMD alone (control), skin permeation and penetration experiments were undertaken by using Franz diffusion cell. The biggest challenge in this study was to develop a method to quantify the copolymer. For this purpose, the gel permeation chromatography (GPC) was used. It was found that, compared to PMD, copolymer only penetrated the upper epidermal layer and did not permeate the skin (pig ear), indicating that polymer-drug conjugation can be used to avoid or minimise permeation of the parent compound into the systemic circulation. Hence, potential side effects associated with PMD application can be avoided.

The design of formulations that contact human tissues requires toxicological testing and, in particular, topically applied formulations require skin irritation testing. The classical test used to assess skin irritation of the compounds is the Draize test (Draize et al., 1944). Over time, due to ethical as well as scientific reasons, alternative methods have been sought using lower animal models (Callens et al., 2001). Chapter six reports a novel method to quickly screen out potential strong irritants by using planaria as a model, based upon the hypothesis that the greater the irritation potential of a compound then the greater will be the fluoresence accumulation inside the flatworm following short term exposure to irritants. Using reported irritation defined by their primary irritation index values, twelve test substances were evaluated, three each from strong-, moderate-, mild- or non-irritants, alongside controls of 1 minute exposure to Artifical Pond Water with or without DMSO, and an untreated planarium to determine autofluorescnece. Autofluorescence was negligible and fluorescence uptake into the control planaria was minimal following short term exposure to the dye; uptake of 4 a.u./cm^2 from APW with DMSO indicates no substantive damage to the outer membrane. Following exposure to the non-irritants, fluorescence was not signficantly different to that of the control animals, with greatest intensity seen for PEG-400 exposure at 5 ± 2.3 a.u./cm^2. Data for the mild-irritants was also not signficiantly different to that of the controls, with benzyl alcohol

causing fluorescence of 4.6 ± 3.9 a.u./cm^2 which rose to 10 ± 5.8 a.u./cm^2 with tri-isobutyl phosphate. The increasing trend in fluorescence intensity continued with the moderate irritants, ranging from decanol (9.5 ± 3.2a.u./cm^2) to linalyl acetate (20 ± 3 a.u./cm^2). As a strong irritant, citronellal (18 ± 6.2 a.u./cm^2) gave similar fluorescence to linalyl acetate but both benzalkonium chloride (53 ± 11.2 a.u./cm^2) and carvacrol (48 ± 12.5 a.u./cm^2) caused catastrophic damage to the membrane resulting in significantly higher fluorescence intensities than all other tests. It was concluded that the fluorescence assay offers a rapid *in vivo* screening tool employing a model that is readily available and easy to maintain and which could act as a pre-screening method to inform subsequent sophisticated and costly assessments of skin irritants. Potentially this assay could be further extended to test irritation potential of various chemicals towards ocular, nasal and vaginal mucosa.

The last chapter of this thesis reported the evaluation of the toxicity of the copolymer poly(AA-*co*-APMD), polyacrylic acid and PMD by using the planaria fluorescence assay. The study showed that the conjugation of the PMD into the copolymer significantly reduces the irritation of the PAA (alone). Moreover, this is as expected from the skin permeation data and most of the copolymer resided at the top layer of the skin, and thus we expect it to exhibit low irritation potential *in vivo*. In order to know the possible mechanism/cause of the irritation of the compounds towards planaria, the effect of pH and logP was studied, revealing that extremes of pH disrupted the planarian membrane while the logP values (available from the data) of different compounds does not have a significant relationship with its increasing or decreasing values.

Overall, the aims of the project have been achieved through successful synthesis and characterisation of the copolymer despite the initial challenges faced. Moreover, it was proven that the PMD can be released from the copolymers by the eastreases and upon the application of the conjugated polymeric system significantly reduced the permeation of PMD through human skin. We were also able to develop a new model to predict the irritation potential of strong irritants towards the skin and based upon that model we successfully evaluated the irritation potential of our copolymer.

8.2. Future Work

This section is broadly divided into two sub sections. First discusses the future work related to this particular study while the second considers broader future uses of polymer-drug conjugates as a drug delivery platform for skin diseases.

8.2.1 Future Work Concerning this Project

The study could not cover all the aspects that should be considered when translating a formulation further towards its regulatory approval and clinical application.

8.2.1.1. Optimising the Conjugate

Despite multiple attempts and modifications to the method or molecular weight or even to the drug carrier, it was not possible to produce an HA-PMD conjugate. However, this carrier (HA) has been successfully conjugated in literature reports (Chen et al., 2014; Huang and Huang,2018). HA is attractive as it is safe, widely used and is known to be a moisturising agent in cosmetic preparation. Studies also show it can penetrate the outer layers of the stratum corneum (but not through the tissue) (Essendoubi et al., 2016) and hence it may help to retain the conjugate on the skin surface for extended periods. It would be of value to further explore the reasons for the non-reactivity and seek alternative approaches for an HA-PMD system.

8.2.1.2. Drug Loading

Whilst drug loading is satisfactory in the pilot work, it remains at ~10% of the copolymer. having it higher for extended drug release may be beneficial. This could be either by changing the monomer, *i.e.* choosing methacrylic acid instead of acrylic acid or may be methacrylic anhydride *etc*

8.2.1.3. Synergistic Effect

Another area that could be possibly explored is the potential combination of repellents like DEET or blend with DEET or may be vanillin for multiple actions of repellency, for example it might help us to cover a broader range of coverage (protection from insect

bites) as compared to the PMD alone, as there are reports that inclusion of 5% vanillin increases the protection time up to 4.5 hours when used in conjunction with citronella oil (Songkro et al., 2012).

8.2.1.4. Formulation

Formulation of the conjugate is an essential step for the ultimate usage (in humans). Whilst the formulation involves challenges, the biggest of which is to prevent the hydrolysis of the ester bond during its long-term storage in the presence of excipients. Thus, requiring strict testing before being formulated. The formulation can be in the form of a topical spray or maybe a hydrogel.

8.2.1.5. *In vivo* Testing

Similarly, another study that could have been done is the in vivo study. However, this study was planned out (6g of copolymer batch was prepared) but could not have been done due to unforeseen circumstances. For this purpose, we suggest arm-in-cage study which is a standard method to evaluate the efficacy of any insect repellent formulation, involving the use of either human volunteers or the animals (rabbits), where a formulation is applied (typically on arms in humans) followed by the calculation of the number of mosquito bites usually up to 24 hours. In the end, the obtained data is compared with the control (Logan et al., 2010).

8.2.2 Future Potential of Polymer-Drug Conjugates for Skin Drug Delivery

Over the last two decades, the application of PDCs to diseases other than cancer has increased, including for topical delivery though this remains a relatively under researched area. As macromolecular constructs, passive diffusion through the intact stratum corneum barrier is not feasible and hence the focus is on targeting to the follicles or use in conditions where the skin barrier is damaged such as psoriasis or wound healing. Thus, opportunities exist for similar barrier dysfunctioning conditions such as atopic dermatitis, scabies or cutaneous leishmaniasis (Smith, 2007).

One opportunity is in treating cutaneous leishmaniasis (CL). There are two major problems associated with the use of current drug regimen for the treatment of CL; (1) they are administered in the form of cutaneous injections which are painful and (2) they have elevated toxicity and carry substantial side effects restricting their use (Croft et al., 2006). The features important for consideration to develop a PDC for CL are that as the outer protective barrier of the skin, *i.e.,* SC is damaged so delivery should be feasible. Secondly, the target site where the parasitized macrophages are located is accessible but requires site-specific delivery as is feasible with conjugates which can ideally be taken up by the *Leishmania* infected macrophages and release the drug within phagolysosomes. It has been reported that the macrophages infected with the *Leishmania* parasite require more glucose as energy source for their survival (Hassani and Olivier, 2013; Liu and Uzonna, 2012), therefore polymeric polysaccharides such as neoglycoproteins, xanthan and HA could be suitable polymers as these polysaccharides can be taken up by the receptor mediated endocytosis using mannose receptors on the macrophages. Moreover, *Leishmania* infected macrophages are rich in a protease enzyme called cathepsin, thus requiring a linker that is susceptible to proteases so can release the drug of choice within the parasite-phorous vacuole of macrophage.

Scabies caused by *Sarcoptes scabiei* is another common skin infestation affecting more than 200 million people worldwide, characterised by intense itching and discomfort *for which* there are various drawbacks associated with treatments. For example, there are reports of neurotoxicity associated with the systemic absorption of topically administered lindane, whilst some literature shows the development of resistance against ivermectin in humans (Khalil et al., 2017). The main aspects that should be considered when designing a PDC system for topical therapy of scabies is to deliver the drug at the site of infestation, *i.e.* the lower SC of the skin (Morgan et al., 2013). The possible solution can be conjugating permethrin, ivermectin or lindane with polypeptides or hyaluronic acid (HA) that are proven to enhance the permeation of the drug through SC but at the same time preventing the systemic absorption as compared to the drug applied alone topically (Witting et al., 2015).

During the last two decades the occurrence of the skin fungal infections has been increasing and are increasingly difficult to treat with a growing population of patients with co-morbidity. For fungal therapies, conventional formulations are widely used, irrespective of where the

fungal pathogen is residing within the skin, *i.e.,* whether in the SC or deeper skin layers. The treatment of deeply seated fungal infections such as invasive aspergillosis and candidiasis is problematic. Moreover, the application of ineffective formulations can provoke adverse effects including allergic reactions (Kumar et al., 2014). To avoid some of the above difficulties, one approach could be to use PDCs with an anti-fungal drug conjugated to a polypeptide or a low molecular weight HA, so that it can penetrate into the skin thus releasing the drug at the site of the infection. This may result in avoidance of the side effects associated with the allergic reactions on skin.

8.4. **Significance of the Key Findings**

To the best of our knowledge, till this date, there is no published work relating to the use of PDCs on the intact skin to decrease the permeation of a compound. Thus, this work for the first time reports the use of PDC as a drug delivery system to decrease the permeation as well as extend the release of the drug, *i.e.* PMD. The findings in this thesis provides a mean to extend this technology, *i.e.* PDCs to other volatile compounds like perfumes, which can be beneficial not only to extend their efficacy (smell) but also to avoid any side effects associated with the permeation of volatile compounds as well as it can also be used to avoid any skin irritation that normally is associated with abrupt release of the drug once a formulation is applied onto the skin.
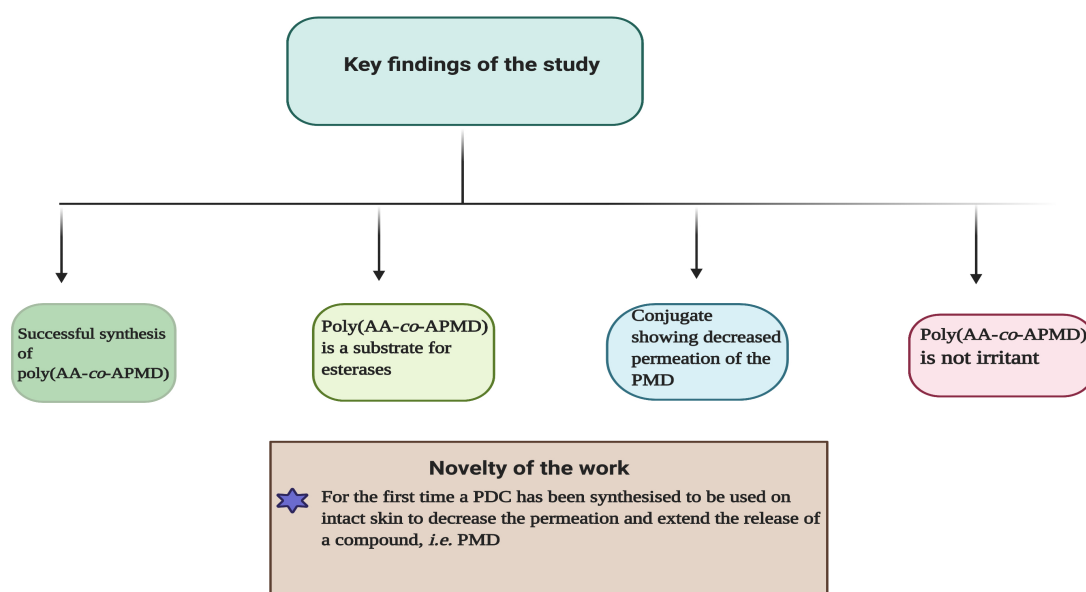

Figure 8.1. Key findings of this thesis

References

Callens, C., Adriaens, E., Dierckens, K., Remon, J.P., 2001. Toxicological evaluation of a bioadhesive nasal powder containing a starch and Carbopol® 974 P on rabbit nasal mucosa and slug mucosa. J. Control. Release 76, 81–91. https://doi.org/https://doi.org/10.1016/S0168-3659(01)00419-9

Carroll, S.P., Loye, J., 2006. PMD, a registered botanical mosquito repellent with deet-like efficacy. J. Am. Mosq. Control Assoc. 22, 507–514. https://doi.org/10.2987/8756-971X(2006)22

Chen, B., Miller, R., Dhal, P., 2014. Hyaluronic Acid-Based Drug Conjugates: State-of-the-Art and Perspectives. J. Biomed. Nanotechnol. 10, 4–16. https://doi.org/10.1166/jbn.2014.1781

Croft, S.L., Sundar, S., Fairlamb, A.H., 2006. Drug resistance in leishmaniasis. Clin. Microbiol. Rev. 19, 111–126. https://doi.org/10.1128/CMR.19.1.111-126.2006

Essendoubi, M., Gobinet, C., Reynaud, R., Angiboust, J.F., Manfait, M., Piot, O., 2016. Human skin penetration of hyaluronic acid of different molecular weights as probed by Raman spectroscopy. Ski. Res. Technol. 22, 55–62. https://doi.org/10.1111/srt.12228

Hassani, K., Olivier, M., 2013. Immunomodulatory impact of leishmania-induced macrophage exosomes: a comparative proteomic and functional analysis. PLoS Negl Trop Dis 7, e2185.

Huang, G., Huang, H., 2018. Application of hyaluronic acid as carriers in drug delivery. Drug Deliv. 25, 766–772. https://doi.org/10.1080/10717544.2018.1450910

Khalil, S., Abbas, O., Kibbi, A.G., Kurban, M., 2017. Scabies in the age of increasing drug resistance. PLoS Negl. Trop. Dis. 11, e0005920–e0005920. https://doi.org/10.1371/journal.pntd.0005920

Kumar, L., Verma, S., Bhardwaj, A., Vaidya, S., Vaidya, B., 2014. Eradication of superficial fungal infections by conventional and novel approaches: a comprehensive review. Artif. Cells, Nanomedicine, Biotechnol. 42, 32–46. https://doi.org/10.3109/21691401.2013.769446

Liu, D., Uzonna, J.E., 2012. The early interaction of Leishmania with macrophages and dendritic cells and its influence on the host immune response. Front. Cell. Infect. Microbiol. 2, 83. https://doi.org/10.3389/fcimb.2012.00083

Morgan, M.S., Arlian, L.G., Markey, M.P., 2013. Sarcoptes scabiei mites modulate gene expression in human skin equivalents. PLoS One 8, e71143–e71143. https://doi.org/10.1371/journal.pone.0071143

Smith, J.G.J., 2007. Burden of skin disease. J. Am. Acad. Dermatol. https://doi.org/10.1016/j.jaad.2006.09.008

Witting, M., Boreham, A., Brodwolf, R., Vávrová, K., Alexiev, U., Friess, W., Hedtrich, S., 2015. Interactions of hyaluronic Acid with the skin and implications for the dermal delivery of biomacromolecules. Mol. Pharm. 12, 1391–1401. https://doi.org/10.1021/mp500676e

Zeller, H., Marrama, L., Sudre, B., Bortel, W. Van, Warns-Petit, E., 2013. Mosquito-borne disease surveillance by the European Centre for Disease Prevention and Control. Clin. Microbiol. Infect. 19, 693–698. https://doi.org/https://doi.org/10.1111/1469-0691.12230